frontiers | Research Topics

Community series in cell network in antitumor immunity of pediatric and adult solid tumors, volume II

Edited by
Ombretta Melaiu and Silvia Pesce

Coordinated by
Elin Bernson

Published in
Frontiers in Immunology

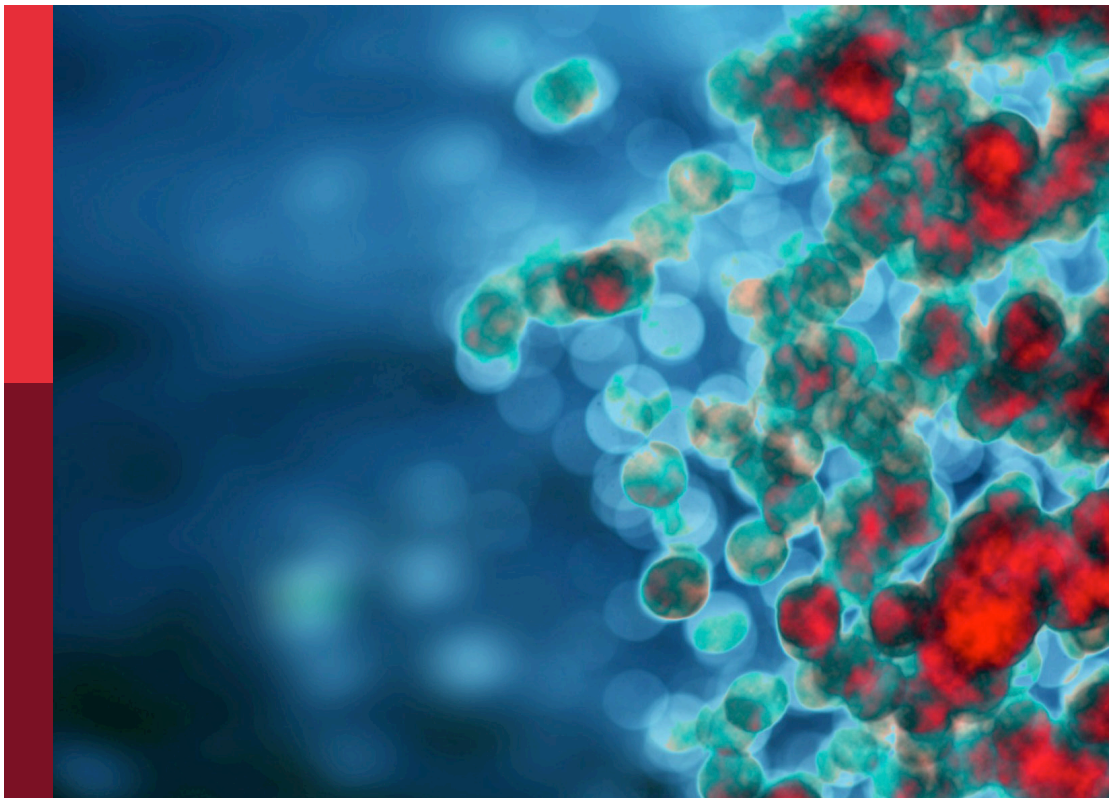

ISSN 1664-8714
ISBN 978-2-8325-6598-8
DOI 10.3389/978-2-8325-6598-8

Generative AI statement
Any alternative text (Alt text) provided alongside figures in the articles in this ebook has been generated by Frontiers with the support of artificial intelligence and reasonable efforts have been made to ensure accuracy, including review by the authors wherever possible. If you identify any issues, please contact us.

About Frontiers

Frontiers is more than just an open access publisher of scholarly articles: it is a pioneering approach to the world of academia, radically improving the way scholarly research is managed. The grand vision of Frontiers is a world where all people have an equal opportunity to seek, share and generate knowledge. Frontiers provides immediate and permanent online open access to all its publications, but this alone is not enough to realize our grand goals.

Frontiers journal series

The Frontiers journal series is a multi-tier and interdisciplinary set of open-access, online journals, promising a paradigm shift from the current review, selection and dissemination processes in academic publishing. All Frontiers journals are driven by researchers for researchers; therefore, they constitute a service to the scholarly community. At the same time, the *Frontiers journal series* operates on a revolutionary invention, the tiered publishing system, initially addressing specific communities of scholars, and gradually climbing up to broader public understanding, thus serving the interests of the lay society, too.

Dedication to quality

Each Frontiers article is a landmark of the highest quality, thanks to genuinely collaborative interactions between authors and review editors, who include some of the world's best academicians. Research must be certified by peers before entering a stream of knowledge that may eventually reach the public - and shape society; therefore, Frontiers only applies the most rigorous and unbiased reviews. Frontiers revolutionizes research publishing by freely delivering the most outstanding research, evaluated with no bias from both the academic and social point of view. By applying the most advanced information technologies, Frontiers is catapulting scholarly publishing into a new generation.

What are Frontiers Research Topics?

Frontiers Research Topics are very popular trademarks of the *Frontiers journals series*: they are collections of at least ten articles, all centered on a particular subject. With their unique mix of varied contributions from Original Research to Review Articles, Frontiers Research Topics unify the most influential researchers, the latest key findings and historical advances in a hot research area.

Find out more on how to host your own Frontiers Research Topic or contribute to one as an author by contacting the Frontiers editorial office: frontiersin.org/about/contact

Community series in cell network in antitumor immunity of pediatric and adult solid tumors, volume II

Topic editors
Ombretta Melaiu — University of Rome Tor Vergata, Italy
Silvia Pesce — University of Genoa, Italy

Topic coordinator
Elin Bernson — University of Gothenburg, Sweden

Citation
Melaiu, O., Pesce, S., Bernson, E., eds. (2025). *Community series in cell network in antitumor immunity of pediatric and adult solid tumors, volume II*.
Lausanne: Frontiers Media SA. doi: 10.3389/978-2-8325-6598-8

Table of contents

frontiers | Frontiers in Immunology

TYPE Editorial
PUBLISHED 27 June 2025
DOI 10.3389/fimmu.2025.1649643

OPEN ACCESS

EDITED AND REVIEWED BY
Peter Brossart,
University of Bonn, Germany

*CORRESPONDENCE
Silvia Pesce
silvia.pesce@unige.it
Ombretta Melaiu
Ombretta.Melaiu@uniroma2.it

†These authors have equally contributed to this work

RECEIVED 18 June 2025
ACCEPTED 20 June 2025
PUBLISHED 27 June 2025

CITATION
Melaiu O, Bernson E and Pesce S (2025) Editorial: Community series in cell network in antitumor immunity of pediatric and adult solid tumors, volume II.
Front. Immunol. 16:1649643.
doi: 10.3389/fimmu.2025.1649643

Editorial: Community series in cell network in antitumor immunity of pediatric and adult solid tumors, volume II

Ombretta Melaiu[1*†], Elin Bernson[2,3] and Silvia Pesce[4*†]

[1]Department of Clinical Sciences and Translational Medicine, University of Rome Tor Vergata, Rome, Italy, [2]Sahlgrenska Center for Cancer Research, University of Gothenburg, Gothenburg, Sweden, [3]Department of Obstetrics and Gynecology, Institute of Clinical Sciences, Sahlgrenska Academy, University of Gothenburg, Gothenburg, Sweden, [4]Department of Experimental Medicine University of Genoa, IRCCS Ospedale Policlinico San Martino, Genova, Italy

KEYWORDS

tumor microenvironment (TME), tumor-infiltrating immune cells, biomarkers, tumor immunity, immunotherapy

Editorial on the Research Topic
Community series in cell network in antitumor immunity of pediatric and adult solid tumors, volume II

This Research Topic has been curated to provide insights into the intricate interactions within the tumour microenvironment (TME) and their impact on cancer progression and treatment outcomes. The Research Topic features a variety of studies focused on impact that different immune and stromal cell types have in solid tumours, shedding light on emerging immunotherapeutic strategies and multi-omics approaches that enhance our understanding of this intricate field. This Research Topic specifically includes four original research articles, one case report, two brief research communications, and three comprehensive literature reviews.

Early cancer detection remains a cornerstone of improved oncology outcomes (1). Two studies both by Rebaudi et al. and Rebaudi et al., one on oral squamous cell carcinoma (OSCC) (Rebaudi et al.) and the other on oral leukoplakia (Rebaudi et al.), which is a precursor to potentially malignant oral disorders (PMOD), demonstrated the feasibility and reliability of non-invasive sampling using a cytobrush in conjunction with biomarker analysis. Using a customised ELISA immunoassay, the researchers could distinguish between malignant and healthy tissue by analysing selected biomarkers, such as EGFR, Ki67, p53, and immune checkpoint-related proteins (PD-L1, HLA-E, and B7-H6). These results corroborate histopathological gold standards and provide dynamic immunophenotypic data from living tissue.

Another key factor in gauging the severity of a tumour is pinpointing crucial genetic and immunohistochemical markers (2). Biatta et al. examined the concordance between *TP53* mutations and p53 immunohistochemical staining patterns in high-grade serous ovarian carcinoma (HGSOC). Null p53 expression, which corresponds to disruptive *TP53* mutations, were associated with significantly reduced overall survival. This offers clinicians an immunohistochemical surrogate marker over genetic analysis for this aggressive disease. Meanwhile, a review of neuroblastoma by D'Amico et al., explored the remarkable cellular

plasticity that enables tumour cell transition between adrenergic (ADRN) and mesenchymal (MES) states. These transitions impact therapeutic resistance and immunogenicity, with MES cells emerging as favourable immunotherapy targets in scenarios where strategies mitigate interconversion and facilitate immune engagement.

Interestingly, a significant portion of this editorial's work has focused on the importance of natural killer (NK) cells, which are pivotal players in the anti-tumour immune system (3). For instance, one of the most notable contributions in this Research Topic is the identification of PLAC1 as a novel ligand for several NK cell-activating receptors (NKARs), including NKG2D and NKp30. Romania et al. demonstrated through a high-throughput shRNA screen that PLAC1 expression enhances NK cell-mediated cytotoxicity. The overexpression of PLAC1 in a wide range of tumours, while remaining largely absent in normal tissues, makes it an ideal candidate for both biomarker development and immunotherapeutic targeting.

Yet, the TME often presents formidable immunosuppressive barriers (4). Karlsson et al., revealed Galectin-3 as a key immune modulator found in ascites and cyst fluid of patients with HGSOC. By priming neutrophils to produce reactive oxygen species (ROS), Galectin-3 indirectly impairs NK cell function, reinforcing the need for strategies that can neutralize suppressive signals within the TME.

Meanwhile, Mariotti et al. have improved our understanding of NK cell regulation by discovering that soluble PD-1 (sPD-1) enhances NK cell cytotoxicity. Produced endogenously by NK cells themselves, sPD-1 binds PD-L1 and suggests a novel autocrine or paracrine regulatory mechanism with potential therapeutic value. Animal models, too, are evolving to meet the demands of next-generation immunotherapy research (5). A comprehensive review by Parodi et al., maps the trajectory of NK cell studies from traditional murine systems to sophisticated humanized mouse models, reinforcing their continued importance in translational immunology.

In addition to NK cells, other components of the TME were also considered, including macrophages and neutrophils (6, 7). In this regard, a comprehensive review by Di Ceglie et al., on the roles of macrophages and neutrophils underscores their dual potential to either support or suppress tumour growth, depending on the local cytokine milieu and cell-cell interactions. As key modulators within the TME, their crosstalk with other immune cells, including NK cells, can influence the success of immunotherapies. Authors suggested that targeting these interactions holds promise as a novel means of reprogramming the immune landscape to favour anti-tumour responses.

Finally, in the case of pancreatic ductal adenocarcinoma (PDAC), a notoriously aggressive form of cancer (8), the dense desmoplastic stroma, which is driven by cancer-associated fibroblasts (CAFs), impedes the penetration of therapeutics and modulates immune responses. Using imaging mass cytometry, Erreni et al. profiled CAF subpopulations with unprecedented resolution and identified 19 phenotypically distinct clusters. Notably, specific CAF populations, such as CAFs 10 and 11, were enriched at the tumour-stroma interface and were associated with poorer prognoses. These fibroblasts co-localised with CD44+ macrophages and contributed to extracellular matrix remodelling, creating barriers to T cell infiltration. These findings highlight the functional heterogeneity of CAFs and their potential as therapeutic targets, particularly in efforts to re-engineer the tumour stroma to improve drug delivery and immune infiltration.

Together, these studies provide a roadmap for achieving a more systems-level understanding of cancer, from diagnosis through treatment. The convergence of non-invasive diagnostics, microenvironmental mapping, and molecular stratification paves the way for personalized interventions that not only target the tumour but reshape the ecosystem in which it thrives.

Whether through NK cell modulation, CAF profiling, or non-invasive biomarker discovery, the unifying theme is clear: precision oncology must be built on a foundation of deep biological insight, real-time monitoring, and therapeutic flexibility.

Author contributions

OM: Formal Analysis, Data curation, Visualization, Conceptualization, Writing – original draft, Funding acquisition. EB: Writing – review & editing, Validation, Visualization. SP: Formal Analysis, Data curation, Visualization, Conceptualization, Writing – original draft, Funding acquisition.

Funding

The author(s) declare that financial support was received for the research and/or publication of this article. This work was supported by funds from PRIN-MIUR 2022 grant n. 2022ZFFALH – P.I.: O.M and PRIN-MIUR PNRR 2022, grant n. P2022PKFNB - P.I.: S.P.

Acknowledgments

We express our gratitude to all the authors who have contributed to this Research Topic and to the reviewers for their valuable work. We hope that the reader will find this Research Topic motivating and helpful.

Conflict of interest

The authors declare that the research was conducted in the absence of any commercial or financial relationships that could be construed as a potential conflict of interest.

Generative AI statement

The author(s) declare that no Generative AI was used in the creation of this manuscript.

Publisher's note

References

1. Crosby D, Bhatia S, Brindle KM, Coussens LM, Dive C, Emberton M, et al. Early detection of cancer. *Science*. (2022) 375:eaay9040. doi: 10.1126/science.aay9040

2. Le M, Oishi N, Mochizuki K, Kondo T. Immunohistochemical detection of cancer genetic abnormalities. *Pathol Res Pract*. (2024) 255:155109. doi: 10.1016/j.prp.2024.155109

3. Wolf NK, Kissiov DU, Raulet DH. Roles of natural killer cells in immunity to cancer, and applications to immunotherapy. *Nat Rev Immunol*. (2023) 23:90–105. doi: 10.1038/s41577-022-00732-1

4. Liu W, Zhou H, Lai W, Hu C, Xu R, Gu P, et al. The immunosuppressive landscape in tumor microenvironment. *Immunol Res*. (2024) 72:566–82. doi: 10.1007/s12026-024-09483-8

5. Zhou R, Tang X, Wang Y. Emerging strategies to investigate the biology of early cancer. *Nat Rev Cancer*. (2024) 24:850–66. doi: 10.1038/s41568-024-00754-y

6. Guan F, Wang R, Yi Z, Luo P, Liu W, Xie Y, et al. Tissue macrophages: origin, heterogenity, biological functions, diseases and therapeutic targets. *Signal Transduct Target Ther*. (2025) 10:93. doi: 10.1038/s41392-025-02124-y

7. Eruslanov E, Nefedova Y, Gabrilovich DI. The heterogeneity of neutrophils in cancer and its implication for therapeutic targeting. *Nat Immunol*. (2025) 26:17–28. doi: 10.1038/s41590-024-02029-y

8. Shah A, Johnson E, Ponnusamy MP, Batra SK. Emerging pathways yielding opportunities for future treatments in pancreatic ductal adenocarcinoma. *Expert Opin Ther Targets*. (2025) 29:309–26. doi: 10.1080/14728222.2025.2507035

frontiers | Frontiers in Immunology

TYPE Review
PUBLISHED 14 June 2023
DOI 10.3389/fimmu.2023.1209237

OPEN ACCESS

EDITED BY
Ombretta Melaiu,
University of Rome Tor Vergata, Italy

REVIEWED BY
Valeria Leuci,
University of Turin, Italy
Valeria Lucarini,
Sapienza University of Rome, Italy
Jaya Lakshmi Thangaraj,
University of California, San Diego, United States
Adeleh Taghi Khani,
Beckman Research Institute, United States

*CORRESPONDENCE
Massimo Vitale
massimo.vitale@hsanmartino.it
Paola Orecchia
paola.orecchia@hsanmartino.it

†These authors have contributed equally to this work

‡These authors share senior authorship

RECEIVED 20 April 2023
ACCEPTED 02 June 2023
PUBLISHED 14 June 2023

CITATION
Parodi M, Astigiano S, Carrega P, Pietra G, Vitale C, Damele L, Grottoli M, Guevara Lopez MdlL, Ferracini R, Bertolini G, Roato I, Vitale M and Orecchia P (2023) Murine models to study human NK cells in human solid tumors. *Front. Immunol.* 14:1209237. doi: 10.3389/fimmu.2023.1209237

Murine models to study human NK cells in human solid tumors

Monica Parodi[1†], Simonetta Astigiano[2†], Paolo Carrega[3], Gabriella Pietra[1,4], Chiara Vitale[1,4], Laura Damele[1], Melania Grottoli[4], Maria de la Luz Guevara Lopez[4], Riccardo Ferracini[5,6], Giulia Bertolini[7], Ilaria Roato[5], Massimo Vitale[1*‡] and Paola Orecchia[1*‡]

[1]Unità Operativa UO Patologia e Immunologia Sperimentale, IRCCS Ospedale Policlinico San Martino, Genova, Italy, [2]Animal Facility, IRCCS Ospedale Policlinico San Martino Genova, Genova, Italy, [3]Laboratory of Immunology and Biotherapy, Department of Human Pathology, University of Messina, Messina, Italy, [4]Dipartimento di Medicina Sperimentale, Università di Genova, Genova, Italy, [5]Department of Surgical Sciences, Bone and Dental Bioengineering Laboratory, C.I.R Dental School, University of Turin, Turin, Italy, [6]Department of Surgical Sciences (DISC), University of Genoa, Genoa, Italy, [7]"Epigenomics and Biomarkers of Solid Tumors", Fondazione IRCCS Istituto Nazionale dei Tumori, Milan, Italy

Since the first studies, the mouse models have provided crucial support for the most important discoveries on NK cells, on their development, function, and circulation within normal and tumor tissues. Murine tumor models were initially set to study murine NK cells, then, ever more sophisticated human-in-mice models have been developed to investigate the behavior of human NK cells and minimize the interferences from the murine environment. This review presents an overview of the models that have been used along time to study NK cells, focusing on the most popular NOG and NSG models, which work as recipients for the preparation of human-in-mice tumor models, the study of transferred human NK cells, and the evaluation of various enhancers of human NK cell function, including cytokines and chimeric molecules. Finally, an overview of the next generation humanized mice is also provided along with a discussion on how traditional and innovative *in-vivo* and *in-vitro* approaches could be integrated to optimize effective pre-clinical studies.

KEYWORDS

natural killer cells, humanized mice, solid tumor, human-in-mouse model, tumor immunity

Introduction

Natural Killer (NK) cells are Innate Lymphoid Cells (ILCs) playing a crucial role in the anti-tumor and antiviral immunity (1–4). They carry out their function both by influencing and supporting the activity of different immune cell types (including myeloid cells and T lymphocytes), and by directly killing the target cells (5–8). Through the release of chemoattractant factors (CCL3, CCL4, CCL5, HMGB1) and cytokines (IFN-γ, TNFα,

and GM-CSF), they can favor recruitment of immune cells, including NK cells (9, 10), and promote Th1-type inflammatory responses, while through the expression of cell death receptors and, especially, the release of cytotoxic granules they exert a potent lytic activity against tumor and virally infected cells. The activation of the different NK cell functions is orchestrated by the cytokine milieu and, more specifically, it depends on the type of cellular interactions involving NK cells. The cell-to-cell contact with normal cells, certain immune cells, or altered cells can give rise to inhibitory, regulatory, or lytic immune synapses respectively (11), with different patterns of engaged NK receptors, including: inhibitory, activating, or cytokine receptors. In different species, the discrimination between normal cells and altered tumor or virally infected cells is carried out through the action of MHC-I-specific inhibitory receptors, and activating receptors recognizing stress-induced molecules or ectopically expressed antigens. In humans, major inhibitory receptors are represented by certain Killer Ig-like Receptors (KIRs) and the CD94:NKG2A heterodimer, while the most known tumor-recognizing receptors include the Natural Cytotoxicity Receptors (NCRs) (NKp46, NKp30, and NKp44), NKG2D, and DNAM-1 (12, 13). Remarkably, the coordinated engagement of some inhibitory and activating receptors, together with cytokine receptors are involved in complex regulatory cross-talks with immune cells.

This picture of NK cell function and mechanics is the result of the many studies that have been carried out *in vitro* over the 90s and across the millennium to dissect single molecular pathways and cellular interactions. These results were then impressively expanded with the advent of new global and in-depth cell analytical approaches, such as the "omics" and "single cell RNA-seq". Application of these techniques led to the identification and fine molecular characterization of new functional NK cell subsets, as naïve or adaptive NK cells, or tumor-associated NK cells (14–16). Despite such important technical advances have significantly extended the power of human *in vitro* and *ex-vivo* studies, the still open issues on NK cell differentiation, circulation, homing, tissue residency, and tumor penetration cannot disregard the option of the animal studies.

Along the timeline of the NK cell studies, the utilization of murine models proved crucial for the initial evaluation of the real anti-tumor effects of NK cells and gave the first molecular hints on the role of MHC-I recognition (17–20). Additional studies provided supportive information on how NK cells differentiate, acquire and regulate their cytolytic potential (through the "licensing/arming" process), and, even more strikingly, persist *in vivo* as memory-like cells (21–24). These new insights are providing important hints for the selection and preparation of optimized NK cell effectors for anti-tumor immuno-therapies, with promising results in the field of hematological malignancies. On the other hand, the successful exploitation of NK cells in the cure of solid tumors is still limited by the active role of the local tumor microenvironment (TME), which hinders infiltration and effector capabilities of NK cells (25, 26). Several *in vitro* studies have contributed to the fine dissection of the different molecular mechanisms underlying the suppressive/escape properties of the TME. Nevertheless, the murine models are providing the crucial answers on how each of these mechanisms, and its targeting, could impact on the real anti-tumor efficacy of NK cells within the complexity of the TME. Given the importance of this issue, many efforts are being spent to generate ever more effective models to study solid tumors, moving from the full murine to the human-in-mice or humanized models, trying to overcome the not-always obvious problems related to the inter-species differences.

Mouse models for the study of mouse cancer

Murine models are well-characterized systems useful to gain insights into human biology and various pathological conditions, including cancer. Indeed, through the development of specific strains with stable and well-known genetic background, the murine system offers defined and reproducible experimental conditions without losing the complexity of living organisms.

The initial studies to identify and molecularly characterize the anti-tumor functions of NK cells *in vivo* were performed on mice injected with murine malignant cells. By the use of a C57BL strain and its "beige" variant, characterized by reduced NK cell activity related to the beige-J spontaneous mutation *Lystbg-J*, it was demonstrated the active role of NK cells in contrasting tumor growth (18, 19). Then, experiments based on the injection of H-2 mismatched or H-2 negative tumor cells in mice bearing given H-2 haplotypes provided important information on the role of the MHC-I-specific NK receptors (27, 28). Finally, the development of induced or spontaneous tumorigenesis mouse models combined with the generation of specific gene silencing (KO mice) were crucial to demonstrate the key role of certain activating NK receptors *in vivo*. Thus, for instance, in the model of transgenic adenocarcinoma of the mouse prostate (TRAMP) the targeting of the *klrk1* gene (TRAMP-NKG2D-KO mice) resulted in higher tumor incidence and the development of larger tumors (29). Similarly, the inactivation of the *cd226* gene (DNAM-1-KO mice) favoured the growth of the (3-MethylColanthrene (MCA)-induced fibrosarcoma in BALB/c mice (30). Finally, the inactivation of the *Ncr1* gene affected the ability of C57BL/6 mice to control melanoma and lung carcinoma metastases, or lymphoma induced by tumor cell line injection (31, 32).

The "mouse in mouse" studies provided important hints for the characterization of the role of human NK cells in the context of the solid tumors, as many murine NK cell receptors presented human homologues, and homologies between human and mice also emerged studying the development of NK cells, the regulation of their functional properties, and the acquisition of memory-like features. However, although these models have been exceedingly important in advancing our knowledge, there are limits and functional differences that have to be accounted for, especially, considering the translation of the obtained data to the design of new immunotherapy strategies (33). In this context, it has become ever more important the development of models enabling the study of human environments in the mouse.

Mouse models for the study of human cancer

The growth of human tissues and cells in a different species (xenotransplant) requires evasion from the immune system to prevent rejection. Xenotransplants became possible after the discovery, in 1962, of the nu/nu spontaneous mutation (34). Nu/nu Nude mice lacked the thymus, showed T-cell deficiency and impaired B-cell functionality, but retained macrophages and NK cells. Another spontaneous mutation affecting the immune system was discovered in 1983 in C.B-17 mice. Such autosomal recessive mutation, named *Prkdcscid*, affects the gene encoding for the protein kinase, DNA activated, catalytic polypeptide (PRKDC) and gives rise to severe combined immunodeficiency (SCID) in the mice. SCID mice (i.e. homozygous *Prkd*^{scid} mutants) lacked both T and B cells and had reduced NK cells (35), however their phenotype was "leaky" and clones of functioning B and T cells could randomly develop in young animals (36). Altered immunity was also observed in nonobese diabetic (NOD) mice (37, 38). These mice were obtained by a combination of inbreeding and selective breeding from a progeny of an outbred Jcl:ICR mouse, and were initially selected as a tool to study autoimmune diabetes, given their genetic predisposition to the development of the disease. However, NOD mice were also characterized by defects in the innate immunity, including the NK cell compartment, and were then considered for the preparation of new immunocompromised models. In particular, by crossing C.B-17 *Prkdc*^{scid} males with NOD/ShiLtSz females, it was generated the NOD-SCID mouse strain. Transfer of the SCID mutation onto a non-obese diabetic (NOD) background eliminated the leaky phenotype of the SCID model and generated the NOD-SCID mouse strain that rapidly became the best choice for transplant studies using freshly isolated human tumour cells, selected cancer stem cells, or tumour fragments (39, 40). NOD-SCID mice lack T and B lymphocytes and display reduced NK cell function, resulting in increased xenotransplant engraftment. However, they have a limited lifespan (7-8 months), due to the frequent spontaneous development of thymic lymphomas (41). Despite their limits, nu/nu, SCID and NOD-SCID mice have represented the most used strains for xenotransplant of human tumour cell lines in the last 50 years. A great improvement in the rate of human cell engraftment was then obtained with the backcrossing of NOD-SCID mice with either truncated or deleted interleukin-2 receptor common gamma chain giving origin to the NOG (42) or NSG (43, 44) strains, respectively. Specifically, in the early 2000s the NOD.Cg-Prkdc^{scid}Il2rg^{tm1Sug} (NOG) strain was developed at the Central Institute for Experimental Animals, Japan, by backcrossing NOD/ShiJic-Prkdc^{scid} mice with IL2rg^{tm1Sug}/ShiJic mice, carrying a truncation of the intracellular signalling domain of the IL2 receptor gamma chain. The NOD-SCID gamma NOD.Cg-Prkdc^{scid}Il2rg^{tm1Wjl}/Szj (NSG) strain, instead, a brand from the Jackson Laboratories (USA), was developed by backcrossing NOD-SCID mice with B6.129S4-IL2rg$^{tmWjl/J}$ (IL2Rγ^{null}) carrying the knock-out of the IL2 receptor gamma chain. NSG and NOG mice lack mature T and B cells, NK cells, and complement, have defective macrophages and dendritic cells (DCs) and gave a great impulse to the development of humanized mice models. In particular, these mice represent elective recipients for the functional studies on circulating tumor cells.

Cancer tissue represents a quite complex biological system, with its peculiar microenvironment and heterogeneity of the malignant and non-malignant components (45, 46). Therefore, the strategies to generate human tumor tissues in immunocompromised mice were generally conceived with the aim of reproducing at best such original complexity. A valid approach in this field has been the setting up of Patient Derived Tumour Xenografts (PDX), i.e. the engraftment of small pieces of freshly collected tumour samples in immunocompromised mice. PDXs warrant the conservation of the original tumor components (47–49) and, for that reason, are widely used for maintenance and therapy response experiments. In one study on lung cancer PDX, it has also been shown that lymphocytes present in the transplanted tumor (tumor infiltrating lymphocytes - TIL) could partly reconstitute the immune system in the mouse. Remarkably, in these mice, the combined treatment with IL-15 and PD-1 inhibition could induce tumor regression, which was dependent on human (tumor-derived) NK and T cells (50). Therefore, the model could provide important information on the interaction of the immune system with the tumor in the autologous setting. The use of this model, however, appear to be limited by the possible variability of the TIL component in different engrafted tumor fragments. Moreover, it should be considered that murine stroma can replace human one after two passages in the mice, and a cross-talk between the human tumor component and murine tumor-associated cells can easily take place in these models.

Another approach comes from the observation that certain human tumor cell populations, especially those containing a cancer stem cell component, can generate malignant lesions, partly recapitulating the original tumor complexity, once injected into immunocompromised mice. Following this observation, several human-in-mice tumor models have been reproduced and studied through the injection of selected tumor cells in NOD-SCID or NSG mice. An interesting example is represented by the attempt to reproduce a bone metastasis of human breast cancer or NSCLC in a human bone fragment that has been subcutaneously implanted in SCID mice (51, 52). In the case of NSCLC, it has been possible to identify a subset of human NSCLC cells endowed with metastasis-initiating-cell properties. Those cells, which were marked by the CD133^{+}CXCR4^{+}EpCAM^{-} phenotype, were shown to colonize the bone implant and to generate tumor lesions.

The immunocompromised mice are optimal recipients for the generation and development of human tumours, but their altered, non-human, immune system represents an issue. Indeed, cancer is a dynamic disease, showing plasticity in its cellular and extracellular components, and its dynamics is often influenced by the interaction with the host and, signally, by the selective pressure of the immune system (46). Therefore, the lack of the human immune system in

these murine models represents a limit, both for the attainment/maintenance of reliable tumor units, and for the studies focused on the development of immunotherapy strategies.

For this reason, there has been a flourishing interest in the "*humanized mice models*": immunocompromised mice transplanted with hematopoietic precursors and/or lymphoid tissues capable of reproducing in the mice several types of human immune cells.

Humanized mice

Engraftment of human lymphoid cells in SCID mice was first reported in 1988 by Mosier and co-workers, who injected intraperitoneally human peripheral blood mononuclear cells (PBMC) from EBV-positive donors and obtained "*stable long-term reconstitution of a functional human immune system*" (53). However, only human T and B cells could be satisfactorily maintained in these mice, while engraftment of other hematopoietic lineages was not effective. An additional problem was represented by the development in the animals of xenogeneic graft-versus-host-disease (GvHD), which usually took place 4-6 weeks after transfer of huPBMC, thus shortening the available observation time (54, 55). Nevertheless, given its relatively easy preparation, this model has been used over time, and, recently, the generation of NSG mice carrying a deletion of the MHC-I or II genes has been proposed to overcome the problem of xenogeneic GvHD (56).

Encouraging results were also obtained by transferring $CD34^+$ human hematopoietic stem cells (HSC) from cord blood into newborn BALB/c $Rag2^{-/-}\gamma c^{-/-}$ mice by intrahepatic injection. However, the reconstitution level remained low (57). The use of NOD-SCID mice carrying the deletion of the *Rag-1* or *Rag-2* gene did not change significantly the outcome (58). In these models, T cell function was limited, probably due the absence of human lymphoid organs supporting T cell maturation, selection, and activation. To overcome this problem, in a new study, $CD34^+$ HSC were transferred into NOD-SCID mice that were previously transplanted with human foetal liver and thymic tissue in the renal capsule (hu-bone marrow-liver-thymus - BLT) (59, 60). hu-BLT mouse model exhibits a full reconstitution of human immune cell repertoire, with T cells capable of mounting HLA-II- and HLA-I-restricted specific responses. These models were initially prepared to assess the immune response to viral infections (namely HIV), and were then adapted for studies of onco-immunology (61). Their employment for the study of NK cells in the tumor, however, appeared to be limited by the fact that BLT-mice developed relative low numbers of, poorly functional, NK cells.

The advent of the next generation murine models is now providing specific tools to study restricted human immune cell types in selected human tumors. These models are generated by using "knock in" and "knock out" strategies in immunocompromised mouse background, and can reach considerable complexity (62). Table 1 summarizes the main models that can be used for the study of human NK cells *in vivo*.

An important issue that is generally considered in the setting of humanized mice regards murine cytokines, which may be poorly expressed in immunocompromised mice and, due to the evolutionary divergence, quite different from their human counterparts. Therefore, several models have been developed expressing human cytokines, generally in NOG or NSG background, with the aim to improve development or persistence of given human immune cells, including NK cells (Table 1).

Katano et al. established transgenic NOG mice sub-strains expressing either human IL-2 (NOG-hIL-2 Tg) or human IL-15 (NOG-hIL-15 Tg) (63, 64). In NOG-hIL-2 Tg mice, human cord blood-derived HSCs could mature and give rise to differentiated KIR^+ NK cells expressing IL-2–activated phenotype; while in NOG-hIL-15 Tg mice, the high levels of IL-15 in the blood could support survival of NK cells from transferred human PBMC. hIL-15 has also been expressed in NSG, and the strain NSG-IL-15 Tg is now commercially available (65). Recently, to improve the development of human NK cells, Matsuda et al. created hIL-7 and hIL-15 double knock-in (hIL-7xhIL-15 KI) NSG mice (66). Compared to NSG mice, these mice showed increased ability to develop human NK cells after engraftment of human hematopoietic stem cells. A hIL-15 and human signal regulatory protein alpha (hSIRPα) double knock-in mouse on a $Rag2^{-/-}$ $il2rg^{-/-}$ background (SRG-15) was described to support efficient development of innate lymphoid cell subsets and NK cells, including tissue resident cells (69, 72). Even more complex knock in mice have been generated that express different combinations of human factors such as IL-3, IL-15, GM-CSF, M-CSF, SIRPα, and thrombopoietin: NSG-SGM3, MISTRG and BRGSF (see Table 1). On the whole, these latter strains support the development of human myeloid cells, which in turn can produce IL-15 and improve development of functional human NK cells (67, 68, 70, 71). Finally, a potentially interesting humanized model is also represented by the Nonirradiated NOD.B6.SCID $Il2rg^{-/-}$ $kit^{w41/w41}$ (NBSGW) mouse, which was obtained by the crossing of NSG strain with the C57BL/6.-Kit^{W-41J}/J strain (73). This model has the interesting advantage of supporting the human HSC engraftment without the need for pre-transplant conditioning (i.e. γ-irradiation), which could negatively affect the host microenvironment for the HSC development (74). An ovarian cancer PDX has been now developed in NBSGW mice, engrafted with human cord blood-derived HSC, to study the tumor immune environment within the peritoneal cavity (75). To date, such NBSGW model has not been used yet to study human NK cells.

Some of the above-mentioned next generation humanized mice have been assayed in different xenogeneic solid tumor models to study various immune cell types, especially T cells and myeloid cells, and only rarely NK cells (Table 2). Indeed, as yet, the large majority of the studies on NK cells have been done on "traditional" NOG or NSG mice. Nevertheless, the strategy of transferring human NK cells in such immunocompromised mice proved effective to evaluate which NK cell preparation, or way of cell activation, would be more suitable to overcome the tumor escape mechanisms and to deliver efficient NK cells into the tumor niches.

10.3389/fimmu.2023.1209237

TABLE 1 Summary of "first" and "next" generation immunodeficient mouse strains to study human NK cells in human solid tumors.

Mouse strain	Full name	Features of mouse strain	References when first described
NOD-SCID	NOD.C.B-17-*Prkdc*^{scid}	- Impaired T and B cell lymphocyte development - deficient NK cell function	(39)
Hu-BLT	NOD SCID Rag2$^{-/-}\gamma c^{-/-}$	- Co-transplantation of human fetal thymus and fetal liver into the renal capsule of mice - Injection of HSC in mice - T, B, Myeloid development	(59, 60)
NOG	NOD.Cg-Prkdc^{scid}Il2rg^{tm1Sug}	- Truncated intracytoplasmic domain of IL2 receptor gamma chain - Defective mouse NK cell development	(42)
NSG	NOD.Cg-Prkdc^{scid}Il2rg^{tm1Wjl}/Szj	- IL2 receptor gamma chain deficiency - lack mature T cells, B cells and functional NK cells - deficient in cytokine signaling	(43, 44)
NOG-IL2	NOD SCID Il2rg^{null} hIL2 tg	- Similar to NOG - Transgenic expression of human IL2 - human NK cell proliferation	(63)
NOG-IL15	NOD SCID Il2rg^{null} hIL15 tg	- Similar to NOG - Transgenic expression of human IL15 - human NK cell proliferation - human NK cells produce granzyme A and perforin upon stimulation	(64)
NSG-IL15	NOD SCID Il2rg$^{-/-}$ hIL15 tg	- Transgenic expression of human IL15 - human NK cell proliferation and maturation - human NK cells produce granzyme A and perforin	(65)
NSG-IL7-IL15	NOD SCID Il2rg$^{-/-}$ hIL7 KI hIL15 KI	- Transgenic expression of human IL15 and IL7 - Efficient development of human NK cells - Human NK cells undergo maturation process and exhibit cytotoxicity	(66)
NSG-SGM3	NOD SCID Il2rg$^{-/-}$ hIL3/hGMCSF tg hSCF tg	- Transgenic expression of human IL3, GM-CSF and SCF - Development of human myeloid cells (compared to NSG) - Increased levels of human NK cells	(67, 68)
SRG-15	Balb/c x 129 Rag2$^{-/-}$ Il2rg$^{-/-}$ hSIRPA KI hIL15 KI	- Expression of human SIRPa enables mouse phagocytes to tolerate human cells - Development of human ILC1 and NK cell subsets	(69)
MISTRG	Balb/c x 129 Rag2$^{-/-}$ Il2rg$^{-/-}$ hMCSF KI hIL3/hGMCSF KI hSIRPA KI hTHPO KI	- Development of functional human myeloid cells and NK cells	(70)
BRGSF	Balb/c Rag2$^{-/-}$ Il2rg$^{-/-}$ SIRPA^{NOD} Flk2 $^{-/-}$	- Development of functional human myeloid cells and NK cells	(71)

NOD, nonobese diabetic; Scid, severe combined immunodeficient; Il2rg, interleukin 2 receptor gammal; prkdc, protein kinase DNA-activated catalytic polypeptide; BLT, Bone Marrow-Liver-Thymus; hIL2 tg, humaninterleukin 2 transgenic; hIL15 tg, human interleukin 15 transgenic; hIL7 KI, human interleukin 7 knock-in; HSC, haematopoietic stem cells; hIL3/hGMCSF, human interleukin 3/human Granulocyte-macrophage colony-stimulating factor knock-in; hMCSF KI, macrophage colony-stimulating factor knock-in.

Human NK cell transfer in human-in-mice tumor models

As mentioned above, the human-in-mice tumor models, combined with human NK cell transfer, represent a suitable mean to assess the real effects of NK cells at the tumor site. Through these studies, it is possible to gain knowledge on spatial localization of NK cells within the tumor, and understand their impact on stroma, tumor cells and other immune cell populations. Likewise, it is possible to characterize phenotype and function of tumor-infiltrating NK cells, and, also, to gain information on their persistence. Therefore, on the whole, these models offer a platform to test possible approaches to optimize survival, function, and safety of adoptively transferred human NK cells. As described below, the animal model receiving human NK cells is generally represented by the NSG mice.

Study of NK cells exposed to cytokines

One of the major limitations to the efficacy of adoptive NK cell therapy is represented by the poor tumor-infiltrating capacity of transferred NK cells (90). The generation of sufficient NK cell numbers for adoptive immunotherapy represents an additional issue. Several strategies, often involving the use of priming cytokines, are employed to expand ex vivo NK cells exhibiting

10.3389/fimmu.2023.1209237

TABLE 2 Next-generation humanized mice used in preclinical studies for solid tumors.

Humanized mouse model	Solid tumor engrafment	Studied human immune cells	References
NOG-IL2	Melanoma Uveal and cutaneous melanoma Cutaneous melanoma	TIL CAR T TIL	(76) (77) (78)
NOG-IL15*	-	-	–
NSG-IL-15	Human sarcoma Melanoma Non-small-cell-lung-cancer	NK cells T cells, NK cells T cells, NK cells	(79) (65) (80)
NSG-IL7-IL15*	-	-	–
NSG-SGM3	Head and neck cancer (HNC) Clear-cell renal cell carcinoma Metastatic breast cancer Metastatic melanoma Melanoma Atypical teratoid/rhabdoid tumors and central nervous system primitive neuroectodermal tumors Glioblastoma Ovarian cancer Ovarian cancer	T cells CAR T cells Myeloid cells Myeloid cells Dendritic cells CTL T cells Macrophage T cells	(81) (82) (83) (84) (85) (86) (87) (88) (89)
SRG-15*	–	–	–
MISTRG*	–	–	–
BRGSF*	–	–	–

*Humanized mouse models not yet employed in preclinical studies.

distinct phenotypes, which can be correlated with their anti-tumor potency *in vitro* and *in vivo* (91). Cytokines are then used *in vivo* to sustain persistency and activation of transferred NK cells.

IL-2 has been the most commonly used cytokine to expand NK cells ex vivo and to boost proliferation of adoptively transferred NK cells *in vivo* (92–95). These IL-2-based therapies, however, generally demonstrated poor efficacy at the bed side, even showing negative side effects. The limits of IL-2 were essentially related to its ability to induce Tregs (with consequent suppressive effects on NK cells) (96–98) and to promote Activation Induced Cell Death (AICD) on NK cells. This latter aspect could be particularly relevant in the context of the solid tumors, as IL-2-primed NK cells undergo AICD following interaction with endothelial cells, with a possible negative impact on extravasation and tumor infiltration (99). Finally, it cannot be disregarded that IL-2 can contribute to the vascular leak syndrome, an important adverse effect that limits its use in therapy (100). In the attempt to improve suitability of IL-2 for immunotherapy, engineered IL-2 molecules (termed superkines) have been developed. Compared to IL-2, IL-2superkines induced superior expansion of cytotoxic T cells, more prolonged and more intense NK cell activation, and improved anti-tumour responses in different syngeneic mouse models (101–103). These studies, however have not yet been conducted using human-in-mice models.

Combining IL-2 with other cytokines to pre-activate NK cells before transfer could improve NK cell efficiency, limiting the IL-2-related negative effects. A candidate for such approach may be IL-21, which has been shown to induce expansion of non-terminally differentiated $CD56^{bright}$ NK cells (104) and functional NK cell maturation (105, 106). The efficacy of human NK cells that were expanded ex vivo using feeder cells + IL-2 + IL-21 was analysed in NSG mice injected with a human melanoma cell line. Adoptive transfer of such pre-activated NK cells resulted in increased *in vivo* persistence, as compared to NK cells pre-treated with IL-2 alone, and in significant inhibition of melanoma-induced lung metastases (107).

IL-15 has been proposed as valid alternative to IL-2 to stimulate NK cells for therapeutic protocols. IL-15 and IL-2 are structurally similar, share two of the three subunits of their receptors (namely, IL-2Rβ/CD122 and γ_c/CD132), and are both capable of activating NK cells. However, the presence of distinctive receptor alpha subunits (IL-15Rα/CD125, and IL-2Rα/CD25) accounts for their different behaviour *in vitro* and *in vivo*. Thus, for example, IL-15 supports NK cell survival, proliferation and effector functions, but, different from IL-2, it has no stimulatory effect on the CD25+ Tregs (108). In addition, IL-15 can be associated to the IL-15Rα and trans presented to NK and T cells by different immune and non-immune IL-15Rα+ cells (109, 110). In different pre-clinical models of solid tumors, IL-15, alone or in combination with additional cytokines (i.e. IL-2, IL-12, and IL-18), has been assayed to stimulate human NK cells before transfer, and/or to support human NK cell persistency after transfer. For example, in a study aimed at evaluating the anti-tumor properties of human NK cells generated *ex vivo* from HSPC, recombinant IL-15 was infused together with NK cells in NSG mice bearing ovarian carcinoma, and this infusion was then followed by a further boost of IL-15 (111). The study, showed efficacy of HSPC-derived NK cells in reducing tumor burden, and was then followed by a clinical trial (NCT: 03539406), which is still ongoing. In this study, patients with recurrent ovarian cancer, pre-treated or not with chemotherapy, are infused intra-peritoneally with allogeneic NK cells generated from UCB CD34+ HSPC. Once completed, this trial will give crucial

information on feasibility, safety and toxicity of this innovative therapeutic approach. In a xenografted mouse model of colon rectal cancer (CRC), human NK cells were first expanded *in vitro* in the presence of IL-15 and IL-2, then were transferred into the mice combining infusion of NK cells and IL-2. Further boosts of IL-2 were given to the mice to maintain NK cells *in vivo*. NK cell transfer induced a delay in tumor growth at an early stage (112).

To improve biological activity and to extend *in vivo* half-life of IL-15 (≈40 min), a super-agonistic molecular complex has been developed that combines mutated activating IL-15, the trans-presenting IL-15Rα sushi domain and IgG1-Fc (113). Such super-agonist, termed N-803 (also known as ALT-803) has been tested in an ovarian carcinoma model, where it was demonstrated to promote HPC-NK cell expansion and functionality (114, 115). First reported clinical trials (NCT: 01885897) (NCT: 01727076) of ALT-803 in cancer patients revealed that it is well tolerated and stimulates NK cell activation and expansion and CD8+ T cells, but not Tregs (116, 117).

IL-15 is also the main component of the IL-12/15/18 cytokine cocktail known to induce the so-called cytokine-induced memory-like (CIML) NK cells. These cells, which can be easily induced *in vitro* from PB NK cells, display enhanced anti-tumor effector functions that can be preserved *in vitro* and even increased *in vivo* (118–120). CIML-NK cells have been initially considered for the cure of hematologic malignancies, and clinically assessed for the immunotherapy of acute myeloid leukemia (AML) (NCT: 01898793) (118, 120). Interestingly, in this clinical study CIML NK cells were shown to persist in the patients, and further differentiate. With regard to solid tumors, CIML NK cells have not yet been assessed in clinics, however they revealed potent anti-tumor activity after transfer in xenogenic melanoma and ovarian cancer NSG mouse models (121, 122). As CIML NK cells have been shown to express CD25, mice bearing the melanoma xenograft were given serial boosts of IL-2 to support persistency and activation of transferred NK cells.

An additional interesting anti-tumor effector lymphocyte population is represented by Cytokine Induced Killer (CIK) T cells. These effectors, which can be expanded *in vitro* by exposure to IFN-γ and IL-2, are characterized by the expression of the CD56 NK cell marker and the activating NKG2D receptor. Remarkably, NKG2D supports their TCR-independent anti-tumor activity, which has been demonstrated both *in vitro* and in xenogeneic tumor models developed into NOD-SCID mice (123–125). Given the promising results obtained *in vitro* and *in vivo*, the use of CIK could contribute to innovative clinical approaches for both hematologic and solid malignancies (126, 127).

Study of CAR-NK and NK cell engagers

Innovative tools to enhance and address anti-tumor NK cell function are represented by engineered chimeric activating receptors (CARs), whose expression is induced on NK cells by transduction protocols to generate CAR-NK, or by multivalent soluble molecules, which are developed as NK cell engagers. In both the cases, the effectiveness of the effector molecules or cells has been evaluated in xenogeneic tumor models.

CARs are generally constituted by a single-chain Fragment variable (scFv), recognizing a specific tumor-expressed antigen, combined with an intracytoplasmic tail of activating transducing molecules (such as the CD3ζ chain). Once expressed on transduced T or NK cells, CARs drive recognition of tumor cells and the subsequent triggering of the effector functions. CARs have been initially set to enhance and address T cell anti-tumor activity and several studies have already been done on these engineered effectors. Therapy with CAR-T, however, appears to be still hampered by several issues, including T cell exhaustion, the appearance of suppressive/regulatory responses, the induction of the cytokine release syndrome (CRS), and even GVHD (128). Given their features, NK cells could be advantageously employed to generate CAR-effectors with minimized side effects.

CAR-NK have been developed especially for hematological malignancies (129, 130), while for solid tumors the studies are still limited. An interesting CAR-NK effector targeting solid tumors has been prepared by transducing *ex-vivo* expanded human NK cells to express the DAP-12-anti-HLA-G CAR. HLA-G molecules are ligands for the inhibitory immune receptors, LILRB1 and LILRB2 (also known as ILT2 and ILT4) (131), and are frequently expressed by solid tumors, therefore, anti-HLA-G CAR-NK can both target tumor cells and relieve immunosuppression. These anti-HLA-G CAR-NK showed tumor cytotoxicity in orthotopic xenograft models of triple negative breast cancer and glioblastoma, developed in NSG mice (132).

Several bivalent or trivalent NK cell engagers have been synthesized and defined with different acronyms depending on the used technical platform and the originating lab. Bi- or tri-specific killer engagers (BiKE or TriKE) consist of a single-chain Fragment variable (scFv) targeting tumor specific antigens, a scFv targeting activating receptors on NK cells (generally CD16), and (in the case of TriKEs) an additional domain generally targeting cytokine receptors to support activation and survival of NK cells (133, 134). The therapeutic efficacy of BiKEs/TRiKEs with different tumor antigen specificities has been demonstrated in various xenograft tumor models, using NSG recipients and evaluating transferred human NK cells (135–138). In a study, the authors analysed the effectiveness of both the engager (which was the bi-specific anti-CD30/CD16 antibody) and of different NK cell effectors, by transferring into the mice either CIML-NK or cord blood-derived NK cells (139).

Recently, a trifunctional NK cell engager (NKCE) triggering simultaneously NKp46 and CD16 on NK cells and targeting a tumor antigen has been developed (140). An upgrade of this engager is then represented by the tetraspecific antibody-based natural killer cell engager therapeutics (ANKETs), which adds the ability to engage IL-R2b to the previous multiple specificity (141). For the preclinical studies, engagers with surrogate anti murine NKp46 were generated and evaluated for their capability to trigger murine NK cells in SCID mice injected with the RAJI or other human lymphoma cells. In some cases, the RAGko huNKp46Tg mice were used to better track NK cells in the tissues, as in these mice NK cells expressed both the human and the murine NKp46, and could be stained by anti-human NKp46 abs without the interference of the anti-murine ANKET.

Several engagers proved promising in the preclinical models, so that phase I/II clinical trials in advanced solid tumors are ongoing (133).

Other ways to enhance NK cell activity to solid tumors

As mentioned above, the use of irradiated feeder cells combined with cytokines represents a possible strategy to obtain large-scale expansion and activation of NK cells. A recently proposed approach involves, as feeder cells, the NK-92 cell line engineered to express OX40L and to secrete neoleukin-2/15, an artificial peptide that binds with high affinity the human IL-2Rβγ complex. These engineered NK-92 cells were irradiated and used to expand ex vivo-derived human NK cells, which were then transferred in three different xenogeneic tumor mouse models: lung, liver, or ovarian cancers, all developed into NOD-SCID mice. In these experiments, NK-92-induced NK cells showed stronger capability to infiltrate the tumors and a higher antitumor effect compared to NK cells expanded with IL-2 (142).

Chemical approach to increase the antitumor activity of NK cells was reported by Choi et al. who showed how 25kDa branched polyethyleneimine (25KbPEI) could enhance cytotoxicity and migration properties of human NK cells. 25KbPEI-induced NK cells were transferred into xenogeneic breast and ovarian cancer models, which were developed in SCID/nude and NSG mice respectively. In both models 25KbPEI-induced NK cells were demonstrated more effective than IL-2-induced NK cells in infiltrating the tumor and limiting its growth (143).

Study of the strategies to sensitize tumor cells to NK cell activity

More recently, human tumor xenografts in NSG mice have also been used to evaluate strategies directly targeting the tumor to increase its susceptibility to NK cells. Most strategies are focused on the study of genotoxic or non-genotoxic agents acting on the DNA-Damage-Response (DDR) or related pathways, which lead to increased expression of activating NK Receptor ligands (144). These agents are first evaluated *in vitro* and then validated *in vivo*. Thus, for example, in a xenogeneic neuroblastoma model, mice were given nutlin3a, a non-toxic p53-activating molecule that was demonstrated to increase expression of NKG2D- and DNAM-1-ligands on tumor cells. These mice, compared to those receiving vehicle alone, showed increased NK cell infiltration in their tumor xenografts and reduced tumor growth following human NK cell transfer (95). Analogously, in a xenogeneic ovarian carcinoma model, it has been demonstrated that the chemotherapeutic drug gemcitabine increased the expression of NKG2D ligands and death receptors on tumor cells, and the adoptive transfer of NK cells in combination with gemcitabine additively decreased ovarian cancer growth (145). Finally, in a recent study, combined high-dose radiotherapy and adoptive human NK cell transfer resulted in improved tumor control over monotherapies in NSG mice engrafted with melanoma and pancreatic tumor cells. Such improvement, however, appeared to be related to the radiotherapy-induced CXCL8 release by tumor cells and subsequent recall of CD56dim cytotoxic NK cells (146).

Final considerations and future development

The increasingly sophisticated analytic tools for the *in-vivo* and *ex-vivo* characterization of tumors are improving clinical decision making, and also, provide means for conducting research directly in the patients. These new approaches add support to the preclinical research but do not replace its fundamental phases, which comprise the studies *in vitro* to dissect molecular and cellular processes, and the validation studies *in vivo*.

The "traditional" 2D *in vitro* cultures address important questions on specific biological, genetic and epigenetic features and on the direct cellular effects of drugs or cytokines, while animal models are amply used to evaluate the actual significance

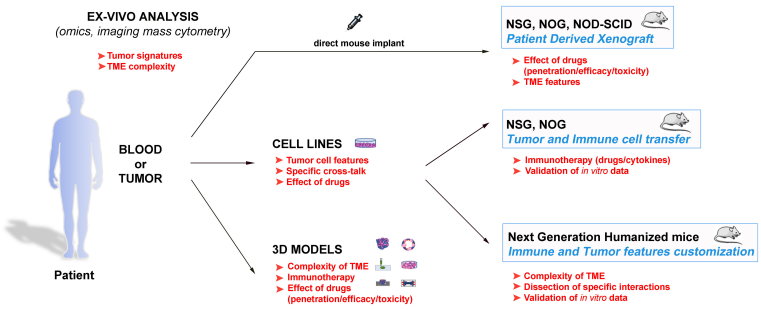

FIGURE 1
Schematic representation of the different available approaches to get insights in the tumour biology, and to design innovative and personalized therapies. These strategies span from the direct evaluation of the patients' samples with advanced analytic techniques to the tumour complexity reproduction and the data validation in both *in vitro* and *in vivo* models. The main goals of the various approaches are indicated in red, and suggest how they can be inter-connected to obtain optimal results.

of the dissected processes and to test therapeutic efficacy of drugs and dose-limiting toxicity of clinical treatments. On the other hand, the animal studies are generally expensive, time-consuming, and, for years, they have been based on a limited range of models (147, 148). Furthermore, there are ethical issues, which, for the animal welfare, limit the use of animals to what is strictly necessary. The principle of the 3Rs (Replacement, Reduction, and Refinement) is presently applied in all projects involving the use of animals. In particular, the Replacement is supported by the development and use of predictive and robust models and tools, based on the latest *in vitro* technologies, to address important scientific questions (149).

In this context, the setting of the 3D cultures has been proposed as an important tool for the development of innovative *in vitro* assays and models of neoplastic cell growth with potentially high clinical relevance. By the setting of 3D models, it is tempting to partly reproduce the complexity of the TME, in terms of extra-cellular matrix, cell types, vasculature, and oxygen, nutrients and catabolites distribution. If fully realized, these 3D tumor models would be a powerful mean to study a number of tumor-related processes, to validate specific findings, and to test the efficacy/toxicity of drug treatments, replacing the employment of animals (150, 151). This goal, however, is presently far to be achieved, as it is not easy to set a reliable balance among all the different fundamental components within a single *in vitro*-generated structure.

Therefore, the employment of animals remains indispensable for the preclinical studies, especially considering the recent development of the next generation humanized mouse models (65, 76–79, 81–89) (Table 2). Indeed, these models can reproduce ever more accurately the complexity of the immune response within the TME, and also offer the interesting perspective of dissecting *in vivo* crucial frames of such complexity. In this context, these models also represent suitable tools to study the behaviour of human NK cells. In conclusion, a powerful strategy to efficiently struggle against cancer should consider the wise integration of the different available tools to gain precise data on the single malignancies, to dissect molecular and cellular pathways, and to evaluate new related therapeutic strategies (Figure 1). In this scenario, in which different strategies are connected, the animal models maintain a pivotal role.

Author contributions

MP, SA, MV, and PO contributed to conception and the outline of the review article. All authors contributed to the article and approved the submitted version.

Funding

Fondazione AIRC, grant number IG 2020 id. 25023 (MV); Italian Ministry of Health (project RF-2018-12366714 (MV, GB); 5permille 2022-24 IRCCS Ospedale Policinico San Martino (to GP); Ricerca Corrente 2022-24 IRCCS Ospedale Policlinico San Martino (to GP and SA); Fondazione CRT 2020 (to IR).

Conflict of interest

The authors declare that the research was conducted in the absence of any commercial or financial relationships that could be construed as a potential conflict of interest.

The reviewer VL declared a shared affiliation with the authors RF and IR to the handling editor at the time of review.

Publisher's note

References

1. Vivier E, Artis D, Colonna M, Diefenbach A, Di Santo JP, Eberl G, et al. Innate lymphoid cells: 10 years on. *Cell* (2018) 174(5):1054–66. doi: 10.1016/j.cell.2018.07.017

2. Cantoni C, Grauwet K, Pietra G, Parodi M, Mingari MC, De Maria A, et al. Role of NK cells in immunotherapy and virotherapy of solid tumors. *Immunotherapy* (2015) 7(8):861–82. doi: 10.2217/imt.15.53

3. Sivori S, Meazza R, Quintarelli C, Carlomagno S, Della Chiesa M, Falco M, et al. NK cell-based immunotherapy for hematological malignancies. *J Clin Med* (2019) 8 (10). doi: 10.3390/jcm8101702

4. Bjorkstrom NK, Strunz B, Ljunggren HG. Natural killer cells in antiviral immunity. *Nat Rev Immunol* (2022) 22(2):112–23. doi: 10.1038/s41577-021-00558-3

5. Crinier A, Narni-Mancinelli E, Ugolini S, Vivier E. SnapShot: natural killer cells. *Cell* (2020) 180(6):1280– e1. doi: 10.1016/j.cell.2020.02.029

6. Moretta A, Marcenaro E, Sivori S, Della Chiesa M, Vitale M, Moretta L. Early liaisons between cells of the innate immune system in inflamed peripheral tissues. *Trends Immunol* (2005) 26(12):668–75. doi: 10.1016/j.it.2005.09.008

7. Bellora F, Castriconi R, Dondero A, Reggiardo G, Moretta L, Mantovani A, et al. The interaction of human natural killer cells with either unpolarized or polarized macrophages results in different functional outcomes. *Proc Natl Acad Sci U S A.* (2010) 107(50):21659–64. doi: 10.1073/pnas.1007654108

8. Scordamaglia F, Balsamo M, Scordamaglia A, Moretta A, Mingari MC, Canonica GW, et al. Perturbations of natural killer cell regulatory functions in respiratory allergic diseases. *J Allergy Clin Immunol* (2008) 121(2):479–85. doi: 10.1016/j.jaci.2007.09.047

9. Fauriat C, Long EO, Ljunggren HG, Bryceson YT. Regulation of human NK-cell cytokine and chemokine production by target cell recognition. *Blood* (2010) 115 (11):2167–76. doi: 10.1182/blood-2009-08-238469

10. Parodi M, Pedrazzi M, Cantoni C, Averna M, Patrone M, Cavaletto M, et al. Natural killer (NK)/melanoma cell interaction induces NK-mediated release of chemotactic high mobility group box-1 (HMGB1) capable of amplifying NK cell recruitment. *Oncoimmunology* (2015) 4(12):e1052353. doi: 10.1080/2162402X.2015.1052353

11. Mace EM, Orange JS. Multiple distinct NK-cell synapses. *Blood* (2011) 118 (25):6475–6. doi: 10.1182/blood-2011-10-381392

12. Vitale M, Cantoni C, Della Chiesa M, Ferlazzo G, Carlomagno S, Pende D, et al. An historical overview: the discovery of how NK cells can kill enemies, recruit defense troops, and more. *Front Immunol* (2019) 10:1415. doi: 10.3389/fimmu.2019.01415

13. Pende D, Falco M, Vitale M, Cantoni C, Vitale C, Munari E, et al. Killer ig-like receptors (KIRs): their role in NK cell modulation and developments leading to their clinical exploitation. *Front Immunol* (2019) 10:1179. doi: 10.3389/fimmu.2019.01179

14. Schlums H, Cichocki F, Tesi B, Theorell J, Beziat V, Holmes TD, et al. Cytomegalovirus infection drives adaptive epigenetic diversification of NK cells with altered signaling and effector function. *Immunity* (2015) 42(3):443–56. doi: 10.1016/j.immuni.2015.02.008

15. Freud AG, Mundy-Bosse BL, Yu J, Caligiuri MA. The broad spectrum of human natural killer cell diversity. *Immunity* (2017) 47(5):820–33. doi: 10.1016/j.immuni.2017.10.008

16. Brownlie D, Scharenberg M, Mold JE, Hard J, Kekalainen E, Buggert M, et al. Expansions of adaptive-like NK cells with a tissue-resident phenotype in human lung and blood. *Proc Natl Acad Sci U.S.A.* (2021) 118(11). doi: 10.1073/pnas.2016580118

17. Kiessling R, Klein E, Pross H, Wigzell H. "Natural" killer cells in the mouse. II. cytotoxic cells with specificity for mouse moloney leukemia cells. characteristics of the killer cell. *Eur J Immunol* (1975) 5(2):117–21. doi: 10.1002/eji.1830050209

18. Karre K, Klein GO, Kiessling R, Klein G, Roder JC. *In vitro* NK-activity and *in vivo* resistance to leukemia: studies of beige, beige//nude and wild-type hosts on C57BL background. *Int J Cancer.* (1980) 26(6):789–97. doi: 10.1002/ijc.2910260613

19. Aboud M, Kingsmore S, Segal S. Role of natural killer cells in controlling local tumor formation and metastatic manifestation of different 3LL Lewis lung carcinoma cell clones. *Nat Immun* (1993) 12(1):17–24.

20. Bennett M. Biology and genetics of hybrid resistance. *Adv Immunol* (1987) 41:333–445. doi: 10.1016/S0065-2776(08)60034-6

21. Sun JC, Beilke JN, Lanier LL. Adaptive immune features of natural killer cells. *Nature* (2009) 457(7229):557–61. doi: 10.1038/nature07665

22. Sun JC. Re-educating natural killer cells. *J Exp Med* (2010) 207(10):2049–52. doi: 10.1084/jem.20101748

23. Kim S, Poursine-Laurent J, Truscott SM, Lybarger L, Song YJ, Yang L, et al. Licensing of natural killer cells by host major histocompatibility complex class I molecules. *Nature* (2005) 436(7051):709–13. doi: 10.1038/nature03847

24. Sojka DK, Tian Z, Yokoyama WM. Tissue-resident natural killer cells and their potential diversity. *Semin Immunol* (2014) 26(2):127–31. doi: 10.1016/j.smim.2014.01.010

25. Vitale M, Cantoni C, Pietra G, Mingari MC, Moretta L. Effect of tumor cells and tumor microenvironment on NK-cell function. *Eur J Immunol* (2014) 44(6):1582–92. doi: 10.1002/eji.201344272

26. Stojanovic A, Cerwenka A. Natural killer cells and solid tumors. *J Innate Immun* (2011) 3(4):355–64. doi: 10.1159/000325465

27. Hoglund P, Ljunggren HG, Ohlen C, Ahrlund-Richter L, Scangos G, Bieberich C, et al. Natural resistance against lymphoma grafts conveyed by h-2Dd transgene to C57BL mice. *J Exp Med* (1988) 168(4):1469–74. doi: 10.1084/jem.168.4.1469

28. Glas R, Sturmhofel K, Hammerling GJ, Karre K, Ljunggren HG. Restoration of a tumorigenic phenotype by beta 2-microglobulin transfection to EL-4 mutant cells. *J Exp Med* (1992) 175(3):843–6. doi: 10.1084/jem.175.3.843

29. Guerra N, Tan YX, Joncker NT, Choy A, Gallardo F, Xiong N, et al. NKG2D-deficient mice are defective in tumor surveillance in models of spontaneous malignancy. *Immunity* (2008) 28(4):571–80. doi: 10.1016/j.immuni.2008.02.016

30. Iguchi-Manaka A, Kai H, Yamashita Y, Shibata K, Tahara-Hanaoka S, Honda S, et al. Accelerated tumor growth in mice deficient in DNAM-1 receptor. *J Exp Med* (2008) 205(13):2959–64. doi: 10.1084/jem.20081611

31. Halfteck GG, Elboim M, Gur C, Achdout H, Ghadially H, Mandelboim O. Enhanced *in vivo* growth of lymphoma tumors in the absence of the NK-activating receptor NKp46/NCR1. *J Immunol* (2009) 182(4):2221–30. doi: 10.4049/jimmunol.0801878

32. Glasner A, Ghadially H, Gur C, Stanietsky N, Tsukerman P, Enk J, et al. Recognition and prevention of tumor metastasis by the NK receptor NKp46/NCR1. *J Immunol* (2012) 188(6):2509–15. doi: 10.4049/jimmunol.1102461

33. Rangarajan A, Weinberg RA. Opinion: comparative biology of mouse versus human cells: modelling human cancer in mice. *Nat Rev Cancer.* (2003) 3(12):952–9. doi: 10.1038/nrc1235

34. Flanagan SP. 'Nude', a new hairless gene with pleiotropic effects in the mouse. *Genet Res* (1966) 8(3):295–309. doi: 10.1017/s0016672300010168

35. Bosma GC, Custer RP, Bosma MJ. A severe combined immunodeficiency mutation in the mouse. *Nature* (1983) 301(5900):527–30. doi: 10.1038/301527a0

36. Bosma MJ, Carroll AM. The SCID mouse mutant: definition, characterization, and potential uses. *Annu Rev Immunol* (1991) 9:323–50. doi: 10.1146/annurev.iy.09.040191.001543

37. Leiter EH. The NOD mouse: a model for analyzing the interplay between heredity and environment in development of autoimmune disease. *ILAR J* (1993) 35(1):4–14. doi: 10.1093/ilar.35.1.4

38. Makino S, Kunimoto K, Muraoka Y, Mizushima Y, Katagiri K, Tochino Y. Breeding of a non-obese, diabetic strain of mice. *Jikken Dobutsu.* (1980) 29(1):1–13. doi: 10.1093/ilar.35.1.4

39. Shultz LD, Schweitzer PA, Christianson SW, Gott B, Schweitzer IB, Tennent B, et al. Multiple defects in innate and adaptive immunologic function in NOD/LtSz-scid mice. *J Immunol* (1995) 154(1):180–91. doi: 10.4049/jimmunol.154.1.180

40. Hesselton RM, Greiner DL, Mordes JP, Rajan TV, Sullivan JL, Shultz LD. High levels of human peripheral blood mononuclear cell engraftment and enhanced susceptibility to human immunodeficiency virus type 1 infection in NOD/LtSz-scid/scid mice. *J Infect Dis* (1995) 172(4):974–82. doi: 10.1093/infdis/172.4.974

41. Hudson WA, Li Q, Le C, Kersey JH. Xenotransplantation of human lymphoid malignancies is optimized in mice with multiple immunologic defects. *Leukemia* (1998) 12(12):2029–33. doi: 10.1038/sj.leu.2401236

42. Ito M, Hiramatsu H, Kobayashi K, Suzue K, Kawahata M, Hioki K, et al. NOD/SCID/gamma(c)(null) mouse: an excellent recipient mouse model for engraftment of human cells. *Blood* (2002) 100(9):3175–82. doi: 10.1182/blood-2001-12-0207

43. Ishikawa F, Yasukawa M, Lyons B, Yoshida S, Miyamoto T, Yoshimoto G, et al. Development of functional human blood and immune systems in NOD/SCID/IL2 receptor gamma chain(null) mice. *Blood* (2005) 106(5):1565–73. doi: 10.1182/blood-2005-02-0516

44. Shultz LD, Lyons BL, Burzenski LM, Gott B, Chen X, Chaleff S, et al. Human lymphoid and myeloid cell development in NOD/LtSz-scid IL2R gamma null mice engrafted with mobilized human hemopoietic stem cells. *J Immunol* (2005) 174(10):6477–89. doi: 10.4049/jimmunol.174.10.6477

45. Fidler IJ, Kripke ML. Metastasis results from preexisting variant cells within a malignant tumor. *Science* (1977) 197(4306):893–5. doi: 10.1126/science.887927

46. Saha S, Pradhan N BN, Mahadevappa R, Minocha S, Kumar S. Cancer plasticity: investigating the causes for this agility. *Semin Cancer Biol* (2023) 88:138–56. doi: 10.1016/j.semcancer.2022.12.005

47. Siolas D, Hannon GJ. Patient-derived tumor xenografts: transforming clinical samples into mouse models. *Cancer Res* (2013) 73(17):5315–9. doi: 10.1158/0008-5472.CAN-13-1069

48. Rygaard J, Povlsen CO. Heterotransplantation of a human malignant tumour to "Nude" mice. *Acta Pathol Microbiol Scand* (1969) 77(4):758–60. doi: 10.1111/j.1699-0463.1969.tb04520.x

49. Gao H, Korn JM, Ferretti S, Monahan JE, Wang Y, Singh M, et al. High-throughput screening using patient-derived tumor xenografts to predict clinical trial drug response. *Nat Med* (2015) 21(11):1318–25. doi: 10.1038/nm.3954

50. Le DT, Huynh TR, Burt B, Van Buren G, Abeynaike SA, Zalfa C, et al. Natural killer cells and cytotoxic T lymphocytes are required to clear solid tumor in a patient-derived xenograft. *JCI Insight* (2021) 6(13). doi: 10.1172/jci.insight.140116

51. Kuperwasser C, Dessain S, Bierbaum BE, Garnet D, Sperandio K, Gauvin GP, et al. A mouse model of human breast cancer metastasis to human bone. *Cancer Res* (2005) 65(14):6130–8. doi: 10.1158/0008-5472.CAN-04-1408

52. Bertolini G, D'Amico L, Moro M, Landoni E, Perego P, Miceli R, et al. Microenvironment-modulated metastatic CD133+/CXCR4+/EpCAM- lung cancer-initiating cells sustain tumor dissemination and correlate with poor prognosis. *Cancer Res* (2015) 75(17):3636–49. doi: 10.1158/0008-5472.CAN-14-3781

53. Mosier DE, Gulizia RJ, Baird SM, Wilson DB. Transfer of a functional human immune system to mice with severe combined immunodeficiency. *Nature* (1988) 335(6187):256–9. doi: 10.1038/335256a0

54. King MA, Covassin L, Brehm MA, Racki W, Pearson T, Leif J, et al. Human peripheral blood leucocyte non-obese diabetic-severe combined immunodeficiency interleukin-2 receptor gamma chain gene mouse model of xenogeneic graft-versus-host-like disease and the role of host major histocompatibility complex. *Clin Exp Immunol* (2009) 157(1):104–18. doi: 10.1111/j.1365-2249.2009.03933.x

55. Yue X, Petersen F, Shu Y, Kasper B, Magatsin JDT, Ahmadi M, et al. Transfer of PBMC from SSc patients induces autoantibodies and systemic inflammation in Rag2-/-/IL2rg-/- mice. *Front Immunol* (2021) 12:677970. doi: 10.3389/fimmu.2021.677970

56. Brehm MA, Kenney LL, Wiles MV, Low BE, Tisch RM, Burzenski L, et al. Lack of acute xenogeneic graft- versus-host disease, but retention of T-cell function following engraftment of human peripheral blood mononuclear cells in NSG mice deficient in MHC class I and II expression. *FASEB J* (2019) 33(3):3137–51. doi: 10.1096/fj.201800636R

57. Traggiai E, Chicha L, Mazzucchelli L, Bronz L, Piffaretti JC, Lanzavecchia A, et al. Development of a human adaptive immune system in cord blood cell-transplanted mice. *Science* (2004) 304(5667):104–7. doi: 10.1126/science.1093933

58. Goldman JP, Blundell MP, Lopes L, Kinnon C, Di Santo JP, Thrasher AJ. Enhanced human cell engraftment in mice deficient in RAG2 and the common cytokine receptor gamma chain. *Br J Haematol* (1998) 103(2):335–42. doi: 10.1046/j.1365-2141.1998.00980.x

59. Melkus MW, Estes JD, Padgett-Thomas A, Gatlin J, Denton PW, Othieno FA, et al. Humanized mice mount specific adaptive and innate immune responses to EBV and TSST-1. *Nat Med* (2006) 12(11):1316–22. doi: 10.1038/nm1431

60. Brainard DM, Seung E, Frahm N, Cariappa A, Bailey CC, Hart WK, et al. Induction of robust cellular and humoral virus-specific adaptive immune responses in human immunodeficiency virus-infected humanized BLT mice. *J Virol* (2009) 83(14):7305–21. doi: 10.1128/JVI.02207-08

61. Vatakis DN, Bristol GC, Kim SG, Levin B, Liu W, Radu CG, et al. Using the BLT humanized mouse as a stem cell based gene therapy tumor model. *J Vis Exp* (2012) 70):e4181. doi: 10.3791/4181

62. Chuprin J, Buettner H, Seedhom MO, Greiner DL, Keck JG, Ishikawa F, et al. Humanized mouse models for immuno-oncology research. *Nat Rev Clin Oncol* (2023) 20(3):192–206. doi: 10.1038/s41571-022-00721-2

63. Katano I, Takahashi T, Ito R, Kamisako T, Mizusawa T, Ka Y, et al. Predominant development of mature and functional human NK cells in a novel human IL-2-producing transgenic NOG mouse. *J Immunol* (2015) 194(7):3513–25. doi: 10.4049/jimmunol.1401323

64. Katano I, Nishime C, Ito R, Kamisako T, Mizusawa T, Ka Y, et al. Long-term maintenance of peripheral blood derived human NK cells in a novel human IL-15-transgenic NOG mouse. *Sci Rep* (2017) 7(1):17230. doi: 10.1038/s41598-017-17442-7

65. Aryee KE, Burzenski LM, Yao LC, Keck JG, Greiner DL, Shultz LD, et al. Enhanced development of functional human NK cells in NOD-scid-IL2rg(null) mice expressing human IL15. *FASEB J* (2022) 36(9):e22476. doi: 10.1096/fj.202200045R

66. Matsuda M, Ono R, Iyoda T, Endo T, Iwasaki M, Tomizawa-Murasawa M, et al. Human NK cell development in hIL-7 and hIL-15 knockin NOD/SCID/IL2rgKO mice. *Life Sci Alliance* (2019) 2(2). doi: 10.26508/lsa.201800195

67. Sippel TR, Radtke S, Olsen TM, Kiem HP, Rongvaux A. Human hematopoietic stem cell maintenance and myeloid cell development in next-generation humanized mouse models. *Blood Adv* (2019) 3(3):268–74. doi: 10.1182/bloodadvances.2018023887

68. Wunderlich M, Chou FS, Sexton C, Presicce P, Chougnet CA, Aliberti J, et al. Improved multilineage human hematopoietic reconstitution and function in NSGS mice. *PloS One* (2018) 13(12):e0209034. doi: 10.1371/journal.pone.0209034

69. Herndler-Brandstetter D, Shan L, Yao Y, Stecher C, Plajer V, Lietzenmayer M, et al. Humanized mouse model supports development, function, and tissue residency of human natural killer cells. *Proc Natl Acad Sci U S A.* (2017) 114(45):E9626–E34. doi: 10.1073/pnas.1705301114

70. Rongvaux A, Willinger T, Martinek J, Strowig T, Gearty SV, Teichmann LL, et al. Development and function of human innate immune cells in a humanized mouse model. *Nat Biotechnol* (2014) 32(4):364–72. doi: 10.1038/nbt.2858

71. Lopez-Lastra S, Masse-Ranson G, Fiquet O, Darche S, Serafini N, Li Y, et al. A functional DC cross talk promotes human ILC homeostasis in humanized mice. *Blood Adv* (2017) 1(10):601–14. doi: 10.1182/bloodadvances.2017004358

72. Shan L, Flavell RA, Herndler-Brandstetter D. Development of humanized mouse models for studying human NK cells in health and disease. *Methods Mol Biol* (2022) 2463:53–66. doi: 10.1007/978-1-0716-2160-8_5

73. McIntosh BE, Brown ME, Duffin BM, Maufort JP, Vereide DT, Slukvin II, et al. Nonirradiated NOD,B6.SCID Il2rgamma-/- Kit(W41/W41) (NBSGW) mice support multilineage engraftment of human hematopoietic cells. *Stem Cell Rep* (2015) 4(2):171–80. doi: 10.1016/j.stemcr.2014.12.005

74. Hess NJ, Lindner PN, Vazquez J, Grindel S, Hudson AW, Stanic AK, et al. Different human immune lineage compositions are generated in non-conditioned NBSGW mice depending on HSPC source. *Front Immunol* (2020) 11:573406. doi: 10.3389/fimmu.2020.573406

75. Steinkamp MP, Lagutina I, Brayer KJ, Schultz F, Burke D, Pankratz VS, et al. Humanized patient-derived xenograft models of disseminated ovarian cancer recapitulate key aspects of the tumor immune environment within the peritoneal cavity. *Cancer Res Commun* (2023) 3(2):309–24. doi: 10.1158/2767-9764.CRC-22-0300

76. Ny L, Rizzo LY, Belgrano V, Karlsson J, Jespersen H, Carstam L, et al. Supporting clinical decision making in advanced melanoma by preclinical testing in personalized immune-humanized xenograft mouse models. *Ann Oncol* (2020) 31(2):266–73. doi: 10.1016/j.annonc.2019.11.002

77. Forsberg EMV, Lindberg MF, Jespersen H, Alsen S, Bagge RO, Donia M, et al. HER2 CAR-T cells eradicate uveal melanoma and T-cell therapy-resistant human melanoma in IL2 transgenic NOD/SCID IL2 receptor knockout mice. *Cancer Res* (2019) 79(5):899–904. doi: 10.1158/0008-5472.CAN-18-3158

78. Jespersen H, Lindberg MF, Donia M, Soderberg EMV, Andersen R, Keller U, et al. Clinical responses to adoptive T-cell transfer can be modeled in an autologous immune-humanized mouse model. *Nat Commun* (2017) 8(1):707. doi: 10.1038/s41467-017-00786-z

79. Rademacher MJ, Cruz A, Faber M, Oldham RAA, Wang D, Medin JA, et al. Sarcoma IL-12 overexpression facilitates NK cell immunomodulation. *Sci Rep* (2021) 11(1):8321. doi: 10.1038/s41598-021-87700-2

80. Flieswasser T, Van den Eynde A, Freire Boullosa L, Melis J, Hermans C, Merlin C, et al. Targeting CD70 in combination with chemotherapy to enhance the anti-tumor immune effects in non-small cell lung cancer. *Oncoimmunology* (2023) 12(1):2192100. doi: 10.1080/2162402X.2023.2192100

81. Zenga J, Awan MJ, Frei A, Petrie E, Sharma GP, Shreenivas A, et al. Chronic stress promotes an immunologic inflammatory state and head and neck cancer growth in a humanized murine model. *Head Neck.* (2022) 44(6):1324–34. doi: 10.1002/hed.27028

82. Wang Y, Buck A, Grimaud M, Culhane AC, Kodangattil S, Razimbaud C, et al. Anti-CAIX BBzeta CAR4/8 T cells exhibit superior efficacy in a ccRCC mouse model. *Mol Ther Oncolytics.* (2022) 24:385–99. doi: 10.1016/j.omto.2021.12.019

83. Scherer SD, Riggio AI, Haroun F, DeRose YS, Ekiz HA, Fujita M, et al. An immune-humanized patient-derived xenograft model of estrogen-independent, hormone receptor positive metastatic breast cancer. *Breast Cancer Res* (2021) 23(1):100. doi: 10.1186/s13058-021-01476-x

84. Yu CI, Martinek J, Wu TC, Kim KI, George J, Ahmadzadeh E, et al. Human KIT + myeloid cells facilitate visceral metastasis by melanoma. *J Exp Med* (2021) 218(6). doi: 10.1084/jem.20182163

85. Lee YS, O'Brien LJ, Walpole CM, Pearson FE, Leal-Rojas IM, Masterman KA, et al. Human CD141(+) dendritic cells (cDC1) are impaired in patients with advanced melanoma but can be targeted to enhance anti-PD-1 in a humanized mouse model. *J Immunother Cancer* (2021) 9(3). doi: 10.1136/jitc-2020-001963

86. Garcia-Moure M, Gonzalez-Huarriz M, Labiano S, Guruceaga E, Bandres E, Zalacain M, et al. Delta-24-RGD, an oncolytic adenovirus, increases survival and promotes proinflammatory immune landscape remodeling in models of AT/RT and CNS-PNET. *Clin Cancer Res* (2021) 27(6):1807–20. doi: 10.1158/1078-0432.CCR-20-3313

87. Zhai L, Ladomersky E, Lauing KL, Wu M, Genet M, Gritsina G, et al. Infiltrating T cells increase IDO1 expression in glioblastoma and contribute to decreased patient survival. *Clin Cancer Res* (2017) 23(21):6650–60. doi: 10.1158/1078-0432.CCR-17-0120

88. Klichinsky M, Ruella M, Shestova O, Lu XM, Best A, Zeeman M, et al. Human chimeric antigen receptor macrophages for cancer immunotherapy. *Nat Biotechnol* (2020) 38(8):947–53. doi: 10.1038/s41587-020-0462-y

89. Odunsi A, McGray AJR, Miliotto A, Zhang Y, Wang J, Abiola A, et al. Fidelity of human ovarian cancer patient-derived xenografts in a partially humanized mouse model for preclinical testing of immunotherapies. *J Immunother Cancer* (2020) 8(2). doi: 10.1136/jitc-2020-001237

90. Chiossone L, Dumas PY, Vienne M, Vivier E. Natural killer cells and other innate lymphoid cells in cancer. *Nat Rev Immunol* (2018) 18(11):671–88. doi: 10.1038/s41577-018-0061-z

91. Nayyar G, Chu Y, Cairo MS. Overcoming resistance to natural killer cell based immunotherapies for solid tumors. *Front Oncol* (2019) 9:51. doi: 10.3389/fonc.2019.00051

92. Miller JS, Soignier Y, Panoskaltsis-Mortari A, McNearney SA, Yun GH, Fautsch SK, et al. Successful adoptive transfer and *in vivo* expansion of human haploidentical NK cells in patients with cancer. *Blood* (2005) 105(8):3051–7. doi: 10.1182/blood-2004-07-2974

93. Curti A, Ruggeri L, D'Addio A, Bontadini A, Dan E, Motta MR, et al. Successful transfer of alloreactive haploidentical KIR ligand-mismatched natural killer cells after infusion in elderly high risk acute myeloid leukemia patients. *Blood* (2011) 118(12):3273–9. doi: 10.1182/blood-2011-01-329508

94. Chen M, Li Y, Wu Y, Xie S, Ma J, Yue J, et al. Anti-tumor activity of expanded PBMC-derived NK cells by feeder-free protocol in ovarian cancer. *Cancers (Basel)* (2021) 13(22). doi: 10.3390/cancers13225866

95. Veneziani I, Infante P, Ferretti E, Melaiu O, Battistelli C, Lucarini V, et al. Nutlin-3a enhances natural killer cell-mediated killing of neuroblastoma by restoring p53-dependent expression of ligands for NKG2D and DNAM-1 receptors. *Cancer Immunol Res* (2021) 9(2):170–83. doi: 10.1158/2326-6066.CIR-20-0313

96. Mitra S, Leonard WJ. Biology of IL-2 and its therapeutic modulation: mechanisms and strategies. *J Leukoc Biol* (2018) 103(4):643–55. doi: 10.1002/JLB.2RI0717-278R

97. Ahmadzadeh M, Rosenberg SA. IL-2 administration increases CD4+ CD25(hi) Foxp3+ regulatory T cells in cancer patients. *Blood* (2006) 107(6):2409–14. doi: 10.1182/blood-2005-06-2399

98. Wei S, Kryczek I, Edwards RP, Zou L, Szeliga W, Banerjee M, et al. Interleukin-2 administration alters the CD4+FOXP3+ T-cell pool and tumor trafficking in patients with ovarian carcinoma. *Cancer Res* (2007) 67(15):7487–94. doi: 10.1158/0008-5472.CAN-07-0565

99. Rodella L, Zamai L, Rezzani R, Artico M, Peri G, Falconi M, et al. Interleukin 2 and interleukin 15 differentially predispose natural killer cells to apoptosis mediated by endothelial and tumour cells. *Br J Haematol* (2001) 115(2):442–50. doi: 10.1046/j.1365-2141.2001.03055.x

100. Mortara L, Balza E, Bruno A, Poggi A, Orecchia P, Carnemolla B. Anti-cancer therapies employing IL-2 cytokine tumor targeting: contribution of innate, adaptive and immunosuppressive cells in the anti-tumor efficacy. *Front Immunol* (2018) 9:2905. doi: 10.3389/fimmu.2018.02905

101. Levin AM, Bates DL, Ring AM, Krieg C, Lin JT, Su L, et al. Exploiting a natural conformational switch to engineer an interleukin-2 'superkine'. *Nature* (2012) 484(7395):529–33. doi: 10.1038/nature10975

102. Merchant R, Galligan C, Munegowda MA, Pearce LB, Lloyd P, Smith P, et al. Fine-tuned long-acting interleukin-2 superkine potentiates durable immune responses in mice and non-human primate. *J Immunother Cancer* (2022) 10(1). doi: 10.1136/jitc-2021-003155

103. Wolf NK, Blaj C, Picton LK, Snyder G, Zhang L, Nicolai CJ, et al. Synergy of a STING agonist and an IL-2 superkine in cancer immunotherapy against MHC I-deficient and MHC i(+) tumors. *Proc Natl Acad Sci U S A.* (2022) 119(22):e2200568119. doi: 10.1073/pnas.2200568119

104. Wendt K, Wilk E, Buyny S, Schmidt RE, Jacobs R. Interleukin-21 differentially affects human natural killer cell subsets. *Immunology* (2007) 122(4):486–95. doi: 10.1111/j.1365-2567.2007.02675.x

105. Kasaian MT, Whitters MJ, Carter LL, Lowe LD, Jussif JM, Deng B, et al. IL-21 limits NK cell responses and promotes antigen-specific T cell activation: a mediator of the transition from innate to adaptive immunity. *Immunity* (2002) 16(4):559–69. doi: 10.1016/S1074-7613(02)00295-9

106. Brady J, Hayakawa Y, Smyth MJ, Nutt SL. IL-21 induces the functional maturation of murine NK cells. *J Immunol* (2004) 172(4):2048–58. doi: 10.4049/jimmunol.172.4.2048

107. Granzin M, Stojanovic A, Miller M, Childs R, Huppert V, Cerwenka A. Highly efficient IL-21 and feeder cell-driven ex vivo expansion of human NK cells with

therapeutic activity in a xenograft mouse model of melanoma. *Oncoimmunology* (2016) 5(9):e1219007. doi: 10.1080/2162402X.2016.1219007

108. Zhou Y, Husman T, Cen X, Tsao T, Brown J, Bajpai A, et al. Interleukin 15 in cell-based cancer immunotherapy. *Int J Mol Sci* (2022) 23(13). doi: 10.3390/ijms23137311

109. Anton OM, Peterson ME, Hollander MJ, Dorward DW, Arora G, Traba J, et al. Trans-endocytosis of intact IL-15Ralpha-IL-15 complex from presenting cells into NK cells favors signaling for proliferation. *Proc Natl Acad Sci U S A.* (2020) 117(1):522–31. doi: 10.1073/pnas.1911678117

110. Ferlazzo G, Pack M, Thomas D, Paludan C, Schmid D, Strowig T, et al. Distinct roles of IL-12 and IL-15 in human natural killer cell activation by dendritic cells from secondary lymphoid organs. *Proc Natl Acad Sci U S A.* (2004) 101(47):16606–11. doi: 10.1073/pnas.0407522101

111. Hoogstad-van Evert JS, Cany J, van den Brand D, Oudenampsen M, Brock R, Torensma R, et al. Umbilical cord blood CD34(+) progenitor-derived NK cells efficiently kill ovarian cancer spheroids and intraperitoneal tumors in NOD/SCID/IL2Rg(null) mice. *Oncoimmunology* (2017) 6(8):e1320630. doi: 10.1080/2162402X.2017.1320630

112. Lanuza PM, Alonso MH, Hidalgo S, Uranga-Murillo I, Garcia-Mulero S, Arnau R, et al. Adoptive NK cell transfer as a treatment in colorectal cancer patients: analyses of tumour cell determinants correlating with efficacy *In vitro* and in vivo. *Front Immunol* (2022) 13:890836. doi: 10.3389/fimmu.2022.890836

113. Han KP, Zhu X, Liu B, Jeng E, Kong L, Yovandich JL, et al. IL-15:IL-15 receptor alpha superagonist complex: high-level co-expression in recombinant mammalian cells, purification and characterization. *Cytokine* (2011) 56(3):804–10. doi: 10.1016/j.cyto.2011.09.028

114. Van der Meer JMR, Maas RJA, Guldevall K, Klarenaar K, de Jonge P, Evert JSH, et al. IL-15 superagonist n-803 improves IFNgamma production and killing of leukemia and ovarian cancer cells by CD34(+) progenitor-derived NK cells. *Cancer Immunol Immunother.* (2021) 70(5):1305–21. doi: 10.1007/s00262-020-02749-8

115. Felices M, Chu S, Kodal B, Bendzick L, Ryan C, Lenvik AJ, et al. IL-15 super-agonist (ALT-803) enhances natural killer (NK) cell function against ovarian cancer. *Gynecol Oncol* (2017) 145(3):453–61. doi: 10.1016/j.ygyno.2017.02.028

116. Romee R, Cooley S, Berrien-Elliott MM, Westervelt P, Verneris MR, Wagner JE, et al. First-in-human phase 1 clinical study of the IL-15 superagonist complex ALT-803 to treat relapse after transplantation. *Blood* (2018) 131(23):2515–27. doi: 10.1182/blood-2017-12-823757

117. Margolin K, Morishima C, Velcheti V, Miller JS, Lee SM, Silk AW, et al. Phase I trial of ALT-803, a novel recombinant IL15 complex, in patients with advanced solid tumors. *Clin Cancer Res* (2018) 24(22):5552–61. doi: 10.1158/1078-0432.CCR-18-0945

118. Romee R, Rosario M, Berrien-Elliott MM, Wagner JA, Jewell BA, Schappe T, et al. Cytokine-induced memory-like natural killer cells exhibit enhanced responses against myeloid leukemia. *Sci Transl Med* (2016) 8(357):357ra123. doi: 10.1126/scitranslmed.aaf2341

119. Ni J, Holsken O, Miller M, Hammer Q, Luetke-Eversloh M, Romagnani C, et al. Adoptively transferred natural killer cells maintain long-term antitumor activity by epigenetic imprinting and CD4(+) T cell help. *Oncoimmunology* (2016) 5(9):e1219009. doi: 10.1080/2162402X.2016.1219009

120. Berrien-Elliott MM, Cashen AF, Cubitt CC, Neal CC, Wong P, Wagner JA, et al. Multidimensional analyses of donor memory-like NK cells reveal new associations with response after adoptive immunotherapy for leukemia. *Cancer Discovery* (2020) 10 (12):1854–71. doi: 10.1158/2159-8290.CD-20-0312

121. Uppendahl LD, Felices M, Bendzick L, Ryan C, Kodal B, Hinderlie P, et al. Cytokine-induced memory-like natural killer cells have enhanced function, proliferation, and *in vivo* expansion against ovarian cancer cells. *Gynecol Oncol* (2019) 153(1):149–57. doi: 10.1016/j.ygyno.2019.01.006

122. Marin ND, Krasnick BA, Becker-Hapak M, Conant L, Goedegebuure SP, Berrien-Elliott MM, et al. Memory-like differentiation enhances NK cell responses to melanoma. *Clin Cancer Res* (2021) 27(17):4859–69. doi: 10.1158/1078-0432.CCR-21-0851

123. Sangiolo D, Mesiano G, Gammaitoni L, Leuci V, Todorovic M, Giraudo L, et al. Cytokine-induced killer cells eradicate bone and soft-tissue sarcomas. *Cancer Res* (2014) 74(1):119–29. doi: 10.1158/0008-5472.CAN-13-1559

124. Gammaitoni L, Giraudo L, Leuci V, Todorovic M, Mesiano G, Picciotto F, et al. Effective activity of cytokine-induced killer cells against autologous metastatic melanoma including cells with stemness features. *Clin Cancer Res* (2013) 19 (16):4347–58. doi: 10.1158/1078-0432.CCR-13-0061

125. Wendel P, Reindl LM, Bexte T, Kunnemeyer L, Sarchen V, Albinger N, et al. Arming immune cells for battle: a brief journey through the advancements of T and NK cell immunotherapy. *Cancers (Basel)* (2021) 13(6). doi: 10.3390/cancers13061481

126. Vaseq R, Sharma A, Li Y, Schmidt-Wolf IGH. Revising the landscape of cytokine-induced killer cell therapy in lung cancer: focus on immune checkpoint inhibitors. *Int J Mol Sci* (2023) 24(6). doi: 10.3390/ijms24065626

127. Introna M, Correnti F. Innovative clinical perspectives for CIK cells in cancer patients. *Int J Mol Sci* (2018) 19(2). doi: 10.3390/ijms19020358

128. Mhaidly R, Verhoeyen E. Humanized mice are precious tools for preclinical evaluation of CAR T and CAR NK cell therapies. *Cancers (Basel).* (2020) 12(7). doi: 10.3390/cancers12071915

129. Caruso S, De Angelis B, Carlomagno S, Del Bufalo F, Sivori S, Locatelli F, et al. NK cells as adoptive cellular therapy for hematological malignancies: advantages and hurdles. *Semin Hematol* (2020) 57(4):175–84. doi: 10.1053/j.seminhematol.2020.10.004

130. Caruso S, De Angelis B, Del Bufalo F, Ciccone R, Donsante S, Volpe G, et al. Safe and effective off-the-shelf immunotherapy based on CAR.CD123-NK cells for the treatment of acute myeloid leukaemia. *J Hematol Oncol* (2022) 15(1):163. doi: 10.1186/s13045-022-01376-3

131. Carosella ED, Rouas-Freiss N, Tronik-Le Roux D, Moreau P, LeMaoult J. HLA-G: an immune checkpoint molecule. *Adv Immunol* (2015) 127:33–144. doi: 10.1016/bs.ai.2015.04.001

132. Jan CI, Huang SW, Canoll P, Bruce JN, Lin YC, Pan CM, et al. Targeting human leukocyte antigen G with chimeric antigen receptors of natural killer cells convert immunosuppression to ablate solid tumors. *J Immunother Cancer* (2021) 9(10). doi: 10.1136/jitc-2021-003050

133. Lian G, Mak TS, Yu X, Lan HY. Challenges and recent advances in NK cell-targeted immunotherapies in solid tumors. *Int J Mol Sci* (2021) 23(1). doi: 10.3390/ijms23010164

134. Myers JA, Miller JS. Exploring the NK cell platform for cancer immunotherapy. *Nat Rev Clin Oncol* (2021) 18(2):85–100. doi: 10.1038/s41571-020-0426-7

135. Vallera DA, Oh F, Kodal B, Hinderlie P, Geller MA, Miller JS, et al. A HER2 tri-specific NK cell engager mediates efficient targeting of human ovarian cancer. *Cancers (Basel)* (2021) 13(16). doi: 10.3390/cancers13163994

136. Vallera DA, Ferrone S, Kodal B, Hinderlie P, Bendzick L, Ettestad B, et al. NK-Cell-Mediated targeting of various solid tumors using a B7-H3 tri-specific killer engager in vitro and *In vivo*. *Cancers (Basel)* (2020) 12(9). doi: 10.3390/cancers12092659

137. Kaminski MF, Bendzick L, Hopps R, Kauffman M, Kodal B, Soignier Y, et al. TEM8 tri-specific killer engager binds both tumor and tumor stroma to specifically engage natural killer cell anti-tumor activity. *J Immunother Cancer* (2022) 10(9). doi: 10.1136/jitc-2022-004725

138. Kennedy PR, Vallera DA, Ettestad B, Hallstrom C, Kodal B, Todhunter DA, et al. A tri-specific killer engager against mesothelin targets NK cells towards lung cancer. *Front Immunol* (2023) 14:1060905. doi: 10.3389/fimmu.2023.1060905

139. Kerbauy LN, Marin ND, Kaplan M, Banerjee PP, Berrien-Elliott MM, Becker-Hapak M, et al. Combining AFM13, a bispecific CD30/CD16 antibody, with cytokine-activated blood and cord blood-derived NK cells facilitates CAR-like responses against CD30(+) malignancies. *Clin Cancer Res* (2021) 27(13):3744–56. doi: 10.1158/1078-0432.CCR-21-0164

140. Gauthier L, Morel A, Anceriz N, Rossi B, Blanchard-Alvarez A, Grondin G, et al. Multifunctional natural killer cell engagers targeting NKp46 trigger protective tumor immunity. *Cell* (2019) 177(7):1701–13 e16. doi: 10.1016/j.cell.2019.04.041

141. Demaria O, Gauthier L, Vetizou M, Blanchard Alvarez A, Vagne C, Habif G, et al. Antitumor immunity induced by antibody-based natural killer cell engager therapeutics armed with not-alpha IL-2 variant. *Cell Rep Med* (2022) 3(10):100783. doi: 10.1016/j.xcrm.2022.100783

142. Guo M, Sun C, Qian Y, Zhu L, Ta N, Wang G, et al. Proliferation of highly cytotoxic human natural killer cells by OX40L armed NK-92 with secretory neoleukin-2/15 for cancer immunotherapy. *Front Oncol* (2021) 11:632540. doi: 10.3389/fonc.2021.632540

143. Choi SH, Kim HJ, Park JD, Ko ES, Lee M, Lee DK, et al. Chemical priming of natural killer cells with branched polyethylenimine for cancer immunotherapy. *J Immunother Cancer* (2022) 10(8). doi: 10.1136/jitc-2022-004964

144. Zingoni A, Ardolino M, Santoni A, Cerboni C. NKG2D and DNAM-1 activating receptors and their ligands in NK-T cell interactions: role in the NK cell-mediated negative regulation of T cell responses. *Front Immunol* (2012) 3:408. doi: 10.3389/fimmu.2012.00408

145. Van der Meer JMR, de Jonge P, van der Waart AB, Geerlings AC, Moonen JP, Brummelman J, et al. CD34(+) progenitor-derived NK cell and gemcitabine combination therapy increases killing of ovarian cancer cells in NOD/SCID/IL2Rg(null) mice. *Oncoimmunology* (2021) 10(1):1981049. doi: 10.1080/2162402X.2021.1981049

146. Walle T, Kraske JA, Liao B, Lenoir B, Timke C, von Bohlen Und Halbach E, et al. Radiotherapy orchestrates natural killer cell dependent antitumor immune responses through CXCL8. *Sci Adv* (2022) 8(12):eabh4050. doi: 10.1126/sciadv.abh4050

147. Huh D, Matthews BD, Mammoto A, Montoya-Zavala M, Hsin HY, Ingber DE. Reconstituting organ-level lung functions on a chip. *Science* (2010) 328(5986):1662–8. doi: 10.1126/science.1188302

148. Lv D, Hu Z, Lu L, Lu H, Xu X. Three-dimensional cell culture: a powerful tool in tumor research and drug discovery. *Oncol Lett* (2017) 14(6):6999–7010. doi: 10.3892/ol.2017.7134

149. Diaz L, Zambrano E, Flores ME, Contreras M, Crispin JC, Aleman G, et al. Ethical considerations in animal research: the principle of 3R's. *Rev Invest Clin* (2020) 73(4):199–209. doi: 10.24875/RIC.20000380

150. Bussard KM, Mutkus L, Stumpf K, Gomez-Manzano C, Marini FC. Tumor-associated stromal cells as key contributors to the tumor microenvironment. *Breast Cancer Res* (2016) 18(1):84. doi: 10.1186/s13058-016-0740-2

151. Hirschhaeuser F, Menne H, Dittfeld C, West J, Mueller-Klieser W, Kunz-Schughart LA. Multicellular tumor spheroids: an underestimated tool is catching up again. *J Biotechnol* (2010) 148(1):3–15. doi: 10.1016/j.jbiotec.2010.01.012

frontiers | Frontiers in Immunology

TYPE Original Research
PUBLISHED 06 July 2023
DOI 10.3389/fimmu.2023.1216107

OPEN ACCESS

EDITED BY
Silvia Scaglione,
National Research Council (CNR), Italy

REVIEWED BY
Federica Papaccio,
University of Salerno, Italy
Dominic Augustine,
M. S. Ramaiah University of Applied Sciences, India

*CORRESPONDENCE
Emanuela Marcenaro
emanuela.marcenaro@unige.it
Silvia Pesce
silvia.pesce@unige.it

†These authors share first authorship

‡These authors share senior authorship

RECEIVED 03 May 2023
ACCEPTED 22 June 2023
PUBLISHED 06 July 2023

CITATION
Rebaudi F, De Rosa A, Greppi M, Pistilli R, Pucci R, Govoni FA, Iacoviello P, Broccolo F, Tomasello G, Pesce S, Laganà F, Bianchi B, Di Gaudio F, Rebaudi A and Marcenaro E (2023) A new method for oral cancer biomarkers detection with a non-invasive cyto-salivary sampling and rapid-highly sensitive ELISA immunoassay: a pilot study in humans. *Front. Immunol.* 14:1216107. doi: 10.3389/fimmu.2023.1216107

A new method for oral cancer biomarkers detection with a non-invasive cyto-salivary sampling and rapid-highly sensitive ELISA immunoassay: a pilot study in humans

Federico Rebaudi[1†], Alfredo De Rosa[2†], Marco Greppi[1†], Roberto Pistilli[3], Resi Pucci[3], Flavio Andrea Govoni[3], Paolo Iacoviello[4], Francesco Broccolo[5], Giuseppe Tomasello[6], Silvia Pesce[1*], Francesco Laganà[7], Bernardo Bianchi[7], Francesca Di Gaudio[8‡], Alberto Rebaudi[9‡] and Emanuela Marcenaro[1,10*‡]

[1]Department of Experimental Medicine (DIMES), University of Genova, Genova, Italy, [2]Multidisciplinary Department of Medical-Surgical and Dental Specialties, University of Campania "Luigi Vanvitelli", Napoli, Italy, [3]Oral and Maxillofacial Surgery, San Camillo-Forlanini Hospital, Roma, Italy, [4]Department of Maxillofacial and Plastic Reconstructive Surgery, E.O. Ospedali Galliera, Genova, Italy, [5]Department of Biological and Environmental Sciences and Technologies, University of Salento, Lecce, Italy, [6]Private Practice, Lugano, Switzerland, [7]IRCCS Ospedale San Martino, Unità Operativa Complessa di Chirurgia Maxillofacciale e Odontoiatra, Genova, Italy, [8]Department of Health Promotion, Mother and Child Care, Internal Medicine and Medical Specialties, University of Palermo, CQRC (Quality Control and Chemical Risk) Hospital Company, Hospitals Reunited Villa Sofia Cervello, Palermo, Italy, [9]Private Practice, President of Bio.C.R.A. (Biomaterials Clinical-Histological Research Association), Genova, Italy, [10]IRCCS Ospedale Policlinico San Martino, Genova, Italy

Introduction: Oral squamous cell carcinoma (OSCC) accounts for approximately 90% of oral malignancies and has a 5-year mortality rate close to 50%. A consistent part (70%) of all oral cancers is diagnosed at an advanced stage since available screening techniques are ineffective. Therefore, it would be urgent to improve them. The diagnostic gold standard is tissue biopsy with histological and immunohistochemical assessment. This method presents some limitations. Biopsy is invasive and the histopathological evaluation is semi-quantitative, and the absolute abundance of the target cannot be reliably determined. In addition, tissue is highly processed and may lead to loss of information of the natural state. The search for classical and new clinical biomarkers on fragments of tissue/cells collected with a cytobrush is a highly hopeful technique for early detection and diagnosis of OSCC, because of its non-invasive sampling and easy collection method.

Methods: Here we analyzed cytobrush biopsies samples collected from the oral cavity of 15 patients with already diagnosed OSCC by applying an innovative high-sensitivity ELISA technique, in order to verify if this approach may provide useful information for detection, diagnosis, and prognosis of OSCC. To this end, we selected six biomarkers, already used in clinical practice for the diagnosis of

OSCC (EGFR, Ki67, p53) or selected based on recent scientific and clinical data which indicate their presence or over-expression in cells undergoing transformation and their role as possible molecular targets in immunecheckpoints blockade therapies (PD-L1, HLA-E, B7-H6).

Results: The selected tumor biomarkers were highly expressed in the tumor core, while were virtually negative in healthy tissue collected from the same patients. These differences were highly statistically significant and consistent with those obtained using the gold standard test clearly indicating that the proposed approach, i.e. analysis of biomarkers by a custom ELISA technique, is strongly reliable.

Discussion: These preliminary data suggest that this non-invasive rapid phenotyping technique could be useful as a screening tool for phenotyping oral lesions and support clinical practice by precise indications on the characteristics of the lesion, also with a view to the application of new anti-tumor treatments, such as immunotherapy, aimed at OSCC patients.

KEYWORDS

oral cancer, screening, tumor biomarkers, natural killer cells, immunotherapy, ELISA immunoassay, cytobrush, immune checkpoints

1 Introduction

Oral cancer is the sixth most common malignancy worldwide (1). Globally, over 400,000 new cases of oral cancer are diagnosed each year. The incidence increases with age, even though cases in subjects younger than 40 years are growing. In more than 90% of cases, oral cancers are squamous cell carcinomas (OSCCs) with a tendency to lymphatic and metastatic spreading (2–5). Oral cancer has poor prognosis, with a 40% overall 5-year survival rate but when diagnosed in the early stage, survival rates can exceed 80% (6–8). The high mortality rate associated with this tumor is attributable to many factors, including generic and non-specific symptoms and absence of validated screening strategies that allow for early diagnosis, thusmost of the oral cancers (70%) are diagnosed late at an advanced stage (II-III-IV) (9–14).

Treatments for advanced stage oral cancer require mutilating interventions and the evolution of the disease leads to a very low quality of life. Oral cancer should be detected at a very early stage which will improve the effectiveness of therapies, to reduce mortality and morbidity (13, 15–18).

Up to now, there are no scientifically approved systems able to detect a lesion in the early phases of tumor transformation (19) other than the conventional clinical visual oral examination (VOE), with the aid of magnifying optics and fluorescent systems as well as the palpation of the oral cavity and neck to detect abnormalities. Currently, surgical biopsy is the most effective method to collect tissue useful for diagnosis (20) and it represents the gold standard as a diagnostic method. However, this approach is invasive and does not allow an early diagnosis because it is done on lesions that are visible at clinical examination. Moreover, the histopathological specimen examination is a method with some limitations because it is semi-quantitative, and the absolute abundance of the target cannot be reliably determined. Furthermore, the tissue is highly processed and may lead to loss of information of the natural state (21). Currently, one the main aims of clinical research is the identification of biomarkers to monitor and discover effective therapeutic strategies. In other fields of medicine, such as gynecology, the early diagnosis of cervical cancer through cytobrush biopsy, PAP test and HPV test, has proven to be very effective in reducing mortality, morbidity, and costs for the community (22). Oral cytobrush was proposed to collect tissue particles, cells, and a small amount of saliva at the same time (23). For this reason, it is a promising method in identifying early disease onset. Recently, the ability to detect molecules with cytobrush from patients with head and neck cancer (24) provided along with saliva samples (25) was claimed to be a unique opportunity to develop noninvasive diagnosis. Nevertheless, no single biomolecule has been shown to meet the real-world requirement for high accuracy in identifying early disease onset, suggesting that multiple biomarkers are needed for high accuracy and sensitivity in detecting OSCC (26). Surgical biopsy is an invasive diagnostic method, while cytobrush technique is suitable for the screening of pathological conditions considering its minimal invasiveness (23). Therefore, it is important to evaluate whether the cytobrush might be sufficient to be used as a reliable standard method to aid in the diagnosis of suspicious oral lesions. To date, the diagnostic precision and accuracy of the cytobrush technique for finding oral cancer biomarkers versus histopathologic diagnosis has not been examined in detail (27).

Our preliminary study aims to establish whether cytobrush biopsy is effective in collecting OSCC selected biomarkers (22, 28–34) from an

oral cancer lesion and to evaluate, from a statistical point of view, its accuracy (as diagnostic effectiveness) and precision (as discriminatory effectiveness between the tumor lesion and the surrounding healthy tissue) in order to perform a correct diagnosis by using the Stark Oral Screening® IVD test (Stark S.a.r.l., Principaute de Monaco) and the Femtohunter® device (Stark S.a.r.l.) and comparing its outcome with the biopsy results, taken as the gold standard.

2 Materials and methods

To perform our study, we used a diagnostic system consisting of the Femtohunter® device and Stark Oral Screening® IVD test kits.

2.1 Subjects

Fifteen patients (9 males, 6 Females) with a newly diagnosed primary OSCC (staged I-IV according to the tumor-node-metastasis-TNM criteria) without prior chemotherapy or radiotherapy were enrolled for the study between May 2022 and April 2023.

2.2 Criteria of inclusion

Adult patients (>18years old) diagnosed with oral cancer (confirmed by histological diagnosis), all cancer stages, no previous treatment.

2.3 Criteria of exclusion

Patients without a confirmed diagnosis of oral cancer by histology or immunohistochemistry. Brush samples with evident blood traces or pyrogens with quantitative negative channel noise background values equal to or greater than 20. Brush samples with an insufficient cell load expressed by beta-actin channel value less than or equal to Femtohunter F.M. 2.

2.4 Samples collection

We collected cytobrush biopsies from the patients and analyzed them for the expression of selected biomarkers with a high-sensitivity fully automated ELISA technique. Patients were asked to rinse their mouths with physiologic solution before performing the cytobrush biopsy retrieval. Two non-invasive cytobrush biopsies were taken from the mouth of each patient with cancer. For each patient, the first sample was obtained from the center of the lesion and the second one from surrounding healthy tissue. Each cytobrush was rubbed applying a mild pressure and a rotation over the area under analysis to collect cells and fragments of tissue exfoliation, while limiting bleeding as much as possible. Cytobrush tips were inserted in sealed Eppendorf vials, cataloged, and stored at 0-4°C and then sent to the lab for analysis in refrigerated boxes.

2.5 Selection of biomarkers

We selected six biomarkers:

- EGFR (35–38), p53 (39–41), Ki67 (29, 42–48), already available and consolidated in their diagnostic effectiveness of OSCC;
- PD-L1, B7-H6, HLA-E, selected based on recent scientific and clinical data which indicate their *de novo* or over-expression in cells undergoing transformation as a mechanism of tumor-mediated immune resistance and their role as possible molecular targets in immune checkpoints blockade therapies (30–34).

2.6 Biomarkers detection technique

Two different disposable Stark Oral Screening® test kits (Stark S.a.r.l.) were used for the analysis of the biological samples:

- Stark oral screening quantitative metabolic (REF: SOSFMTCKIT) detection of EGFR/p53/Ki67
- Stark oral screening quantitative NK time (REF.SOSBHPDQNT) detection of B7-H6/PD-L1/HLA-E.

The Stark Oral Screening® test is a patient side *in vitro* diagnostics (IVD) and quantitative test based on a bioluminescent signal response. The Stark Oral Screening® test has a very high sensitivity with the following limit of detection value (LOD) "*In vitro*": LOD = 20 Femtograms/microliter.

Disposable kits are made up of 3 elements:

1) Cytobrush for non-invasive sampling of the biological sample.
2) Reagent slots - A thermoformed tray in two superimposed layers defined in slot caps and test tube slots so designed to keep the solid phase separate from the liquid phase, in order to be able to make the storage at room temperature. The reagent slot has 10 cavities, called "stations" necessary for the correct automatic execution of the ELISA procedure.
3) Slot detector membranes in PVDF - The thermoformed tray has 3 cavities which allow the anchoring of 3 membranes armed with polyclonal antibodies towards markers of interest as well as 1 control membrane.

Disposable kits had to be processed through Femtohunter (Stark Sarl, Principaute de Monaco).

2.7 Data preparation

The biological samples were inserted into the respective cavities of the Stark kit reagent slot to identify:

- EGFR, p53, Ki67 markers (Cod kit SOSFMTCKIT)
- B7-H6, PD-L1, HLA-E markers (Cod Kit SOSBHPDQNT)

The reagent slots, loaded with the biological sample from the patient, were inserted into the automatic ELISA developer device (Femtohunter) with chemiluminescent signal and qualitative and quantitative analysis response. The slot membranes, armed with polyclonal antibodies against the marker of interest, were inserted into the automatic developer device.

The automatic procedure took place in 13 development steps: 12 steps included the correct ELISA procedure and 1 step was focused on chemiluminescent signal detection and analysis.

Each chemiluminescent signal (S) detected with the Femtohunter device (Figure 1) is calibrated at each test by measuring the intensity of the background noise (N), generated by non-specific luminescence on a control PVDF membrane. The N value is then subtracted from the S value present on the PVDF membrane dedicated to the marker. If the result is a positive value (S-N>0) then it assesses that there is a specific signal S for the sought marker, therefore its presence in the sample. The positive value S is then divided by N generating a multiplication factor and allowing the operator to understand how many times the specific signal S is intense compared to the background noise N (Signal/Noise ratio). The obtained S/N value is defined as FM (multiplication factor for the Femtohunter®) and included in the Femtohunter® FM patient report. For instance, the value 2.4 EGFR expresses that there is a chemiluminescent signal S on the PVDF dedicated to EGFR greater 2.4 times the background noise N. The test was considered POSITIVE for a malignant tumor lesion when it showed the Femtohunter® FM > 1.2 for all six markers of interest. The test was considered NEGATIVE for a malignant tumor lesion when it showed a Femtohunter® FM < 1.19 for any of the markers of interest.

2.8 Statistical methods

First, a power analysis (Table 1) was carried out to estimate the minimum number of statistical units necessary to guarantee the test a power of at least 0.8. The significance level chosen is 0,05.

The primary outcome identified to perform the power analysis is the parameter PD-L1.

The reasons why we chose the PD-L1 marker are related to its characteristics:

- PD-L1 is also expressed in oral cancer precancerous lesions (49), and it is usually overexpressed in tumor lesion, so it is a statistically strong parameter.
- PD-L1 expression can render the cancer invulnerable to immune attack. In fact, the PD-1/PD-L1 axis plays an important role in oral cancer therapy. Thus, PD-L1 is not only a guidance for the use of immune checkpoint inhibitors (50), but also a potential prognostic indicator for oral cancer (51). Therefore, focusing on its presence in the sample is not only useful for statistical purposes since it could have a prognostic value.

Empirical data, observed in a first pilot sample, were used to identify the expected value for the "PD-L1 tumor center" variable,

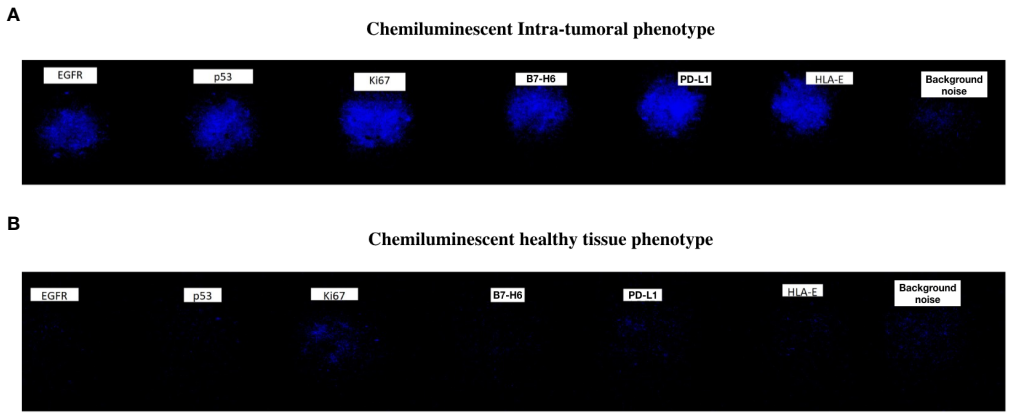

FIGURE 1
An example of Chemiluminescent Phenotype showing the six selected biomarkers in an intra-tumoral sample **(A)** and healthy tissue sample **(B)**.

TABLE 1 Power analysis.

	N	Actual Powerb	Test Assumptions			
			Power	Std. Dev.	Effect Size	Sig.
Test for Mean[a]	**7**	**0,820**	**0,8**	**14,39**	**1,098**	**0,05**
a. One-sided test.						
b. Based on non-central t distribution.						

as no literature data are available. Healthy tissue for the variable PD-L1 has an expected value, by definition, equal to 0, with no standard deviation. Therefore, a one-sample power analysis was performed to compare the expected mean value of "PD-L1 tumor center" with the reference value of 0.

A univariate descriptive analysis of the FM parameters was then carried out by calculating the centrality and variability indexes for quantitative variables. Therefore, nonparametric Wilcoxon tests for paired samples were used to verify whether there was a statistically significant difference, in terms of distribution of EGFR, p53, Ki67, B7-H6, PD-L1 and HLA-E parameter values, between the tumor center and the healthy tissue of the same subjects.

The null hypothesis is H0 = no significant differences in the distribution of parameters between the tumor center and the healthy tissue. An alpha significance level of 0.05 was used in all these analyses.

Healthy patients have not been added to the study, as control is the healthy tissue of the patients themselves, thus making the recruitment of additional patients without pathology superfluous.

In fact, the patients were enrolled in the study because they were diagnosed with OSCC by biopsy, considered as a gold standard, i.e. the most accurate diagnostic examination to confirm a certain diagnostic question, to which every other examination (or any other new examination) must relate to have diagnostic validity (52). Moreover, in this type of statistical evaluation, the use of a cohort as a control would inevitably increase overall bias (i.e. false negatives and false positives).

IBM SPSS Statistics software in version 28 was used for statistical analysis of data.

3 Results

3.1 Power analysis

The PD-L1 parameter, chosen as the primary outcome for the power analysis, shows in the preliminary data an average value of 15,8 with a standard deviation of 14,39 for the tumor center. While the score for PD-L1 parameter in healthy tissue is by definition equal to 0. The final mean PD-L1 score of the 15 enrolled patients, as evident in the table "FM Descriptive statistics for each parameter and Wilcoxon comparison test", turns out to be different (i.e. 13.1) from the mean value hypothesized in the power analysis (i.e. 15.8) since the latter, being by definition an analysis that is carried out "a priori", was carried out on the preliminary data, i.e. on the data relating only to the first 7 patients enrolled (as evidenced by the value "7" in the column called " N" of the Power analysis table), whose mean and standard deviation were respectively 15.8 and 14.39. A one-tail t-test was used for the single-sample mean (H0: $\mu = 0$; H1: $\mu > 0$) (Table 1).

The power analysis showed that the minimum number of statistical units necessary to obtain a power of 0,8 with reference to the PD-L1 parameter is 7 units. Therefore, our sample size can be considered definitely adequate in terms of actual power of the tests and should be able to accurately represent the total population.

3.2 Statistical analyses

After sample collection, data was analyzed obtaining the following results:

Intra-tumoral markers (Table 2): All samples from the tumor center showed 6 over-expressed markers out of 6 markers, except for two subjects who had only 5 markers out of 6.

Healthy tissue markers (Table 3): All samples from the healthy tissue showed 0 to 3 over-expressed markers out of 6 markers.

FM Descriptive statistics for each parameter and Wilcoxon comparison test (Table 4)

The Wilcoxon non parametrical paired test is statistically significant for all six analyzed parameters (EGFR p:0,001; p53 p: <0.001; Ki67 p:0.008; B7-H6 p:0.001; PD-L1 p:<0.001; HLA-E p: <0.001). Therefore, we can reject the null hypothesis that there is no significant difference in the distribution of parameters between the tumor center and healthy tissue. Specifically, all the six parameters have significantly higher values in the tumor center than in healthy tissue (Figure 2).

TABLE 2 Intra-tumoral markers.

		Frequency	Percent	Cumulative Percent
Markers	5 out of 6	2	13,3	13,3
	6 out of 6	13	86,7	100,0
	Total	15	100,0	

TABLE 3 Healthy tissue markers.

		Frequency	Percent	Cumulative Percent
Markers	0 out of 6	5	33,3	33,3
	1 out of 6	7	46,7	80,0
	2 out of 6	2	13,3	93,3
	3 out of 6	1	6,7	100,0
	Total	15	100,0	

TABLE 4 FM Descriptive statistics for each parameter and Wilcoxon comparison test.

	Mean	Standard Deviation	Median	Percentile 25	Percentile 75	p-value
EGFR Tumor tissue	7,7	6,7	5,1	4,8	7,9	0,001***
EGFR Healthy tissue	0,8	2,3	0,0	0,0	0,0	
p53 Tumor tissue	8,0	8,2	5,5	4,3	7,0	<0,001***
p53 Healthy tissue	0,0	0,0	0,0	0,0	0,0	
Ki67 Tumor tissue	9,1	6,1	6,7	5,4	10,5	0,008**
Ki67 Healthy tissue	2,8	4,8	0,0	0,0	4,9	
B7-H6 Tumor tissue	8,0	4,8	6,9	4,6	9,4	0,001***
B7-H6 Healthy tissue	1,4	2,4	0,0	0,0	3,4	
PD-L1 Tumor tissue	13,1	12,4	8,4	5,7	15,8	<0,001***
PD-L1 Healthy tissue	0,0	0,0	0,0	0,0	0,0	
HLA-E Tumor tissue	10,3	6,9	6,9	5,8	15,4	<0,001***
HLA-E Healthy tissue	0,2	0,6	0,0	0,0	0,0	

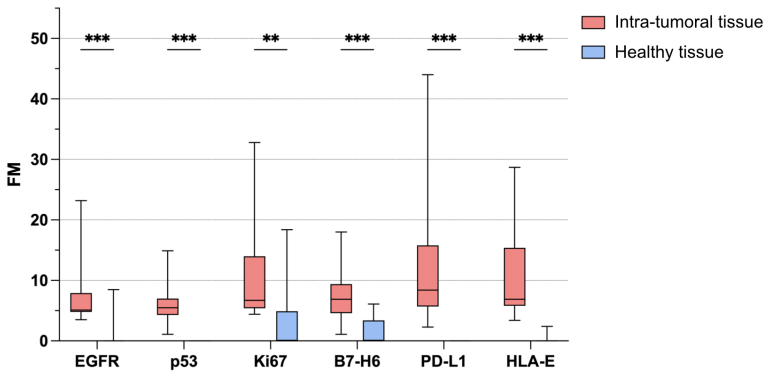

FIGURE 2
Bio-marker detectability in intra-tumoral and healthy tissue samples. Variation in the FM (moltiplicative factor) of each of the six bio-markers between intra-tumoral (red) and healthy (blue) samples in patients with OSCC (N=15). P value of less than 0.01 (**) and less than 0.001 (***) was considered statistically significant.

The bioluminescent phenotype observed in the two different sampling sites (healthy tissue and center of the lesion) differs not only in signal quality but also in quantitative intensity with a signal that is on average 213% more intense in the center of the tumor than in the health tissue, confirming a marked over-expression of markers in the tumor center and a sharp decay or a disappearance of the signal in healthy tissues. This result was independent of tumor staging.

These results are consistent with those obtained using the gold standard test and clearly indicate that the proposed approach (analysis of biomarkers by an automated proprietary ELISA technique) is highly reliable, being able to detect tumor markers only in the core of the tumor and not in the healthy tissue.

4 Discussion

The Femtohunter® is an automatic ELISA developer device that automatically performs the chemiluminescence analysis on samples taken by cytobrush and submitted to the Stark Oral Screening® IVD test, provides the results as a graphical image within 60 minutes, as well as the analytical data of the markers and prints a patient report. The Stark Oral Screening® test is a patient side *in vitro* diagnostics (IVD) and quantitative test based on a bioluminescent signal response. The Stark Oral Screening® test has a very high sensitivity with the following limit of detection (LOD) values of 20 Femtograms/microliter.The aim of the present study was to verify whether the detection of appropriately selected biomarkers in cytobrush biopsies samples by the Femtohunter can discriminate the lesions of OSCC from the surrounding healthy tissue. To this end, we have selected 6 biomarkers, some of these already used in clinical practice for the diagnosis of OSCC (EGFR, p53, Ki67), other selected based on recent scientific and clinical data which indicate their *de novo*- or over-expression in cells undergoing transformation and their role as possible molecular targets in immune checkpoints blockade therapies (B7-H6, PD-L1, HLA-E). The choice of these markers is based on recent evidence of the

important role that the immune system plays in preventing but also in promoting the development of tumors. Indeed, resistance mechanisms are commonly employed by tumors in response to immune pressures exerted by effector cells, such as natural killer (NK) cells and cytotoxic T cells. Among such resistance mechanisms, increased expression of inhibitory receptors on $CD8^+$ T cells and Natural killer (NK) cells constrains their antitumor cytotoxic potential (53, 54). Monoclonal Antibodies (mAbs) that abrogate these inhibitory interactions between immune checkpoint receptors and their ligands have transformed the therapeutic landscape for treatment of solid tumors (54–56). NK cells are lymphocytes of the innate immune system that sense target cells through a panel of activating and inhibitory receptors expressed at their surface. Integration of the opposing signals transduced by the engagement of such receptors defines the functional outcome for NK cells (57). Inhibitory receptors include the KIRs and CD94/NKG2A molecules, and their interaction with classical (HLA-I molecules) and non-classical (HLA-E) on target cells prevents activation of NK cells. Thus, downregulation of normally ubiquitously expressed HLA-I molecules on target cells activates NK cells, a process coined as "missing self" recognition, while the maintaining of HLA-I expression on the tumor surface blocks NK cell ability to kill the tumor. Recently, the PD-1 receptor, originally identified on T cells, has been described on a subset NK cells as an additional inhibitory receptor that can block NK cell function against tumor cells expressing the specific ligands PD-L1 and PD-L2. Thus, in pathological conditions, these inhibitory receptors (primarily NKG2A and PD-1) can function as immune checkpoints by blocking the functional activity of NK cells against tumor cells expressing the relative ligands. These NK cell impairments can be rescued using specific mAbs able to disrupt the receptors/ligands interactions, thus demonstrating a role for these inhibitory receptors as true immune checkpoints (clinicaltrials.gov). For these reasons, these receptors, mainly NKG2A and PD-1, and their relative ligands (HLA-E and PD-L1) are considered possible molecular targets in the immune checkpoint blockade immunotherapy. HLA-E is a non-classical MHC class I molecule that is ubiquitously expressed on hematopoietic cells at low abundance on the cell surface and is sensitive to inflammatory signals. HLA-E binds to the heterodimeric complex CD94/NKG2A (58–61). A humanised mAb binding to the NKG2A receptor, Monalizumab, has been developed, and numerous clinical trials are ongoing across multiple tumor indications (clinicaltrials.gov). Monalizumab can be potentially used in the treatment of oral cancers (30, 61). *In vitro* blockade of NKG2A, alone or in combination with targeting the PD-1 pathway, stimulates NK cell functions but is collectively required to stimulate a strong CD8+ T cell response to $HLA\text{-}E^+$ $PD\text{-}L1^+$ tumors. The combined administration of anti-NKG2A and anti-PD-L1 blocking antibodies unleashes NK and $CD8^+$ T cells and subsequently slows tumor progression in mouse models and preliminary analyses suggest *in vivo* efficacy of Monalizumab when in combination with the EGF receptor (EGFR) blockade antibody (Cetuximab) in recurrent/metastatic squamous cell carcinoma of the head and neck (HNSCC) (30). PD-1/PD-L1 blockade has been tested in clinical trials for various malignancies including metastatic oral carcinoma, with significant response rates and limited side effects. Immunotherapies targeting the PD-1/PD-L1 pathway have particularly proven effective in controlling tumor growth through the reinvigoration of $CD8^+$ T cells and/or NK cells across numerous tumor settings, including oral cancer (30). PD-L1 expression has also been proposed as a prognostic marker for different types of cancers with mixed results. Based on these data and considering the high expression of HLA-E and PD-L1 on the surface of oral cancer cells (30), we selected these two molecules as potential OSCC biomarkers. Regarding the selection of B7-H6 as a possible additional marker of oral cancer, we should consider that NK cells (and other immune cells) also express a series of activating receptors, including the so-called Natural Cytotoxicity Receptors (NCR), that include NKp46 (NCR1), NKp44 (NCR2) and NKp30 (NCR3). NKp30 was identified at the end of the 1990s as a novel 30-kDa triggering receptor expressed by all resting and activated human NK cells (57, 62). Cells expressing NKp30 ligands are sensitive to the cytotoxicity of human NK cells. The identification of B7-H6 as a counter structure of the NCR3 NKp30 shed light on the molecular basis of NK cell immunosurveillance. B7-H6, a member of the B7 family of immune modulators, is expressed in a variety of tumor cell types while minimally or not expressed in normal tissues. Expression of B7-H6 on the tumor cell surface can markedly enhance the sensitivity of tumor cells to NK cells. Several studies suggest that NK cells can potentially eliminate B7-H6-positive tumor cells in cancer patients. However, as clinically observed, most of the human tumors are found to be B7-H6+ rather than B7-H6–, which suggests the functional compromise of the B7-H6 ligand-NKp30 receptor system in cancer patients to permit the growth of B7-H6+ tumor cells (33). A study evaluating different doses of BI 76504, an anti-B7-H6/Anti-CD3 bispecific antibody, given alone and given with Ezabenlimab (an anti-PD-1 drug) to patients with advanced solid tumors (including oral cancers) having the B7-H6 marker is currently recruiting participants (clinicaltrials.gov). BI 765049 is an immunoglobulin G (IgG)-like bispecific T-cell engaging antibody directed against both NCR3 (NKp30) ligand 1 (NCR3LG1; B7-H6) and T-cell surface antigen CD3, with potential immunostimulating and antineoplastic activities. Upon administration, anti-B7-H6/anti-CD3 bispecific antibody BI 765049 targets and binds to both B7-H6 on tumor cells and CD3 on T cells. This results in the cross-linking of B7-H6-expressing tumor cells and T-cells, redirects cytotoxic T lymphocytes (CTLs) to B7-H6-expressing tumor cells, which leads to the CTL-mediated cell death of B7-H6-expressing tumor cells. Thus, considering these clinical data, and the presence of B7-H6 in certain cancers including oral cancers, and its ability to modulate immune cell function that can be exploited in immunotherapeutic approaches, we selected this molecule as a further OSCC biomarker to detect in our system. To confirm the validity of this technique, multiple cytobrush samples were collected from the oral cavity of 15 patients with already diagnosed OSCC in order to search the selected markers. Patients had diagnosed oral cancers ranging from stage I to IV, representing the full spectrum of OSCC. Cytobrush samples analyzed with the novel high-sensitivity ELISA technique demonstrated reliability, specificity, discriminatory value, and low cost. These results are

consistent with those obtained using the gold standard test and clearly indicate that the proposed approach is highly reliable, being able to detect tumor markers only in the core of the tumor and not in the healthy tissue. This innovative approach could pave the way for the realization of a new method of screening and phenotyping of oral lesions with advantages on patients' health and possible simplification of screening procedures for obtaining early diagnosis. Many patients are currently being discharged after a negative biopsy result of a suspected precancerous lesion or potentially malignant oral disorders. On the contrary, these patients should be placed on a regular follow-up schedule to prevent a precancerous lesion from turning into cancer over time. Although biopsy with histological examination is universally recognized as the best diagnostic system available today, it cannot be used for a screening or periodic monitoring of potentially malignant oral disorders, precancerous lesions or suspicious lesions that could evolve, because it is invasive and could leave a scar that could alter the outcome of future diagnoses. A screening test is not intended to be diagnostic but aims to capture patients with such abnormal oral findings and to accelerate the referral and application of more specific diagnostic procedures by a specialist.

Human saliva has been considered a valuable source for protein or nucleic acid biomarkers for various infections, systemic and non-systemic diseases (63). Exfoliated cancer cells may release proteins and free molecules representing gene expression changes associated with tumor development into the saliva, thus salivary proteins provide a strong option for development of non-invasive, point-of-care assays for screening/early detection of oral cancers. Among the proteins verified, CD44, S100A7 and S100P showed significant potential for use as early detection markers in patients with dysplastic leukoplakia and OSCC (64).

In a previous study, Lichieh Julie Chu et al. identified matrix metalloproteinase-1 (MMP-1) as one of the most promising salivary biomarkers for OSCC and developed a sensitive ELISA for MMP-1 with good performance in detection of OSCC. More recently, they developed a time-saving rapid strip test (RST) and demonstrated that salivary MMP-1 levels measured using RST and ELISA were highly comparable and both assays could effectively distinguish between OSCC and non-cancerous groups (65).

The technique proposed in the present paper aims to be non-invasive and capable in the future of phenotyping suspicious lesions based on the number and quantitative level of tumor markers present on a lesion. Moreover, the source in which to search for the markers has been carefully evaluated, preferring cytobrush samples containing fragments of tissue and cells directly from the suspicious lesions where the markers would be much more concentrated than samples of blood, saliva, or other organic fluids. Such a technique aims in the future to become valuable as an aid for obtaining an early diagnosis and help clinicians in setting up a prompt therapy in case of malignant positivity. This technique was also designed to be also rapid, cost effective and patient-side. The small number of cases does not allow the authors to indicate the materials and methods adopted for the present study as a new diagnostic tool that can be used for point of care screening, although, from a statistical perspective, the number of samples is already significant enough to validate our observations. Therefore, the extremely positive and encouraging results of our study require the future evaluation of larger samples to confirm its potential value for the early detection of oral cancer and the assessment of disease progression.

5 Conclusions

In conclusion, our study strongly suggests that the search of selected tumor markers on brush biopsy could be successful for the detection of oral cancers and precancers.The proposed technique consists in a rapid non-invasive possible alternative or companion examination to the gold standard (biopsy). This procedure quantitatively and qualitatively evaluates the presence of six markers proven to be associated with neoplastic transformation. The results showed how each of the six markers selected is significatively overrepresented in the neoplastic lesion compared to the healthy tissue, therefore the combined evaluation of the six markers could be able to determine the presence of neoplastic formations with high accuracy.

Statistical power analysis showed that the study sample has the necessary size, anyway it would be very interesting, in future works, to further expand the sample population to confirm the effectiveness of the proposed test on a large statistical base. If the results of the present study are confirmed for a large sample as well, this technique could be applied to define the phenotype of precancerous lesions based on the markers expressed, paving the way to an innovative method of screening to prevent oral cancer.

Data availability statement

The original contributions presented in the study are included in the article. Further inquiries can be directed to the corresponding authors.

Ethics statement

The studies involving human participants were reviewed and approved by ethics committee of the Liguria Region, Genova, Italy (n. 326/2018 and n127/2022-DB id12223). The patients/participants provided their written informed consent to participate in this study.

Author contributions

FR, ADR, MG designed, performed research, and interpreted data; RoP, ReP, FG, PI, FL, BB provided patient's profile; GT, MG, SP performed statistical analyses, FB, FDG revised the article; AR, EM designed and performed research, interpreted data, wrote the article. All authors contributed to the article and approved the submitted version.

Funding

The research leading to these results has received funding from AIRC under IG 2021 – ID. 26037 project – P.I. Marcenaro Emanuela. Additional grants from. University of Genova: Compagnia di San Paolo (2019.866) (G.L. EM). MG was supported by a FIRC-AIRC fellowship for Italy.

Acknowledgments

The authors want to thank: Riccardo Moffa, Angelo Simone Parodi, Dr. Giuseppe Di Meo, and Dr. Francesca Carrano (Stark Sarl Monaco), Dr. Giuseppe Signorini, Galliera Hospital, Genova, Italy; Prof. Maria Contaldo and Dr. Ciro Emiliano Boschetti (Università degli studi della Campania Luigi Vanvitelli, Napoli, Italy); Dr. Danny Amore and Franco Solari.

Conflict of interest

The authors declare that the research was conducted in the absence of any commercial or financial relationships that could be construed as a potential conflict of interest.

Publisher's note

References

1. Warnakulasuriya S. Global epidemiology of oral and oropharyngeal cancer. *Oral Oncol* (2009) 45:309–16. doi: 10.1016/J.ORALONCOLOGY.2008.06.002

2. Dhanuthai K, Rojanawatsirivej S, Thosaporn W, Kintarak S, Subarnbhesaj A, Darling M, et al. Oral cancer: a multicenter study. *Med Oral Patol Oral Cir Bucal* (2018) 23:e23–9. doi: 10.4317/MEDORAL.21999

3. Kane SV, Gupta M, Kakade AC, D'Cruz A. Depth of invasion is the most significant histological predictor of subclinical cervical lymph node metastasis in early squamous carcinomas of the oral cavity. *Eur J Surg Oncol* (2006) 32:795–803. doi: 10.1016/J.EJSO.2006.05.004

4. Montero PH, Patel SG. Cancer of the oral cavity. *Surg Oncol Clin N Am* (2015) 24:491. doi: 10.1016/J.SOC.2015.03.006

5. Rivera C. Essentials of oral cancer. *Int J Clin Exp Pathol* (2015) 8:11884.

6. Abati S, Bramati C, Bondi S, Lissoni A, Trimarchi M. Oral cancer and precancer: a narrative review on the relevance of early diagnosis. *Int J Environ Res Public Health* (2020) 17:1–14. doi: 10.3390/IJERPH17249160

7. González-Moles MÁ, Aguilar-Ruiz M, Ramos-García P. Challenges in the early diagnosis of oral cancer, evidence gaps and strategies for improvement: a scoping review of systematic reviews. *Cancers* (2022) 14:4967. doi: 10.3390/CANCERS14194967

8. Silverman S, Kerr AR, Epstein JB. Oral and pharyngeal cancer control and early detection. *J Cancer Educ* (2010) 25:279–81. doi: 10.1007/S13187-010-0045-6

9. Akbulut N, Oztas B, Kursun S, Evirgen S. Delayed diagnosis of oral squamous cell carcinoma: a case series. *J Med Case Rep* (2011) 5:291. doi: 10.1186/1752-1947-5-291

10. Goy J, Hall SF, Feldman-Stewart D, Groome PA. Diagnostic delay and disease stage in head and neck cancer: a systematic review. *Laryngoscope* (2009) 119:889–98. doi: 10.1002/LARY.20185

11. Mauceri R, Bazzano M, Coppini M, Tozzo P, Panzarella V, Campisi G. Diagnostic delay of oral squamous cell carcinoma and the fear of diagnosis: a scoping review. *Front Psychol* (2022) 13:1009080. doi: 10.3389/FPSYG.2022.1009080

12. Mercadante V, Paderni C, Campisi G. Novel non-invasive adjunctive techniques for early oral cancer diagnosis and oral lesions examination. *Curr Pharm Des* (2012) 18:5442–51. doi: 10.2174/138161212803307626

13. Gómez I, Seoane J, Varela-Centelles P, Diz P, Takkouche B. Is diagnostic delay related to advanced-stage oral cancer? a meta-analysis. *Eur J Oral Sci* (2009) 117:541–6. doi: 10.1111/J.1600-0722.2009.00672.X

14. McCullough MJ, Prasad G, Farah CS. Oral mucosal malignancy and potentially malignant lesions: an update on the epidemiology, risk factors, diagnosis and management. *Aust Dent J* (2010) 55 Suppl 1:61–5. doi: 10.1111/J.1834-7819.2010.01200.X

15. Feller L, Lemmer J, Feller L, Lemmer J. Oral squamous cell carcinoma: epidemiology, clinical presentation and treatment. *J Cancer Ther* (2012) 3:263–8. doi: 10.4236/JCT.2012.34037

16. Groome PA, Rohland SL, Hall SF, Irish J, MacKillop WJ, O'Sullivan B. A population-based study of factors associated with early versus late stage oral cavity cancer diagnoses. *Oral Oncol* (2011) 47:642–7. doi: 10.1016/J.ORALONCOLOGY.2011.04.018

17. McGurk M, Chan C, Jones J, O'Regan E, Sherriff M. Delay in diagnosis and its effect on outcome in head and neck cancer. *Br J Oral Maxillofac Surg* (2005) 43:281–4. doi: 10.1016/J.BJOMS.2004.01.016

18. Ford PJ, Farah CS. Early detection and diagnosis of oral cancer: strategies for improvement. *J Cancer Policy* (2013) 1:e2–7. doi: 10.1016/J.JCPO.2013.04.002

19. Cicciù M, Cervino G, Fiorillo L, D'Amico C, Oteri G, Troiano G, et al. Early diagnosis on oral and potentially oral malignant lesions: a systematic review on the VELscope® fluorescence method. *Dent J (Basel)* (2019) 7. doi: 10.3390/DJ7030093

20. Shanti RM, Tanaka T, Stanton DC. Oral biopsy techniques. *Dermatol Clin* (2020) 38:421–7. doi: 10.1016/J.DET.2020.05.003

21. Yang EC, Tan MT, Schwarz RA, Richards-Kortum RR, Gillenwater AM, Vigneswaran N. Noninvasive diagnostic adjuncts for the evaluation of potentially premalignant oral epithelial lesions: current limitations and future directions. *Oral Surg Oral Med Oral Pathol Oral Radiol* (2018) 125:670. doi: 10.1016/J.OOOO.2018.02.020

22. Patel KR, Vajaria BN, Singh RD, Begum R, Patel PS. Clinical implications of p53 alterations in oral cancer progression: a review from India. *Exp Oncol* (2018) 40:10–18. doi: .

23. Sahebjamee M, Mansourian A, Etemad-Moghadam S, Shamshiri AR, Derakhshan S. Conventional versus papanicolaou-stained cytobrush biopsy in the diagnosis of oral squamous cell carcinoma. *Oral Health Dent Manag* (2014) 13:619–22.

24. Gissi DB, Morandi L, Colella G, De Luca R, Campisi G, Mauceri R, et al. Clinical validation of 13-gene DNA methylation analysis in oral brushing samples for detection of oral carcinoma: an Italian multicenter study. *Head Neck* (2021) 43:1563–73. doi: 10.1002/HED.26624

25. Aro K, Kaczor-Urbanowicz K, Carreras-Presas CM. Salivaomics in oral cancer. *Curr Opin Otolaryngol Head Neck Surg* (2019) 27:91–7. doi: 10.1097/MOO.0000000000000502

26. Chu HW, Chang KP, Hsu CW, Chang IYF, Liu HP, Chen YT, et al. Identification of salivary biomarkers for oral cancer detection with untargeted and targeted quantitative proteomics approaches. *Mol Cell Proteomics* (2019) 18:1796–806. doi: 10.1074/MCP.RA119.001530

27. Mehrotra R, Hullmann M, Smeets R, Reichert TE, Driemel O. Oral cytology revisited. *J Oral Pathol Med* (2009) 38:161–6. doi: 10.1111/J.1600-0714.2008.00709.X

28. Rajaram P, Chandra P, Ticku S, Pallavi B, Rudresh K, Mansabdar P. Epidermal growth factor receptor: role in human cancer. *Indian J Dent Res* (2017) 28:687–94. doi: 10.4103/IJDR.IJDR_534_16

29. Swain S, Nishat R, Ramachandran S, Raghuvanshi M, Behura SS, Kumar H. Comparative evaluation of immunohistochemical expression of MCM2 and Ki67 in oral epithelial dysplasia and oral squamous cell carcinoma. *J Cancer Res Ther* (2022) 18:997–1002. doi: 10.4103/JCRT.JCRT_10_20

30. André P, Denis C, Soulas C, Bourbon-Caillet C, Lopez J, Arnoux T, et al. Anti-NKG2A mAb is a checkpoint inhibitor that promotes anti-tumor immunity by unleashing both T and NK cells. *Cell* (2018) 175:1731–1743.e13. doi: 10.1016/J.CELL.2018.10.014

31. Brandt CS, Baratin M, Yi EC, Kennedy J, Gao Z, Fox B, et al. The B7 family member B7-H6 is a tumor cell ligand for the activating natural killer cell receptor NKp30 in humans. *J Exp Med* (2009) 206:1495–503. doi: 10.1084/JEM.20090681

32. Gonçalves AS, Mosconi C, Jaeger F, Wastowski IJ, Aguiar MCF, Silva TA, et al. Overexpression of immunomodulatory mediators in oral precancerous lesions. *Hum Immunol* (2017) 78:752–7. doi: 10.1016/J.HUMIMM.2017.09.003

33. Pesce S, Tabellini G, Cantoni C, Patrizi O, Coltrini D, Rampinelli F, et al. B7-H6-mediated downregulation of NKp30 in NK cells contributes to ovarian carcinoma immune escape. *Oncoimmunology* (2015) 4:e1001224. doi: 10.1080/2162402X.2014.1001224

34. Wang C, Li Y, Jia L, Kim JK, Li J, Deng P, et al. CD276 expression enables squamous cell carcinoma stem cells to evade immune surveillance. *Cell Stem Cell* (2021) 28:1597–1613.e7. doi: 10.1016/J.STEM.2021.04.011

35. Miranda Galvis M, Santos-Silva AR, Freitas Jardim J, Paiva Fonseca F, Lopes MA, de Almeida OP, et al. Different patterns of expression of cell cycle control and local invasion-related proteins in oral squamous cell carcinoma affecting young patients. *J Oral Pathol Med* (2018) 47:32–9. doi: 10.1111/JOP.12601

36. Schinke H, Shi E, Lin Z, Quadt T, Kranz G, Zhou J, et al. A transcriptomic map of EGFR-induced epithelial-to-mesenchymal transition identifies prognostic and therapeutic targets for head and neck cancer. *Mol Cancer* (2022) 21:1–25. doi: 10.1186/S12943-022-01646-1/FIGURES/8

37. Selvan SR, Brichetti JA, Thurber DB, Botting GM, Bertenshaw GP. Functional profiling of head and Neck/Esophageal squamous cell carcinoma to predict cetuximab response. *Cancer Biother Radiopharm* (2021). doi: 10.1089/CBR.2021.0283

38. Tarle M, Müller D, Raguž M, Lukšić I. Significance of nuclear EGFR and ABCG2 expression in malignant transformation of oral potentially malignant disorders. *Head Neck* (2022) 44:2668–77. doi: 10.1002/HED.27174

39. de Lima MAP, Cavalcante RB, da Silva CGL, Nogueira RLM, Macedo GEC, de Galiza LE, et al. Evaluation of HPV and EBV in OSCC and the expression of p53, p16, e-cadherin, COX-2, MYC, and MLH1. *Oral Dis* (2022) 28:1104–22. doi: 10.1111/ODI.13814

40. Gawande M, Chaudhary M, Sharma P, Hande A, Patil S, Sonone A. Expression of p53 at invasive front of oral squamous cell carcinoma and negative histopathological surgical margins to establish correlation at 3-year survival. *J Oral Maxillofac Pathol* (2020) 24:582. doi: 10.4103/JOMFP.JOMFP_106_20

41. Kakkar V, Sarin V, Chatterjee A, Manjari M, Chopra I. Expression of cyclin-D1 and p53 as prognostic markers in treatment of oral squamous cell carcinoma. *Indian J Otolaryngol Head Neck Surg* (2022) 74:6136–45. doi: 10.1007/S12070-021-02716-4

42. Dash KC, Mahapatra N, Bhuyan L, Panda A, Behura SS, Mishra P. An immunohistochemical study showing ki-67 as an analytical marker in oral malignant and premalignant lesions. *J Pharm Bioallied Sci* (2020) 12:S274–8. doi: 10.4103/JPBS.JPBS_83_20

43. de Souza Martins Câmara AC, Gonzaga AKG, dos Santos Pereira J, Queiroz SIML, da Silveira ÉJD, Pinto LP, et al. Immunohistochemical comparative analysis of IMP-3 and KI-67 in actinic cheilitis and lower lip squamous cell carcinoma. *Oral Maxillofac Surg* (2022) 26:587–93. doi: 10.1007/S10006-021-00990-8

44. Dumitru CS, Ceausu AR, Comsa S, Raica M. Loss of e-cadherin expression correlates with ki-67 in head and neck squamous cell carcinoma. *In Vivo (Brooklyn)* (2022) 36:1150. doi: 10.21873/INVIVO.12814

45. Gadbail A, Sarode S, Chaudhary M, Gondivkar S, Tekade S, Yuwanati M, et al. Ki-67, CD105, and α-smooth muscle actin expression in oral squamous cell carcinoma corresponds with different forms of tobacco consumption habits. *J Cancer Res Ther* (2022) 18:S197–204. doi: 10.4103/JCRT.JCRT_1307_20

46. Nazar M, Naz I, Mahmood MK, Hashmi SN. Immunohistochemical expression of cyclin D1 and ki-67 in primary and metastatic oral squamous cell carcinoma. *Asian Pac J Cancer Prev* (2020) 21:37. doi: 10.31557/APJCP.2020.21.1.37

47. Segura IG, Secchi DG, Galíndez MF, Carrica A, Bologna-Molina R, Brunotto M, et al. Connexin 43, bcl-2, bax, Ki67, and e-cadherin patterns in oral squamous cell carcinoma and its relationship with GJA1 rs12197797 C/G. *Med Oral Patol Oral Cir Bucal* (2022) 27:e366–74. doi: 10.4317/MEDORAL.25298

48. Shen Y, Xu Z, Liu M, Piao S, Li J. Evaluation of CK19 and VEGF gene expression, ki67 antigen, p53 protein, c-erb-B2, and their relationship in oral squamous cell carcinoma. *Cell Mol Biol (Noisy-le-grand)* (2022) 67:233–9. doi: 10.14715/CMB/2021.67.5.32

49. Dave K, Ali A, Magalhaes M. Increased expression of PD-1 and PD-L1 in oral lesions progressing to oral squamous cell carcinoma: a pilot study. *Sci Rep* (2020) 10:1–11. doi: 10.1038/s41598-020-66257-6

50. Shilova O, Shramova E, Proshkina G, Deyev S. Natural and designed toxins for precise therapy: modern approaches in experimental oncology. *Int J Mol Sci* (2021) 22:4975. doi: 10.3390/IJMS22094975

51. Huang Z, Zheng S, Ding S, Wei Y, Chen C, Liu X, et al. Prognostic role of programmed cell death ligand-1 expression in head and neck cancer treated with programmed cell death protein-1/programmed cell death ligand-1 inhibitors: a meta-analysis based on clinical trials. *J Cancer Res Ther* (2021) 17:676–87. doi: 10.4103/JCRT.JCRT_1606_20

52. Versi E. "Gold standard" is an appropriate term. *BMJ : Br Med J* (1992) 305:187. doi: 10.1136/BMJ.305.6846.187-B

53. Pesce S, Greppi M, Grossi F, Del Zotto G, Moretta L, Sivori S, et al. PD/1-PD-Ls checkpoint: insight on the potential role of NK cells. *Front Immunol* (2019) 10:1242/BIBTEX. doi: 10.3389/FIMMU.2019.01242/BIBTEX

54. Pesce S, Trabanelli S, Di Vito C, Greppi M, Obino V, Guolo F, et al. Cancer immunotherapy by blocking immune checkpoints on innate lymphocytes. *Cancers* (2020) 12:3504. doi: 10.3390/CANCERS12123504

55. Myers JA, Miller JS. Exploring the NK cell platform for cancer immunotherapy. *Nat Rev Clin Oncol* (2020) 18:85–100. doi: 10.1038/s41571-020-0426-7

56. Topalian SL, Taube JM, Anders RA, Pardoll DM. Mechanism-driven biomarkers to guide immune checkpoint blockade in cancer therapy. *Nat Rev Cancer* (2016) 16:275–87. doi: 10.1038/NRC.2016.36

57. Di Vito C, Mikulak J, Zaghi E, Pesce S, Marcenaro E, Mavilio D. NK cells to cure cancer. *Semin Immunol* (2019) 41:101272. doi: 10.1016/J.SMIM.2019.03.004

58. Boyington JC, Riaz AN, Patamawenu A, Coligan JE, Brooks AG, Sun PD. Structure of CD94 reveals a novel c-type lectin fold: implications for the NK cell-associated CD94/NKG2 receptors. *Immunity* (1999) 10:75–82. doi: 10.1016/S1074-7613(00)80008-4

59. Carretero M, Cantoni C, Bellón T, Bottino C, Biassoni R, Rodríguez A, et al. The CD94 and NKG2-a c-type lectins covalently assemble to form a natural killer cell inhibitory receptor for HLA class I molecules. *Eur J Immunol* (1997) 27:563–7. doi: 10.1002/EJI.1830270230

60. Sivori S, Vitale M, Bottino C, Marcenaro E, Sanseverino L, Parolini S, et al. CD94 functions as a natural killer cell inhibitory receptor for different HLA class I alleles: identification of the inhibitory form of CD94 by the use of novel monoclonal antibodies. *Eur J Immunol* (1996) 26:2487–92. doi: 10.1002/EJI.1830261032

61. Van Hall T, André P, Horowitz A, Ruan DF, Borst L, Zerbib R, et al. Monalizumab: inhibiting the novel immune checkpoint NKG2A. *J Immunother Cancer* (2019) 7:263. doi: 10.1186/S40425-019-0761-3

62. Pende D, Parolini S, Pessino A, Sivori S, Augugliaro R, Morelli L, et al. Identification and molecular characterization of NKp30, a novel triggering receptor involved in natural cytotoxicity mediated by human natural killer cells. *J Exp Med* (1999) 190:1505–16. doi: 10.1084/JEM.190.10.1505

63. Xiao H, Wong DT. Proteomics and its applications for biomarker discovery in human saliva. *Bioinformation* (2011) 5:294. doi: 10.6026/97320630005294

64. Sivadasan P, Gupta MK, Sathe G, Sudheendra HV, Sunny SP, Renu D, et al. Salivary proteins from dysplastic leukoplakia and oral squamous cell carcinoma and their potential for early detection. *J Proteomics* (2020) 212:103574. doi: 10.1016/J.JPROT.2019.103574

65. Chu LJ, Chang Y-T, Chien C-Y, Chung H-C, Wu S-F, Chen C-J, et al. Clinical validation of a saliva-based matrix metalloproteinase-1 rapid strip test for detection of oral cavity cancer. *BioMed J* (2023). doi: 10.1016/J.BJ.2023.04.002

frontiers | Frontiers in Immunology

TYPE Brief Research Report
PUBLISHED 10 August 2023
DOI 10.3389/fimmu.2023.1229341

OPEN ACCESS

EDITED BY
Silvia Pesce,
University of Genoa, Italy

REVIEWED BY
Daniel Olive,
Aix Marseille Université, France
Michael A. Caligiuri,
City of Hope National Medical Center,
United States

*CORRESPONDENCE
Lorenzo Moretta
lorenzo.moretta@opbg.net

RECEIVED 26 May 2023
ACCEPTED 25 July 2023
PUBLISHED 10 August 2023

CITATION
Mariotti FR, Ingegnere T, Landolina N, Vacca P, Munari E and Moretta L (2023) Analysis of the mechanisms regulating soluble PD-1 production and function in human NK cells.
Front. Immunol. 14:1229341.
doi: 10.3389/fimmu.2023.1229341

Analysis of the mechanisms regulating soluble PD-1 production and function in human NK cells

Francesca Romana Mariotti[1], Tiziano Ingegnere[1], Nadine Landolina[1,2], Paola Vacca[2], Enrico Munari[3] and Lorenzo Moretta[1]*

[1]Tumor Immunology Unit, Bambino Gesù Children's Hospital, IRCCS, Rome, Italy, [2]Lymphoid Cells of Innate Immunity Unit, Bambino Gesù Children's Hospital, IRCCS, Rome, Italy, [3]Pathology Unit, Department of Molecular and Translational Medicine, University of Brescia, Brescia, Italy

NK cells represent important effectors that play a major role in innate defences against pathogens and display potent cytolytic activity against tumor cells. An array of surface receptors finely regulate their function and inhibitory checkpoints, such as PD-1, can dampen the immune response inducing an immunosuppressive state. Indeed, PD-1 expression in human NK cells correlated with impaired effector function and tumor immune evasion. Importantly, blockade of the PD-1/PD-L1 axis has been shown to reverse NK cell exhaustion and increase their cytotoxicity. Recently, soluble counterparts of checkpoint receptors, such as soluble PD-1 (sPD-1), are rising high interest due to their biological activity and ability to modulate immune responses. It has been widely demonstrated that sPD-1 can modulate T cell effector functions and tumor growth. Tumor-infiltrating T cells are considered the main source of circulating sPD-1. In addition, recently, also stimulated macrophages have been demonstrated to release sPD-1. However, no data are present on the role of sPD-1 in the context of other innate immune cell subsets and therefore this study is aimed to unveil the effect of sPD-1 on human NK cell function. We produced the recombinant sPD-1 protein and demonstrated that it binds PD-L1 and that its presence results in increased NK cell cytotoxicity. Notably, we also identified a pathway regulating endogenous sPD-1 synthesis and release in human NK cells. Secreted endogenous sPD-1, retained its biological function and could modulate NK cell effector function. Overall, these data reveal a pivotal role of sPD-1 in regulating NK-mediated innate immune responses.

KEYWORDS

NK cells, soluble PD-1, cancer, neuroblastoma, immunotherapy

Introduction

Natural Killer (NK) cells are potent immune effector cells that play a major role in innate defences against viruses and tumors (1). Through an array of inhibitory and activating surface receptors, able to recognize specific ligands induced by virus infection or tumor transformation, NK cells are able to discriminate between healthy and neoplastic cells (2, 3). Indeed, while on one side activating receptors allow recognition and killing of tumor cells, on the other side inhibitory receptors, recognize the HLA class-I molecule expressed on healthy cells preventing their killing and counterbalancing NK cell activation (4–6). However, during cancer progression, the transformed cells might decrease or even lose MHC expression increasing their susceptibility to NK cell-mediated killing. In this context, NK cells are considered powerful weapons against tumors characterized by a very low or absent expression of HLA-I, such as Neuroblastoma (NB) (7–9). Nevertheless, neoplastic cells have developed different mechanisms which sharply dampen NK cell anti-tumour activity. In this context, inhibitory checkpoints have been shown to play a pivotal role in regulating the immune response. Their interactions with specific ligands, often overexpressed or expressed *de novo* by transformed cells, activates a signaling cascade that can dampen NK cell effector function thus promoting tumor growth. One of the major inhibitory checkpoints is represented by the Programmed Cell Death-1 (PD-1) protein that specifically interacts with Programmed Cell Death Ligand 1 and 2 (PD-L1, PD-L2) that have been found to be expressed on different tumors, including NB (10). Several studies have demonstrated that PD-1 can be detected on human NK cells and this expression is associated with impaired NK cell function (11–14). Of note, the PD-1/PD-L1 axis represents a mechanism widely adopted by tumor cells to escape the anti-tumor immune control and blockade of this interaction has been shown to recover NK cell function increasing their cytolytic activity (11, 15).

Recently, soluble counterparts of checkpoint receptors and ligands, in particular of PD-1 (sPD-1) and PD-L1 (sPD-L1), are rising high interest because they could positively or negatively regulate the immune response and are considered novel prognostic markers and therapeutic targets (16–18). sPD-1 originates from an alternative splicing event where the Exon3, containing the coding sequence for the transmembrane domain of PD-1, is deleted from the mRNA transcript (19). Thus, the ΔExon3 isoform, lacking the sequence determining membrane localization, encodes for the soluble form of PD-1. Even though it was reported that no soluble form of sPD-1 could be detected in freshly isolated PBMC from HD, it has been suggested that tumor-specific T cells might be the prime source of circulating sPD-1. While it has recently demonstrated that stimulated macrophages are also able to express sPD-1, no data are available on sPD-1 production by other cell subsets involved in anti-tumor response (20). Of note sPD-1, comprising the extracellular domain required for ligands binding, retains the biological function of the full length PD-1 protein. Accordingly, it is able to interact with PD-1 ligands and thus, blocking their interaction with membrane PD-1 it can regulate the immune response (21). Moreover, few studies indicate that prolonged engagement of PD-Ls by sPD-1 can deliver a reverse signaling altering cell functions (22, 23).

Several *in vitro* and *in vivo* studies on mouse models, aimed to investigate the anti-cancer effect of sPD-1, demonstrated that sPD-1 blockade of PD-L1 could increase activation and cytotoxicity of T cells as well as promote reduction of tumor growth (24–27). Similarly, enhancement of anti-tumor immunity was observed when sPD-1 was combined with gene-therapeutic agents further confirming the broad and pivotal anti-cancer properties of sPD-1 (28, 29). In addition, it has been demonstrated that release of sPD-1 strengthen CAR-T cytotoxicity against $CD19^+$ pediatric acute lymphoblastic leukemia cell line and breast cancer cells further demonstrating how sPD-1 could represent a successful therapeutic strategy (30, 31). Importantly, soluble checkpoints are also considered novel therapeutic targets and potential biomarkers. Indeed, high levels of both sPD-1 and sPD-L1 forms have been detected in plasma/serum of different cancer patients, compared to healthy donors (HDs), and have been associated with tumor prognosis, therapeutic response and overall survival (OS) (32–37). Although, several studies demonstrated the pivotal role of sPD-1 in controlling cytotoxic T cells anti-cancer function, there is a lack of knowledge on the role of sPD-1 toward human NK cells. Therefore, in this study we aimed to investigate, on one side whether human NK cell function could be affected by sPD-1 and, on the other side, the mechanisms regulating its production and release.

Materials and methods

Human samples

Buffy coats were collected from healthy donors (HD) admitted to the blood transfusion service of IRCCS Bambino Gesù Children's Hospital after obtaining informed consent. The Ethical Committee of IRCCS Bambino Gesù Children's Hospital approved (AIRC IG2017#19920) and conducted the study in accordance with the tenants of the Declaration of Helsinki.

Cells lines

Human neuroblastoma SKNAS and IMR-32 cell lines were purchased from American Type Culture Collection (ATCC, Rockville, MDA) and were cultured in Dulbecco's Modified Eagle Medium high glucose (Euroclone MI, IT) supplemented with 2 mM l-glutamine (Euroclone), 1% penicillin-streptomycin-neomycin mixture (Euroclone) and 10% heat-inactivated Fetal bovine Serum (FBS) (Euroclone). To detect PD-L1expression, SKNAS and IMR32 cell lines were incubated with anti-PD-L1-PeCF594 (BD Erembodegem, Belgium) and anti-PD-L2-PE-Vio615 (Miltenyi Biotec, Bergisch Gladbach, Germany) for 30 min at 4°C. After wash, samples were acquired using the Cytoflex S (Beckman Coulter) flow cytometer and analysed with the CytExpert 2.4 software (Beckman Coulter, Brea, CA, USA) and the Kaluza software (Beckman Coulter, Brea, CA, USA).

Isolation and stimulation of NK cells

PBMC were obtained after density gradient centrifugation over Ficoll Lumpholyte®-H (Cederlane, Burlington Canada). Highly purified (≥ 95%) $CD56^+$, $CD3^-$ Peripheral Blood NK (PB-NK) cells were isolated with the Rosette Sep and purity of isolated NK cells was verified incubating NK cells with CD-56-PeCy7 and CD3-APC antibodies. For PD-1 induction, NK cells were stimulated for six days with a cocktail of cytokines consisting of IL-12 (10 ng/ml), IL-15 (25 ng/ml), IL-18 (100 ng/ml) (all purchased from Myltenyi) and DMSO (1:2000; SIGMA) (control NK cells) or 1mM Dexamethasone (Stimulated NK cells) (1:2000, SIGMA) (stimulated NK cells). To verify PD-1 expression, NK cells were stained with CD56-Pe-Cy7 and PD-1-PE (130-117-384, Miltenyi) mAbs 30 min 4°C and acquired using the Cytoflex S (Beckman Coulter) flow cytometer and analysed with the CytExpert 2.4 software.

Analysis of cytotoxic activity, degranulation and IFN-γ accumulation

For cytotoxicity analysis, control and stimulated NK cells were incubated with SKNAS or IMR-32 cell lines at an effector-to-target (E:T) ratio ranging from 40:1 to 0.3:1. For analysis of both recombinant and endogenous sPD-1, target cells were previously treated with sPD-1 or conditioned media for 30 min at 37°C and then incubated with NK cells. Cytotoxicity was assessed using a flow cytometric assay for NK-cell killing developed by McGinnes (38) and modified as follow: target cells were stained with 5uM of Cell Tracker Green (CMFDA, Invitrogen) for 15 min at 37C. After wash, target cells were incubated with recombinant sPD-1 at 37C for 30 min and then with the effector NK cells. After 4 hrs incubation propidium iodide (Sigma-Aldrich) was added. Live and dead (Td) target cells were identified as $CMFDA^+$ PI^- and $CMFDA^+$ PI^+, respectively. Specific lysis was calculated as dead target cells (Td) of target cells cultured with effector cells minus Td of target cells cultured alone. To assess degranulation, NK cells were incubated for 4 hrs with SKNAS cells in the presence or not of sPD-1 at 1:1 Effector/Target (E/T) ratio. Monensin (BD, GolgiStop), Golgi Plug (BD) and CD107a-APC (BD) were added to the cocultures. After incubation, cells were stained for surface markers with the following antibodies: CD56-PeCy7 and PD-1-PE. For IFN-γ accumulation NK cells were incubated with SKNAS target cells for four hours in the presence or not of sPD-1. Monensin (BD, GolgiStop), Golgi Plug (BD) were added to the coculture. After incubation, cells were stained with CD56-PeCy7 and PD-1-PE for 30 min at 4°C. After wash cells were fixed and permeabilized with 1% Formalin and 0.1% of Saponin, respectively and then incubated with IFN-γ APC-eF780 (eBiosciences) for 30 min at RT. All samples were acquired with the Cytoflex S flow cytometer and samples were analysed with the CyteExpert and Kaluza software.

Protein extract and Western Blot analysis

For protein extraction, NK cells pellet were resuspended in RIPA buffer with 1X Halt Protease and phosphatase inhibitor cocktail (Thermo Fisher Scientific, Waltham, Massachusetts, USA), incubated on ice for 20 min and centrifuged for 15 min at 21.130 g at 4°C. Supernatants were recovered and protein concentration was measured with the BCA assay (Perkin Elmer, Waltham, Massachusetts, USA) according to manufacturer's instruction. For Western Blotting, protein extracts were fractionated by SDS-page gel electrophoresis and transferred to a PVDF membrane (Ge Healthcare, Little Chalfont, UK). Membrane was initially incubated in TBST with 5% nonfat dry milk (Cell Signaling Technology, Danvers, Massachusetts, USA) with gentle agitation for 60 min, and then with TBST with 3% nonfat dry milk containing the following antibodies: α-PD-1 1:1000 (Abnova, Taipei, Taiwan), α-β-Actin 1:10000 (Sigma-Aldrich), Streptavidin-HRP (NEL 75000 1EA, Perkin Elmer) and anti-mouse-HRP (Cell Signaling Technology). Signals were developed with the ECL prime system (Ge Healthcare) according to manufacturer's instruction and detected with the Uvitec Mini HD9 technology (Uvitec Ltd, Rugby, UK). Quantifications were performed using the Ninealliance© software (Uvitec).

mRNA extraction and real-time PCR

To isolate RNA, NK cells pellets were resuspended in Trizol (Ambion). Chloroform was added and after incubation on ice for 10 minutes, samples were centrifuged at 12,000g for 15 min at 4°C. The aqueous phase was removed and RNA was then isolated with the Qiagen RNeasy Plus Micro kit (Qiagen, Hilden, Germany) according to manufacturer's instruction. cDNAs were synthetized by random priming using the Superscript® IV First-Strand Synthesis System (Invitrogen) according to the manufacturer's instruction. Quantitative Real-time PCR was performed with the QuantStudio 6 Flex PCR (Applied Biosystems) using the PowerUp SYBR Green Master mix (Applied Biosystems) according to manufacturer's instruction. Relative quantification of mRNA was determined by the ΔCt method. PD-1ΔExon3 mRNA expression was normalized against ActinB expression. Primers for real time are as follow: PD-1- ΔExon3 F 5'- AGGGTGACAGGGACAATAGG -3'; PD-1- ΔExon3 R 5'- CCATAGTCCACAGAGAACAC -3'; ActB-F 5'-ACCGCGAGAAGATGACCCAGA-3'; ActB-R 5'-GGATAGCACAGCCTGGATAGCAA-3'.

sPD-1 ELISA

sPD-1 levels were quantified by enzyme –linked immunosorbent assays (ELISA) using the human PD-1 antibody duoset kit (DY1086, R&D Systems) and the DuoSet ELISA Ancillary Reagent kit 2 (DY008, R&D). Plates were coated over night with capture antibody (2 ug/ml). After washes (3 x 300ul with Wash Buffer 1X), 100ul of Reagent Diluent were added to each well and plate was incubated for 1 hr at 700rpm. After a washing step as before, plate incubated with 100ul of sample or standards for 2 hrs with gentle shaking. Calibration curve consisted of 1:2 dilutions of the standard material ranging from 2,5 ng/ml to 0,0097 ng/ml. Plate was subsequently washed and incubated with 100ul of Detection

Antibody (200ng/ml) for 2 hrs with gentle shaking. After repeating the washing step, 100ul of Streptavidin-HRP was added to each well. Plate was incubated in the dark for 40 min, washed and then treated with 100ul of Substrate Solution for 20 min. After addition of 50ul of Stop Solution, optical density was measured using the Synergy H1 Reader (Biotek, Winooski, USA). Sample were read at 450 nm and 540 nm wavelengths and to correct optical imperfection reading at 540nm was subtracted to reading at 450 nm. sPD-1 concentrations (pg/ml) were calculated using the four-point-fit calibration curve of standard dilutions.

Luminex

Analysis of soluble forms of inhibitory checkpoints was performed using the MILLIPLEX MAP kit Human Immuno-Oncology Checkpoint Protein Panel 1 HCKP1-11K (Merck) according to manufacturer's instruction.

Cloning

The pEX-A258-sPD-1-Tev-T2A-tGFP plasmid, containing the sequence for the PD-1 ΔExon3 isoform in frame with Twin-Strep Tag, T2A and turbo GFP (tGFP) tags with the HindIII and BamHI restriction sites at the 5' and 3'ends respectively, was obtained from Eurofins Genomics. Sequence verification was performed after each cloning step and congruence was 100%. After transformation into MAX Efficiency® DH5α (Invitrogen) bacterial cells, colonies were selected on Ampicillin (Sigma) plates and DNA was isolated with the QIAprep Spin Miniprep Kit (27106, Qiagen). DNA samples were restricted with BamHI, HindIII and PvuI (New England Biolabs) and products, along with the 1Kb DNA ladder (N3232S, New England Biolabs) were separated by electrophoresis on a 1% agarose gel. Images were collected using the Uvitec Mini HD9 transilluminator system. The band corresponding to the sequence of interest was isolated from the gel with the MinElute Gel Extraction Kit (28604, Qiagen) according to manufacturer instruction. The eluted DNA samples was cloned into the pcDNA3.1 vector, previously restricted with BamHI and HindIII, using the T4 DNA ligase (M0202S, NEB). After antibiotic selection (Ampicillin), DNA was isolated as described before, restricted with BamHI and HindIII enzymes and separated on 1% agarose gel to confirm efficient cloning of the sequence of interest.

Recombinant sPD-1 protein expression and purification

BL21 DE3 bacterial cells (Invitrogen) transformed with the pCDNA3.1-sPD-1 plasmid were grown in Terrific Broth (Sigma) over night at 30°C and then stimulated with IPTG 1mM (Promega) for 4 hrs. After centrifugation at 3200g 30min at 4°C, cell pellet was resuspended in 20 ml of Sonication Buffer (Hepes 100mM, NaCl 500mM, DTT 1mM and EDTA 0,1mM) and then sonicated as follow: 40% amplitude with 40 sec on/off for 10 times. Sample was centrifuged at 21000g for 30min at 4°C and sPD-1 protein was then purified with the Strep-Tactin®XT purification column according to manufacturer instructions. The purified sample was transferred into Amicon Ultra-4 10K centrifugal filter devices (Merck), centrifuged at 3000g for 20min at 4°C and washed as follow: 4ml of Storage Buffer (NaCl 330mM, Tris-HCl pH6.8 11mM, EDTA 0,11mM and DTT 1,1 mM) at 3000g for 20 min at 4°C for 8 times. Protein concentration was measured with the BCA assay (Perkin Elmer, Waltham, Massachusetts, USA) according to manufacturer's instruction.

Coomassie staining

Purified protein sample was fractionated by SDS-Page gel electrophoresis and detected by Coomassie blu dye staining. After run, gel was incubated with the Fixing solution (50% methanol and 10% acetic acid) for 1hr and then stained (50% methanol, 10% acetic acid and 0.1% Coomassie Brilliant Blue R-250) for 20min with gentle agitation. Gel was incubated in the Distaining solution (40% methanol and 10% acetic acid) replenishing the solution several times until background of the gel was fully distained. Gel was stored in 5% acetic acid solution and images were acquired with the Uvitec Mini HD9 technology.

sPD-1 and sPD-L1 binding

SKNAS and IMR32 cells were firstly treated with PBS and 1% FBS for 30 min and then incubated with 1μg or 5μg of recombinant sPD-1 for 30min at 37°C. After washing, samples were incubated with Streptavidin-PE (Biolegend) antibody 1:50 or PD-L1 1:50 for 30min at 4°C. To demonstrate the specificity of sPD-1 for PD-L1, SKNAS were initially incubated with IgG1 Isotype control (DDXCH01P-100, Novus Biological) or Atezolizumab (A2004, Selleckchem) for 30 min at 4°C and subsequently with recombinant sPD-1 for 30min at 37°C. After washing, samples were incubated with anti-Streptavidin-PE (Biolegend) antibody for 30min at 4°C. Binding of Atezolizumab to PD-L1 was performed incubating SKNAS with IgG1 Isotype control or Atezolizumab for 30 min at 4°C and then with anti-PDL1 for 30 min at 4°C. SKNAS treated with PBS were used as control. All samples were acquired using the Cytoflex S as described before. For analysis of sPD-1 and sPD-L1 binding SKNAS, Ctrl and Stimulated NK cells were incubated with the conditioned media for 1 hours at 37°C and, after washes, samples were incubated with PD-1 or PD-L1 antibody. Binding of Nivolumab (A2002, Selleckchem) to PD-1 was performed incubating stimulated NK cells with IgG4 control Isotype (DDXCH04P-100, Novus Biological) or Nivolumab for 30 min at 4°C and then with anti-PD1 for 30 min at 4°C. Stimulated NK cells, treated with PBS were used as control.

Statistical analysis

Statistical analyses were performed using the GraphPad Prism 6.0 (La Jolla, CA, USA) software. Values were expressed as mean ± SEM. P values less than 0.05 were considered statistically significant. * P< 0.05, ** P< 0.01 *** P< 0.001.

Results

In the recent years, soluble counterparts of the inhibitory checkpoints, in particular sPD-1 and sPD-L1, have gained attention due to their ability to regulate immune responses. Importantly, these soluble forms retain the ability to bind their ligands and therefore they can inhibit PD-1/PD-DL1 interaction. Indeed, local delivery of sPD-1 in the tumor microenvironment (TME), has been demonstrated to enhance T cell cytotoxicity through PD-L1 binding and the consequent blockade of the PD-1/PD-L1 axis. However, little is known on its biological effect on NK cell function and on the mechanisms regulating its release. Therefore, we decided to investigate whether sPD-1could be able to modulate NK cell effector function. For this purpose, we first synthetized the recombinant sPD-1 protein. To this end, the designed the sPD-1-T2A-tGFP sequence was subcloned into the pcDNA3.1 plasmid and then transformed into the BL21 bacterial cells for protein induction (Figures S1A, B). Coomassie staining confirmed that the purified protein was of approximately 20 kDa (Figure 1A, left panel), as expected for the recombinant sPD-1 protein. To further evaluate the purity of the isolated protein and also confirm that it effectively corresponded to the soluble counterpart of PD-1 we performed western blot analysis using the α-Streptavidin and α-PD-1 antibodies. As reported in the right panel of Figure 1A, hybridization with α-Streptavidin antibody allowed detection of one band corresponding to the isolated recombinant sPD-1 protein. In line with this data, incubation with the α-PD-1 antibody allowed detection of the same band observed with the Streptavidin antibody, thus confirming that the recombinant sPD-1 protein was efficiently purified (Figure 1A, right panel). To better characterize the isolated sPD-1 protein, we then investigated whether it retained the functional capability of binding to PD-1 ligands. For this purpose two NB cell lines, SKNAS and IMR-32, that differentially express PD-L1 while having almost undetectable levels of the PD-L2 receptor, were used (Figure 1B). The SKNAS and IMR-32 cell lines were incubated alone or with different amounts (1-5 μg) of the recombinant protein and sPD1/PD-L1 interaction was detected as binding of the α-Streptavidin antibody to the Strep-tag present on sPD-1. As reported in Figure 1C a shift in the Streptavidin signal could be observed only when sPD-1 was added to the cell cultures, demonstrating that the recombinant protein was able to bind PD-L1 expressed on both cell lines. Interestingly, the intensity of the signal proportionally increased with the amount of sPD-1 (Figure 1C). To demonstrate the specificity of sPD-1/PD-L1 interaction, we used Atezolizumab, a fully humanized IgG1 monoclonal antibody (mAb) that engages PD-L1. Indeed, following incubation of SKNAS with Atezolizumab, IgG1 isotype or PBS, abrogation of PD-L1 signal was observed only in the presence of the anti-PD-L1 mAb (Figure 1D, left panel). Therefore, to investigate whether mAb treatment would affect PD-L1 engagement by sPD-1, SKNAS were incubated with PBS, Atezolizumab or control IgG1 isotype antibody and subsequently treated with recombinant sPD-1. The interaction between PD-L1 and sPD-1 was analysed by Streptavidin signal and samples treated with PBS represented the negative control. As expected, sPD-1 binding was detected in SKNAS cells treated with PBS and the control isotype while in tumor cells that have been previously treated with Atezolizumab loss of streptavidin signal was detected, demonstrating that masking of PD-L1 prevented sPD-1 binding to its molecular target (Figure 1D, right panel). To further investigate the property of sPD-1 binding, the PD-L1 Mean Fluorescent Intensity (MFI) of both SKNAS and IMR32 was analysed. In line with previous data, a partial reduction of PD-L1 MFI was observed in both the NB cell lines incubated with recombinant sPD-1, showing that sPD-1-dependent engagement of PD-L1 could reduce antibody binding (Figure 1E). No significant differences regarding PD-L1 MFI were detected upon treatment with 5μg of recombinant sPD-1 (data not shown). Together, these data demonstrate that we efficiently purified the recombinant soluble counterpart of PD-1. Importantly, the isolated sPD-1 protein retained its ability to specifically bind PD-L1 expressed on NB tumor cell lines, as demonstrated by the abrogation of sPD-1/PD-L1 interaction upon treatment with Atezolizumab.

We then asked whether the interaction between sPD-1 and PD-L1, expressed on tumor cells, could affect the ability of NK cells to kill NB target cell lines. For this purpose, freshly isolated NK cells were stimulated *in vitro*, as previously described by our group, with IL-12/IL-15/IL-18 in the presence of DMSO (Ctrl) or Dexamethasone (Stim), in order to induce the expression of PD-1 on the cell membrane (13). Indeed, increase of membrane PD-1 expression was detected in stimulated NK cells compared to control cells (Figure 2A). Recently, it has been shown that incubation of NK cells with the same cytokine milieu induces PD-L1 membrane upregulation (39). In line with published data, Ctrl NK cells showed a massive PD-L1 expression (Figure 2A left panel). Interestingly, stimulated NK cells do not express PD-L1 at the surface indicating that these receptors are regulated by different mechanisms (Figure 2A right panel). Therefore, to investigate any effect of sPD-1 in regulating the immune response we performed the following experiments on Stimulated NK cells that being PD-1^{+} PD-$L1^{-}$ ensure that sPD-1 would bind exclusively to PD-L1 expressed on tumor cells. To analyse the effector functions of stimulated NK cells, cytotoxicity was analysed after 4 hrs incubation with SKNAS or IMR-32 cell lines, in the presence or in the absence of recombinant sPD-1. As reported in Figure 2B an increase of NK cell killing was detected, against both NB cell lines, only when sPD-1 was present in the culture medium demonstrating that sPD-1 dependent blockade of PD-1/PD-L1 axis would promote NK cell effector function. In line with these data, increase of degranulation and IFN-γ accumulation were detected in the presence of sPD-1 compared to untreated samples (Figure 2C left and right panels).

10.3389/fimmu.2023.1229341

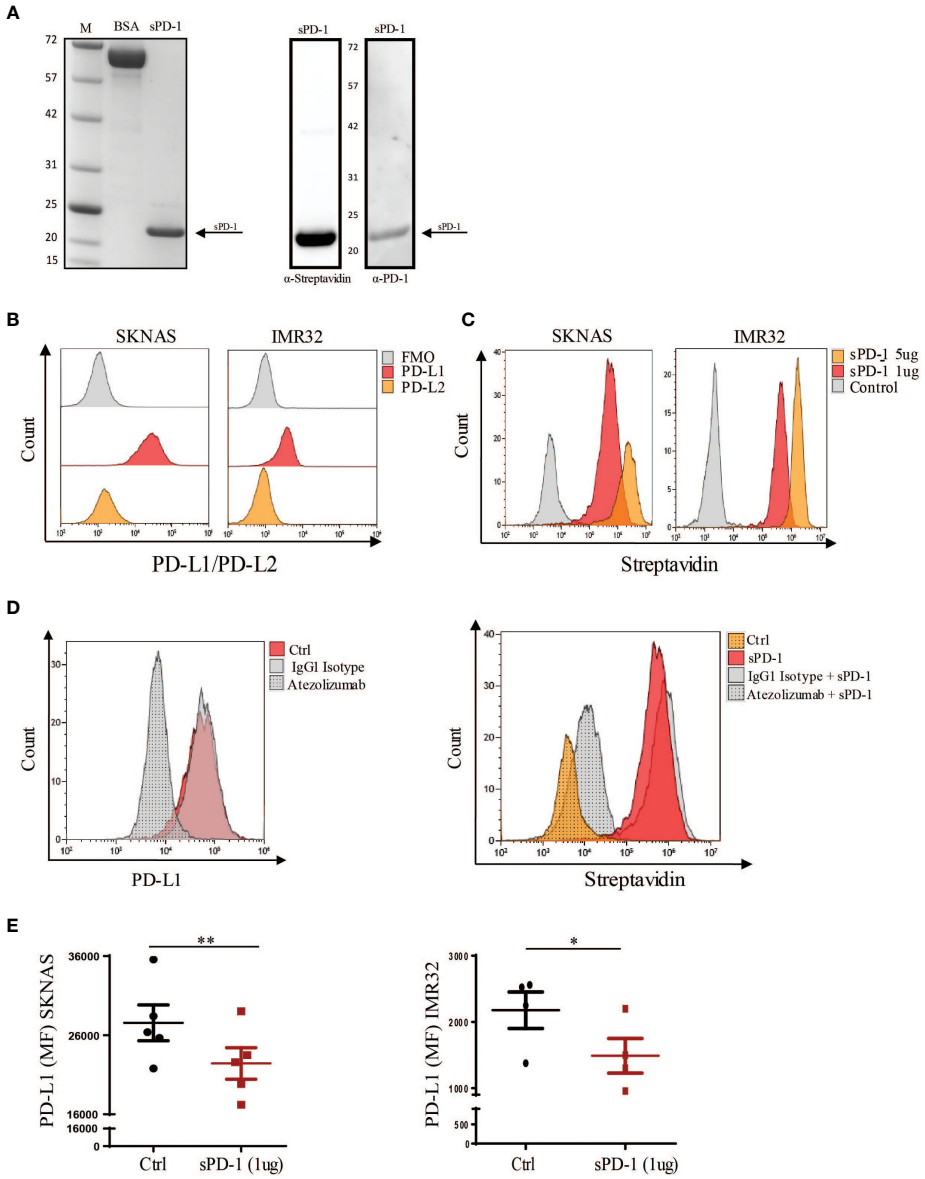

FIGURE 1
Characterization of the isolated recombinant sPD-1 protein. **(A)** Gel-based proteomic analysis of purified sPD-1. Left panel: Coomassie staining of the isolated recombinant sPD-1 revealed a band of approximately 20 kDa corresponding to sPD-1 molecular weight. BSA sample was used as a control. Right panel: western blot analysis allowed detection of the recombinant sPD-1 protein with both the anti-Streptavidin-HRP and anti-PD-1 antibodies. **(B)** SKNAS and IMR-32 cell lines were analysed for PD-L1 and PD-L2 expression. Only PD-L1 could be detected on the surface of both cell lines. **(C)** Analysis of recombinant sPD-1 binding to PD-L1 ligand. Flow cytometry analysis demonstrated that recombinant sPD-1 was able to bind PD-L1 expressed by SKNAS and IMR-32 cell lines. **(D)** SKNAS were incubated with PBS, IgG1 Isotype or Atezolizumab and then analysed for PD-L1 expression. Abrogation of PD-L1 signal occurred only when tumor cells were treated with Atezoliumab (left panel). Binding of sPD-1 to tumor expressed PD-L1 was abrogated when NB cells were previously incubated with Atezolizumab. **(E)** Incubation of PD-L1^{+} SKNAS and IMR-32 cell lines with recombinant sPD-1 resulted in a decreased PD-L1 signal. MFI from ctrl (not stained) samples was subtracted from their corresponding stained samples. Values are mean ± SEM. Statistical significance has been determined by Paired T test, $p< 0.01$ **; $p<0.05$ *.

To further investigate the effect of sPD-1 on the regulation of the immune response, we compared its effect with Nivolumab, an IgG4 humanized mAb able to block membrane PD-1. Indeed, Nivolumab incubation abrogated PD-1 detection on Stimulated NK cells compared to Ctrl and IgG4 isotype-treated cells (Figure 2D, left panel). Cytotoxicity was analysed between stimulated NK cells treated or not with Nivolumab in the presence or in the absence of sPD-1. As previously demonstrated, increased tumor cell killing was detected in Stimulated NK cells incubated with sPD-1 compared to ctrl cells (-sPD-1) (Figure 2D right panel). Similarly, higher cytotoxicity was detected in Nivolumab-treated cells only in the presence of sPD-1. Interestingly, Nivolumab-treated NK cells exerted an effector function similar to Ctrl cells and it was significantly lower as compared to the same conditions incubated with recombinant sPD-1. No significant differences, except at the higher E:T ratio,

10.3389/fimmu.2023.1229341

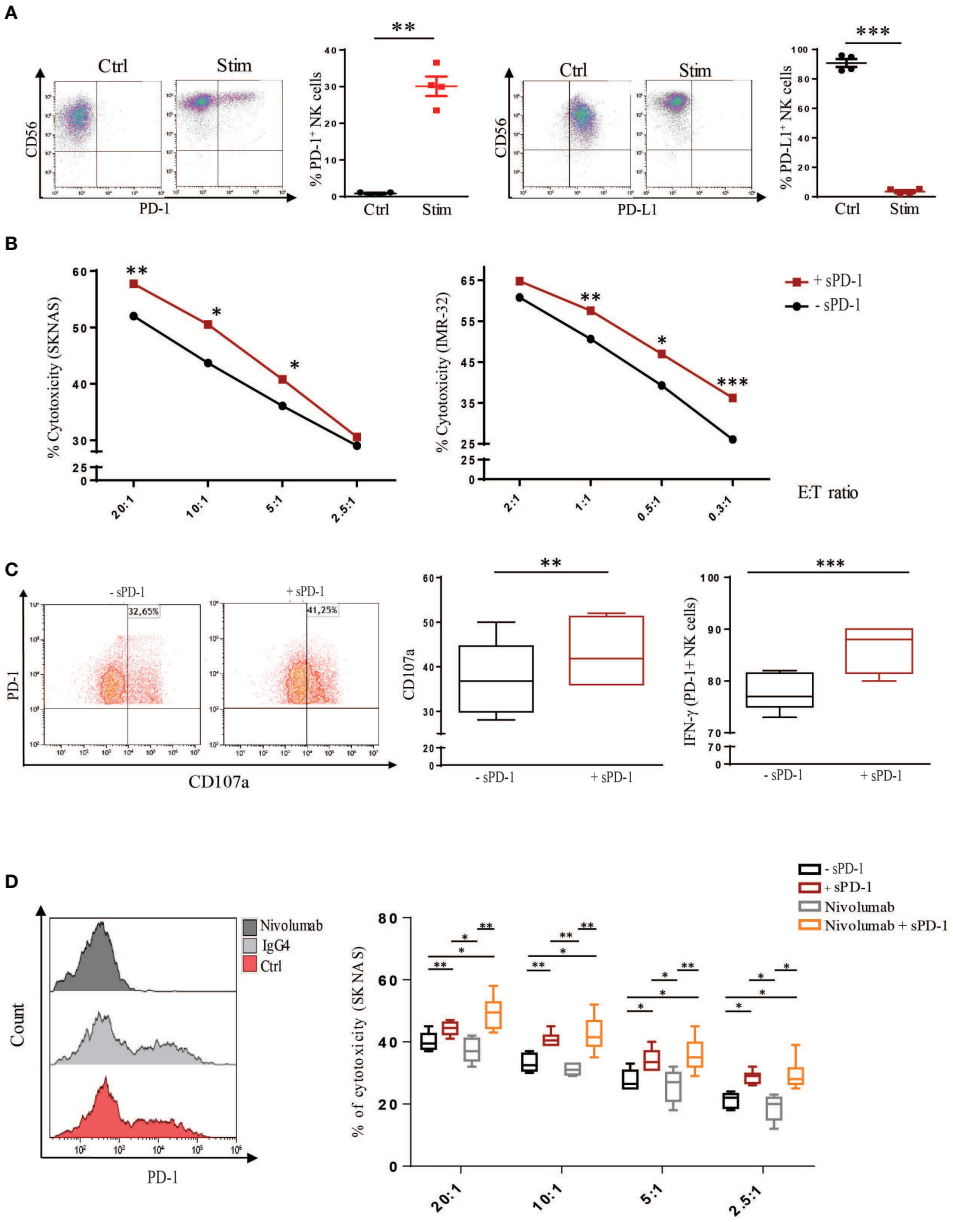

FIGURE 2
Recombinant sPD-1 can modulate NK cell effector function. **(A)** Control and stimulated NK cells were analysed for membrane PD-1 and PD-L1 expression. Membrane-bound PD-1 was detected only in stimulated NK cells compared to control cells. Conversely, while Ctrl NK cells expressed PD-L1, it was barely detectable on stimulated NK cells. One representative experiment has been shown. Quantifications of four different experiments have been reported. Values are mean ± SEM. Statistical significance has been determined by Paired T test, p< 0.01 **; p< 0.001 ***. **(B)** NB cell lines were incubated with stimulated NK cells, expressing PD-1, with or without recombinant sPD-1. An increase in cytotoxicity toward both SKNAS (n=7) and IMR-32 (n=8) cell lines at different Effector **(E)** Target (T) ratios was observed only when recombinant sPD-1 was present in the co-culture. Data have been compared using paired T test, p< 0.05 *; p< 0.01 **, p< 0.001 ***. **(C)** Similarly, in the presence of recombinant sPD-1 an increase in degranulation (left and middle panels) and accumulation of IFN-γ (right panel) of NK cells were observed. Values are mean ± SEM. Statistical significance has been determined by Paired T test, p< 0.01 **, p< 0.001 ***. **(D)** Comparison of sPD-1 and Nivolumab treatments on cytotoxicity of stimulated NK cells. Incubation with Nivolumab abrogated PD-1 signal compared to Ctrl and IgG4 samples (left panel). Increase of cytotoxicity toward SKNAS cell line at different E:T ratio was observed in both the analysed conditions (treated or not with Nivolumab) only in the presence of sPD-1. Values are mean ± SEM. Data have been compared using paired T test, p< 0.05 *; p< 0.01 **, p< 0.001 ***.

could be observed between the two sPD-1 treated samples indicating that, in this condition, Nivolumab treatment does not further improve NK cell killing (Figure 2D right panel). These data demonstrate that recombinant sPD-1, through its interaction with PD-L1 expressed by tumor cells, can partially block the inhibitory axis thus improving human NK cell effector function toward NB cell lines.

As discussed above, the soluble form of the PD-1 checkpoint inhibitor has been detected in the plasma of cancer patients. However, despite its clinical importance little is known on cell

subsets involved in its production and the mechanisms of its release. As mentioned before, our group recently demonstrated that stimulation with a specific combination of cytokines and Dexamethasone, resulted in PD-1 surface expression in human NK cells (13). Therefore, we asked whether the same stimulus could also induce for sPD-1 production and release. To this end, human NK cells, isolated from HDs, were stimulated or not (Ctrl) as previously described and then analysed for sPD-1 synthesis and release. As reported in Figure 3A, while the ΔExon3 transcript could be barely detected in Ctrl NK cells, its expression levels were highly increased upon stimulation. In line with this data, sPD-1 protein could be detected only in stimulated NK cells indicating that the increase of the ΔExon3 mRNA transcription correlated with a rise in protein translation (Figure 3B). To investigate if the increase in protein translation was associated also to sPD-1 release supernatants from both Ctrl and stimulated NK cells were analysed. As expected, increased sPD-1 levels were detected only in the medium from stimulated NK cells compared to Ctrl samples (Figure 3C). All together, these data demonstrate that human NK cells, when properly stimulated, are able to increase both sPD-1 mRNA transcription and protein synthesis as well as its release in the surrounding medium revealing that NK cells may represent a source for circulating sPD-1.

We then studied whether endogenous sPD-1, produced by NK cells, retained its ability to interact with PD-L1 and whether this engagement would affect NK cell effector function. For this purpose human NK cells were stimulated or not in order to obtain different conditioned supernatants (SN) that were then used to treat tumor cells and study the sPD-1 biological function (Figure 4A). Even though we previously demonstrated that sPD-1 could be detected only in the SN from stimulated NK cells we could not exclude that the two conditioned media would differ exclusively for sPD-1 expression. Therefore, we analysed the expression of soluble forms of different inhibitory checkpoints in the two SN. Interestingly, in the media derived from Ctrl NK cells sPD-L1 and sPD-L2 levels were higher compared to SN from stimulated NK cells (Figure 4B). Conversely, sPD-1 was the only soluble form upregulated in SN from stimulated NK cells. Of note, these data are in line with PD-1 and PD-L1 membrane expression on NK cells. To investigate whether endogenous sPD-1 would be able to bind PD-L1, both Ctrl NK cells and SKNAS were incubated with the different SN and PD-L1 expression was analysed. Reduction of PD-L1 MFI was observed in both samples only when incubated with the medium containing sPD-1 (Figure 4C left and middle panels). Interestingly, a reduction of PD-1 MFI occurred only in Stimulated NK cells incubated with SN containing sPD-Ls indicating that these soluble forms were able to interact with membrane PD-1 reducing antibody binding (Figure 4C right panel). We further investigated whether the interaction between endogenous sPD-1 and PD-L1 could have an effect on NK cell function as previously detected with the recombinant sPD-1 protein. Thus, SKNAS cells and stimulated human NK cells were incubated together using the supernatants from ctrl and stimulated NK cells in order to compare blockade of the PD-1/PD-L1 axis acting on PD-1 or tumor expressing PD-L1, respectively. Except for the higher E:T ratio, where increased cytotoxicity was observed in the presence of SN from stimulated NK cells no significant differences could be observed even though there is a trend of higher cell killing when PD-L1 ligand is bound (Figure 4D).

Discussion

In cancer, the PD-1/PD-L1 axis has been the subject of intense investigations and its blockade, through the development of mAbs disrupting this interaction, has revolutionized tumor immunotherapies. Recently, the soluble counterpart of PD-1 has gained interest due to its prognostic and predictive value in tumor patients, which has opened a new paradigm of investigation in different cancer types. In addition, sPD-1, retaining the function proper of full-length PD-1, is able to engage with membrane-bound ligands and enhance T cell-dependent anti-tumor immune responses limiting the binding of PD-1^+ cells with PD-Ls^+ neoplastic cells. In this context, we investigated the role of sPD-1 toward human NK cell function and the mechanisms regulating its expression. In particular, we purified a recombinant form of sPD-1 able to interact with PD-L1 expressed by tumor cell lines. The sPD-1/PD-L1 interaction was specific as demonstrated by the abrogation of sPD-1 binding upon treatment of tumor cells with Atezolizumab and by reduction of PD-L1 MFI indicating that sPD-1might act as a decoy for anti-PD-L1 antibody. Importantly, sPD-1-dependent blockade of PD-L1 pathway was able to modulate the anti-tumor immune response of human NK cells. Indeed, we observed an increase of tumor cell killing, degranulation and IFN-g accumulation in the presence of sPD-1 as compared to ctrl (-sPD-1) samples.

Considering the biological importance of the circulating soluble form of PD-1, we focused our attention on mechanisms regulating endogenous sPD-1 production. In a previous work, investigating the expression of PD-1 in human NK cells, we demonstrated that resting and *in vitro* activated NK cells, isolated from HDs, expressed the PD-1 ΔExon3 mRNA isoform, even though no sPD-1 protein could be detected in the cytoplasm or in the culture supernatants (40). Moreover, sPD-1 was detected in the pleural effusions (PE) of lung cancer patients and the ΔExon3 mRNA transcript was detected in NK cells purified from the same PE. Therefore, we argued that human NK cells could be involved in sPD-1 production. Indeed, we demonstrated that specific stimulation of human NK cells leads to increase sPD-1 transcription, synthesis and release in the culture medium. These data unveil a novel mechanism regulating sPD-1 production and also demonstrates that human NK cells are capable of releasing sPD-1. Of note, analysing the different SN we confirmed that released of sPD-1 would occur only in Stimulated NK cells and showed that ctrl NK cells are able to release sPD-L1 and sPD-L2 in the culture medium indicating that NK cells could be considered a source for sPD-Ls circulating forms.

Interestingly, binding assays showed decreased PD-L1 and PD-1 MFI upon treatment of NK and SKNAS cells with SN from stimulated and ctrl NK cells, respectively indicating that soluble checkpoint inhibitors retained the ability to interact with their specific targets and thus could act as decoy for antibody binding. However, comparing PD-L1 and PD-1 blockade, taking advantage of the different conditioned media, no significant differences could be observed.

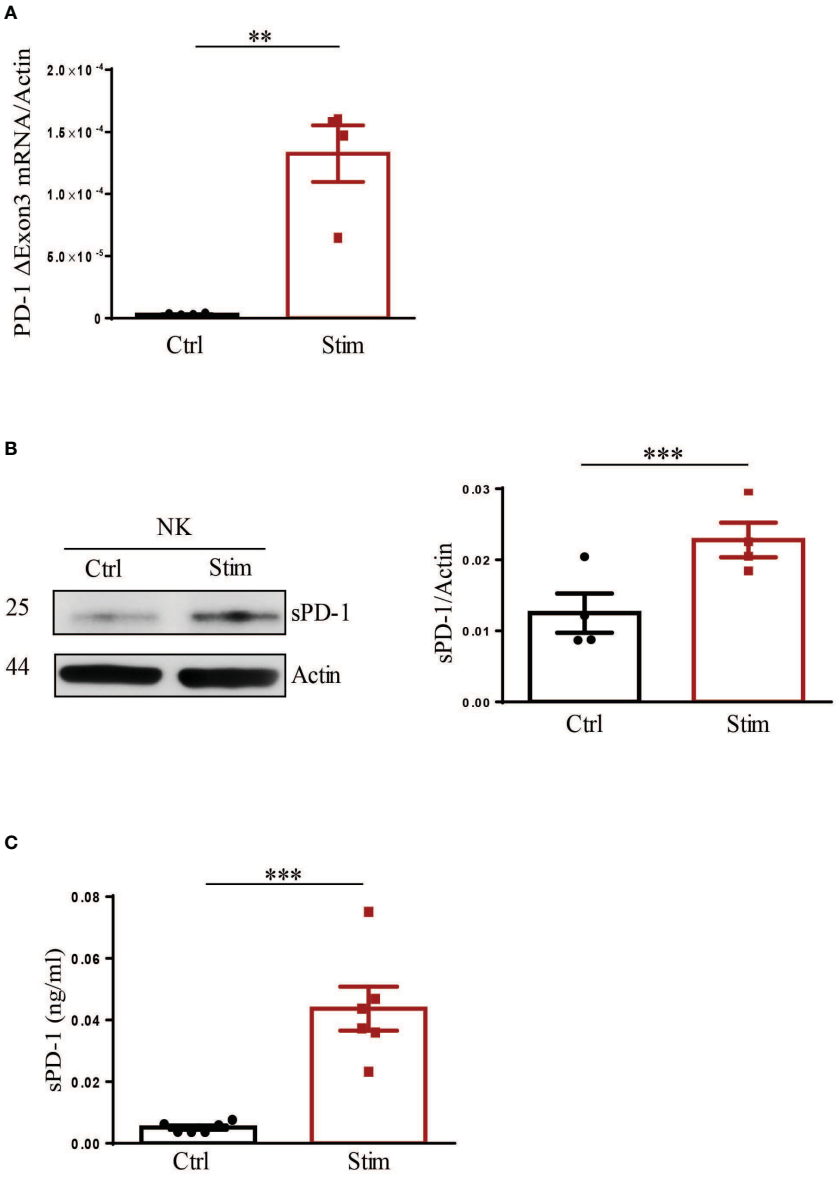

FIGURE 3
Stimulation of NK cells leads to production and release of endogenous sPD-1. Control (Ctrl) and stimulated (stim) NK cells were analysed for endogenous sPD-1 expression. **(A)** Real-time analysis demonstrated a huge increase of the ΔExon3 mRNA transcript in stimulated compared to ctrl NK cells. **(B)** Western blot analysis demonstrated that an increase in sPD-1 protein level could be observed in NK cells upon stimulation. **(C)** Supernatant of both Ctrl and Stimulated NK cells were analysed by ELISA. High levels of endogenous sPD-1 were detected in the medium derived from stimulated NK cells, while in sample from Ctrl NK cells endogenous sPD-1 could be barely detected. All values are mean ± SEM. Statistical significance has been determined by Paired T test, p< 0.01 **; p< 0.001 ***.

Despite our demonstration of the involvement of human NK cells in producing sPD-1 and its role in regulating antitumor immune response, some limitations of this study must be considered. The recombinant sPD-1 protein, being produced in bacteria, does not present the posttranslational modifications (PTMs) proper of full-length PD-1 and known to be important for its function and therefore in our setting we could not investigate how the PTMs would affect recombinant sPD-1 function. In addition, the effects of endogenous soluble forms on NK cell effector function are less marked compared to the modulation observed with the recombinant sPD-1 protein. This could be explained by the fact that the average amount of released sPD-1 and sPD-L1 by stimulated and ctrl human NK cells is quite low and it might not be sufficient to efficiently block the PD-1/PD-L1 pathway and modulate NK cell anti-tumor activity. Indeed, median values of circulating sPD-1 in serum/plasma of cancer patients can span from almost 400 pg to even 8 ng or more (27, 32). Moreover, in the TME, due to the close cellular interactions and to the presence of several cytokines and other soluble factors, the concentrations of sPD-1 may actually be quite higher. Therefore, in the present set up, it is conceivable that we underestimate the real contribution of endogenous sPD-1 on human NK cell function. In this context, it would be interesting to purify the endogenous sPD-1 protein in order to deeper investigate its biological function and

10.3389/fimmu.2023.1229341

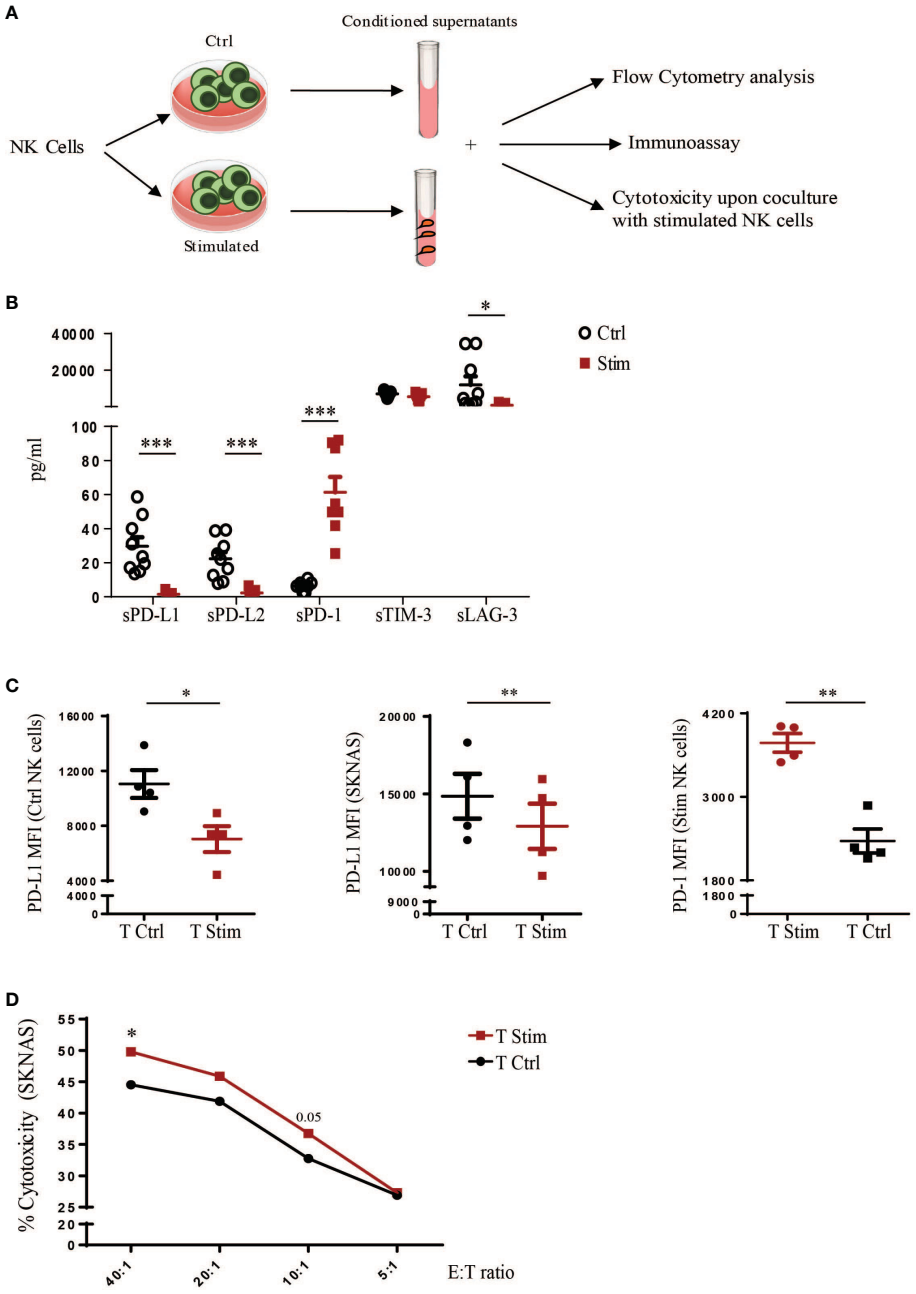

FIGURE 4
Effects of endogenous sPD-1 on human NK cell function. **(A)** Schematic representation of the designed experiments to investigate the functional activity of endogenous soluble forms released by human NK cells. **(B)** Luminex assay on the SN to evaluate the expression of soluble forms of different inhibitory checkpoints released by human NK cells in the two treatment conditions. All values are mean ± SEM. Statistical significance has been determined by Paired T test, p< 0.05 *; p< 0.001 ***. **(C)** Ctrl and Stimulated NK cells and SKNAS cell line were incubated with conditioned medium deriving from unstimulated (Ctrl) or stimulated (Stim) NK cells and binding of endogenous sPD-1, and sPD-Ls present in the medium, was analysed by flow cytometry as decrease in PD-L1 and PD-1 MFI. Values are mean ± SEM. Statistical significance has been determined by Paired T test, p< 0.05 *; p< 0.01 **. **(D)** Cytotoxicity of stimulated NK cells toward SKNAS cell line at the indicated Effector (E): Target (T) ratios upon incubation with conditioned media. Values (% of cytotoxicity) represent the mean of nine independent experiments. Data have been analysed using paired T test, p< 0.05 *.

define the amount sufficient for enhancing NK-mediated function. Indeed, there is a lack of information in the literature on the role played by sPD-1 in the context of pediatric tumors and the presented data might suggest that sPD-1 could play a role as an immune regulator in NB.

In conclusion, we identified a mechanism regulating sPD-1 synthesis and release in human NK cells demonstrating that this innate cells can also be considered a source for circulating sPD-1. Moreover, our present study provides a first insight on the effect of sPD-1 on human NK cell effector function, confirming that sPD-1,

retaining its ability to bind PD-L1, can disrupt the PD-1/PD-L1 axis and counteract the inhibitory effect of this interaction.

Overall, these data confirm the important role played by sPD-1 in regulating the anti-tumor immune response and suggest that sPD-1 could be considered a novel additional tool for anti-cancer therapies in paediatric tumors.

Data availability statement

The original contributions presented in the study are included in the article/Supplementary Material. Further inquiries can be directed to the corresponding author.

Ethics statement

The studies involving human participants were reviewed and approved by Ethical Committee of Bambino Gesù Children's Hospital, IRCCS. The patients/participants provided their written informed consent to participate in this study.

Author contributions

FM designed and performed experiments, interpreted data and wrote the manuscript. TI and NL performed experiments and reviewed the manuscript. EM reviewed the manuscript. PV and LM discussed results and reviewed the manuscript. All authors contributed to the article and approved the submitted version.

Funding

This work was supported by Associazione Italiana per la ricerca sul Cancro (project no. 5x1000 2018 Id 21147 to LM, project no. IG 2017 Id 19920 to LM, IG2022 Id.27065 to PV) and by Current Research found 5x1000 project no. 202305_IMMUNO_MARIOTTI to FRM. FRM was supported by Fondazione Umberto Veronesi. NL is supported by the i-CARE fellowship awarded by AIRC and from the European Union's Horizon 2020 research and innovation program under the Marie Skłodowska-Curie (grant agreement No. 800924NL). This work was supported also by the Italian Ministry of Health with "Current research funds".

Conflict of interest

The authors declare that the research was conducted in the absence of any commercial or financial relationships that could be construed as a potential conflict of interest.

Publisher's note

Supplementary material

The Supplementary Material for this article can be found online at: https://www.frontiersin.org/articles/10.3389/fimmu.2023.1229341/full#supplementary-material

SUPPLEMENTARY FIGURE 1
Construction of the pCDNA3.1-sPD-1-Twin-Strep-tag-T2A-GFP plasmid. **(A)** Left panel: schematic representation of the region, within the pEX-A258 plasmid, containing the sPD-1 coding sequence in frame with the TEV site and the Twin-Strep-tGFP sequence. HindIII and BamHI restriction enzyme sequences were introduced at the beginning and the end of the described region, respectively. Right panel: upon DH5alpha bacterial cells transfection, positive colonies were screened by HindIII, BamHI and PvuI restriction and samples were separated on agarose gel. The red arrow indicates the band of 2187 bp corresponding to the sPD-1-Twin-Strep-tGFP region. **(B)** Circular map of the pCDNA3.1-sPD-1-Twin-Strep-tag-T2A-GFP plasmid upon subcloning of the sPD-1-Twin-Strep-tGFP region (left panel). Colonies grown in selective plates were analysed by HindIII and BamHI restriction and samples were run on agarose gel (right panel). The red arrow indicates the sPD-1-Twin-Strep-tGFP band.

References

1. Wolf NK, Kissiov DU, Raulet DH. Roles of natural killer cells in immunity to cancer, and applications to immunotherapy. *Nat Rev Immunol* (2023) 23:90–105. doi: 10.1038/S41577-022-00732-1

2. Kumar S. Natural killer cell cytotoxicity and its regulation by inhibitory receptors. *Immunology* (2018) 154:383–93. doi: 10.1111/IMM.12921

3. Sivori S, Vacca P, Del Zotto G, Munari E, Mingari MC, Moretta L. Human NK cells: surface receptors, inhibitory checkpoints, and translational applications. *Cell Mol Immunol* (2019) 16:430–41. doi: 10.1038/s41423-019-0206-4

4. Barrow AD, Martin CJ, Colonna M. The natural cytotoxicity receptors in health and disease. *Front Immunol* (2019) 10:909/BIBTEX. doi: 10.3389/FIMMU.2019.00909/BIBTEX

5. Moretta A, Bottino C, Vitale M, Pende D, Cantoni C, Cristina M, et al. Activating receptors and coreceptors involved in human natural killer cell-mediated cytolysis. *Annu Rev Immunol* (2001) 19:197–223. doi: 10.1146/annurev.immunol.19.1.197

6. Kamiya T, Seow SV, Wong D, Robinson M, Campana D. Blocking expression of inhibitory receptor NKG2A overcomes tumor resistance to NK cells. *J Clin Invest* (2019) 129:2094–106. doi: 10.1172/JCI123955

7. Bottino C, Dondero A, Bellora F, Moretta L, Locatelli F, Pistoia V, et al. Natural killer cells and neuroblastoma: tumor recognition, escape mechanisms, and possible novel immunotherapeutic approaches. *Front Immunol* (2014) 5:56. doi: 10.3389/fimmu.2014.00056

8. Bottino C, Della Chiesa M, Sorrentino S, Morini M, Vitale C, Dondero A, et al. Strategies for potentiating NK-mediated neuroblastoma surveillance in autologous or HLA-haploidentical hematopoietic stem cell transplants. *Cancers* (2022) 14:4548. doi: 10.3390/CANCERS14194548

9. Wu SY, Fu T, Jiang YZ, Shao ZM. Natural killer cells in cancer biology and therapy. *Mol Cancer* (2020) 19:1–26. doi: 10.1186/S12943-020-01238-X/TABLES/3

10. Dondero A, Pastorino F, Della Chiesa M, Corrias MV, Morandi F, Pistoia V, et al. PD-L1 expression in metastatic neuroblastoma as an additional mechanism for

limiting immune surveillance. *Oncoimmunology* (2016) 5:e1064578. doi: 10.1080/2162402X.2015.1064578

11. Pesce S, Greppi M, Tabellini G, Rampinelli F, Parolini S, Olive D, et al. Identification of a subset of human natural killer cells expressing high levels of programmed death 1: A phenotypic and functional characterization. *J Allergy Clin Immunol* (2017) 139:335–346.e3. doi: 10.1016/j.jaci.2016.04.025

12. Tumino N, Martini S, Munari E, Scordamaglia F, Besi F, Mariotti FR, et al. Presence of innate lymphoid cells in pleural effusions of primary and metastatic tumors: Functional analysis and expression of PD-1 receptor. *Int J Cancer* (2019) 145:1660–8. doi: 10.1002/ijc.32262

13. Quatrini L, Vacca P, Tumino N, Besi F, Di Pace AL, Scordamaglia F, et al. Glucocorticoids and the cytokines IL-12, IL-15, and IL-18 present in the tumor microenvironment induce PD-1 expression on human natural killer cells. *J Allergy Clin Immunol* (2021) 147:349–60. doi: 10.1016/j.jaci.2020.04.044

14. Trefny MP, Kaiser M, Stanczak MA, Herzig P, Savic S, Wiese M, et al. PD-1+ natural killer cells in human non-small cell lung cancer can be activated by PD-1/PD-L1 blockade. *Cancer Immunol Immunother* (2020) 69:1505–17. doi: 10.1007/s00262-020-02558-z

15. Oyer JL, Gitto SB, Altomare DA, Copik AJ. PD-L1 blockade enhances anti-tumor efficacy of NK cells. *Oncoimmunology* (2018) 7. doi: 10.1080/2162402X.2018.1509819

16. Gu D, Ao X, Yang Y, Chen Z, Xu X. Soluble immune checkpoints in cancer: production, function and biological significance. *J Immunother Cancer* (2018) 6. doi: 10.1186/S40425-018-0449-0

17. Tominaga T, Akiyoshi T, Yamamoto N, Taguchi S, Mori S, Nagasaki T, et al. Clinical significance of soluble programmed cell death-1 and soluble programmed cell death-ligand 1 in patients with locally advanced rectal cancer treated with neoadjuvant chemoradiotherapy. *PloS One* (2019) 14. doi: 10.1371/JOURNAL.PONE.0212978

18. Oh SY, Kim S, Keam B, Kim TM, Kim DW, Heo DS. Soluble PD-L1 is a predictive and prognostic biomarker in advanced cancer patients who receive immune checkpoint blockade treatment. *Sci Rep* (2021) 11. doi: 10.1038/S41598-021-99311-Y

19. Nielsen C, Ohm-Laursen L, Barington T, Husby S, Lillevang ST. Alternative splice variants of the human PD-1 gene. *Cell Immunol* (2005) 235:109–16. doi: 10.1016/j.cellimm.2005.07.007

20. Antonsen KW, Hviid CVB, Hagensen MK, Sørensen BS, Møller HJ. Soluble PD-1 (sPD-1) is expressed in human macrophages. *Cell Immunol* (2021) 369. doi: 10.1016/J.CELLIMM.2021.104435

21. Khan M, Zhao Z, Arooj S, Fu Y, Liao G. Soluble PD-1: predictive, prognostic, and therapeutic value for cancer immunotherapy. *Front Immunol* (2020) 11:587460. doi: 10.3389/fimmu.2020.587460

22. Kuipers H, Muskens F, Willart M, Hijdra D, van Assema FBJ, Coyle AJ, et al. Contribution of the PD-1 ligands/PD-1 signaling pathway to dendritic cell-mediated CD4+ cell activation. *Eur J Immunol* (2006) 36:2472–82. doi: 10.1002/EJI.200635978

23. Jalali S, Price-Troska T, Bothun C, Villasboas J, Kim HJ, Yang ZZ, et al. Reverse signaling via PD-L1 supports Malignant cell growth and survival in classical Hodgkin lymphoma. *Blood Cancer J* (2019) 9. doi: 10.1038/S41408-019-0185-9

24. Elhag OAO, Hu XJ, Wen-Ying Z, Li X, Yuan YZ, Deng LF, et al. Reconstructed adeno-associated virus with the extracellular domain of murine PD-1 induces antitumor immunity. *Asian Pac J Cancer Prev* (2012) 13:4031–6. doi: 10.7314/APJCP.2012.13.8.4031

25. He L, Zhang G, He Y, Zhu H, Zhang H, Feng Z. Blockade of B7-H1 with sPD-1 improves immunity against marine hepatocarcinoma. *Anticancer Res* (2005) 25:3309–13.

26. Amancha PK, Hong JJ, Rogers K, Ansari AA, Villinger F. *In vivo* blockade of the programmed cell death-1 pathway using soluble recombinant PD-1-Fc enhances CD4+ and CD8+ T cell responses but has limited clinical benefit. *J Immunol* (2013) 191:6060–70. doi: 10.4049/jimmunol.1302044

27. He J, Pan Y, Guo Y, Li B, Tang Y. Study on the expression levels and clinical significance of PD-1 and PD-L1 in plasma of NSCLC patients. *J Immunother* (2020) 43. doi: 10.1097/CJI.0000000000000315

28. Qiu H, Liu S, Xie C, Long I, Feng Z. Regulating immunity and inhibiting tumor growth by the recombinant peptide sPD-1-CH50. *Anticancer Res* (2009) 29:5089–94.

29. Shin SP, Seo HH, Shin JH, Park HB, Lim DP, Eom HS, et al. Adenovirus expressing both thymidine kinase and soluble PD1 enhances antitumor immunity by strengthening CD8 T-cell response. *Mol Ther* (2013) 21:688–95. doi: 10.1038/MT.2012.252

30. Xia W, Chen J, Hou W, Chen J, Xiong Y, Li H, et al. Engineering a HER2-CAR-NK cell secreting soluble programmed cell death protein with superior antitumor efficacy. *Int J Mol Sci* (2023) 24:6843. doi: 10.3390/IJMS24076843

31. Zhang A, Sun Y, Wang S, Du J, Gao X, Yuan Y, et al. Secretion of human soluble programmed cell death protein 1 by chimeric antigen receptor-modified T cells enhances anti-tumor efficacy. *Cytotherapy* (2020) 22:734–43. doi: 10.1016/J.JCYT.2020.05.007

32. Bian B, Fanale D, Dusetti N, Roque J, Pastor S, Chretien AS, et al. Prognostic significance of circulating PD-1, PD-L1, pan-BTN3As, BTN3A1 and BTLA in patients with pancreatic adenocarcinoma. *Oncoimmunology* (2019) 8. doi: 10.1080/2162402X.2018.1561120

33. Pedersen JG, Sokac M, Sørensen BS, Luczak AA, Aggerholm-Pedersen N, Birkbak NJ, et al. Increased soluble PD-1 predicts response to nivolumab plus ipilimumab in melanoma. *Cancers (Basel)* (2022) 14. doi: 10.3390/cancers14143342

34. Sorensen SF, Demuth C, Weber B, Sorensen BS, Meldgaard P. Increase in soluble PD-1 is associated with prolonged survival in patients with advanced EGFR-mutated non-small cell lung cancer treated with erlotinib. *Lung Cancer* (2016) 100:77–84. doi: 10.1016/j.lungcan.2016.08.001

35. Kruger S, Legenstein ML, Rösgen V, Haas M, Modest DP, Westphalen CB, et al. Serum levels of soluble programmed death protein 1 (sPD-1) and soluble programmed death ligand 1 (sPD-L1) in advanced pancreatic cancer. *Oncoimmunology* (2017) 6. doi: 10.1080/2162402X.2017.1310358

36. Dorman K, Gerckens M, Kruger S, Krueger K, Mayer Z, Rupp A, et al. Serum biomarker panel diagnostics in pancreatic ductal adenocarcinoma: the clinical utility of soluble interleukins, IFN-γ, TNF-α and PD-1/PD-L1 in comparison to established serum tumor markers. *J Cancer Res Clin Oncol* (2022) 149(6)2463–2474. doi: 10.1007/s00432-022-04112-z

37. Meyo MT, Jouinot A, Giroux-Leprieur E, Fabre E, Wislez M, Alifano M, et al. Predictive value of soluble PD-1, PD-L1, VEGFA, CD40 ligand and CD44 for nivolumab therapy in advanced non-small cell lung cancer: A case-control study. *Cancers (Basel)* (2020) 12. doi: 10.3390/CANCERS12020473

38. McGinnes K, Chapman G, Marks R, Ronald P. A fluorescence NK assay using flow cytometry. *J Immnological Methods* (1986) 86:7–15. doi: 10.1016/0022-1759(86)90258-9

39. Dong W, Wu X, Ma S, Wang Y, Nalin AP, Zhu Z, et al. The mechanism of anti-PD-L1 antibody efficacy against PD-L1-negative tumors identifies NK cells expressing PD-L1 as a cytolytic effector. *Cancer Discovery* (2019) 9:1422–37. doi: 10.1158/2159-8290.CD-18-1259

40. Mariotti FR, Petrini S, Ingegnere T, Tumino N, Besi F, Scordamaglia F, et al. PD-1 in human NK cells: evidence of cytoplasmic mRNA and protein expression. *Oncoimmunology* (2019) 8. doi: 10.1080/2162402X.2018.1557030

frontiers | Frontiers in Immunology

TYPE Brief Research Report
PUBLISHED 23 August 2023
DOI 10.3389/fimmu.2023.1221605

OPEN ACCESS

EDITED BY
Hailin Tang,
Sun Yat-sen University Cancer Center (SYSUCC), China

REVIEWED BY
Xinyao Yi,
Central South University, China
Yue Sui,
The University of Hong Kong, Hong Kong SAR, China
Yong Zhang,
The Second Affiliated Hospital of Xi'an Jiaotong University, China

*CORRESPONDENCE
Valerio G. Vellone
valerio.vellone@unige.it
Emanuela Marcenaro
emanuela.marcenaro@unige.it

†These authors have contributed equally to this work

‡These authors share last authorship

RECEIVED 12 May 2023
ACCEPTED 08 August 2023
PUBLISHED 23 August 2023

CITATION
Biatta CM, Paudice M, Greppi M, Parrella V, Parodi A, De Luca G, Cerruti GM, Mammoliti S, Caroti C, Menichini P, Fronza G, Pesce S, Marcenaro E and Vellone VG (2023) The fading guardian: clinical relevance of TP53 null mutation in high-grade serous ovarian cancers. *Front. Immunol.* 14:1221605. doi: 10.3389/fimmu.2023.1221605

The fading guardian: clinical relevance of TP53 null mutation in high-grade serous ovarian cancers

Chiara M. Biatta[1†], Michele Paudice[1,2†], Marco Greppi[3†], Veronica Parrella[1], Alessia Parodi[1], Giuseppa De Luca[4], Gianna Maria Cerruti[4], Serafina Mammoliti[5], Cinzia Caroti[6], Paola Menichini[7], Gilberto Fronza[7], Silvia Pesce[3], Emanuela Marcenaro[3,8*‡] and Valerio G. Vellone[1,9*‡]

[1]Department of Surgical Sciences and Integrated Diagnostics (DISC), University of Genoa, Genoa, Italy, [2]Pathology University Unit, IRCCS Ospedale Policlinico S. Martino, Genoa, Italy, [3]Department of Experimental Medicine (DIMES), University of Genova, Genoa, Italy, [4]Molecular Diagnostic Unit, IRCCS Ospedale Policlinico S. Martino, Genoa, Italy, [5]Oncology Unit, IRCCS San Martino IST, Genoa, Italy, [6]Oncology University Unit, IRCCS Ospedale Policlinico San Martino, Genoa, Italy, [7]Mutagenesis and Cancer Prevention Unit, IRCCS Ospedale Policlinico S.Martino, Genoa, Italy, [8]IRCCS Ospedale Policlinico San Martino, Genova, Italy, [9]Pathology Unit, IRCCS Istituto Giannina Gaslini, Genoa, Italy

Background: we evaluated the concordance between immunohistochemical p53 staining and TP53 mutations in a series of HGSOC. Moreover, we searched for prognostic differences between p53 overexpression and null expression groups.

Methods: patients affected by HGSOC were included. For each case p53 immunohistochemical staining and molecular assay (Sanger sequencing) were performed. Kaplan-Meier survival analyses were undertaken to determine whether the type of TP53 mutation, or p53 staining pattern influenced overall survival (OS) and progression free survival (PFS).

Results: 34 HGSOC were considered. All cases with a null immunohistochemical p53 expression (n=16) showed TP53 mutations (n=9 nonsense, n=4 in-frame deletion, n=2 splice, n=1 in-frame insertion). 16 out of 18 cases with p53 overexpression showed TP53 missense mutation. Follow up data were available for 33 out of 34 cases (median follow up time 15 month). We observed a significant reduction of OS in p53 null group [HR = 3.64, 95% CI 1.01-13.16].

Conclusion: immunohistochemical assay is a reliable surrogate for TP53 mutations in most cases. Despite the small cohort and the limited median follow up, we can infer that HGSOC harboring p53 null mutations are a more aggressive subgroup.

KEYWORDS

high grade serous ovarian carcinoma, TP53, immunohistochemistry, sanger sequencing, ovarian cancer

1 Introduction

Epithelial ovarian cancer (EOC) is the fifth most common cause of female cancer death in the developed world. It affects every year 21,750 women in the USA of whom 13,940 will die of the disease (1). Despite aggressive surgeries and combined chemotherapies, the prognosis remains worrisome. The reason for this high mortality rate is the late presentation, meaning that more than 70% of EOC are diagnosed at stage III or IV with a 5-year Overall Survival of approximately 15-30%.

In recent years the therapeutic landscape for EOC has seen a revolution expected for thirty years with the introduction, the PARP-inhibitors, changing the prognosis of the BRCA mutated subgroup of EOC. In SOLO-1, which investigated Olaparib in newly diagnosed advanced BRCA mutated ovarian cancer, the 3-years risk of disease progression or death was 70% lower with Olaparib than with placebo (60% vs. 27%, HR 0.30) (2).

EOC is not a single disease. Its histopathology is heterogeneous and each EOC subtype harbors genetic mutations that are being assessed for their potential to predict the efficacy of molecularly targeted treatments (3). The most frequent subgroup, accounting for 70% of all EOCs, is high-grade serous ovarian cancer (HGSOC), which is considered to originate from serous tubal intra-epithelial carcinoma (STIC) and is characterized by mutation in TP53 gene in 95% of cases.TP53 is the most frequently mutated gene in cancer, with mutations identified in at least 50% of human malignancy. The protein p53 is a homotetrameric transcription factor with tumor suppression functions. It controls the expression of hundreds of target genes in order to maintain homeostasis and genome integrity. It can activate DNA repair proteins when DNA has sustained damage, arrest cell growth by holding the cell cycle at the G1/S transition, allowing DNA repair, and initiate apoptosis if DNA damage proves to be irreparable. It's also involved in senescence, autophagy as well as processes that oppose oncogenic metabolic reprogramming (4).

In normal condition, wild-type p53 is maintained at low levels by the E3 ubiquitin ligase MDM2 that polyubiquitinates p53, marking it for proteasomal degradation. In response to cellular stress, several mechanisms, disrupt the MDM2-p53 association, leading to the stabilization and the activation of p53 (5).

More recent research has focused on the epigenomic control of p53 providing evidence that microRNAs and long noncoding RNAs can play a role in the epigenomic control of p53 expression. These findings suggest that epigenetic changes may be a promising target for cancer prevention and treatment (6, 7).

Over 36,000 TP53 mutations have been reported, and for this reason, it is challenging to find a drug that could be effective for all mutations. Approximately 80% of TP53 mutations are missense mutations and lead to an overexpression of mutp53 in the cells that can be promptly identified by immunohistochemistry (IHC). The other mutations as frame-shift, nonsense and splice-site mutations are collectively known as p53-null mutations and they result in the absence of an encoded protein.

In this setting it is evident how relevant the identification of molecular prognostic factors is, which could potentially identify subgroups of tumors with greater aggressiveness and which require therapeutic modulation with more aggressive treatments and close follow-ups.

Here we describe how p53-null mutations have implications in prognosis and in the aggressiveness of HGSOC and how a simple and inexpensive diagnostic tool as IHC can be used as an alternative to Sanger sequencing in discriminating between null and missense mutations of TP53.

2 Materials and methods

2.1 Tumor samples

Our cohort consisted of 36 gynecological tumors (serous ovarian, fallopian tube and peritoneal carcinomas) collected from IRCCS Ospedale Policlinico San Martino. 34 HGSOC, one low-grade serous tumor (LGSOC), and one mucinous carcinoma were included in the final analysis as study controls. 29/34 HGSOCs were at an advanced stage, classified as FIGO (International Federation of Gynecology and Obstetrics) III or IV, whereas 5/34 were at an early stage, classified as FIGO I or II.

Survival and other clinical data were available for many patients. Based on immunohistochemical analysis of p53 protein expression, we matched p53 null mutation cohort, non-otherwise selected, with p53 protein overexpressed cohort consecutive unselected with similar histopathologic features. We divided the patients into two cohorts: one characterized by p53 null mutations, and one characterized by p53 overexpression.

After histopathological HGSOC diagnosis, if deemed suitable, patients underwent primary debulking surgery (PDS) followed by six cycles of chemotherapy. If complete surgical debulking was not judged feasible, two sets of three cycles of neoadjuvant chemotherapy (NACT) interspersed by interval debulking surgery (IDS) were performed. The standard regimen of chemotherapy contains Carboplatin AUC5 plus Paclitaxel 175 mg/m^2 every three weeks with addition of Bevacizumab or Olaparib based on BRCA status, when investigated. In case of disease recurrence, after considering secondary debulking surgery (SDS) for a subset of selected cases, patients received second line chemotherapy according to common guidelines. None of the patients had intraoperative complications. One of them was also affected by metastatic non-small cell lung cancer (NSCLC) and one already had EOC metastasis.

Progression Free Survival (PFS) was defined as time from the date of biopsy/surgery and consensual diagnosis of HGSOC to the date of progression diagnosed with imaging and laboratory techniques. Overall Survival (OS) was counted from the date of biopsy/surgery and consensual diagnosis of HGSOC to the date of death or last follow up as recorded in hospital medical records, doctors' rooms, and publicly available death notices. Written informed consent was obtained from all subjects. All methods were carried out in accordance with the approved guidelines.

Matched formalin fixed paraffin embedded samples were obtained from our diagnostic pathology laboratory (IRCCS Ospedale Policlinico San Martino). Among the study samples, we included four kinds of specimens: 1 FNAB (Fine Needle Aspiration

Biopsy), 13 LPS (laparoscopy), 18 primary debulking and 2 secondary debulking surgery (after disease relapse). This retrospective series of HGOSC specimens was prepared according to standard protocols. In brief: after the surgical excision, all the specimens were sent unfixed to the pathology units where they were fixed in 10% buffered formalin (12–18 hours); after grossing, the samples were routinely processed, and paraffin embedded to obtain histological slides stained in hematoxylin and eosin (H&E). The paraffin blocks were kept in dedicated archives, at room temperature, in cardboard boxes kept away from dust, light and heat sources.

Two pathologists [VGV, CMB] to confirm diagnosis, supported by standard immunohistochemistry biomarkers panel (Cytokeratin 7, Cytokeratin 20, Vimentin, WT1, Napsin-A, ER, PR, Ki67 and p53), histological grade and pathological stage, reviewed all tumor tissue. Following initial surgery, patients were staged according to the FIGO criteria.

Sections were ascertained from tumors for determination of percent tumor cells following H&E staining and for DNA extraction. Tumors containing at least 5% of tumor cells were selected for this study (5).

The most significant paraffin block was selected for molecular analysis according to the following criteria: optimal fixation/storage, high representativeness of the entire neoplasia, high tumor cellularity, low percentage of stroma cell, fibrosis and necrosis. From selected samples, manual macrodissection was performed and sections (three sections of 10μm thickness) were obtained for molecular analyses.

2.2 p53 immunohistochemistry

One tumor-rich sample per case, a 3-μm-thick section from a formalin-fixed, paraffin embedded tumor tissue block, was selected for immunohistochemical analysis. Staining was detected with the automated ultraView Universal DAB procedure on the BenchMark ULTRA IHC/ISH Staining Module, Ventana with anti-p53 (clone DO7, prediluted,Ventana, Innovation Park Dr. Tucson, AZ, USA). Ventana Medical Systems' (Ventana) CONFIRM anti-p53 (DO-7) a mouse monoclonal antibody (IgG1, kappa) directed against human p53. The antibody is intended for laboratory use to qualitatively identify by light microscopy wild type and mutant p53 in sections of formalin-fixed, paraffin-embedded tissue on a Ventana automated slide stainer.

Nuclear staining was considered a positive reaction. The extent of nuclear staining was estimated to the nearest 5% level of positive tumor cells, reporting the actual percentage for each case.

All stains were done within one week after sectioning. Stained slides were examined by an experienced surgical pathologist [VGV, CMB, MP] who was blinded to molecular data.

The percentage of cells showing positive nuclear staining was estimated and report-ed in three categories: ≥50% positively stained nuclei (overexpression); >1% and <50% stained nuclei (partial expression); ≤1% positively stained nuclei (no expression/null) (5).

2.3 Sanger sequencing molecular analysis

All samples underwent Sanger sequencing using the identical DNA. PCR primers and conditions for amplifying genomic DNA sequences within exons 2-11 of TP53 gene were those recommended by the International Agency for Research on Cancer (IARC) TP53 database (https://p53.iarc.fr/Download/TP53_SangerSequencing_IARC.pdf).

Briefly, PCR products were purified with the enzyme ExoSap-IT (USB) and consequently, sequencing reaction done with BigDye. Terminator v3.1 Cycle Sequencing Kit (Applied Biosystems). Subsequently, products were purified, and sequencing was performed on 3500 Genetic Analyzer capillary sequencing instrument (Applied Biosystems).

Electropherograms were analyzed by visual inspection of sequences imported in MacVector software. Variants found were compared against the human TP53 reference genomic sequence NC_000017.10 (transcript NM_000546.5) and biological/clinical significance (if present) carried out thanks to IARC and Cosmic databases (5).

The Limit of Detection (LoD) of mutational testing by Sanger sequencing in our lab is extimated approximately 12-15%. Considering the issue of heterozygosity, the minimal neoplastic component present in the section should be quantitatively double the instrumental LoD, according to SIAPeC-IAP (Italian Society of Anatomic Pathology) recommendations. For example, a sample with 10% tumor cells should be tested with an assay with LoD of at least 5% (8).

2.4 Statistical analyses

Clinicopathological and laboratory data was imported in MSExcel™ spreadsheet and analyzed with dedicated statistical software MedCalc. The Chi-squared test was used to evaluate the association between categorical data while continuous values were com-pared using Kruskal-Wallis test.

Kaplan-Meier survival analyses compared by the log-rank (Mantel-Cox) test were undertaken to determine whether the type of TP53 mutation, or p53 staining pattern influenced overall (OS) and progression free survival (PFS) in HGSOCs. $p<0.05$ was considered statistically significant.

3 Results

Clinicopathological characteristics of the cohort studied are summarized in Table 1. The mean age at diagnosis of both cohorts was 66.3 years (range 48 – 79), being 68.8 (range 48 – 79) in p53 null group and 64.1 (range 54 – 78) in p53 overexpressed group. The slight age difference at diagnosis between the two cohorts was statistically significant. The median follow up was about 15 months (range 1 – 57), evaluated on 33 patients being one lost to follow up. All of them were high-grade serous ovarian carcinomas (HGSOCs) and one (2,9%) had a second clear cell component.

10.3389/fimmu.2023.1221605

TABLE 1 Clinicopathological characteristics.

	p53 null (n=16)	p53 overexpressed (n=18)
Mean age (years)	68.8 ± 7.1	64.1 ± 7.5
Mean follow-up (months)	13.5 ± 10.2	16.8 ± 12.8
Early stage (FIGO I-II)	1	4
Advanced stage (FIGO III-IV)	15	14
NACT	5	5
No debulking surgery	3	0
Macro residual disease (MDR)	3 + 3	3
mOS(months)	13.5 ± 10.2	16.8 ± 12.8
mPFS(months)	7.4 ± 8.8	10.4 ± 9.1
Deaths	7	3

The tumor cellularity (%) of the samples, sometimes obtained through macrodissection, was very high (57.8 ± 21.8), regardless of the type of specimen. No statistical difference in tumor cellularity was observed between samples belonging to p53 null and p53 overexpressed groups (Figure 1).

Among all biomarkers included in standard immunohistochemistry panel used in HGSOC diagnosis, only Progesterone (PR) showed statistically significant difference, being less expressed in cases belonging to p53 overexpressed cohort.

Neither ER (Estrogen) nor proliferation index Ki67 expression showed statistical significance (Figure 1).

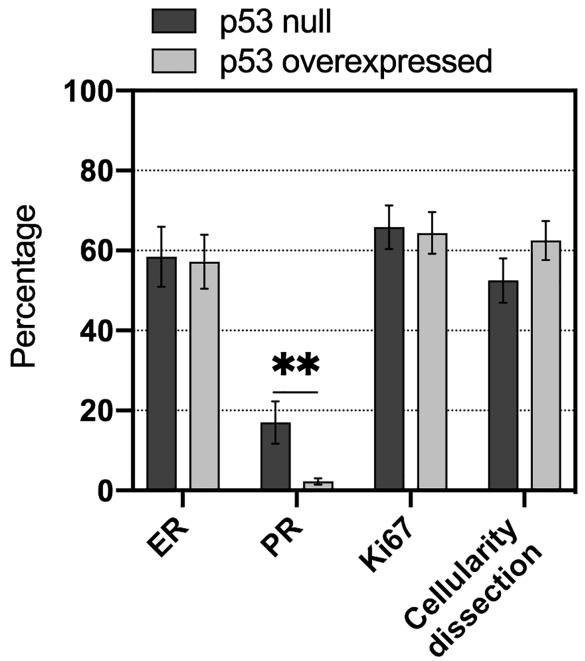

FIGURE 1
Comparison of immunohistochemistry expression of biomarkers routinely used in HGSOC diagnosis. ER, Estrogen Receptor; PR, Progesteron receptor. **p value>0.01.

There was a significant association of p53 null with increased risk of HGSOC-related death [HR = 3.64, 95% CI 1.01-13.16] compared with p53 overexpressed (Figure 2A).

Analogously, an even more significant association of p53 null with increased risk of HGSOC-related death within 24 months of follow up [HR = 6.09, 95% CI 1.52-24.51] was observed compared with p53 overexpressed (Figure 2B). Conversely, the difference in PFS was not statistically significant between the two groups.

All 34 HGSOCs (100%) showed aberrant p53 immunohistochemical expression, whereas the two study controls (LGSOC and mucinous carcinoma) had wild-type TP53, with p53 expression respectively 20% and 5% (Supplementary Figure 1).

Of 34 HGSOCs, analyzed for TP53 mutation by Sanger sequencing, 94,1% (32/34) tumors contained mutations of potential biological and clinical interests. In 16 out of 18 (88.9%) p53 overexpressed samples, we identified at least a missense mutation, in some cases associated to synonymous mutations, all occurring in the p53 DBD; of the remaining 2 (11.1%) we couldn't find any mutation between exons 2–11 of TP53 gene in one, while the other has not been evaluated due to poor DNA quality. The p53 null immuno-labeling pattern was always associated to mutations: 4 nucleotide deletions (25%), 1 nucleotide insertion (6.3%), 2 splice-site mutations (12.5%), and 9 nonsense mutations (56.3%). Not surprisingly, all samples with nonsense mutations exhibited no p53 staining (p53 null).

p53 neutral polymorphism was not included in further analysis. By combining two immunohistochemical staining patterns (p53 null and p53 overexpression), the immunohistochemical analysis correlated with the mutational analysis in 94.1% of cases.

Immunohistochemical and mutational analysis data are summarized in Figure 3A.

The majority of TP53 mutations with p53 null immunophenotype identified in this study (81.25%; 13/16) were located in the p53 DBD, with the exception of p.Thr81fs, p.Arg306* and p.Glu51*. 'Hot-spot' codons for mutation included p.Arg175 (found twice in p53 overexpressed group) residing within the p53 DBD, that have previously been recognized as TP53 mutational 'hot-spots' in human malignancy, as well as p.Gly245Ser(Figure 3B). Both of these mutp53 have been recognized to be GOF mutations (9).

Most of the mutations identified in the study samples through Sanger sequencing and studied on IARC and Cosmic databases resulted pathogenic or likely pathogenic. But 4 of them had not yet been described.

4 Discussion

4.1 p53 immunohistochemistry as surrogate marker for mutational TP53 status

Individual examination of HGSOCs diagnosed according to current criteria revealed that p53 was abnormally expressed in 100% of these tumors. The definition of abnormal expression was taken

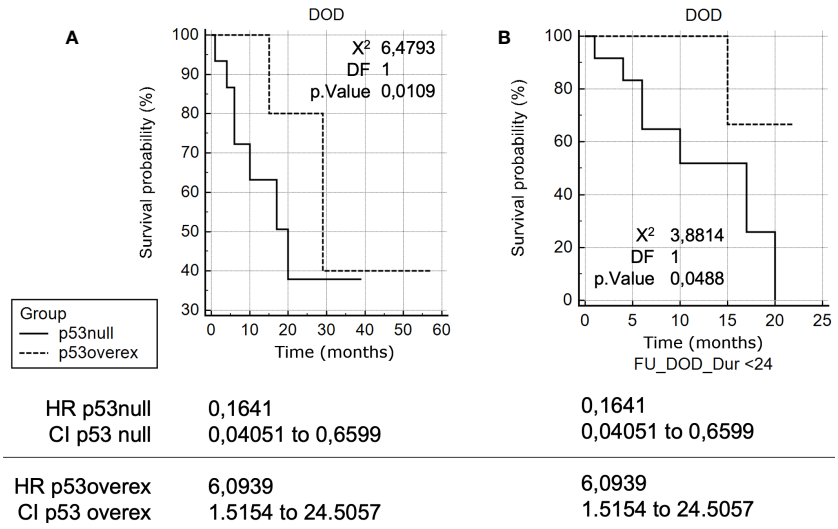

FIGURE 2
(A) Kaplan-Meier survival curve analyses in HGSOCs. Kaplan-Meier survival curve analysis of TP53 mutation-positive HGSOCs for Death Of the Disease (DOD), in months, of patients with p53 overexpression compared to patients with p53 null. **(B)** Kaplan-Meier survival curve analyses in HGSOCs (24 months). Kaplan-Meier survival curve analysis of TP53 mutation-positive HGSOCs for DOD.

from a previous study (10) in which p53 was either completely negative or overexpressed in more than 50% of tumor cell nuclei.

Notably, the frequency of abnormal expression was similar to the reported frequency of TP53 mutations, present in approximately 94% of HGSOCs. This range highlights the limitations of previous TP53 mutation studies, as the methods used were not sensitive and were not expected to detect all mutations leading to loss of expression of the functional p53

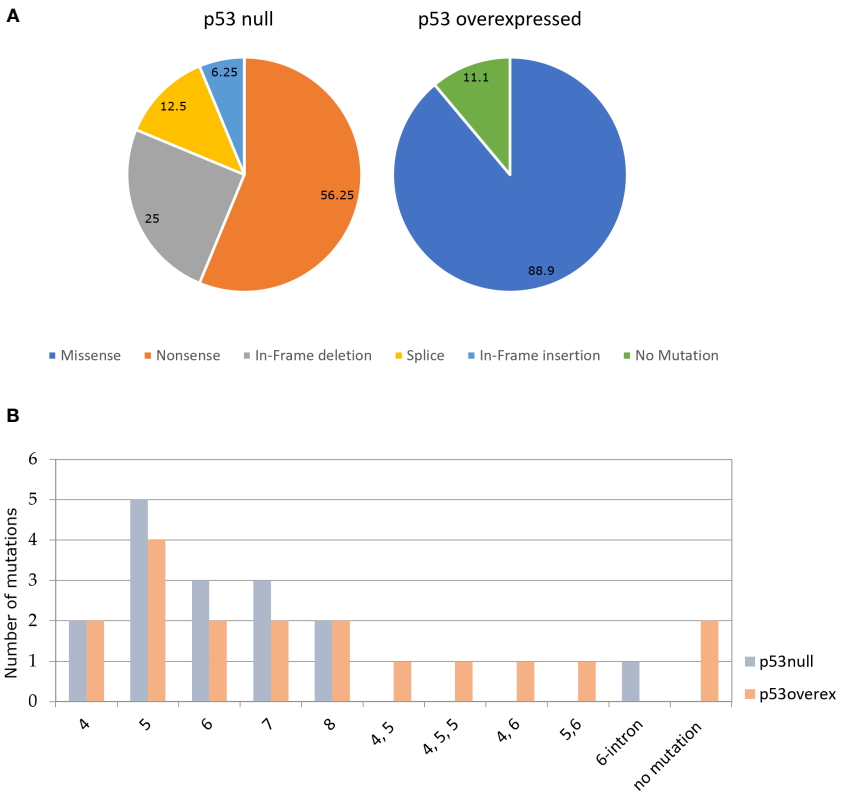

FIGURE 3
(A) Percentage of the different types of TP53 in p53 null (N=16) and p53 overexpressed (N=18). **(B)** Percentage of mutations in each exon of TP53 in p53 null and p53 overexpressed.

protein. Technical limitations include the inability to study only some exons, only mRNA, to assess deletions and inversions, and to sequence insufficient depth to detect somatic mutations present in mixed tumor cell and normal cell samples.

Analysis of p53 expression by immunohistochemistry is a rapid, inexpensive, and widely available method that may be useful as a surrogate marker for TP53 mutation status, but its ability to predict mutation status using both current standards for interpretation of p53 expression and comprehensive and detailed analysis of TP53 has been predicted that missense mutations in TP 53 are associated with accumulation of p53 protein in the nucleus and overexpression should indicate missense mutation. Havrilesky et al. found that 69% of TP53 mutations detected in advanced ovarian cancer were missense, and overexpression. Havrilesky et al. estimated that p53 overexpression by immunostaining (defined in their study as >30% of cells staining positive, although strong staining was seen in 75-100% of cells in most of these cases) (9) concluded ha TP53 overexpression is a fully sensitive marker for the detection of missense mutations (100%), but it is also seen in cases with other mutations (insertions, deletions, nonsense mutations) or undetectable mutations. The lack of TP53 mutations detectable by p53 overexpression (8/98,8% in their study) is problematic due to the small number of cases. It is unclear whether this lack of specificity is due to false-positive immunostaining results or false-negative mutation analysis results. Recently, it has been suggested that if immunostaining for p53 is completely negative, this should be associated with mutations undergoing non-sense degradation with high sensitivity and specificity, but there is relatively little data linking this immunostaining pattern to mutation analysis (11, 12). Yemelynova et al. reported 14 cases in which loss of p53 expression and localized expression predicted TP53 mutations from wild type with 88% sensitivity and 100% specificity (11).

In our study, the frequency of null mutations was completely consistent with case series in which we observed a complete absence of p53 expression (100%). Although this rate seems high, there may be a bias in the TP53 mutations recorded, as many studies limit their analysis to exons 5-8 and omit null mutations outside exons 5-8. Further studies with a larger number of cases are needed to determine how reliable this correlation is.

4.2 TP53 null mutations and unfavorable outcome

Our second finding was that HGSOCs with complete absence of p53 expression were associated with an unfavorable outcome. This confirmed an observation first made some years ago (13, 14). In particular, Shahin et al, revealed that HGSOCs harboring TP53 null mutation had an increased risk for tumor-related death [HR 2.17 (1.35–3.51)] compared with TP53 missense mutation.

We found a risk for death of similar magnitude [HR 3.63 (1.01–13.15)] for patients with no expression in p53. Limiting follow up to 24 months makes this data even more pronounced [HR 6.09 (1.52–24.51), p<0.01] suggesting that p53 null HGSOCs are a sub-group of ovarian cancer with a particularly adverse presentation.

These differences support the possibility of biological differences related to the nature of the TP53 mutation. Findings like similar frequency of macro residual disease (MRD) and similar requirement of NACT administration in both groups of our study didn't take into account that 3 patients (~19%) belonging to p53 null group were not deemed suitable to PDS against no patient in the p53 overexpressed group. Indeed, they received first line chemotherapy instead of NACT and certainly had pelvic and abdominal disease when chemotherapy was started.

Our findings are somehow in contrast to previous meta-analyses that found that p53 overexpression is a risk factor for shorter survival in women with ovarian cancer (15). While these meta-analyses were adequately powered to show a modest effect, the authors clearly acknowledge the bias of studying different heterogeneous histologic types in terms of initial stage, outcome and response to chemotherapy (16). Furthermore, the inclusion of non-HGSOC patients without p53 abnormalities and with good prognosis hinders attempts to understand the clinical significance of different p53 expression patterns. Indeed, biomarker studies in cohorts with mixed disease types are more likely to identify type-specific (diagnostic) markers rather than type-independent prognostic markers, and the adverse outcomes identified may be related to histologic type rather than p53 overexpression.

Since these tumors usually lack p53 abnormalities, the presence of these mutations can be associated with a poor prognosis across all cancer stages because p53 alterations are associated with an unfavorable subgroup of ovarian carcinoma (HGSOC).

This controversy demonstrates the importance of examining prognostic biomarkers in homogeneous tumor cohorts.

These data are preliminary considering the small number of patients, the limited median follow up and the fact that one of the three patients not feasible for PDS was also affected by metastatic non-small cell lung cancer (NSCLC). Nevertheless, we can infer that HGSOC harboring p53 null mutations are a more aggressive subgroup, especially in its clinical presentation. This notion should lead the clinician, once more, to be as timely as possible, in the effort of not wasting the chance to eradicate a pathology that can briefly escape from the intent of cure.

In the last years we have been facing outstanding improvements in targeted therapy in the whole oncologic landscape. Regarding ovarian cancer, after years of limited therapeutic innovation, PARP inhibitors Olaparib, Niraparib, Rucaparib and Veliparib are showing important clinical benefit for patients with BRCA mutations or HRD deficiency (2, 17–19).

In this perspective, research on TP53 gene is very attractive as it is altered in 95% of HGSOCs and it is the most mutated gene in cancer.

New drugs that restore the wild-type structure and function of mutant p53 are underway and missense p53 proteins, which are found at high levels in cells due to loss of MDM2 regulation and other mechanisms, appear to be a promising drug target (20). The most promising compound is PRIMA-MET (APR246), a prodrug that after hydrolytic conversion to its active substance (Methylene Quinuclidinone) binds to cysteine in p53 and reactivates p53 wild-type functions. Nowadays there are 10 ongoing clinical trials with

APR-246 and the combination of APR-246 plus Azacitidine for the treatment of MDS started phase 3 in January 2019.

Moreover, the large number of diverse p53 mutations and the notion that specific mutp53 have different forms and cellular effects, are leading to the investigation of others therapeutic strategies to selectively target specific classes of mutations including prevention of p53 degradation by MDM2/4 antagonists, disruption of aggregates of mutp53 and other selective strategies aiming to target the single specific mutation. Even for p53 null-mutations, which appear to be the most difficult mutation to restore, a combination treatment with nonsense-mediated mRNA decay (NMD) inhibitor has shown an increase in tumor cell elimination, shedding light on a field unexplored so far.

Despite the recent progress described the significance of TP53 mutations as well as the effect of specific TP53 mutations (especially GOF TP53 mutation) on EOCs are to be better understood. Only with a deeper knowledge of p53 biology it will be possible to develop targeted drugs against a critically important protein for development of HGSOCs and many others cancer types.

5 Conclusions

Ours is a small but homogeneous single-center study, which reports the real-life results that can be obtained through well-established and standardized methods available in numerous surgical pathology units around the world.

Immunohistochemical staining for p53 demonstrated excellent correlation with Sanger sequencing results, allowing patients to be divided into two subgroups with different prognoses. Overall, in our population high-grade serous carcinoma confirmed a severe prognosis with p53-null patients having an even more severe prognosis and who could benefit from differentiated therapeutic protocols with close follow-ups and more aggressive treatments.

Our results appear encouraging and could be the starting point for a larger, multi-center study with a numerosity permitting a multivariate analysis.

Data availability statement

The original contributions presented in the study are included in the article/Supplementary Material. Further inquiries can be directed to the corresponding authors.

Ethics statement

The studies involving humans were approved by Liguria Region, Genova, Italy (n127/2022-DB id12223). The studies were conducted in accordance with the local legislation and institutional requirements. The participants provided their written informed consent to participate in this study.

Author contributions

Conceptualization, CB, VV, EM. Methodology, GL, AP. Software, MG, SP. Formal analysis, GL. Investigation, GC. Resources, VP. Data curation, GF. Writing-original draft preparation, CB. Writing-review and editing, MP. Visualization, CC and SM. Supervision and project administration, EM and VV. All authors contributed to the article and approved the submitted version.

Funding

The research leading to these results has received funding from AIRC under IG 2021 – ID. 26037 project – P.I. Marcenaro Emanuela. MG was supported by a FIRC-AIRC fellowship for Italy.

Acknowledgments

A special thanks to Mrs. Giorgia Anselmi and Mrs. Romana Conte for technical support.

Conflict of interest

The authors declare that the research was conducted in the absence of any commercial or financial relationships that could be construed as a potential conflict of interest.

Publisher's note

Supplementary material

The Supplementary Material for this article can be found online at: https://www.frontiersin.org/articles/10.3389/fimmu.2023.1221605/full#supplementary-material

SUPPLEMENTARY FIGURE 1
(200x) hematoxylin-eosin staining (up) and differences of p53 staining (down) between p53 wildtype mucinous carcinoma (left), HGSOC p53 null (center), and HGSOC p53 overexpressed (right).

References

1. Cancer Facts & Figures. *American Cancer Society* (2020). Available at: https://www.cancer.org/research/cancer-facts-statistics/all-cancer-facts-figures/cancer-facts-figures-2020.html.

2. Moore K, Colombo N, Scambia G, Kim BG, Oaknin A, Friedlander M, et al. Maintenance olaparib in patients with newly diagnosed advanced ovarian cancer. *N Engl J Med* (2018) 379(26):2495–505. doi: 10.1056/NEJMoa1810858

3. Jayson GC, Kohn EC, Kitchener HC, Ledermann JA. Ovarian cancer. *Lancet* (2014) 384(9951):1376–88. doi: 10.1016/S0140-6736(13)62146-7

4. Menendez D, Inga A, Resnick MA. The expanding universe of p53 targets. *Nat Rev Cancer* (2009) 9(10):724–37. doi: 10.1038/nrc2730

5. Cole AJ, Dwight T, Gill AJ, Dickson KA, Zhu Y, Clarkson A, et al. Assessing mutant p53 in primary high-grade serous ovarian cancer using immunohistochemistry and massively parallel sequencing. *Sci Rep* (2016) 6(1):26191. doi: 10.1038/srep26191

6. Yuan K, Lan J, Xu L, Feng X, Liao H, Xie K, et al. Long noncoding RNA TLNC1 promotes the growth and metastasis of liver cancer via inhibition of p53 signaling. *Mol Cancer* (2022) 21(1):105. doi: 10.1186/s12943-022-01578-w

7. Tang H, Wang Z, Liu Q, Liu X, Wu M, Li G. Disturbing miR-182 and -381 inhibits BRD7 transcription and glioma growth by directly targeting LRRC4. *PloS One* (2014) 9 (1):e84146. doi: 10.1371/journal.pone.0084146

8. Martin L, Grigoryan A, Wang D, Wang J, Breda L, Rivella S, et al. Identification and characterization of small molecules that inhibit nonsense-mediated RNA decay and suppress nonsense p53 mutations. *Cancer Res* (2014) 74(11):3104–13. doi: 10.1158/0008-5472.CAN-13-2235

9. Havrilesky L, Darcy KM, Hamdan H, Priore RL, Leon J, Bell J, et al. Prognostic Significance of *p53* Mutation and p53 Overexpression in Advanced Epithelial Ovarian Cancer: A Gynecologic Oncology Group Study. *JCO* (2003) 21(20):3814–25. doi: 10.1200/JCO.2003.11.052

10. Lassus H, Leminen A, Lundin J, Lehtovirta P, Butzow R. Distinct subtypes of serous ovarian carcinoma identified by p53 determination. Supplementary data associated with this article can be found at doi: 10.1016/S0090-8258(03)00608-5. *Gynecol Oncol* (2003) 91(3):504–12. doi: 10.1016/j.ygyno.2003.08.034

11. Yemelyanova A, Vang R, Kshirsagar M, Lu D, Marks MA, Shih IM, et al. Immunohistochemical staining patterns of p53 can serve as a surrogate marker for TP53 mutations in ovarian carcinoma: an immunohistochemical and nucleotide sequencing analysis. *Mod Pathol* (2011) 24(9):1248–53. doi: 10.1038/modpathol.2011.85

12. Nenutil R, Smardova J, Pavlova S, Hanzelkova Z, Muller P, Fabian P, et al. Discriminating functional and non-functional p53 in human tumours by p53 and MDM2 immunohistochemistry. *J Pathol* (2005) 207(3):251–9. doi: 10.1002/path.1838

13. Köbel M, Reuss A, Du Bois A, Kommoss S, Kommoss F, Gao D, et al. The biological and clinical value of p53 expression in pelvic high-grade serous carcinomas. *J Pathol* (2010) 222(2):191–8. doi: 10.1002/path.2744

14. Shahin MS, Hughes JH, Sood AK, Buller RE. The prognostic significance of p53 tumor suppressor gene alterations in ovarian carcinoma. *Cancer* (2000) 89(9):2006–17. doi: 10.1002/1097-0142(20001101)89:9<2006::AID-CNCR18>3.0.CO;2-7

15. de Graeff P, Crijns APG, De Jong S, Boezen M, Post WJ, De Vries EGE, et al. Modest effect of p53, EGFR and HER-2/neu on prognosis in epithelial ovarian cancer: a meta-analysis. *Br J Cancer* (2009) 101(1):149–59. doi: 10.1038/sj.bjc.6605112

16. Köbel M, Kalloger SE, Huntsman DG, Santos JL, Swenerton KD, Seidman JD, et al. Differences in tumor type in low-stage versus high-stage ovarian carcinomas. *Int J Gynecol Pathol* (2010) 29(3):203–11. doi: 10.1097/PGP.0b013e3181c042b6

17. González-Martín A, Pothuri B, Vergote I, DePont Christensen R, Graybill W, Mirza MR, et al. Niraparib in patients with newly diagnosed advanced ovarian cancer. *N Engl J Med* (2019) 381(25):2391–402. doi: 10.1056/NEJMoa1910962

18. Coleman RL, Oza AM, Lorusso D, Aghajanian C, Oaknin A, Dean A, et al. Rucaparib maintenance treatment for recurrent ovarian carcinoma after response to platinum therapy (ARIEL3): a randomised, double-blind, placebo-controlled, phase 3 trial. *Lancet* (2017) 390(10106):1949–61. doi: 10.1016/S0140-6736(17)32440-6

19. Coleman RL, Fleming GF, Brady MF, Swisher EM, Steffensen KD, Friedlander M, et al. Veliparib with first-line chemotherapy and as maintenance therapy in ovarian cancer. *N Engl J Med* (2019) 381(25):2403–15. doi: 10.1056/NEJMoa1909707

20. Kogan S, Carpizo D. Pharmacological targeting of mutant p53. *Transl Cancer Res* (2016) 5(6):698–706. doi: 10.21037/tcr.2016.11.74

frontiers | Frontiers in Immunology

TYPE Review
PUBLISHED 02 October 2023
DOI 10.3389/fimmu.2023.1268645

OPEN ACCESS

EDITED BY
Sansana Sawasdikosol,
Icahn School of Medicine at Mount Sinai,
United States

REVIEWED BY
Gabriella Pietra,
University of Genoa, Italy
Beisi Xu,
St. Jude Children's Research Hospital,
United States
Simon Keane,
University of Gothenburg, Sweden

*CORRESPONDENCE
Doriana Fruci
doriana.fruci@opbg.net

RECEIVED 28 July 2023
ACCEPTED 18 September 2023
PUBLISHED 02 October 2023

CITATION
D'Amico S, Tempora P, Gragera P, Król K, Melaiu O, De Ioris MA, Locatelli F and Fruci D (2023) Two bullets in the gun: combining immunotherapy with chemotherapy to defeat neuroblastoma by targeting adrenergic-mesenchymal plasticity. *Front. Immunol.* 14:1268645. doi: 10.3389/fimmu.2023.1268645

Two bullets in the gun: combining immunotherapy with chemotherapy to defeat neuroblastoma by targeting adrenergic-mesenchymal plasticity

Silvia D'Amico[1], Patrizia Tempora[1], Paula Gragera[1], Kamila Król[1], Ombretta Melaiu[1,2], Maria Antonietta De Ioris[1], Franco Locatelli[1,3] and Doriana Fruci[1]*

[1]Department of Paediatric Haematology/Oncology and Cell and Gene Therapy, Bambino Gesù Children Hospital, Istituto di Ricovero e Cura a Carattere Scientifico (IRCCS), Rome, Italy, [2]Department of Clinical Sciences and Translational Medicine, University of Rome "Tor Vergata", Rome, Italy, [3]Department of Pediatrics, Catholic University of the Sacred Heart, Rome, Italy

Neuroblastoma (NB) is a childhood tumor that originates in the peripheral sympathetic nervous system and is responsible for 15% of cancer-related deaths in the pediatric population. Despite intensive multimodal treatment, many patients with high-risk NB relapse and develop a therapy-resistant tumor. One of the phenomena related to therapeutic resistance is intratumor heterogeneity resulting from the adaptation of tumor cells in response to different selective environmental pressures. The transcriptional and epigenetic profiling of NB tissue has recently revealed the existence of two distinct cellular identities in the NB, termed adrenergic (ADRN) and mesenchymal (MES), which can spontaneously interconvert through epigenetic regulation. This phenomenon, known as tumor plasticity, has a major impact on cancer pathogenesis. The aim of this review is to describe the peculiarities of these two cell states, and how their plasticity affects the response to current therapeutic treatments, with special focus on the immunogenic potential of MES cells. Furthermore, we will discuss the opportunity to combine immunotherapy with chemotherapy to counteract NB phenotypic interconversion.

KEYWORDS

neuroblastoma, tumor microenvironment, adrenergic to mesenchymal transition, tumor plasticity, drug resistance, metronomic chemotherapy, immunotherapy

1 Introduction

Neuroblastoma (NB) is a malignant tumor arising from primitive neuronal crest cells of the developing sympathetic nervous system (SNS), and is the most common extracranial solid tumor in children, responsible for 15% of childhood cancer deaths (1, 2). Patients with high-risk NB receive a very intensive multimodal treatment regime, including induction chemotherapy, surgery, high-dose treatment with allogeneic stem cell transplantation and radiotherapy. This is then followed by isotretinoin and anti-GD2 monoclonal antibody to treat any residual disease (3). Although most high-risk NB patients initially respond to treatment, often with complete clinical remission, many of these relapse by developing therapy-resistant tumors (4). The onset of chemoresistance is a phenomenon typically related to intratumoral heterogeneity (ITH) (4).

NB ITH originally demonstrated in isogenic tumor-derived cell lines consisted on the presence of multiple cell types that differed in morphology, tumorigenic properties, and biochemical markers (5, 6). Based on their characteristics, the cells were defined as: (i) neuroblastic (type N), (ii) substrate-adherent (type S) and (iii) intermediate (type I) with a mixed and more aggressive phenotype, referred to as 'malignant NB stem cells' (5, 6).

Recent gene expression and epigenetic profiling of 33 different NB cell lines have provided insight into the details of NB ITH. van Groningen and colleagues identified two predominant cell identities, named adrenergic (ADRN) and mesenchymal (MES), that can spontaneously interconvert through epigenetic regulation (7–9). The phenotypic characteristics of these two cell populations are largely determined by the activation of specific transcriptional circuitries: while ADRN cells express markers of sympatho-adrenergic differentiation, MES cells appear undifferentiated and more similar to their neural crest progenitors (7, 8). Interestingly, the ADRN and MES classification coincides with the characteristics previously described for N/I-type and S-type cells, respectively (10).

The potential for interconversion between different cell states, is known as tumour plasticity and has recently been proposed as a new 'emerging hallmark of cancer' (11). Indeed, it can lead to the expression of phenotypic characteristics that may be advantageous in the presence of selective pressures and contribute to drug resistance and cancer progression.

In this review, we focus on the peculiarities of ADRN and MES cell states, and how their plasticity may influence the response to current therapeutic standards. Furthermore, we discuss how the combination of chemotherapy and immunotherapy has the potential to successfully target the dual nature of NB, possibly improving the prognosis of these young patients.

2 Plasticity of neuroblastoma: from adrenergic to mesenchymal cell lineage and back

Several studies have demonstrated that it is possible to induce ADRN/MES trans-differentiation *in vitro* by acting on lineage-specific core regulatory circuits (CRCs). In 2017, Van Groningen and colleagues showed that the over-expression of the Paired related homeobox protein 1 (PRRX1) gene, a MES-specific CRC transcription factor (TF), is able of reprogramming the transitional and epigenetic landscape of ADRN cells towards a MES state (7). Two years later, the same group described Neurogenic locus notch homolog protein 3 (NOTCH3) as a master regulator of ADRN-to-MES reprogramming (12). To date, specific CRCs have been described for ADRN and MES, consisting of 18 and 20 TFs, respectively (7) (Figure 1).

Many other genes have been identified to contribute to the maintenance of a specific transcriptional program. Yu and colleagues found different levels of telomeric protein expression and telomerase activity between ADRN and MES subclones (13). Accordingly, pharmacological conversion of ADRN into MES cells induced a robust change in the expression of telomere-binding proteins (13). Telomerase inhibition (TERT) was sufficient to induce a reversible switch from ADRN to MES without affecting telomere length, thus suggesting that TERT might exert a role in maintaining the ADRN phenotype independently of its telomere maintenance-related functions (13). Similarly, DNA topoisomerase 2-beta (TOP2B) was found to be required to maintain the ADRN-like transcriptional signature of SH-SY5Y cells and to suppress the alternative MES-like epigenetic state (14). Indeed, silencing of TOP2B in SH-SY5Y cells resulted in downmodulation of 47% of genes included in the ADRN signature and upregulation of 38% of genes identified in the MES signature (14). A recent study by Pan and colleagues shows that the TOP2B inhibitor CX-5461 causes DNA damage leading NB cells to apoptosis after 24 hours of treatment (15). The treatment is selective and more effective in MYCN-amplified NBs (15), in which the oncogene stabilizes the ADRN CRC (16). Inhibition of TOP2B, therefore, rather than inducing trans-differentiation from ADRN to MES, might select for the MES tumor component by specifically killing the ADRN tumor component.

Recently, a regulatory polymorphism of the LIM-domain-only 1 (*LMO1*) gene has been described to genetically determine NB fate by promoting the ADRN cell state (17). LMO1 is a transcriptional coregulator whose overexpression synergizes with MYCN to accelerate tumor formation and metastasis in a NBL-zebrafish model (18). Despite the lack of a DNA-binding domain, LMO1 mediates protein-protein interactions within ADRN CRCs and is essential for establishing ADRN cell identity (19). It has been observed that the G allele of the G → T polymorphism at the rs2168101 locus within the first intron of the *LMO1* gene predisposes to NB (20). This polymorphism, being located within a GATA domain, regulates the binding of TFs such as GATA3, and consequently affects the expression levels of LMO1. The authors showed that the protective T allele, by impairing the binding of GATA3 and reducing LMO1 expression, decreased the rate of NB initiation in MYCN-driven tumors that were restricted to the MES cell state. Whole-genome sequencing (WGS) of NB showed that tumors homozygous for the T allele (rs2168101(T;T)) have a MES cell state and are typically at low-risk NB at diagnosis (17).

It is currently unclear whether NB cells can adopt a pure MES phenotype *in vivo*, as two single-cell RNA sequencing (scRNA-seq)

10.3389/fimmu.2023.1268645

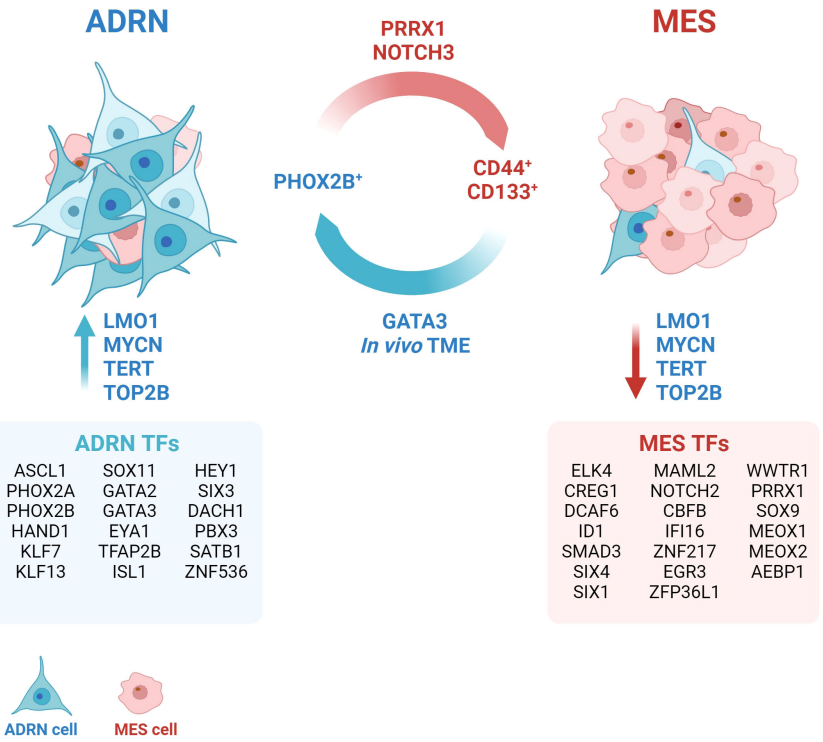

FIGURE 1
Neuroblastoma plasticity. The interconversion from the adrenergic state (ADRN) to the mesenchymal state (MES) occurs spontaneously and bidirectionally *in vivo*. The tumor microenvironment (TME) exerts a strong pressure towards the ADRN state. The transition can be induced through the activation or overexpression of specific transcription factors (TFs), such as GATA3, PRRX1, NOTCH3. The definition of cell identity is based on fundamental core regulatory circles that group different TFs (ADRN TFs and MES TFs) and establish typical gene expression signatures. Several accessory proteins, such as LMO1, TERT, TOP2B contribute to the maintenance of the transcriptional state. Created with BioRender.com.

analyses did not identify MES-like cells in primary tumours (21, 22), and a third identified ADRN tumour cells with only a few MES-like features (23, 24). The existence of a population with similar characteristics has also been suggested on the basis of scRNA-seq analysis of 10 neuroblastic tumour samples (25). The authors described a population of "transitional cells" expressing genes involved in sympathoadrenal development, but also rapid tumor proliferation and spread, suggesting a more aggressive phenotype. In an independent cohort of NB patients, high expression of the "transitional signature" was shown to be predictive of a worse prognosis than ADRN or MES expression patterns (25). A more recent study emphasizes the intrinsic plasticity properties of NB cells and the dependence of cell identity on external signals from the environment (26). PHOX2B and CD44 have been identified as specific markers of ADRN and MES, respectively, thereby being able to separate and culture the ADRN ($CD44^-$) and MES ($CD44^+$) components of different cell lines with a mixed phenotype (26). The authors also observed that ADRN cells were able to acquire CD44 expression in culture over time and that this phenomenon was influenced by the composition of the culture medium. Conversely, $CD44^+$ cells did not acquire PHOX2B expression, thus maintaining their MES identity *in vitro* (26). The xenografts derived from $CD44^+$ and $CD44^-$ cells showed a predominant ADRN identity, demonstrating the strong ability of the tumour microenvironment (TME) to drive NB cells towards ADRN differentiation. However, this is not sufficient to suppress the plasticity potential of the cells, which still retain the ability to transdifferentiate in the MES direction when isolated from the xenograft and cultured *in vitro* (26). By integrating scRNA-seq data from 18 NB biopsies and 15 patient-derived xenografts (PDXs), the authors demonstrated that human primary NB cells also acquire a predominantly ADRN phenotype (26). However, clusters of cells referred to as "bridging cells" or "noradrenergic-mesenchymal cells", display characteristics intermediate between the two main cell identities (26). This specific cell population could be responsible of the potential plasticity of the tumour.

3 Cell plasticity as a driver of resistance

Dynamic and heterogeneous interconversion between tumour cell subtypes has been associated with malignant progression and responses to therapy in several cancer types, such as prostate cancer, basal cell carcinoma and lung cancer (11). Numerous efforts have been made to identify the regulatory determinants of this dynamic phenotypic plasticity and to define lineage-specific therapies (11).

A scRNA-seq analysis of parental and etoposide- or cisplatin-resistant cells shed light on the link between NB plasticity and resistance to treatment (27). This analysis showed that drug treatment induces the formation of cell subpopulations with distinct transcriptome profiles. Drug resistance was associated

10.3389/fimmu.2023.1268645

with the modification of drug targets and the expression of genes involved in DNA double-strand break (DSB) repair, such as BARD1, BRCA1 and PARP1 (27). Cisplatin-resistant cells were highly enriched in ADRN genes, compared to parental cells where the MES signature was prevalent. In contrast, etoposide-resistant cells were equally enriched in MES and ADRN genes, suggesting a higher plasticity potential (27).

A subsequent study isolated the ADRN and MES components of some NB cell lines and analysed their response to conventional chemotherapy, providing further evidence of how cell identity influences drug response. The authors demonstrated that MES populations show marked intrinsic resistance to conventional chemotherapy *in vitro* compared to their ADRN counterpart (26) (Figure 2). Furthermore, a genome-wide epigenetic profiling study of 60 NBs identified four major epigenetic subtypes driven by super-enhancer (28). Among these, the one showing higher MES characteristics was enriched in relapsed disease, suggesting a connection between the MES phenotype and recurrence (28).

The International Society of Paediatric Oncology Europe Neuroblastoma Group (SIOPEN) developed the Rapid COJEC regimen as an induction chemotherapy step (29, 30). The regimen consists of a combination of five chemotherapeutic drugs (cisplatin, carboplatin, cyclophosphamide, etoposide and vincristine) spread over three cycles, administrated alternatively in eight 10-days cycles (29, 30). Most high-risk NB patients relapse after an initial response to treatment and develop therapy-resistant tumours. To investigate the mechanisms underlying resistance to the most common therapeutic strategy in clinical practice, Mañas and colleagues developed a treatment schedule that mimics COJEC induction therapy to treat mice carrying PDXs (31). They analysed the transcriptomic and genomic changes occurring in NBs during treatment and at relapse showing that chemotherapy-resistant NBs are enriched with an immature MES-like signature resembling multipotent Schwann cell precursors, while NBs that respond Favourably to treatment show a committed ADRN phenotype similar to normal neuroblasts (31).

The acquisition of MES features may also confer resistance to differentiating agents, target therapies and anti-GD2 immunotherapy. *In vitro*, MES NB cell lines, such as SH-EP, do not undergo differentiation in response to all-trans retinoic acid (ATRA) treatment compared to their ADRN counterparts (SH-SY5Y and SK-N-BE (2)-C) (32). ATRA induces upregulation of the retinoic acid (RA) signalling markers RARA and RARB only in ADRN cell lines (32) (Figure 2). Accordingly, Zimmerman and colleagues demonstrated that retinoids-induced differentiation of NB cells depends on reprogramming of the adrenergic CRC and establishment of a new retino-sympathetic CRC that causes proliferative arrest and sympathetic differentiation (16). It has been reported that MES cells endogenously produce RA to promote cell motility (33), suggesting that a RA signalling

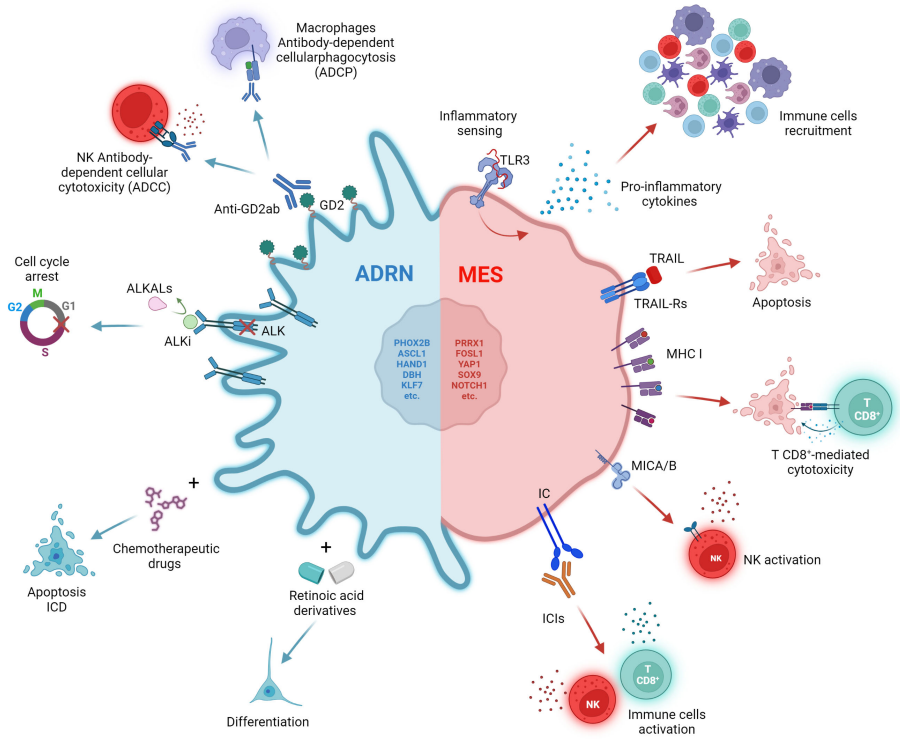

FIGURE 2
Impact of therapies on ADRN and MES states. The ADRN and MES identities are characterized by distinct vulnerabilities to therapies. The ADRN state is sensitive to differentiating and chemotherapeutic agents. The high expression of GD2 and ALK can be exploited through the use of anti-GD2 antibodies and ALK inhibitors (ALKi). The MES state displays a reduced expression of ALK and GD2, and a high immunogenicity characterized by high levels of inflammatory sensing, expression of MHC class I (MHC-I), MICA/B and immune checkpoint (IC) molecules on the cell surface, potentially emerging as a good target for ICI therapy. Created with BioRender.com.

pathway might be constitutively active in MES-type cells, but not associated with differentiation. Khazeem and colleagues reported similar results investigating the role of TOP2B in RA-induced gene expression and differentiation and the balance between ADRN and MES transcription programs in SH-SY5Y (14). They show that non-expression of TOP2B hinders the induction of many ATRA-response-associated genes by shifting cell identity towards a more MES phenotype. This suggests that the reduced neural differentiation stimulated by RA in TOP2B-null cells may be a result of weakened ADRN transcriptional signatures (14).

When analysing GD2 expression and publicly available RNA-seq data for 23 NB cell lines, Mabe and colleagues found that GD2-high and GD2-low expression cell lines were strongly correlated with ADRN and MES signatures, respectively (34) (Figure 2). Moreover, induction of ADRN to MES conversion trough overexpression of PRRX1 or NOTCH3 reduced GD2 expression and response to anti-GD2 therapy (34). They proposed that the transition from an ADRN state to a MES state reduces GD2 expression by downregulation of ST8SIA1, a gene encoding for GD3 synthase (GD3S), through the activation of EZH2, a core subunit of the polycomb repressive complex 2 (PRC2) (34).

The MES-like phenotype has been recently associated with resistance to ALK inhibitors (ALKi) due to the absence of ALK expression even in presence of tumour-driving ALK mutations, suggesting a role of ADRN-to-MES conversion in relapse (35). ALK-mutated SH-SY5Y xenografts acquire resistance to ALKi when reprogrammed by inducible expression of NOTCH3 into a MES phenotype, providing evidence that MES cells with a mutant ALK gene can escape targeted ALKi (35) (Figure 2). By comparing the expression profile of 8 MES and 28 ADRN cell lines, the authors discovered the differential expression of 90 apoptosis-related genes (35). In particular, several genes involved in the extrinsic apoptosis pathway were preferentially expressed in MES cells including caspase-8. Soluble recombinant human TNF-related apoptosis-inducing ligand (TRAIL), an activator of the extrinsic apoptosis pathway, was efficient in selectively inducing apoptosis in MES cells (Figure 2). The combination of ALKi and TRAIL delayed relapses in a subset of SH-SY5Y xenograft, demonstrating that dual targeting of both ADRN and MES could be an effective strategy in the treatment of NB (35).

Taken together, this evidence reinforces the role of cell identity and plasticity as resistance factors and supports the evidence that the MES phenotype contributes to resistance to conventional chemotherapy and the onset of relapse.

4 Immunotherapy to target the mesenchymal population

Although heterogeneous, NB has been widely described as a 'cold tumor', i.e., characterized by a lack of T-cell infiltration and therefore unable to trigger a strong immune response (36, 37). NB is characterized by a low mutational load and reduced expression of the major histocompatibility complex (MHC) class I (38, 39). An aspect that should not be underestimated is the level of inflammatory signaling in cancer cells, which has the potential to influence immune cell trafficking and recognition of cancer cells through cytokine secretion. Lower baseline inflammatory signaling has also been associated with resistance to immune checkpoint blockade (ICB) (40, 41). The study of the functional response of a group of 20 NB cell lines to different inflammatory stimuli revealed that the epigenetic state influences the inflammatory sensing and cytokines release of NB (42). All cell lines displayed a functional interferon gamma (IFNγ) signaling and except for one, showed dysfunctional detection of cytosolic DNA by cGAS-STING (42). However, heterogeneity in the detection of double-stranded RNA (dsRNA) by Toll-like receptor 3 (TLR3) and other dsRNA sensors was shown when cells treated with the dsRNA-mimetic drug poly(I:C) (42). While all non-responsive cell lines were in the ADRN state, six of the seven cell lines that showed a robust response to poly(I:C) were in the epigenetic MES state and showed increased expression of both pro-inflammatory cytokines and antigen presentation components (42) (Figure 2). Moreover, the forced switch of non-responsive cell lines from the ADRN state to the MES state was sufficient to restore TLR3 response signaling. A subsequent analysis of scRNA-seq data from 10 untreated high-risk NBs confirmed that tumors with stronger MES signatures had higher levels of basal inflammatory transcripts than those with stronger ADRN signatures (42).

Another study further investigated the immunological aspect of NB by analyzing RNA-seq data from 498 well-annotated primary human NB tumors and scRNA-seq data from a total of 40 tumors (43). The analytical effort led to the identification of four clusters, one of which, named C3, was found to be enriched for the expression of genes involved in immune activation and escape (43). The C3 cluster included many of the tumors with a higher MES score, again suggesting that a MES identity is associated with higher immunogenicity (43). In addition, the author showed that overexpression of PRRX1, but not its dysfunctional form, is sufficient to induce conversion of the ADRN SH-SY5Y cell line to a MES phenotype and to increase the expression of genes involved in antigen presentation and dysfunctional sensing of cytosolic DNA. Expression of MHC class I and the MICA and MICB ligands of the activating receptor NKG2D, is also increased on the cell surface (43) (Figure 2).

Transcriptional analysis of seven paired NB tumors, obtained at diagnosis and at relapse, confirmed the clinical relevance of this finding (43). In two cases, tumors acquired MES features at relapse, and this was accompanied by increased expression of cytotoxic T- and NK-cell signatures and immune checkpoint inhibitors PD-1 and CTLA-4 (43) (Figure 2). Similar data were obtained from scRNA-seq analysis of a pair of independent tumors (43). Thus, resistance or relapse associated with the transition from an ADRN to a MES phenotype is accompanied by an increase in immune cell infiltration. The expression of immune-related genes is strongly correlated with the epigenetic state of the tumor. This hypothesis was further confirmed by Cornel and colleagues who discovered the ability of the histone deacetylase inhibitor (HDACi) entinostat to increase the susceptibility of NB cells to $CD8^+$ T cell- and NK cell-mediated killing (44). The effect of entinostat was mediated by increased surface expression of MHC class I and other components of the antigen processing and presentation machinery, such as

TAP1, TAP2 and immunoproteasome subunits, as well as the NK activating ligands MICA and MICB. Consistent with Sengupta findings (43), this increase in immunogenicity has been correlated with a shift towards a more MES cell lineage (44).

Evidence to date suggests that immunogenicity may be the Achilles' heel of MES cells, representing an important opportunity to be exploited to make NBs susceptible to immunotherapy. Furthermore, the association of drug resistance features with the MES phenotype is now complemented by evidence of increased vulnerability to the immune system, opening new perspectives for future therapeutic combinations.

5 A combinatorial approach to target ADRN and MES populations

Several studies have shown that MES cells are more resistant to conventional treatments and are enriched in post-therapy and relapse tumors (26, 28, 31). However, by analyzing the expression of ADRN and MES mRNAs in serial bone marrow samples from high-risk NB, van-Wezel found that ADRN mRNAs and MES mRNAs have distinct temporal dynamics. Specifically, ADRN mRNAs levels were high at diagnosis and during relapse, but decreased during treatment. In contrast, MES mRNAs expression increased during treatment and was associated with patients who eventually relapsed (45). Beyond differences in therapeutic response, this result suggests that MES cells still retain a great deal of plasticity and can convert to ADRN when the selective pressure exerted by therapies is removed. This implies that an effective clinical response cannot be achieved without simultaneously targeting all the different cell states that the NB can acquire, thus rendering plasticity useless as an escape mechanism. Although current treatment protocols are not designed for this purpose, some studies are moving in this direction. Consistently, it has been proposed the dual targeting of ADRN and MES components through the combination of ALKi and TNF-related apoptosis-inducing ligand (TRAIL) (35).

The prevalence of the low-immunogenic ADRN phenotype partly explains the lack of T-cell infiltration and poor response to ICIs in this tumor type. Recent studies describing the MES phenotype as more immunogenic offer the possibility to exploit this feature and improve the efficacy of ICIs. With this in mind, forcing the NB towards a more MES identity could be an interesting strategy to sensitize the tumor to immunotherapy. Cornel and colleagues have demonstrated that epigenetic drugs, such as HDACi, can reprogram NB cells towards a more MES and immunogenic phenotype, capable of stimulating killing by effector $CD8^+$ T cells and NK cells (44). However, a high MES score can also be associated with higher expression of genes involved in immune evasion, such as the immune checkpoint (43). HDACi and ICIs could act synergistically on two different fronts: the former by overcoming the tumor's poor immunogenicity through epigenetic regulation, and the latter by counteracting the immune evasion properties of the MES phenotype.

The evidence that chemotherapy-resistant NBs exhibit MES features (31), suggests that the chemotherapy itself induces a selective pressure towards the MES status. From this perspective, combining of chemotherapy and immunotherapy could represent strategy to prevent relapse, by disfavoring the establishment of a chemotherapy-resistant MES identity.

To date, the combination of immunotherapy and chemotherapy has been little explored in the treatment of pediatric cancers. It is widely believed that chemotherapy-induced immunosuppression may render immunotherapy ineffective. However, several chemotherapy drugs, including those already used in the treatment of NB, have been shown to induce immunogenic cell death (ICD) when administered at low doses (46). ICD is a particular type of cell death that can elicit immune activation by exposing the host immune system to tumor antigens and damage-associated molecular patterns (DAMPs) (47, 48) (Figure 2).

Based on this, we recently proposed a chemo-immunotherapy approach combining low-dose mitoxantrone (MTX) with PD-1 and TGFβ blockade (49). This combination treatment was able to induce increased expression of several chemokines involved in the recruitment of lymphoid and myeloid cell populations, such as dendritic cells (DC) and NK cells (49), which are associated with improved survival of patients with NB and other cancers (50).

6 Discussion

NB cells represent a dynamic entity strongly influenced by the TME and therapeutic treatments. Their plasticity underlines the ability to optimize their survival by acquiring phenotypic traits that become favorable under specific conditions. It has been shown that in both mouse and human models the TME tends to force NB cells towards a predominantly ADRN identity (26). However, analysis of pairs of tumors taken at onset and relapse has shown that a MES phenotype can be acquired during therapy (31, 43). This is associated with increased immunogenicity, suggesting the possible success of an immunotherapeutic approach against NB (43). However, analysis of MES and ADRN mRNA expression in serial bone marrow samples of high-risk NB showed an increase in MES markers only during therapy, whereas ADRN mRNAs returned to elevated levels during relapse, suggesting that the drug-induced shift from ADR to MES might be reversible (45). It has recently been suggested that an immature component of tumor cell with an intermediate phenotype between ADR and MES, termed bridging cells or noradrenergic MES cells, may be responsible for the high plasticity potential of NB (26). In a landscape so variable and susceptible to external influences, targeting the tumor based on its current condition may not be a winning strategy. Future therapeutic approaches must consider the different transcriptional programs that might be undertaken by the tumor to simultaneously target different cell identities and reduce the tumor's chances of escaping cell death. Combinatorial therapies including an immunotherapeutic approach could be a viable strategy to exploit the immunogenicity of the chemo-resistant MES-like population and at the same time target the prominent ADRN compartment. Several combinatorial approaches have been proposed, among which metronomic chemotherapy combined with ICIs could present several advantages. Firstly, the possibility of using drugs

that have already been tested in NB patients, counteracting their side effects through dose de-escalation. Furthermore, several cytotoxic drugs have demonstrated the ability to induce ICD when used at low doses; this could counteract the "cold" TME typical of NB and contribute to the enhancement of the effect of ICIs, as observed in previous studies (51, 52). In this regard, we have shown that low-dose MTX combined with immunotherapy restricts NB growth, leading to substantial tumor regression by remodeling the TME (49). Equally important is the fact that the use of metronomic chemotherapy allows treatment to be prolonged over time (53), thus maintaining selective pressure on the ADRN component, while simultaneously targeting the chemoresistant compartment through immunotherapy. Finally, DAMPs released from dying ADRN cells could trigger the release of pro-inflammatory cytokines from the MES counterpart, further enhancing the effect of combinatorial therapy.

Given the great plasticity of NB cells, a targeted approach to ADRN/MES duality may not be sufficient for a lasting therapeutic response. Regardless of the most promising therapeutic approach, new studies are needed to better understand the different transcriptional configurations that NB cells can acquire.

Author contributions

SD'A: Conceptualization, Writing – original draft, Writing – review & editing. PT: Writing – review & editing, Investigation. PG: Writing – review & editing, Data curation. KK: Writing – review & editing, Data curation. OM: Writing – review & editing, Data curation. MD: Writing – review & editing, Data curation. FL: Writing – review & editing, Supervision. DF: Funding acquisition, Writing – original draft, Writing – review & editing, Conceptualization.

Funding

This project has received funding from Associazione Italiana Ricerca sul Cancro (AIRC) IG24345 (DF) and the European Union's Horizon 2020 research and innovation programme under the Marie Skłodowska-Curie grant agreement No 954992. This research was also supported by Fondazione Umberto Veronesi (FUV) fellowship (SD).

Conflict of interest

The authors declare that the research was conducted in the absence of any commercial or financial relationships that could be construed as a potential conflict of interest.

Publisher's note

References

1. Maris JM. Recent advances in neuroblastoma. *N Engl J Med* (2010) 362(23):2202–11. doi: 10.1056/NEJMra0804577

2. Cheung NK, Dyer MA. Neuroblastoma: developmental biology, cancer genomics and immunotherapy. *Nat Rev Cancer* (2013) 13(6):397–411. doi: 10.1038/nrc3526

3. Nguyen R, Thiele CJ. Immunotherapy approaches targeting neuroblastoma. *Curr Opin Pediatr* (2021) 33(1):19–25. doi: 10.1097/MOP.0000000000000982

4. Qiu B, Matthay KK. Advancing therapy for neuroblastoma. *Nat Rev Clin Oncol* (2022) 19(8):515–33. doi: 10.1038/s41571-022-00643-z

5. Biedler JL, Helson L, Spengler BA. Morphology and growth, tumorigenicity, and cytogenetics of human neuroblastoma cells in continuous culture. *Cancer Res* (1973) 33 (11):2643–52.

6. Acosta S, Lavarino C, Paris R, Garcia I, de Torres C, Rodriguez E, et al. Comprehensive characterization of neuroblastoma cell line subtypes reveals bilineage potential similar to neural crest stem cells. *BMC Dev Biol* (2009) 9:12. doi: 10.1186/1471-213X-9-12

7. van Groningen T, Koster J, Valentijn LJ, Zwijnenburg DA, Akogul N, Hasselt NE, et al. Neuroblastoma is composed of two super-enhancer-associated differentiation states. *Nat Genet* (2017) 49(8):1261–6. doi: 10.1038/ng.3899

8. Boeva V, Louis-Brennetot C, Peltier A, Durand S, Pierre-Eugene C, Raynal V, et al. Heterogeneity of neuroblastoma cell identity defined by transcriptional circuitries. *Nat Genet* (2017) 49(9):1408–13. doi: 10.1038/ng.3921

9. Upton K, Modi A, Patel K, Kendsersky NM, Conkrite KL, Sussman RT, et al. Epigenomic profiling of neuroblastoma cell lines. *Sci Data* (2020) 7(1):116. doi: 10.1038/s41597-020-0458-y

10. Yu EY, Cheung NV, Lue NF. Connecting telomere maintenance and regulation to the developmental origin and differentiation states of neuroblastoma tumor cells. *J Hematol Oncol* (2022) 15(1):117. doi: 10.1186/s13045-022-01337-w

11. Hanahan D. Hallmarks of cancer: new dimensions. *Cancer Discovery* (2022) 12 (1):31–46. doi: 10.1158/2159-8290.CD-21-1059

12. van Groningen T, Akogul N, Westerhout EM, Chan A, Hasselt NE, Zwijnenburg DA, et al. A notch feed-forward loop drives reprogramming from adrenergic to mesenchymal state in neuroblastoma. *Nat Commun* (2019) 10(1):1530. doi: 10.1038/s41467-019-09470-w

13. Yu EY, Zahid SS, Aloe S, Falck-Pedersen E, Zhou XK, Cheung NV, et al. Reciprocal impacts of telomerase activity and adrn/mes differentiation state in neuroblastoma tumor biology. *Commun Biol* (2021) 4(1):1315. doi: 10.1038/s42003-021-02821-8

14. Khazeem MM, Casement JW, Schlossmacher G, Kenneth NS, Sumbung NK, Chan JYT, et al. Top2b is required to maintain the adrenergic neural phenotype and for atra-induced differentiation of sh-sy5y neuroblastoma cells. *Mol Neurobiol* (2022) 59 (10):5987–6008. doi: 10.1007/s12035-022-02949-6

15. Pan M, Wright WC, Chapple RH, Zubair A, Sandhu M, Batchelder JE, et al. The chemotherapeutic cx-5461 primarily targets top2b and exhibits selective activity in high-risk neuroblastoma. *Nat Commun* (2021) 12(1):6468. doi: 10.1038/s41467-021-26640-x

16. Zimmerman MW, Durbin AD, He S, Oppel F, Shi H, Tao T, et al. Retinoic acid rewires the adrenergic core regulatory circuitry of childhood neuroblastoma. *Sci Adv* (2021) 7(43):eabe0834. doi: 10.1126/sciadv.abe0834

17. Weichert-Leahey N, Shi H, Tao T, Oldridge DA, Durbin AD, Abraham BJ, et al. Genetic predisposition to neuroblastoma results from a regulatory polymorphism that promotes the adrenergic cell state. *J Clin Invest* (2023) 133(10):e166919. doi: 10.1172/JCI166919

18. Zhu S, Zhang X, Weichert-Leahey N, Dong Z, Zhang C, Lopez G, et al. Lmo1 synergizes with mycn to promote neuroblastoma initiation and metastasis. *Cancer Cell* (2017) 32(3):310–23 e5. doi: 10.1016/j.ccell.2017.08.002

19. Wang L, Tan TK, Durbin AD, Zimmerman MW, Abraham BJ, Tan SH, et al. Ascl1 is a mycn- and lmo1-dependent member of the adrenergic neuroblastoma core regulatory circuitry. *Nat Commun* (2019) 10(1):5622. doi: 10.1038/s41467-019-13515-5

20. Oldridge DA, Wood AC, Weichert-Leahey N, Crimmins I, Sussman R, Winter C, et al. Genetic predisposition to neuroblastoma mediated by a lmo1 super-enhancer polymorphism. *Nature* (2015) 528(7582):418–21. doi: 10.1038/nature15540

21. Kildisiute G, Kholosy WM, Young MD, Roberts K, Elmentaite R, van Hooff SR, et al. Tumor to normal single-cell mrna comparisons reveal a pan-neuroblastoma cancer cell. *Sci Adv* (2021) 7(6):eabd3311. doi: 10.1126/sciadv.abd3311

22. Dong R, Yang R, Zhan Y, Lai HD, Ye CJ, Yao XY, et al. Single-cell characterization of Malignant phenotypes and developmental trajectories of adrenal neuroblastoma. *Cancer Cell* (2020) 38(5):716–33 e6. doi: 10.1016/j.ccell.2020.08.014

23. Jansky S, Sharma AK, Korber V, Quintero A, Toprak UH, Wecht EM, et al. Single-cell transcriptomic analyses provide insights into the developmental origins of neuroblastoma. *Nat Genet* (2021) 53(5):683–93. doi: 10.1038/s41588-021-00806-1

24. Rohrer H. Linking human sympathoadrenal development and neuroblastoma. *Nat Genet* (2021) 53(5):593–4. doi: 10.1038/s41588-021-00845-8

25. Yuan X, Seneviratne JA, Du S, Xu Y, Chen Y, Jin Q, et al. Single-cell profiling of peripheral neuroblastic tumors identifies an aggressive transitional state that bridges an adrenergic-mesenchymal trajectory. *Cell Rep* (2022) 41(1):111455. doi: 10.1016/j.celrep.2022.111455

26. Thirant C, Peltier A, Durand S, Kramdi A, Louis-Brennetot C, Pierre-Eugene C, et al. Reversible transitions between noradrenergic and mesenchymal tumor identities define cell plasticity in neuroblastoma. *Nat Commun* (2023) 14(1):2575. doi: 10.1038/s41467-023-38239-5

27. Avitabile M, Bonfiglio F, Aievola V, Cantalupo S, Maiorino T, Lasorsa VA, et al. Single-cell transcriptomics of neuroblastoma identifies chemoresistance-associated genes and pathways. *Comput Struct Biotechnol J* (2022) 20:4437–45. doi: 10.1016/j.csbj.2022.08.031

28. Gartlgruber M, Sharma AK, Quintero A, Dreidax D, Jansky S, Park YG, et al. Super enhancers define regulatory subtypes and cell identity in neuroblastoma. *Nat Cancer* (2021) 2(1):114–28. doi: 10.1038/s43018-020-00145-w

29. Garaventa A, Poetschger U, Valteau-Couanet D, Luksch R, Castel V, Elliott M, et al. Randomized trial of two induction therapy regimens for high-risk neuroblastoma: hr-nbl1.5 international society of pediatric oncology european neuroblastoma group study. *J Clin Oncol* (2021) 39(23):2552–63. doi: 10.1200/JCO.20.03144

30. Moreno L, Vaidya SJ, Schrey D, Pinkerton CR, Lewis IJ, Kearns PR, et al. Long-term analysis of children with metastatic neuroblastoma treated in the ensg5 randomised clinical trial. *Pediatr Blood Cancer* (2019) 66(4):e27565. doi: 10.1002/pbc.27565

31. Manas A, Aaltonen K, Andersson N, Hansson K, Adamska A, Seger A, et al. Clinically relevant treatment of pdx models reveals patterns of neuroblastoma chemoresistance. *Sci Adv* (2022) 8(43):eabq4617. doi: 10.1126/sciadv.abq4617

32. Gomez RL, Woods LM, Ramachandran R, Abou Tayoun AN, Philpott A, Ali FR. Super-enhancer associated core regulatory circuits mediate susceptibility to retinoic acid in neuroblastoma cells. *Front Cell Dev Biol* (2022) 10:943924. doi: 10.3389/fcell.2022.943924

33. van Groningen T NC, Chan A, Akogul N, Westerhout EM, von Stedingk K, Hamdi M, et al. An immature subset of neuroblastoma cells synthesizes retinoic acid and depends on this metabolite. *bioRxiv* (2021). doi: 10.1101/2021.05.18.444639

34. Mabe NW, Huang M, Dalton GN, Alexe G, Schaefer DA, Geraghty AC, et al. Transition to a mesenchymal state in neuroblastoma confers resistance to anti-gd2 antibody via reduced expression of st8sia1. *Nat Cancer* (2022) 3(8):976–93. doi: 10.1038/s43018-022-00405-x

35. Westerhout EM, Hamdi M, Stroeken P, Nowakowska NE, Lakeman A, van Arkel J, et al. Mesenchymal-type neuroblastoma cells escape alk inhibitors. *Cancer Res* (2022) 82(3):484–96. doi: 10.1158/0008-5472.CAN-21-1621

36. Mina M, Boldrini R, Citti A, Romania P, D'Alicandro V, De Ioris M, et al. Tumor-infiltrating T lymphocytes improve clinical outcome of therapy-resistant neuroblastoma. *Oncoimmunology* (2015) 4(9):e1019981. doi: 10.1080/2162402X.2015.1019981

37. Melaiu O, Mina M, Chierici M, Boldrini R, Jurman G, Romania P, et al. Pd-L1 is a therapeutic target of the bromodomain inhibitor jq1 and, combined with hla class I, a promising prognostic biomarker in neuroblastoma. *Clin Cancer Res* (2017) 23(15):4462–72. doi: 10.1158/1078-0432.CCR-16-2601

38. Forloni M, Albini S, Limongi MZ, Cifaldi L, Boldrini R, Nicotra MR, et al. Nf-kappab, and not mycn, regulates mhc class I and endoplasmic reticulum aminopeptidases in human neuroblastoma cells. *Cancer Res* (2010) 70(3):916–24. doi: 10.1158/0008-5472.CAN-09-2582

39. Lorenzi S, Forloni M, Cifaldi L, Antonucci C, Citti A, Boldrini R, et al. Irf1 and nf-kb restore mhc class I-restricted tumor antigen processing and presentation to cytotoxic T cells in aggressive neuroblastoma. *PloS One* (2012) 7(10):e46928. doi: 10.1371/journal.pone.0046928

40. Cristescu R, Mogg R, Ayers M, Albright A, Murphy E, Yearley J, et al. Pan-tumor genomic biomarkers for pd-1 checkpoint blockade-based immunotherapy. *Science* (2018) 362(6411):eaar3593. doi: 10.1126/science.aar3593

41. Ayers M, Lunceford J, Nebozhyn M, Murphy E, Loboda A, Kaufman DR, et al. Ifn-gamma-related mrna profile predicts clinical response to pd-1 blockade. *J Clin Invest* (2017) 127(8):2930–40. doi: 10.1172/JCI91190

42. Wolpaw AJ, Grossmann LD, Dessau JL, Dong MM, Aaron BJ, Brafford PA, et al. Epigenetic state determines inflammatory sensing in neuroblastoma. *Proc Natl Acad Sci USA* (2022) 119(6):e2102358119. doi: 10.1073/pnas.2102358119

43. Sengupta S, Das S, Crespo AC, Cornel AM, Patel AG, Mahadevan NR, et al. Mesenchymal and adrenergic cell lineage states in neuroblastoma possess distinct immunogenic phenotypes. *Nat Cancer* (2022) 3(10):1228–46. doi: 10.1038/s43018-022-00427-5

44. Cornel AM, Dunnebach E, Hofman DA, Das S, Sengupta S, van den Ham F, et al. Epigenetic modulation of neuroblastoma enhances T cell and nk cell immunogenicity by inducing a tumor-cell lineage switch. *J Immunother Cancer* (2022) 10(12):e005002. doi: 10.1136/jitc-2022-005002

45. van Wezel EM, van Zogchel LMJ, van Wijk J, Timmerman I, Vo NK, Zappeij-Kannegieter L, et al. Mesenchymal neuroblastoma cells are undetected by current mrna marker panels: the development of a specific neuroblastoma mesenchymal minimal residual disease panel. *JCO Precis Oncol* (2019) 3:PO.18.00413. doi: 10.1200/PO.18.00413

46. Wu J, Waxman DJ. Immunogenic chemotherapy: dose and schedule dependence and combination with immunotherapy. *Cancer Lett* (2018) 419:210–21. doi: 10.1016/j.canlet.2018.01.050

47. Galluzzi L, Vitale I, Warren S, Adjemian S, Agostinis P, Martinez AB, et al. Consensus guidelines for the definition, detection and interpretation of immunogenic cell death. *J Immunother Cancer* (2020) 8(1):e000337. doi: 10.1136/jitc-2019-000337

48. Kroemer G, Galassi C, Zitvogel L, Galluzzi L. Immunogenic cell stress and death. *Nat Immunol* (2022) 23(4):487–500. doi: 10.1038/s41590-022-01132-2

49. Lucarini V, Melaiu O, D'Amico S, Pastorino F, Tempora P, Scarsella M, et al. Combined mitoxantrone and anti-tgfbeta treatment with pd-1 blockade enhances antitumor immunity by remodelling the tumor immune landscape in neuroblastoma. *J Exp Clin Cancer Res* (2022) 41(1):326. doi: 10.1186/s13046-022-02525-9

50. Melaiu O, Chierici M, Lucarini V, Jurman G, Conti LA, De Vito R, et al. Cellular and gene signatures of tumor-infiltrating dendritic cells and natural-killer cells predict prognosis of neuroblastoma. *Nat Commun* (2020) 11(1):5992. doi: 10.1038/s41467-020-19781-y

51. Shi F, Huang X, Hong Z, Lu N, Huang X, Liu L, et al. Improvement strategy for immune checkpoint blockade: A focus on the combination with immunogenic cell death inducers. *Cancer Lett* (2023) 562:216167. doi: 10.1016/j.canlet.2023.216167

52. Li Z, Lai X, Fu S, Ren L, Cai H, Zhang H, et al. Immunogenic cell death activates the tumor immune microenvironment to boost the immunotherapy efficiency. *Adv Sci (Weinh)* (2022) 9(22):e2201734. doi: 10.1002/advs.202201734

53. Andre N, Orbach D, Pasquier E. Metronomic maintenance for high-risk pediatric Malignancies: one size will not fit all. *Trends Cancer* (2020) 6(10):819–28. doi: 10.1016/j.trecan.2020.05.007

frontiers | Frontiers in Immunology

TYPE Review
PUBLISHED 14 February 2024
DOI 10.3389/fimmu.2024.1341390

OPEN ACCESS

EDITED BY
Silvia Pesce,
University of Genoa, Italy

REVIEWED BY
Yves Delneste,
Institut National de la Santé et de la Recherche Médicale (INSERM), France
Nicola Tamassia,
University of Verona, Italy

*CORRESPONDENCE
Sebastien Jaillon
sebastien.jaillon@humanitasresearch.it

†These authors have contributed equally to this work

RECEIVED 20 November 2023
ACCEPTED 29 January 2024
PUBLISHED 14 February 2024

CITATION
Di Ceglie I, Carnevale S, Rigatelli A, Grieco G, Molisso P and Jaillon S (2024) Immune cell networking in solid tumors: focus on macrophages and neutrophils.
Front. Immunol. 15:1341390.
doi: 10.3389/fimmu.2024.1341390

Immune cell networking in solid tumors: focus on macrophages and neutrophils

Irene Di Ceglie[1†], Silvia Carnevale[1†], Anna Rigatelli[1†], Giovanna Grieco[1,2†], Piera Molisso[1,2†] and Sebastien Jaillon[1,2*]

[1]IRCCS Humanitas Research Hospital, Milan, Italy, [2]Department of Biomedical Sciences, Humanitas University, Milan, Italy

The tumor microenvironment is composed of tumor cells, stromal cells and leukocytes, including innate and adaptive immune cells, and represents an ecological niche that regulates tumor development and progression. In general, inflammatory cells are considered to contribute to tumor progression through various mechanisms, including the formation of an immunosuppressive microenvironment. Macrophages and neutrophils are important components of the tumor microenvironment and can act as a double-edged sword, promoting or inhibiting the development of the tumor. Targeting of the immune system is emerging as an important therapeutic strategy for cancer patients. However, the efficacy of the various immunotherapies available is still limited. Given the crucial importance of the crosstalk between macrophages and neutrophils and other immune cells in the formation of the anti-tumor immune response, targeting these interactions may represent a promising therapeutic approach against cancer. Here we will review the current knowledge of the role played by macrophages and neutrophils in cancer, focusing on their interaction with other immune cells.

KEYWORDS

tumor microenvironment, anti-tumor immunity, tumor-associated macrophages, tumor-associated neutrophils, immune cell network

Introduction

To develop and grow, tumor cells require constant support from cells of the surrounding environment (1–3). Immune cells are key players in this scene where they actively collaborate to either promote or inhibit tumor growth (4, 5). Through the production of numerous immunomodulatory molecules (e.g. cytokines, chemokines and growth factors), tumor cells can modulate the phenotype of immune cells and the positive or negative influence that they exert on the tumor microenvironment (TME) (6, 7). Additionally, tumor-infiltrated immune cells are engaged in a number of mutual interactions which further potentiate or reduce their pro-tumor or anti-tumor activities

(8–10). Tumor-associated macrophages (TAMs) have long been identified as central players of this complex intercellular network (11–13). More recently, neutrophils, traditionally considered only as short-lived front-line fighters against pathogens, have received increasing attention due to their important role in regulating tumor development (14–17).

Being highly plastic and consequently heterogeneous, TAMs and tumor associated neutrophils (TANs) adapt their phenotype and activation state to the surrounding environment (11–21). TAMs and TANs have the capacity to act directly on tumor cells to promote or inhibit their proliferation, and to modulate the anti-tumor or pro-tumor activities of other immune cells (11, 14, 22). Targeting the immune system is now a reality and is emerging as an important therapeutic approach for the treatment of cancer (23, 24). However, a significant percentage of patients do not respond to current available treatments (25). Given the crucial importance of the intercellular crosstalk between immune cells within the TME, novel therapeutic approaches targeting these interactions might be beneficial. In this review, after a short overview concerning TAMs and TANs, we will focus on their complex intercellular interactions with other immune cells, with a particular emphasis on how these interactions can influence tumor development and progression.

Macrophages in the tumor microenvironment

Macrophages are large phagocytic cells of the innate immune system and are found in tissues where they play numerous roles, including defense against invading pathogens and maintenance of tissue homeostasis (19). Macrophages have long been identified as tumor-infiltrating cells and as one of the key regulators of the immune response within the TME (11–13). In a majority of human cancers, a high level of macrophage infiltration has been associated with a poor prognosis, including in gastric cancer, urogenital and head neck cancers, pancreatic ductal adenocarcinoma and breast carcinoma with some notable exceptions such as colorectal cancer and ovarian cancer (26–33).

The majority of TAMs derive from circulating bone marrow (BM)-derived monocytes that migrate into the tumor bed mainly under the influence of chemokines (e.g. C-C motif ligand 2 (CCL2)), cytokine colony stimulating factor 1 (CSF-1), or complement components (26, 34–39). In addition, numerous studies have shown that another important source of TAMs was represented by tissue-resident macrophages (TRMs), which derive from embryonic precursors and are maintained locally (40–45). Interestingly, a difference in origin can influence the function of TAMs within the TME (46, 47).

In addition to their heterogenous origin, TAMs have a high degree of plasticity and constantly adapt in response to the microenvironment further increasing their heterogeneity within the TME (11, 19, 48, 49). Historically, TAMs have been classified into two major polarization states, generally referred to as M1 (or classically activated) and M2 (or alternatively activated) (50–52). M1 polarization can be induced by bacterial products and interferon-γ (IFN-γ) and has been associated with tissue damage and anti-tumor activities (50, 51). In contrast, M2 polarization, induced by cytokines of the type 2 immune response, such as interleukin (IL)-13 and IL-4, has been associated with tissue repair and tumor-promotion (50, 51, 53). Although this dichotomous classification is still commonly used, it is nowadays fully recognized that it is too reductive and does not reflect the extraordinary complexity and heterogeneity of the different phenotypes and activation states of TAMs (13, 21, 52). Novel technologies, including single-cell RNA sequencing and spatial transcriptomic analyses, have led to a better understanding of macrophage complexity and heterogeneity in different tumor contexts. In addition, these technologies have facilitated insight into the localization of macrophages and their interactions with other cells within the TME (54–61).

Macrophages and immune cells cross-talk in the TME

Macrophages and lymphoid cells

The existence of a crosstalk between macrophages and lymphoid cells within the TME has been clearly defined and extensively studied. In various human cancers, TAMs were found in close proximity to different lymphoid cells, including natural killer (NK) cells and T cells (62–64). The final effect of the interaction between macrophages and lymphoid cells can differ depending on the type and the stage of tumors, the presence of immunomodulatory molecules and the location of TAMs within the TME.

A large body of evidence has shown that TAMs can inhibit the anti-tumor activity of lymphoid cells, thereby promoting cancer progression. As a matter of fact, the presence of monocyte/macrophage infiltration was found to be inversely correlated with the presence and activation of NK cells in different human cancers including lung cancer, gastric cancer and hepatocellular carcinoma (HCC) (64–66). In contrast, monocyte/macrophage infiltration was found positively correlated with the presence of regulatory $CD4^+$ T lymphocytes (T-reg) in prostate cancer and colorectal cancer (67, 68). Consistently, CSF-1– CSF-1 receptor (CSF-1R) axis blockade or macrophage recruitment blockade via C-C chemokine receptor type 2 (CCR2)-inhibition could restore immune response against tumor in cancer models (69, 70).

The mechanisms by which TAMs can inhibit the anti-tumor activities of lymphoid cells are numerous ranging from the release of soluble inhibitory mediators and cell-cell contact to the modulation of their recruitment or their exclusion from the tumor bed (Figure 1). The release of tumor growth factor-β (TGF-β) by TAMs can directly inhibits T cell and NK cell effector functions (64, 71–74). In addition, macrophage-derived TGF-β can promote the generation of T-reg lymphocytes via the induction of SMAD3-mediated FOXP3 expression and the upregulation of PD-1 (68, 75). TGF-β availability within the TME can be further amplified by metalloproteinase 9 (MMP-9) secreted by

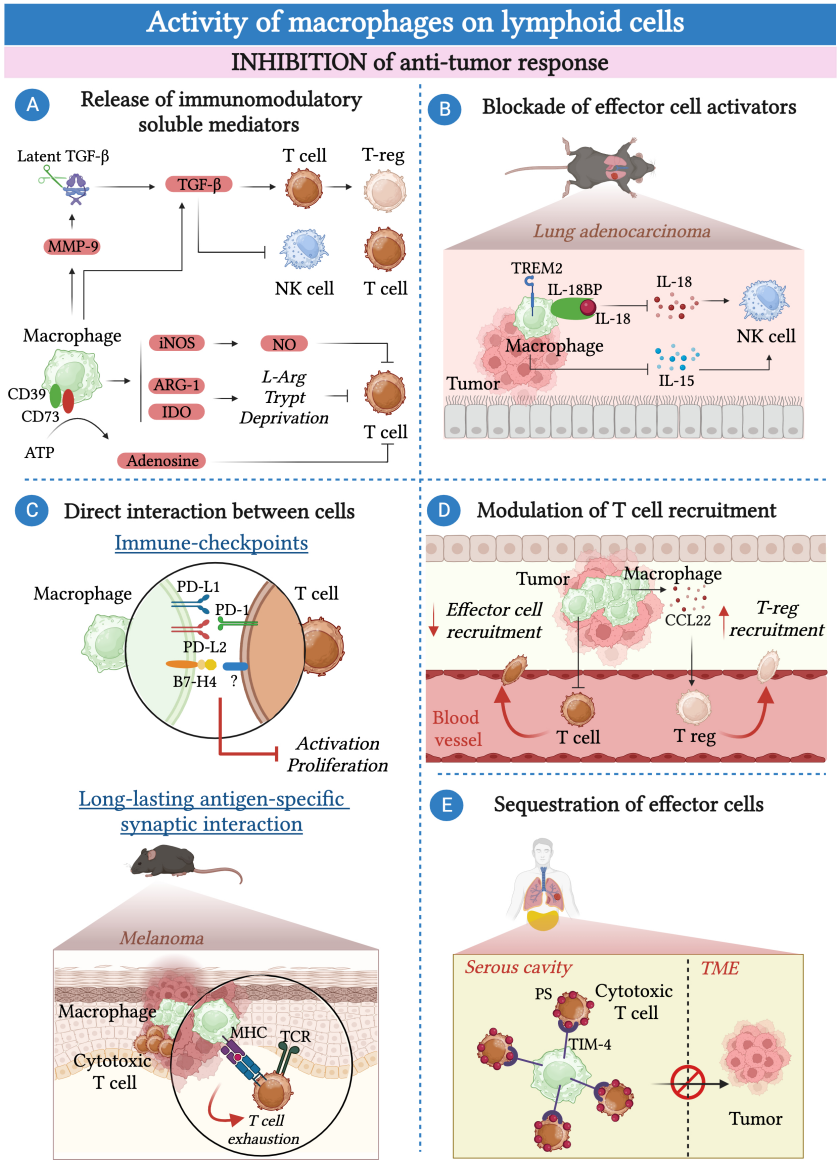

FIGURE 1
Macrophages inhibit the anti-tumor response of lymphoid cells. **(A)** Macrophages secrete a plethora of soluble molecules and immunomodulatory enzymes that inhibit effector cell functions including tumor growth factor β (TGF-β), inducible nitric oxide synthase (iNOS), indoleamine-2,3-dioxygenase (IDO) and arginase-1 (Arg-1). In addition, they produce metalloproteinase 9 (MMP-9) that induces the activation of the latent TGF-β present in the extracellular matrix (ECM). TAMs express CD39 and CD73, which convert the pro-inflammatory ATP present in the TME into the immunosuppressive adenosine. **(B)** In the context of lung carcinoma, triggering receptor expressed on myeloid cells 2 (TREM2)-expressing macrophages suppress the cytokine-mediated activation of NK-cells via the production of IL-18-binding protein (IL-18BP) and by limiting IL-15 production by dendritic cells. **(C)** Macrophages can inhibit the activation of effector cells in a contact-dependent manner. They express immune checkpoints such as programmed cell death ligand 1 (PD-L1), PD-L2 and B7-H4 that, by binding to their ligands, impair the activity of T cells and NK cells. In a mouse model of melanoma, the formation of an antigen-specific interaction between macrophages and T cells leads to T cell exhaustion. **(D)** Macrophages can inhibit the recruitment of effector T cells into the TME whereas they favor the recruitment of T-reg lymphocytes via the secretion of CCL22. **(E)** In pleural and peritoneal body cavities, macrophages expressing T-cell immunoglobulin and mucin domain containing 4 (TIM-4) can sequester $CD8^+$ cytotoxic T cells away from the tumor by binding to phosphatidylserine (PS) expressed on their surface and inhibiting their proliferation.

macrophages, which can cleave and activate latent TGF-β present in the extracellular matrix (ECM) (76).

TAMs can release the immunoregulatory enzymes Arginase-1 (Arg-1) and indoleamine 2,3-dioxygenase (IDO) that, by catalyzing the degradation of L-arginine (L-arg) and L-tryptophan respectively, deprive T cells of essential nutrients, leading to their functional impairment (77–79). A third important immunomodulatory enzyme produced by macrophages is the inducible nitric oxide synthase (iNOS), which catalyzes the production of nitric oxide (NO). In turn, NO has a direct inhibitory effect on T cell proliferation, as well as an indirect effect due to the secondary production of peroxynitrites able to impair the interaction of the major histocompatibility complex (MHC) with the T cell receptor (TCR) via nitration of tyrosines in the TCR-CD8 complex (80–82).

TAMs can exert their pro-tumor activity by blocking the activity of soluble factors that normally contribute to the activation of lymphoid cells. For instance, TAMs can express CD39 and CD73, which are essential in converting the pro-inflammatory adenosine triphosphate (ATP) present in the TME into immunosuppressive adenosine (83). In glioblastoma, kynurenine produced by cancer cells upregulates the expression of hydrocarbon receptor (AHR) in TAMs. In turn, AHR favors the expression of the ectonucleotidase CD39, which, in collaboration with CD73, leads to the dysfunction of $CD8^+$ T cells via the production of adenosine (84, 85).

In a murine model of lung adenocarcinoma, efferocytosis of apoptotic cancer cell by macrophages induced a pro-tumorigenic program controlled by triggering receptor expressed on myeloid cells 2 (TREM2). In particular, $TREM2^+$ macrophages can prevent the recruitment and activation of NK cells by blocking the activities of IL-18 and IL-15 through the production of IL-18 binding protein and by inhibiting the production of IL-15 by tumor-infiltrating dendritic cells (65).

The mechanism by which macrophages can dampen the anti-tumor response goes beyond the secretion of molecules or the interference with soluble mediators and often requires direct cell-cell contact.

TAMs have been found to express high levels of immune checkpoint molecules, including programmed cell death ligand 1 (PD-L1), PD-L2, V-domain Ig suppressor of T cell activation (VISTA) and B7-H4 (11, 86–93). The interaction of these immune checkpoints with their ligands expressed on T cells results in the suppression of the adaptive T cell immune response (94). Consistently, immune checkpoint blockade can restore T cell-mediated anti-tumor immune response (89, 91). In addition to T cells, PD-1, the ligand of PD-L1, can be expressed by a subset of fully mature NK cells, suggesting that NK cells can also serve as a target of PD-L1-mediated inhibition by macrophages (95).

In addition to the expression of immune checkpoints, other mechanisms involving cell-cell contact between macrophages and T cells have been identified and may lead to T cell exhaustion. For instance, TAMs and $CD8^+$ T cells can be engaged in a long-lasting antigen-specific synaptic interaction. This interaction causes only weak stimulation of the TCR, which is insufficient to activate T cells and instead leads to their exhaustion (96).

Furthermore, different lines of evidence suggested the involvement of TAMs in modulating the recruitment of lymphoid cells within the TME. In cervical and breast cancer models, CSF-1R-blockade has been shown to enhance $CD8^+$ T cell infiltration (97). Consistently, LIF-mediated epigenetic silencing of CXCL9, one of the most important chemokines for $CD8^+$ T cells, in macrophages resulted in decreased infiltration of $CD8^+$ T cells into the tumor (98, 99). While they can reduce the recruitment of effector $CD8^+$ T cells in the TME, macrophages have been suggested to facilitate the recruitment of T-reg lymphocytes via the secretion of CCL22 in human ovarian cancer (100). In a mouse model of melanoma, intra-tumoral administration of an anti-CCL22 antibody reduced the recruitment of T-reg lymphocytes and inhibited tumor growth (101).

Macrophages have been implicated in the sequestration of effector T cells away from the tumor bed. Recently, a study showed that serous cavity-resident macrophages expressed high levels of T-cell immunoglobulin and mucin domain containing 4 (TIM-4), a receptor for phosphatidylserine (PS). The interaction between TIM-4 and PS, highly expressed on cytotoxic $CD8^+$ T cells, resulted in the sequestration of $CD8^+$ T cells away from the tumor and inhibited their proliferation (102). Similarly, in samples of human non-small cell lung carcinoma (NSLC),TAMs reduced the motility of the $CD8^+$ T cells present in the stroma surrounding the tumor, limiting their entry into the tumor bed (62).

Although in a large number of studies, TAMs appeared to reduce the anti-tumor activity of lymphoid cells, some works have suggested the existence of macrophages with an opposite function in different tumors (Figure 2). Recently, a study identified a discrete population of human tissue-resident $FOL2R^+$ macrophages present in healthy mammary gland and breast cancer primary tumors endowed with an anti-tumor function. This population of macrophages was localized in the perivascular areas of the tumor stroma where they interacted with $CD8^+$ T cells and promoted their activation (103). Of note, the presence of $FOLR2^+$ macrophages has been associated with increased survival in breast cancer patients (103). In addition to T cells, macrophages have the potential to support the anti-tumor activity of NK cells either via the release of soluble molecules or via direct contact. For instance, in a model of mammary tumor, TAMs expressing the lipid transporter epidermal fatty acid binding proteins-(E-FABP) have been described to have an anti-tumor activity through the activation of NK cells. Specifically, the expression of E-FABP promoted the formation of lipid droplets in TAMs, leading to increased IFN-β production, which, in turn, favored the recruitment of effector cells, particularly NK cells (104). Remarkably, the same study showed that E-FABP was highly expressed in TAMs from women with early-stage disease, and that this expression decreased with disease progression (104). In *in vitro* co-culture experiments, M1-macrophages induced an IL-23 and IFN-β-dependent upregulation of natural killer group 2D (NKG2D) expression, an IL-1β-dependent upregulation of NKp44 expression, and sustained the production of IFN-γ by NK cells via the release of IFN-β and the engagement of the 2B4-CD48 pathway (105). Similarly, M0 and M2 macrophages reprogrammed to M1 via *in vitro* LPS stimulation can promote the cytotoxic activity of NK cells via a contact-dependent mechanism and drive the production of IFN-γ by NK cells via the interaction between DNAX accessory molecule-1 (DNAM-1) and 2B4 and the production of IL-18 (73, 106).

In addition to T cells and NK cells, some evidence suggested that macrophages could promote B cell proliferation via the release of B cell-activating factor (BAFF) or IL-6 (8, 107, 108). However, the relevance of this interaction within the TME remains to be clarified.

The interaction between macrophages and lymphoid cells within the TME is mutual and the phenotype and function of macrophages can also be affected by lymphoid cells (12, 109). For instance, the IFN-γ produced by T-helper (Th)-1 cells, NK cells and cytotoxic $CD8^+$ T cells increases the presentation of antigens by macrophages, the production of pro-inflammatory cytokines and the cytotoxic activity of macrophages against tumor cells (48, 109, 110). In contrast, lymphoid cells found in the TME can also favor a pro-tumor phenotype of macrophages. For instance, $CD4^+$ Th-2

10.3389/fimmu.2024.1341390

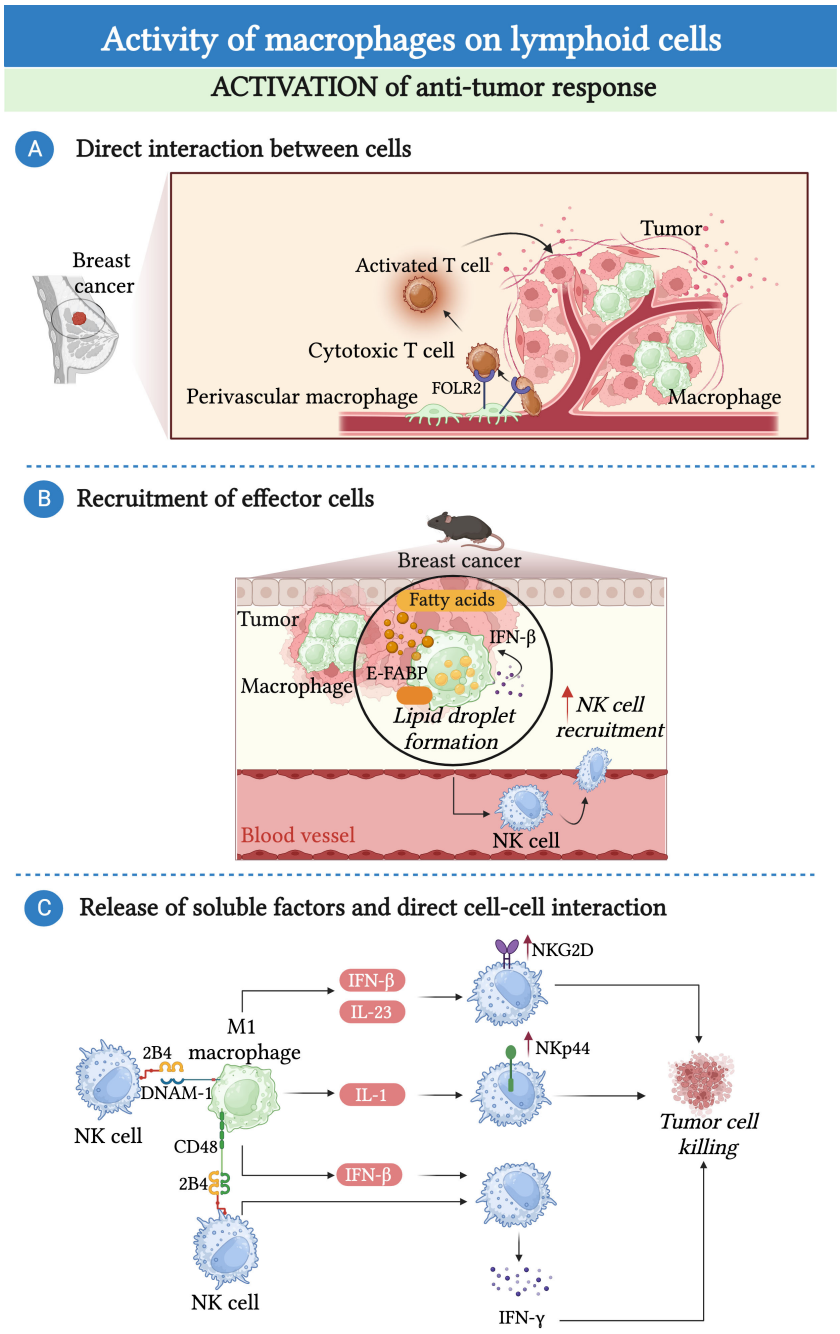

FIGURE 2
Macrophages promote the anti-tumor response of lymphoid cells. **(A)** In the context of breast cancer, a population of folate receptor 2 (FOLR2)-expressing macrophages endowed with anti-tumor properties can establish a prolonged interaction with cytotoxic T cells facilitating their recruitment and activation. **(B)** In a mouse model of mammary tumor, accumulation of lipid droplets in epidermal fatty acid binding proteins (E-FABP)-expressing TAMs induces the production of interferon-β (IFN-β), leading to the recruitment and activation of NK-cells. **(C)** Macrophages have the potential to support the anti-tumor activity of NK cells. M1-macrophages induce an IL-23 and IFN-β-dependent upregulation of NKG2D expression, an IL-1β-dependent upregulation of NKp44 expression, and sustained the production of IFN-γ by NK cells via the release of IFN-β and the interaction of CD48 and DNAX accessory molecule-1 (DNAM-1) with 2B4.

cells, innate lymphoid cells (ILCs)-2- and T-reg lymphocytes that produce IL-4, IL-13 and IL-10 can sustain the formation of M2-like macrophages with a pro-tumor phenotype (111–115). Interestingly, it has been shown that mouse T-reg lymphocytes can indirectly promote the survival of M2-like pro-tumor macrophages. Indeed, by limiting the production of IFN-γ by $CD8^+$ T cells, T- reg lymphocytes prevent the inhibition of sterol regulatory element binding protein 1 (SREBP1)-mediated fatty acid synthesis, which is crucial for the survival of M2-like macrophages (116).

Additionally, NK cells have been shown to be able to kill macrophages. Of note, this macrophage killing activity was found to be especially efficient toward M0 and M2 macrophage subtypes

whereas M1 macrophages were more resistant to lysis due to the higher expression of human leukocytes antigen (HLA) class I molecules (106). Similarly, invariant natural killer T cells (iNKT) have been shown to exert anti-tumor activity by killing macrophages in a CD1d-dependent mechanism (117).

Finally, some studies have highlighted an effect of B cells on macrophages in tumor. In a mouse model of melanoma, adoptive transfer of a subtype of B cells can induce M2-like polarization of TAMs (118).

Macrophages and myeloid cells

While the interaction between macrophages and lymphoid cells has been the subject of numerous studies, their interaction with other myeloid cells has received less attention. Among myeloid cells, dendritic cells are key players in the orchestration of both innate and adaptive immune responses in cancer (119).TAMs produce high levels of vascular endothelial growth factor (VEGF), IL-10, IL-6 and TGF-β which are described to inhibit the activity of dendritic cells (11, 120–124). Besides dendritic cells, macrophages can interact with neutrophils (14). The interaction between these two important myeloid subtypes within the TME will be further discussed in this review.

Neutrophils in the tumor microenvironment

Neutrophils are the most abundant circulating leukocytes in humans. They have long been considered as simple first-line fighters against invading pathogens, but are now recognized as central players in the regulation of tumor development and progression (14, 16). TANs have been found in the TME of several human cancers, including renal cell carcinoma, hepatocellular carcinoma, lung cancer, melanoma, head and neck cancer, glioma, colorectal cancer, sarcomas, pancreatic cancer, breast cancer, gastric cancer, urothelial carcinoma and ovarian cancer (125–136). However, their role is still controversial and may depend on a number of factors, including the different types of cancer, the stage of development and the presence of other cells (14, 17, 137). While in a large number of studies, a high level of TANs has been associated with a poor prognosis for patients, in others, including colorectal cancer and undifferentiated pleomorphic sarcoma (UPS), it has been associated with a better outcome (14, 125, 130, 138–143).

Mature mouse and human neutrophils are constantly released from the BM where they differentiate and mature from progenitors in response to growth factors, in particular granulocyte-colony stimulating factor (G-CSF) and granulocyte macrophage-colony stimulating factor (GM-CSF) (16, 144–149). The process of neutrophil mobilization from the BM has been extensively investigated in mice and is highly dependent on the regulation of the expression of genes coding for CXCR4 and CXCR2 (150). Upon maturation, BM-neutrophils downregulate CXCR4 expression, which is the receptor for CXCL12 produced by BM stromal cells, and increase the expression of CXCR2. The expression of CXCR2 and the presence CXCL2, which is the ligand for CXCR2, in the circulation trigger the release of neutrophils into the peripheral blood (150, 151). The observation of alterations in neutrophil biology among patients with genetic mutations in CXCR4 and CXCR2 implies the significance of these molecules also in human (152, 153). Stress conditions, including cancer, trigger an "emergency granulopoiesis" program during which the process of neutrophil maturation and BM egress is altered, resulting in the release of immature neutrophils into the circulation (154).

Circulating neutrophils express high levels of CXCR1 and CXCR2, which play a major role in their recruitment into the TME (14, 16, 155). Numerous studies have shown the involvement of CXCR1 and CXCR2 ligands, including CXCL1, CXCL2, CXCL5, CXCL6 and CXCL8 (only for humans) in the recruitment of neutrophils into the TME (14, 156–162). Additionally, other inflammatory mediators, including the cytokines TNF-α, IL-17 and IL-1β have been implicated in the recruitment of neutrophils into the TME (14, 163, 164).

While neutrophils were traditionally considered as short-lived effector cells with limited plasticity, a large body of evidence challenged this view and recognized their considerable plasticity and heterogeneity (17, 18, 20). Based on their phenotype and function and mirroring the M1/M2 paradigm, TANs have been classified into anti-tumor (N1) and pro-tumor (N2) neutrophils (14, 165, 166). As mentioned above for macrophages, new studies based on state-of-the-art methodology, including single cell RNA sequencing, mass cytometry by time-of-flight (CyTOF), multiplex immunofluorescence and spatial transcriptomic have revealed a high degree of heterogeneity in TANs (14, 16, 167–171).

Pro-tumor neutrophils can directly promote tumor development by inducing tissue damage and genetic instability through the production of radical oxygen species (ROS) and miRNA, and by stimulating tumor growth through the secretion of cytokines and growth factors (172–177). Additionally, pro-tumor neutrophils can facilitate the formation of tumor metastasis through different mechanisms such as the induction of angiogenesis and ECM remodeling (178–181). In contrast, anti-tumor neutrophils can inhibit tumor growth through the direct killing of tumor cells via the production of ROS and NO or by trogocytosis of antibody-opsonized cancer cells (182, 183).

Besides their direct effect on tumor cells, TANs are engaged in dynamic and continuous interactions with a large variety of tumor infiltrating immune cells, affecting their phenotype and effector functions (14). In turn, these immune cells have a significant impact on neutrophil recruitment, phenotype and function (14, 17).

Neutrophils and immune cells cross-talk in tumor

Neutrophils and lymphoid cells

Neutrophils interact with a variety of lymphoid cells including $CD4^+$ and $CD8^+$ T cells, unconventional T cells, NK cells and B cells. In human samples, neutrophils have often been found co-

localized with other lymphoid cells in the tumor bed or in the tumor-draining lymph nodes (139, 184–186).

Neutrophils have the capacity to either inhibit or activate the effector functions of these lymphoid cells (Figure 3) (15).

Several lines of evidence have suggested that human and mouse neutrophil-derived soluble mediators, such as Arg-1, ROS, reactive nitrogen intermediates (RNI) and prostaglandin E2 (PGE2), played a key role in suppressing the effector functions of T cells and NK cells (17, 165, 187–193). In different mouse tumor models, TANs respond to TGF-β by producing significant amounts of Arg-1, leading to a reduction in the availability of L-arginine (165). Given the fundamental role of L-arginine in T cell metabolism, its deprivation results in T cell dysfunction (165). Accordingly, a population of neutrophils expressing Arg-1 has been found in renal cell carcinoma and NSLC patients with a frequency that negatively correlates with the frequency of CD8+ cytotoxic T lymphocytes (191, 192).

Changes in neutrophil metabolism may be linked to their pro-tumor or anti-tumor activities. In a transplantable mouse model of breast cancer with limited glucose supply, c-Kit^{+} immature neutrophils exhibited increased mitochondrial fatty acid oxidation, resulting in higher production of ROS and inhibition of the T cell response (187). The production of RNI, through iNOS–dependent NO production, was found to hinder T cell activation in mammary tumor-bearing *K14Cre; Cdh1$^{F/F}$; Trp53$^{F/F}$* (KEP) mice (189). Neutrophils found within the TME can exhibit endoplasmic

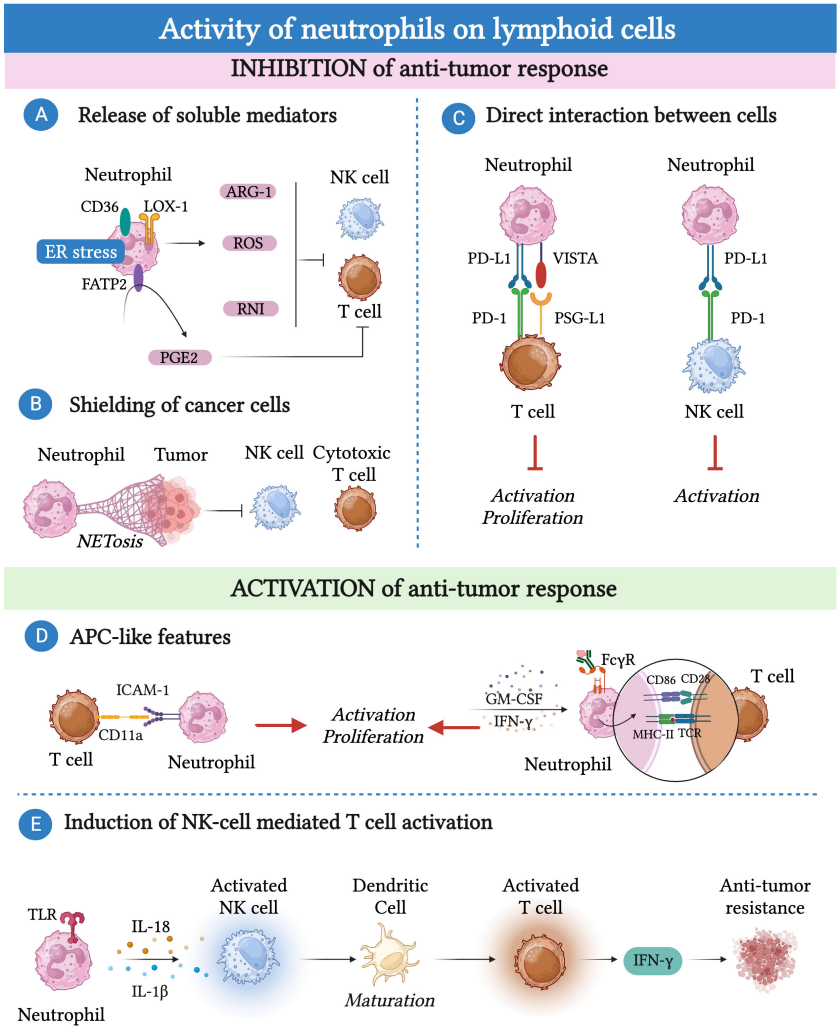

FIGURE 3
Neutrophils can promote or inhibit the anti-tumor response of lymphoid cells. **(A)** Immunosuppression can be mediated by neutrophils via the production of reactive oxygen species (ROS), reactive nitrogen intermediate (RNI) and arginase-1 (Arg-1) or through fatty acid transporter protein 2 (FATP2)-dependent production of prostaglandin E2 (PGE2). **(B)** Neutrophils can indirectly affect the cytotoxic activity of NK cells and CD8^{+} T cells by releasing neutrophil extracellular traps (NETs) that shield cancer cells. **(C)** Neutrophils express immune checkpoints such as programmed cell death 1 ligand 1 (PD-L1) or the V-domain immunoglobulin suppressor of T-cell activation (VISTA) that, by binding to their ligands PD-1 and P-selectin glycoprotein ligand-1 (PSG-L1), cause T cell and NK cell dysfunction. **(D)** Neutrophils can acquire antigen presenting cell-like (APC-like) features under the influence of GM-CSF or interferon (IFN)-γ or upon phagocytosis of antibody-antigen complexes via Fc gamma receptors (FcγRs). Similarly, neutrophils enhance TCR signaling in CD8^{+} T cells through the interaction between CD54/intercellular adhesion molecule 1 (ICAM-1) expressed on neutrophils and CD11a expressed on T cells. **(E)** Tool like receptor (TLR)-stimulated neutrophils can attract and activate NK cells which, in turn, trigger the maturation of dendritic cells resulting in T cell proliferation and IFN-γ production.

reticulum (ER) stress and altered lipid metabolism (188, 194). This phenomenon has been associated with the expression of proteins involved in lipid trafficking and metabolism, such as CD36, lectin-like oxidized low-density lipoprotein receptor-1 (LOX-1), and fatty acid transport protein 2 (FATP2), and with an immunosuppressive phenotype of neutrophils (195). For instance, ER-stressed neutrophils produce higher amounts of ROS and Arg-1, which inhibit T cell proliferation and cytokine production (195, 196). Remarkably, FATP2 expression on neutrophils induced the production of PGE2, which has potent immunosuppressive activity on NK cells and $CD8^+$ T cells (188, 197).

Neutrophils can also indirectly affect NK cell and $CD8^+$ T cell cytotoxic activity through the release of neutrophil extracellular traps (NETs) that shield cancer cells (198). In this context, CXCL chemokines produced by tumor cells induce NETosis in neutrophils, which can coat and protect cancer cells from the cytotoxic activity of NK cells and $CD8^+$ T cells. Interestingly, blockade of protein arginine deiminase 4 (PAD-4), which is essential for the formation of NETs, increased the activity of anti-PD-1 and anti-Cytotoxic T-Lymphocyte Antigen 4 (CTLA-4) immunotherapy in a transplantable mouse model of breast cancer (198).

The interactions between neutrophils and lymphocytes extend beyond the release of soluble mediators, as neutrophils themselves express immune checkpoints such as PD-L1 or VISTA. These molecules can interact with their ligands expressed on T cells and NK cells, leading to their dysfunction (199–204). Neutrophils expressing PD-L1 or VISTA have been found in various types of human and murine cancer, including hepatocellular carcinoma, melanoma, and gastric cancer (199–203).

As mentioned earlier, neutrophils can also interact with lymphoid cells to activate their anti-tumor activity. For instance, in patients with NSLC, neutrophils with antigen-presenting cell (APC)-like features were found and shown to be capable to activate $CD4^+$ and $CD8^+$ T cells (184). Neutrophils can acquire these APC-like features in response to TME-derived GM-CSF and IFN-γ, which induce the expression of MHC-II and CD86 in neutrophils (184). The interaction between these TANs isolated from lung cancer tissue and activated T cells led to increased expression of the costimulatory molecules CD54, CD86, OX40L, and 4-1BBL on the neutrophil surface, which further enhanced T cell proliferation, creating a positive feedback loop (205). Similar findings were observed in colorectal cancer patients, where neutrophils enhanced TCR signaling in $CD8^+$ T cells, in a cell-to-cell contact dependent manner through the interaction between CD54/intercellular adhesion molecule 1 (ICAM-1) expressed on neutrophils and CD11a expressed on T cells (139). Further investigations have demonstrated that the phagocytosis of antibody-antigen complexes via Fc gamma receptors (FcγRs) renders murine and human neutrophils more potent APC-like cells (206).

In addition to T cells, neutrophils can induce NK cell activation through various mechanisms (207, 208). For example, cytokine-stimulated NK cells and neutrophils exchange contact-dependent activation signals involving CD18, ICAM-1 and ICAM-3 (207).

Stimulated neutrophils can attract and activate NK cells trough release of soluble mediators, including IL-1β and IL-18 (208). In turn, activated NK cells can trigger the maturation of dendritic cells, resulting in T cell proliferation and IFN-γ production, suggesting an additional mechanism trough which neutrophils can indirectly control the T cell anti-tumor immune response (208).

In addition to conventional T cells, neutrophils can influence the polarization and activation state of a subset of unconventional T cells, leading to their secretion of IFN-γ. This mechanism required a tripartite interaction between neutrophils, macrophages and unconventional T cells (see below) (143).

The reasons for these dichotomous functions of neutrophils on lymphoid cells are not fully elucidated. Interestingly, a recent study conducted in head and neck cancer (HNC) patients described this neutrophil dual role in tumor-draining lymph nodes, where neutrophils can interact with T cells in a stage-dependent manner (185). In metastasis-free patients, neutrophils transmigrate to lymph-nodes, acquiring APC-like features and promoting T cell anti-tumor activity (185). In contrast, at a later stage, neutrophils acquire PD-L1 expression and suppress T cell activation (185).

Conversely, neutrophils can be influenced by lymphoid cells, which can modulate their recruitment and phenotype to the tumor bed under different conditions (Figure 4) (186, 189, 209, 210). For instance, in a mouse model of breast cancer in KEP mice, γδ T cells in response to IL-1β showed increased production of IL-17 which induced a G-CSF dependent accumulation of neutrophils with an immunosuppressive phenotype in the peripheral blood and metastatic lung (189). In CRC patients, IL-22 producing T cells induced the recruitment of neutrophils, by triggering the production of neutrophil-recruiting chemokines (i.e. CXCL1, CXCL2, CXCL3) by colorectal cancer cells. Importantly, the expression of IL-22 was found associated with the presence of neutrophils and T cells and a favorable prognosis (186).

Recently, in colorectal cancer patients, iNKT cells were found to increase the recruitment of neutrophils with immunosuppressive activity (209). The mechanism was related to the presence of the tumor-associated pathobiont *Fusobacterium nucleatum*, which induced the production of IL-17 and GM-CSF in iNKT. Importantly, the presence of iNKT cells and neutrophils correlated with a worse prognosis, suggesting that targeting this crosstalk could improve patient survival (209). On the other hand, NK cells have been involved in the control of neutrophil pro-tumor activity through an IFN-γ-dependent mechanism in mice (210). In a mouse model of transplantable sarcoma, the absence of NK cells induced neutrophils to acquire a pro-tumor phenotype characterized by the expression of VEGF-A (210) Interestingly, tumor-reprogrammed neutrophils that localize in a unique hypoxic and glycolytic niche exert a potent tumor-supporting, pro-angiogenic function through their high expression of VEGF-A (171). In contrast, NK cells have been suggested to induce neutrophil apoptosis via a NKp46 and FAS–dependent mechanism (211, 212). Remarkably, efferocytosis of apoptotic neutrophils by macrophages has been well documented to promote their shift toward an M2-like pro-tumor phenotype (213).

Neutrophils have been shown to interact also with B cells. Specifically, splenic neutrophils have been described to play a B-cell helper function, promoting the immunoglobulin class switching and the production of antibodies by activated B cells through a

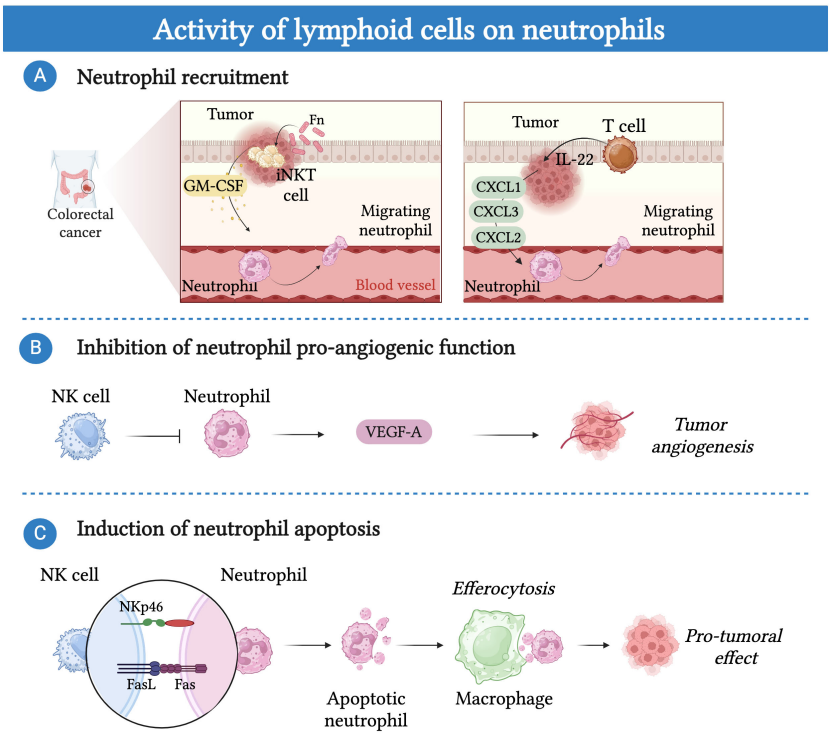

FIGURE 4
Lymphoid cells can modulate the activity of neutrophils. **(A)** Lymphoid cells can regulate the recruitment of neutrophils into the tumor bed. In CRC patients, tumor-associated pathobiont *Fusobacterium nucleatum* (Fn) induces the production of IL-17 and GM-CSF in invariant natural killer T cells (iNKT) resulting in increased neutrophil migration into the tumor bed. Additionally, IL-22 producing T cells induce the recruitment of neutrophils, by triggering the production of neutrophil-recruiting chemokines (i.e. CXCL1, CXCL2, CXCL3) by colorectal cancer cells. **(B)** NK cells control pro-tumor angiogenic function of neutrophils by blocking their secretion of vascular endothelial growth factor (VEGF). **(C)** NK-cells induce neutrophil apoptosis in a NKp46 and FAS-dependent manner. Efferocytosis of apoptotic neutrophils by macrophages promote a shift toward an M2-like pro-tumor phenotype.

mechanism involving BAFF, APRIL and IL-21 (214). However, the involvement of this interaction in cancer has not been investigated.

Neutrophils and myeloid cells

As mentioned above for macrophages, while a significant amount of research has focused on the interaction between neutrophils and lymphoid cells, a limited number of studies have explored the cross-talk between neutrophils and other myeloid cells in the TME (Figure 5) (215).

Neutrophils play a role in promoting the recruitment of other myeloid cells into the tumor bed through the release of chemokines such as CCL2, CCL3, and CCL4, which attract monocytes and dendritic cells (216). Once in the TME, monocytes and dendritic cells produce CXCL8, which favors the recruitment of additional neutrophils, creating a feedback loop that fosters the accumulation of inflammatory cells within the TME (217). Moreover, dendritic cells have been shown to physically interact with neutrophils via dendritic cell-specific intercellular adhesion molecule-3-grabbing non-integrin (DC-SIGN), leading to increased release of TNF-α by neutrophils (217). This interaction enhances the maturation of dendritic cells, thereby improving their capacity to effectively prime T cells and activate their anti-tumor response (217).

Another intriguing hypothesis is that neutrophils could amplify the source of antigens that dendritic cells process and present to T cells (218). Neutrophil-mediated trogoptosis of cancer cells may lead to an increased release of antigens and damage-associated molecular patterns (DAMPs) available for dendritic cells (219–222). This mechanism has been proposed as a potential therapeutic target and strategy to improve dendritic cell-based anti-cancer vaccines.

In a mouse model of breast cancer, it has been shown that neutrophil cytotoxic activity can be modulated by monocytes (223). Breast cancer cells with low spontaneous metastatic potential secrete high levels of CCL2, leading to the recruitment of IFN-γ-producing monocytes. Subsequently, neutrophils upregulate the expression of the transmembrane protein 173 (TMEM173, also known as stimulator of interferon response CGAMP interactor 1 (STING)), which then unleashes their cytotoxic activity (223).

Additionally, neutrophils were found to play a crucial role in potentiating the release of IL-12 by macrophages in the context of 3-methylcholanthrene (3-MCA)-induced sarcomagenesis (143). In turn, IL-12 can activate a subset of unconventional T cells (UTC) that express high levels of IL-12R, resulting in their production of

10.3389/fimmu.2024.1341390

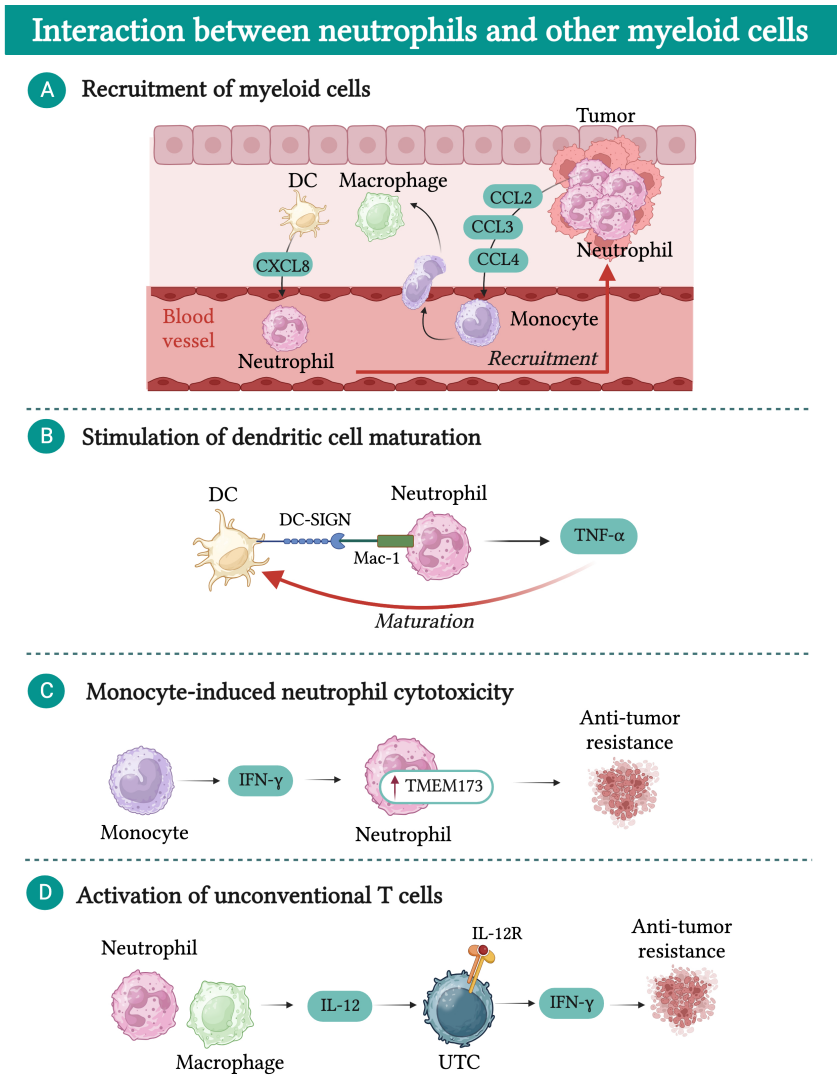

FIGURE 5
Interactions between neutrophils and other myeloid cells in cancer. **(A)** Macrophages and dendritic cells (DCs) are attracted into the tumor bed by chemokines released by neutrophils (e.g. CCL2, CCL3, and CCL4). In turn, macrophages and DCs produce chemokines (e.g. CXCL8) which further fuel neutrophil recruitment. **(B)** DCs physically interact with neutrophils via dendritic cell-specific intercellular adhesion molecule-3-grabbing non-integrin (DC-SIGN), resulting in increased release of tumor necrosis factor α (TNF-α). In turn, TNF-α promotes DC maturation. **(C)** IFN-γ produced by monocytes induces upregulation of transmembrane protein 173 (TMEM173) expression in neutrophils, unleashing their cytotoxic activity. **(D)** In a mouse model of sarcoma, neutrophil-macrophage interaction results in increased production of IL-12 by macrophages, which induces the expression of interferon γ (IFN-γ) in a subset of unconventional αβ T cells (UTCαβ) and favors their anti-tumor activity.

IFN-γ and tumor control (143). To further underscore the importance of the interaction between neutrophils and other myeloid cells, two recent reports investigating the limited success of CSF-1R treatment in preclinical models of cancer revealed that upon TAM depletion, neutrophils acquired a highly immunosuppressive phenotype, counteracting the beneficial effect of macrophage depletion (224, 225).

Conclusion and perspectives

The TME represents a complex ecological niche composed of tumor cells, stromal cells and immune cells constantly engaged in mutual interactions that influence tumor development and progression. TAMs and TANs are crucial components of this niche and affect tumor progression by directly influencing tumor cell proliferation and by shaping the anti-tumor or pro-tumor response of other immune cells. In turn, the phenotypes and activities of TAMs and TANs are continuously regulated by other immune cells present in the TME.

Targeting the immune system represents a therapeutic strategy against cancer. However, a significant percentage of patients do not respond to current available treatments, underlining the need for new therapeutic approaches. As we uncover the complexity of the interactions between macrophages and neutrophils and other immune cells, it becomes evident that targeting these interactions may hold promise for developing novel and effective immunotherapeutic approaches to fight cancer.

Author contributions

ID: Writing – original draft. SC: Writing – original draft. AR: Writing – original draft. GG: Writing – original draft. PM: Writing – original draft. SJ: Writing – review & editing.

Funding

The author(s) declare financial support was received for the research, authorship, and/or publication of this article. SC is recipient of a fellowship from the Italian Association for Cancer Research. ID is financed by the HIgh Profile POst doc program – HIPPO Fondi 5x1000 Italian Ministry of University and Research. The Italian Ministry of Health GR-2018-12365588 and RF-2021-12372202 to SJ, the European Union - Next Generation EU - NRRP M6C2 - Investment 2.1 Enhancement and strengthening of biomedical research in the NHS - PNRR-MAD-2022-12375947 to SJ, the Italian Association for Cancer Research AIRC IG-22815 to SJ; Italian Ministry of University and Research - PRIN 2017K7FSYB to SJ, are gratefully acknowledged.

Acknowledgments

Figures were created with BioRender.com.

Conflict of interest

The authors declare that the research was conducted in the absence of any commercial or financial relationships that could be construed as a potential conflict of interest.

Publisher's note

References

1. Anderson NM, Simon MC. The tumor microenvironment. *Curr Biol* (2020) 30 (16):R921–R5. doi: 10.1016/j.cub.2020.06.081

2. Baghban R, Roshangar L, Jahanban-Esfahlan R, Seidi K, Ebrahimi-Kalan A, Jaymand M, et al. Tumor microenvironment complexity and therapeutic implications at a glance. *Cell Commun Signal* (2020) 18(1):59. doi: 10.1186/s12964-020-0530-4

3. Giraldo NA, Sanchez-Salas R, Peske JD, Vano Y, Becht E, Petitprez F, et al. The clinical role of the TME in solid cancer. *Br J Cancer* (2019) 120(1):45–53. doi: 10.1038/s41416-018-0327-z

4. Galon J, Bruni D. Tumor immunology and tumor evolution: intertwined histories. *Immunity* (2020) 52(1):55–81. doi: 10.1016/j.immuni.2019.12.018

5. Pena-Romero AC, Orenes-Pinero E. Dual effect of immune cells within tumour microenvironment: pro- and anti-tumour effects and their triggers. *Cancers (Basel)* (2022) 14(7):1681. doi: 10.3390/cancers14071681

6. Wu B, Shi X, Jiang M, Liu H. Cross-talk between cancer stem cells and immune cells: potential therapeutic targets in the tumor immune microenvironment. *Mol Cancer* (2023) 22(1):38. doi: 10.1186/s12943-023-01748-4

7. Vinay DS, Ryan EP, Pawelec G, Talib WH, Stagg J, Elkord E, et al. Immune evasion in cancer: Mechanistic basis and therapeutic strategies. *Semin Cancer Biol* (2015) 35 Suppl:S185–S98. doi: 10.1016/j.semcancer.2015.03.004

8. Li M, Jiang P, Wei S, Wang J, Li C. The role of macrophages-mediated communications among cell compositions of tumor microenvironment in cancer progression. *Front Immunol* (2023) 14:1113312. doi: 10.3389/fimmu.2023.1113312

9. Zhou Y, Cheng L, Liu L, Li X. NK cells are never alone: crosstalk and communication in tumour microenvironments. *Mol Cancer* (2023) 22(1):34. doi: 10.1186/s12943-023-01737-7

10. Zhong J, Zong S, Wang J, Feng M, Wang J, Zhang H, et al. Role of neutrophils on cancer cells and other immune cells in the tumor microenvironment. *Biochim Biophys Acta Mol Cell Res* (2023) 1870(7):119493. doi: 10.1016/j.bbamcr.2023.119493

11. Mantovani A, Allavena P, Marchesi F, Garlanda C. Macrophages as tools and targets in cancer therapy. *Nat Rev Drug Discovery* (2022) 21(11):799–820. doi: 10.1038/s41573-022-00520-5

12. DeNardo DG, Ruffell B. Macrophages as regulators of tumour immunity and immunotherapy. *Nat Rev Immunol* (2019) 19(6):369–82. doi: 10.1038/s41577-019-0127-6

13. Cassetta L, Pollard JW. A timeline of tumour-associated macrophage biology. *Nat Rev Cancer* (2023) 23(4):238–57. doi: 10.1038/s41568-022-00547-1

14. Jaillon S, Ponzetta A, Di Mitri D, Santoni A, Bonecchi R, Mantovani A. Neutrophil diversity and plasticity in tumour progression and therapy. *Nat Rev Cancer* (2020) 20(9):485–503. doi: 10.1038/s41568-020-0281-y

15. Carnevale S, Ghasemi S, Rigatelli A, Jaillon S. The complexity of neutrophils in health and disease: Focus on cancer. *Semin Immunol* (2020) 48:101409. doi: 10.1016/j.smim.2020.101409

16. Carnevale S, Di Ceglie I, Grieco G, Rigatelli A, Bonavita E, Jaillon S. Neutrophil diversity in inflammation and cancer. *Front Immunol* (2023) 14:1180810. doi: 10.3389/fimmu.2023.1180810

17. Hedrick CC, Malanchi I. Neutrophils in cancer: heterogeneous and multifaceted. *Nat Rev Immunol* (2022) 22(3):173–87. doi: 10.1038/s41577-021-00571-6

18. Ng LG, Ostuni R, Hidalgo A. Heterogeneity of neutrophils. *Nat Rev Immunol* (2019) 19(4):255–65. doi: 10.1038/s41577-019-0141-8

19. Park MD, Silvin A, Ginhoux F, Merad M. Macrophages in health and disease. *Cell* (2022) 185(23):4259–79. doi: 10.1016/j.cell.2022.10.007

20. Beyrau M, Bodkin JV, Nourshargh S. Neutrophil heterogeneity in health and disease: a revitalized avenue in inflammation and immunity. *Open Biol* (2012) 2 (11):120134. doi: 10.1098/rsob.120134

21. Kloosterman DJ, Akkari L. Macrophages at the interface of the co-evolving cancer ecosystem. *Cell* (2023) 186(8):1627–51. doi: 10.1016/j.cell.2023.02.020

22. Kazakova A, Sudarskikh T, Kovalev O, Kzhyshkowska J, Larionova I. Interaction of tumor–associated macrophages with stromal and immune components in solid tumors: Research progress (Review). *Int J Oncol* (2023) 62(2):32. doi: 10.3892/ijo.2023.5480

23. Abbott M, Ustoyev Y. Cancer and the immune system: the history and background of immunotherapy. *Semin Oncol Nurs* (2019) 35(5):150923. doi: 10.1016/j.soncn.2019.08.002

24. De Cicco P, Ercolano G, Ianaro A. The new era of cancer immunotherapy: targeting myeloid-derived suppressor cells to overcome immune evasion. *Front Immunol* (2020) 11:1680. doi: 10.3389/fimmu.2020.01680

25. Pilard C, Ancion M, Delvenne P, Jerusalem G, Hubert P, Herfs M. Cancer immunotherapy: it's time to better predict patients' response. *Br J Cancer* (2021) 125 (7):927–38. doi: 10.1038/s41416-021-01413-x

26. Mantovani A, Marchesi F, Malesci A, Laghi L, Allavena P. Tumour-associated macrophages as treatment targets in oncology. *Nat Rev Clin Oncol* (2017) 14(7):399–416. doi: 10.1038/nrclinonc.2016.217

27. Zhang QW, Liu L, Gong CY, Shi HS, Zeng YH, Wang XZ, et al. Prognostic significance of tumor-associated macrophages in solid tumor: a meta-analysis of the literature. *PloS One* (2012) 7(12):e50946. doi: 10.1371/journal.pone.0050946

28. Di Caro G, Cortese N, Castino GF, Grizzi F, Gavazzi F, Ridolfi C, et al. Dual prognostic significance of tumour-associated macrophages in human pancreatic adenocarcinoma treated or untreated with chemotherapy. *Gut* (2016) 65(10):1710–20. doi: 10.1136/gutjnl-2015-309193

29. Leek RD, Lewis CE, Whitehouse R, Greenall M, Clarke J, Harris AL. Association of macrophage infiltration with angiogenesis and prognosis in invasive breast carcinoma. *Cancer Res* (1996) 56(20):4625–9.

30. Hanada T, Nakagawa M, Emoto A, Nomura T, Nasu N, Nomura Y. Prognostic value of tumor-associated macrophage count in human bladder cancer. *Int J Urol* (2000) 7(7):263–9. doi: 10.1046/j.1442-2042.2000.00190.x

31. Forssell J, Oberg A, Henriksson ML, Stenling R, Jung A, Palmqvist R. High macrophage infiltration along the tumor front correlates with improved survival in colon cancer. *Clin Cancer Res* (2007) 13(5):1472–9. doi: 10.1158/1078-0432.CCR-06-2073

32. Malesci A, Bianchi P, Celesti G, Basso G, Marchesi F, Grizzi F, et al. Tumor-associated macrophages and response to 5-fluorouracil adjuvant therapy in stage III colorectal cancer. *Oncoimmunology* (2017) 6(12):e1342918. doi: 10.1080/2162402X.2017.1342918

33. Tanaka Y, Kobayashi H, Suzuki M, Kanayama N, Suzuki M, Terao T. Upregulation of bikunin in tumor-infiltrating macrophages as a factor of favorable prognosis in ovarian cancer. *Gynecol Oncol* (2004) 94(3):725–34. doi: 10.1016/j.ygyno.2004.06.012

34. Mantovani A, Bottazzi B, Colotta F, Sozzani S, Ruco L. The origin and function of tumor-associated macrophages. *Immunol Today* (1992) 13(7):265–70. doi: 10.1016/0167-5699(92)90008-U

35. Qian BZ, Li J, Zhang H, Kitamura T, Zhang J, Campion LR, et al. CCL2 recruits inflammatory monocytes to facilitate breast-tumour metastasis. *Nature* (2011) 475 (7355):222–5. doi: 10.1038/nature10138

36. Bottazzi B, Polentarutti N, Acero R, Balsari A, Boraschi D, Ghezzi P, et al. Regulation of the macrophage content of neoplasms by chemoattractants. *Science* (1983) 220(4593):210–2. doi: 10.1126/science.6828888

37. Arwert EN, Harney AS, Entenberg D, Wang Y, Sahai E, Pollard JW, et al. A unidirectional transition from migratory to perivascular macrophage is required for tumor cell intravasation. *Cell Rep* (2018) 23(5):1239–48. doi: 10.1016/j.celrep.2018.04.007

38. Pena CG, Nakada Y, Saatcioglu HD, Aloisio GM, Cuevas I, Zhang S, et al. LKB1 loss promotes endometrial cancer progression via CCL2-dependent macrophage recruitment. *J Clin Invest* (2015) 125(11):4063–76. doi: 10.1172/JCI82152

39. Clarijs R, Schalkwijk L, Ruiter DJ, de Waal RM. EMAP-II expression is associated with macrophage accumulation in primary uveal melanoma. *Invest Ophthalmol Vis Sci* (2003) 44(5):1801–6. doi: 10.1167/iovs.02-0624

40. Ginhoux F, Guilliams M. Tissue-resident macrophage ontogeny and homeostasis. *Immunity* (2016) 44(3):439–49. doi: 10.1016/j.immuni.2016.02.024

41. Ginhoux F, Schultze JL, Murray PJ, Ochando J, Biswas SK. New insights into the multidimensional concept of macrophage ontogeny, activation and function. *Nat Immunol* (2016) 17(1):34–40. doi: 10.1038/ni.3324

42. Casanova-Acebes M, Dalla E, Leader AM, LeBerichel J, Nikolic J, Morales BM, et al. Tissue-resident macrophages provide a pro-tumorigenic niche to early NSCLC cells. *Nature* (2021) 595(7868):578–84. doi: 10.1038/s41586-021-03651-8

43. Zhu Y, Herndon JM, Sojka DK, Kim KW, Knolhoff BL, Zuo C, et al. Tissue-resident macrophages in pancreatic ductal adenocarcinoma originate from embryonic hematopoiesis and promote tumor progression. *Immunity* (2017) 47(2):323–38 e6. doi: 10.1016/j.immuni.2017.07.014

44. Loyher PL, Hamon P, Laviron M, Meghraoui-Kheddar A, Goncalves E, Deng Z, et al. Macrophages of distinct origins contribute to tumor development in the lung. *J Exp Med* (2018) 215(10):2536–53. doi: 10.1084/jem.20180534

45. Bowman RL, Klemm F, Akkari L, Pyonteck SM, Sevenich L, Quail DF, et al. Macrophage ontogeny underlies differences in tumor-specific education in brain Malignancies. *Cell Rep* (2016) 17(9):2445–59. doi: 10.1016/j.celrep.2016.10.052

46. Lahmar Q, Keirsse J, Laoui D, Movahedi K, Van Overmeire E, Van Ginderachter JA. Tissue-resident versus monocyte-derived macrophages in the tumor microenvironment. *Biochim Biophys Acta* (2016) 1865(1):23–34. doi: 10.1016/j.bbcan.2015.06.009

47. Franklin RA, Li MO. Ontogeny of tumor-associated macrophages and its implication in cancer regulation. *Trends Cancer* (2016) 2(1):20–34. doi: 10.1016/j.trecan.2015.11.004

48. Locati M, Curtale G, Mantovani A. Diversity, mechanisms, and significance of macrophage plasticity. *Annu Rev Pathol* (2020) 15:123–47. doi: 10.1146/annurev-pathmechdis-012418-012718

49. Masetti M, Carriero R, Portale F, Marelli G, Morina N, Pandini M, et al. Lipid-loaded tumor-associated macrophages sustain tumor growth and invasiveness in prostate cancer. *J Exp Med* (2022) 219(2):e20210564. doi: 10.1084/jem.20210564

50. Mantovani A, Sozzani S, Locati M, Allavena P, Sica A. Macrophage polarization: tumor-associated macrophages as a paradigm for polarized M2 mononuclear phagocytes. *Trends Immunol* (2002) 23(11):549–55. doi: 10.1016/S1471-4906(02)02302-5

51. Allavena P, Sica A, Garlanda C, Mantovani A. The Yin-Yang of tumor-associated macrophages in neoplastic progression and immune surveillance. *Immunol Rev* (2008) 222:155–61. doi: 10.1111/j.1600-065X.2008.00607.x

52. Murray PJ, Allen JE, Biswas SK, Fisher EA, Gilroy DW, Goerdt S, et al. Macrophage activation and polarization: nomenclature and experimental guidelines. *Immunity* (2014) 41(1):14–20. doi: 10.1016/j.immuni.2014.06.008

53. Stein M, Keshav S, Harris N, Gordon S. Interleukin 4 potently enhances murine macrophage mannose receptor activity: a marker of alternative immunologic macrophage activation. *J Exp Med* (1992) 176(1):287–92. doi: 10.1084/jem.176.1.287

54. Cheng S, Li Z, Gao R, Xing B, Gao Y, Yang Y, et al. A pan-cancer single-cell transcriptional atlas of tumor infiltrating myeloid cells. *Cell* (2021) 184(3):792–809 e23. doi: 10.1016/j.cell.2021.01.010

55. Ma RY, Black A, Qian BZ. Macrophage diversity in cancer revisited in the era of single-cell omics. *Trends Immunol* (2022) 43(7):546–63. doi: 10.1016/j.it.2022.04.008

56. Zhang Q, He Y, Luo N, Patel SJ, Han Y, Gao R, et al. Landscape and dynamics of single immune cells in hepatocellular carcinoma. *Cell* (2019) 179(4):829–45 e20. doi: 10.1016/j.cell.2019.10.003

57. Obradovic A, Chowdhury N, Haake SM, Ager C, Wang V, Vlahos L, et al. Single-cell protein activity analysis identifies recurrence-associated renal tumor macrophages. *Cell* (2021) 184(11):2988–3005 e16. doi: 10.1016/j.cell.2021.04.038

58. Mulder K, Patel AA, Kong WT, Piot C, Halitzki E, Dunsmore G, et al. Cross-tissue single-cell landscape of human monocytes and macrophages in health and disease. *Immunity* (2021) 54(8):1883–900 e5. doi: 10.1016/j.immuni.2021.07.007

59. Andersson A, Larsson L, Stenbeck L, Salmen F, Ehinger A, Wu SZ, et al. Spatial deconvolution of HER2-positive breast cancer delineates tumor-associated cell type interactions. *Nat Commun* (2021) 12(1):6012. doi: 10.1038/s41467-021-26271-2

60. Cortese N, Carriero R, Barbagallo M, Putignano AR, Costa G, Giavazzi F, et al. High-resolution analysis of mononuclear phagocytes reveals GPNMB as a prognostic marker in human colorectal liver metastasis. *Cancer Immunol Res* (2023) 11(4):405–20. doi: 10.1158/2326-6066.CIR-22-0462

61. Donadon M, Torzilli G, Cortese N, Soldani C, Di Tommaso L, Franceschini B, et al. Macrophage morphology correlates with single-cell diversity and prognosis in colorectal liver metastasis. *J Exp Med* (2020) 217(11):e20191847. doi: 10.1084/jem.20191847

62. Peranzoni E, Lemoine J, Vimeux L, Feuillet V, Barrin S, Kantari-Mimoun C, et al. Macrophages impede CD8 T cells from reaching tumor cells and limit the efficacy of anti-PD-1 treatment. *Proc Natl Acad Sci U S A* (2018) 115(17):E4041–E50. doi: 10.1073/pnas.1720948115

63. La Fleur L, Botling J, He F, Pelicano C, Zhou C, He C, et al. Targeting MARCO and IL37R on immunosuppressive macrophages in lung cancer blocks regulatory T cells and supports cytotoxic lymphocyte function. *Cancer Res* (2021) 81(4):956–67. doi: 10.1158/0008-5472.CAN-20-1885

64. Peng LS, Zhang JY, Teng YS, Zhao YL, Wang TT, Mao FY, et al. Tumor-associated monocytes/macrophages impair NK-cell function via TGFbeta1 in human gastric cancer. *Cancer Immunol Res* (2017) 5(3):248–56. doi: 10.1158/2326-6066.CIR-16-0152

65. Park MD, Reyes-Torres I, LeBerichel J, Hamon P, LaMarche NM, Hegde S, et al. TREM2 macrophages drive NK cell paucity and dysfunction in lung cancer. *Nat Immunol* (2023) 24(5):792–801. doi: 10.1038/s41590-023-01475-4

66. Wu Y, Kuang DM, Pan WD, Wan YL, Lao XM, Wang D, et al. Monocyte/macrophage-elicited natural killer cell dysfunction in hepatocellular carcinoma is mediated by CD48/2B4 interactions. *Hepatology* (2013) 57(3):1107–16. doi: 10.1002/hep.26192

67. Erlandsson A, Carlsson J, Lundholm M, Falt A, Andersson SO, Andren O, et al. M2 macrophages and regulatory T cells in lethal prostate cancer. *Prostate* (2019) 79 (4):363–9. doi: 10.1002/pros.23742

68. Ma X, Gao Y, Chen Y, Liu J, Yang C, Bao C, et al. M2-type macrophages induce tregs generation by activating the TGF-beta/smad signalling pathway to promote colorectal cancer development. *Onco Targets Ther* (2021) 14:5391–402. doi: 10.2147/OTT.S336548

69. Zhu Y, Knolhoff BL, Meyer MA, Nywening TM, West BL, Luo J, et al. CSF1/CSF1R blockade reprograms tumor-infiltrating macrophages and improves response to T-cell checkpoint immunotherapy in pancreatic cancer models. *Cancer Res* (2014) 74 (18):5057–69. doi: 10.1158/0008-5472.CAN-13-3723

70. Mitchem JB, Brennan DJ, Knolhoff BL, Belt BA, Zhu Y, Sanford DE, et al. Targeting tumor-infiltrating macrophages decreases tumor-initiating cells, relieves immunosuppression, and improves chemotherapeutic responses. *Cancer Res* (2013) 73(3):1128–41. doi: 10.1158/0008-5472.CAN-12-2731

71. Batlle E, Massague J. Transforming growth factor-beta signaling in immunity and cancer. *Immunity* (2019) 50(4):924–40. doi: 10.1016/j.immuni.2019.03.024

72. Krneta T, Gillgrass A, Poznanski S, Chew M, Lee AJ, Kolb M, et al. M2-polarized and tumor-associated macrophages alter NK cell phenotype and function in a contact-dependent manner. *J Leukoc Biol* (2017) 101(1):285–95. doi: 10.1189/jlb.3A1215-552R

73. Molgora M, Supino D, Mavilio D, Santoni A, Moretta L, Mantovani A, et al. The yin-yang of the interaction between myelomonocytic cells and NK cells. *Scand J Immunol* (2018) 88(3):e12705. doi: 10.1111/sji.12705

74. Li L, Yang L, Wang L, Wang F, Zhang Z, Li J, et al. Impaired T cell function in Malignant pleural effusion is caused by TGF-beta derived predominantly from macrophages. *Int J Cancer* (2016) 139(10):2261–9. doi: 10.1002/ijc.30289

75. Kos K, Salvagno C, Wellenstein MD, Aslam MA, Meijer DA, Hau CS, et al. Tumor-associated macrophages promote intratumoral conversion of conventional CD4(+) T cells into regulatory T cells via PD-1 signalling. *Oncoimmunology* (2022) 11(1):2063225. doi: 10.1080/2162402X.2022.2063225

76. Kessenbrock K, Plaks V, Werb Z. Matrix metalloproteinases: regulators of the tumor microenvironment. *Cell* (2010) 141(1):52–67. doi: 10.1016/j.cell.2010.03.015

77. Geiger R, Rieckmann JC, Wolf T, Basso C, Feng Y, Fuhrer T, et al. L-arginine modulates T cell metabolism and enhances survival and anti-tumor activity. *Cell* (2016) 167(3):829–42 e13. doi: 10.1016/j.cell.2016.09.031

78. Rodriguez PC, Quiceno DG, Zabaleta J, Ortiz B, Zea AH, Piazuelo MB, et al. Arginase I production in the tumor microenvironment by mature myeloid cells inhibits

T-cell receptor expression and antigen-specific T-cell responses. *Cancer Res* (2004) 64 (16):5839–49. doi: 10.1158/0008-5472.CAN-04-0465

79. Munn DH, Shafizadeh E, Attwood JT, Bondarev I, Pashine A, Mellor AL. Inhibition of T cell proliferation by macrophage tryptophan catabolism. *J Exp Med* (1999) 189(9):1363–72. doi: 10.1084/jem.189.9.1363

80. Lu T, Ramakrishnan R, Altiok S, Youn JI, Cheng P, Celis E, et al. Tumor-infiltrating myeloid cells induce tumor cell resistance to cytotoxic T cells in mice. *J Clin Invest* (2011) 121(10):4015–29. doi: 10.1172/JCI45862

81. Lu T, Gabrilovich DI. Molecular pathways: tumor-infiltrating myeloid cells and reactive oxygen species in regulation of tumor microenvironment. *Clin Cancer Res* (2012) 18(18):4877–82. doi: 10.1158/1078-0432.CCR-11-2939

82. Nagaraj S, Gupta K, Pisarev V, Kinarsky L, Sherman S, Kang L, et al. Altered recognition of antigen is a mechanism of CD8+ T cell tolerance in cancer. *Nat Med* (2007) 13(7):828–35. doi: 10.1038/nm1609

83. Antonioli L, Pacher P, Vizi ES, Hasko G. CD39 and CD73 in immunity and inflammation. *Trends Mol Med* (2013) 19(6):355–67. doi: 10.1016/j.molmed.2013.03.005

84. Takenaka MC, Gabriely G, Rothhammer V, Mascanfroni ID, Wheeler MA, Chao CC, et al. Author Correction: Control of tumor-associated macrophages and T cells in glioblastoma via AHR and CD39. *Nat Neurosci* (2019) 22(9):1533. doi: 10.1038/s41593-019-0446-8

85. Mastelic-Gavillet B, Navarro Rodrigo B, Decombaz L, Wang H, Ercolano G, Ahmed R, et al. Adenosine mediates functional and metabolic suppression of peripheral and tumor-infiltrating CD8(+) T cells. *J Immunother Cancer* (2019) 7 (1):257. doi: 10.1186/s40425-019-0719-5

86. Kuang DM, Zhao Q, Peng C, Xu J, Zhang JP, Wu C, et al. Activated monocytes in peritumoral stroma of hepatocellular carcinoma foster immune privilege and disease progression through PD-L1. *J Exp Med* (2009) 206(6):1327–37. doi: 10.1084/jem.20082173

87. Lin H, Wei S, Hurt EM, Green MD, Zhao L, Vatan L, et al. Host expression of PD-L1 determines efficacy of PD-L1 pathway blockade-mediated tumor regression. *J Clin Invest* (2018) 128(2):805–15. doi: 10.1172/JCI96113

88. Brom VC, Burger C, Wirtz DC, Schildberg FA. The role of immune checkpoint molecules on macrophages in cancer, infection, and autoimmune pathologies. *Front Immunol* (2022) 13:837645. doi: 10.3389/fimmu.2022.837645

89. Kryczek I, Zou L, Rodriguez P, Zhu G, Wei S, Mottram P, et al. B7-H4 expression identifies a novel suppressive macrophage population in human ovarian carcinoma. *J Exp Med* (2006) 203(4):871–81. doi: 10.1084/jem.20050930

90. Liu L, Li D, Chen S, Zhao R, Pang D, Li D, et al. B7-H4 expression in human infiltrating ductal carcinoma–associated macrophages. *Mol Med Rep* (2016) 14 (3):2135–42. doi: 10.3892/mmr.2016.5510

91. Li J, Lee Y, Li Y, Jiang Y, Lu H, Zang W, et al. Co-inhibitory molecule B7 superfamily member 1 expressed by tumor-infiltrating myeloid cells induces dysfunction of anti-tumor CD8(+) T cells. *Immunity* (2018) 48(4):773–86 e5. doi: 10.1016/j.immuni.2018.03.018

92. Blando J, Sharma A, Higa MG, Zhao H, Vence L, Yadav SS, et al. Comparison of immune infiltrates in melanoma and pancreatic cancer highlights VISTA as a potential target in pancreatic cancer. *Proc Natl Acad Sci U S A* (2019) 116(5):1692–7. doi: 10.1073/pnas.1811067116

93. Xie X, Zhang J, Shi Z, Liu W, Hu X, Qie C, et al. The expression pattern and clinical significance of the immune checkpoint regulator VISTA in human breast cancer. *Front Immunol* (2020) 11:563044. doi: 10.3389/fimmu.2020.563044

94. Dyck L, Mills KHG. Immune checkpoints and their inhibition in cancer and infectious diseases. *Eur J Immunol* (2017) 47(5):765–79. doi: 10.1002/eji.201646875

95. Pesce S, Greppi M, Tabellini G, Rampinelli F, Parolini S, Olive D, et al. Identification of a subset of human natural killer cells expressing high levels of programmed death 1: A phenotypic and functional characterization. *J Allergy Clin Immunol* (2017) 139(1):335–46 e3. doi: 10.1016/j.jaci.2016.04.025

96. Kersten K, Hu KH, Combes AJ, Samad B, Harwin T, Ray A, et al. Spatiotemporal co-dependency between macrophages and exhausted CD8(+) T cells in cancer. *Cancer Cell* (2022) 40(6):624–38 e9. doi: 10.1016/j.ccell.2022.05.004

97. Strachan DC, Ruffell B, Oei Y, Bissell MJ, Coussens LM, Pryer N, et al. CSF1R inhibition delays cervical and mammary tumor growth in murine models by attenuating the turnover of tumor-associated macrophages and enhancing infiltration by CD8(+) T cells. *Oncoimmunology* (2013) 2(12):e26968. doi: 10.4161/onci.26968

98. Pascual-Garcia M, Bonfill-Teixidor E, Planas-Rigol E, Rubio-Perez C, Iurlaro R, Arias A, et al. LIF regulates CXCL9 in tumor-associated macrophages and prevents CD8(+) T cell tumor-infiltration impairing anti-PD1 therapy. *Nat Commun* (2019) 10 (1):2416. doi: 10.1038/s41467-019-10369-9

99. Dangaj D, Bruand M, Grimm AJ, Ronet C, Barras D, Duttagupta PA, et al. Cooperation between constitutive and inducible chemokines enables T cell engraftment and immune attack in solid tumors. *Cancer Cell* (2019) 35(6):885–900 e10. doi: 10.1016/j.ccell.2019.05.004

100. Curiel TJ, Coukos G, Zou L, Alvarez X, Cheng P, Mottram P, et al. Specific recruitment of regulatory T cells in ovarian carcinoma fosters immune privilege and predicts reduced survival. *Nat Med* (2004) 10(9):942–9. doi: 10.1038/nm1093

101. Furudate S, Fujimura T, Kambayashi Y, Kakizaki A, Hidaka T, Aiba S. Immunomodulatory effect of imiquimod through CCL22 produced by tumor-associated macrophages in B16F10 melanomas. *Anticancer Res* (2017) 37(7):3461–71. doi: 10.21873/anticanres.11714

102. Chow A, SChad S, Green MD, Hellmann MD, Allaj V, Ceglia N, et al. Tim-4(+) cavity-resident macrophages impair anti-tumor CD8(+) T cell immunity. *Cancer Cell* (2021) 39(7):973–88 e9. doi: 10.1016/j.ccell.2021.05.006

103. Nalio Ramos R, Missolo-Koussou Y, Gerber-Ferder Y, Bromley CP, Bugatti M, Nunez NG, et al. Tissue-resident FOLR2(+) macrophages associate with CD8(+) T cell infiltration in human breast cancer. *Cell* (2022) 185(7):1189–207 e25. doi: 10.1016/j.cell.2022.02.021

104. Zhang Y, Sun Y, Rao E, Yan F, Li Q, Zhang Y, et al. Fatty acid-binding protein E-FABP restricts tumor growth by promoting IFN-beta responses in tumor-associated macrophages. *Cancer Res* (2014) 74(11):2986–98. doi: 10.1158/0008-5472.CAN-13-2689

105. Mattiola I, Pesant M, Tentorio PF, Molgora M, Marcenaro E, Lugli E, et al. Priming of human resting NK cells by autologous M1 macrophages via the engagement of IL-1beta, IFN-beta, and IL-15 pathways. *J Immunol* (2015) 195(6):2818–28. doi: 10.4049/jimmunol.1500325

106. Bellora F, Castriconi R, Dondero A, Reggiardo G, Moretta L, Mantovani A, et al. The interaction of human natural killer cells with either unpolarized or polarized macrophages results in different functional outcomes. *Proc Natl Acad Sci U S A* (2010) 107(50):21659–64. doi: 10.1073/pnas.1007654108

107. Craxton A, Magaletti D, Ryan EJ, Clark EA. Macrophage- and dendritic cell–dependent regulation of human B-cell proliferation requires the TNF family ligand BAFF. *Blood* (2003) 101(11):4464–71. doi: 10.1182/blood-2002-10-3123

108. Thies FG, Laurindo MF, Perez EC, Novaes e Brito RR, Mariano M, Popi AF. Cross talk between peritoneal macrophages and B-1 cells in vitro. *PloS One* (2013) 8(5): e62805. doi: 10.1371/journal.pone.0062805

109. Biswas SK, Mantovani A. Macrophage plasticity and interaction with lymphocyte subsets: cancer as a paradigm. *Nat Immunol* (2010) 11(10):889–96. doi: 10.1038/ni.1937

110. Ruffell B, Affara NI, Coussens LM. Differential macrophage programming in the tumor microenvironment. *Trends Immunol* (2012) 33(3):119–26. doi: 10.1016/j.it.2011.12.001

111. Gordon S, Martinez FO. Alternative activation of macrophages: mechanism and functions. *Immunity* (2010) 32(5):593–604. doi: 10.1016/j.immuni.2010.05.007

112. Dannenmann SR, Thielicke J, Stockli M, Matter C, von Boehmer L, Cecconi V, et al. Tumor-associated macrophages subvert T-cell function and correlate with reduced survival in clear cell renal cell carcinoma. *Oncoimmunology* (2013) 2(3): e23562. doi: 10.4161/onci.23562

113. DeNardo DG, Barreto JB, Andreu P, Vasquez L, Tawfik D, Kolhatkar N, et al. CD4(+) T cells regulate pulmonary metastasis of mammary carcinomas by enhancing protumor properties of macrophages. *Cancer Cell* (2009) 16(2):91–102. doi: 10.1016/j.ccr.2009.06.018

114. Yin G, Zhao C, Pei W. Crosstalk between macrophages and innate lymphoid cells (ILCs) in diseases. *Int Immunopharmacol* (2022) 110:108937. doi: 10.1016/j.intimp.2022.108937

115. Tiemessen MM, Jagger AL, Evans HG, van Herwijnen MJ, John S, Taams LS. CD4+CD25+Foxp3+ regulatory T cells induce alternative activation of human monocytes/macrophages. *Proc Natl Acad Sci U S A* (2007) 104(49):19446–51. doi: 10.1073/pnas.0706832104

116. Liu C, Chikina M, Deshpande R, Menk AV, Wang T, Tabib T, et al. Treg cells promote the SREBP1-dependent metabolic fitness of tumor-promoting macrophages via repression of CD8(+) T cell-derived interferon-gamma. *Immunity* (2019) 51 (2):381–97 e6. doi: 10.1016/j.immuni.2019.06.017

117. Song L, Asgharzadeh S, Salo J, Engell K, Wu HW, Sposto R, et al. Valpha24-invariant NKT cells mediate antitumor activity via killing of tumor-associated macrophages. *J Clin Invest* (2009) 119(6):1524–36. doi: 10.1172/JCI37869

118. Wong SC, Puaux AL, Chittezhath M, Shalova I, Kajiji TS, Wang X, et al. Macrophage polarization to a unique phenotype driven by B cells. *Eur J Immunol* (2010) 40(8):2296–307. doi: 10.1002/eji.200940288

119. Wculek SK, Cueto FJ, Mujal AM, Melero I, Krummel MF, Sancho D. Dendritic cells in cancer immunology and immunotherapy. *Nat Rev Immunol* (2020) 20(1):7–24. doi: 10.1038/s41577-019-0210-z

120. Gabrilovich DI, Chen HL, Girgis KR, Cunningham HT, Meny GM, Nadaf S, et al. Production of vascular endothelial growth factor by human tumors inhibits the functional maturation of dendritic cells. *Nat Med* (1996) 2(10):1096–103. doi: 10.1038/nm1096-1096

121. Menetrier-Caux C, Montmain G, Dieu MC, Bain C, Favrot MC, Caux C, et al. Inhibition of the differentiation of dendritic cells from CD34(+) progenitors by tumor cells: role of interleukin-6 and macrophage colony-stimulating factor. *Blood* (1998) 92 (12):4778–91. doi: 10.1182/blood.V92.12.4778

122. Song S, Wang Y, Wang J, Lian W, Liu S, Zhang Z, et al. Tumour-derived IL-10 within tumour microenvironment represses the antitumour immunity of Socs1-silenced and sustained antigen expressing DCs. *Eur J Cancer* (2012) 48(14):2252–9. doi: 10.1016/j.ejca.2011.12.009

123. Thepmalee C, Panya A, Junking M, Chieochansin T, Yenchitsomanus PT. Inhibition of IL-10 and TGF-beta receptors on dendritic cells enhances activation of effector T-cells to kill cholangiocarcinoma cells. *Hum Vaccin Immunother* (2018) 14 (6):1423–31. doi: 10.1080/21645515.2018.1431598

124. Ruffell B, Chang-Strachan D, Chan V, Rosenbusch A, Ho CM, Pryer N, et al. Macrophage IL-10 blocks CD8+ T cell-dependent responses to chemotherapy by suppressing IL-12 expression in intratumoral dendritic cells. *Cancer Cell* (2014) 26 (5):623–37. doi: 10.1016/j.ccell.2014.09.006

125. Jensen HK, Donskov F, Marcussen N, Nordsmark M, Lundbeck F, von der Maase H. Presence of intratumoral neutrophils is an independent prognostic factor in localized renal cell carcinoma. *J Clin Oncol* (2009) 27(28):4709–17. doi: 10.1200/JCO.2008.18.9498

126. Kuang DM, Zhao Q, Wu Y, Peng C, Wang J, Xu Z, et al. Peritumoral neutrophils link inflammatory response to disease progression by fostering angiogenesis in hepatocellular carcinoma. *J Hepatol* (2011) 54(5):948–55. doi: 10.1016/j.jhep.2010.08.041

127. Li YW, Qiu SJ, Fan J, Zhou J, Gao Q, Xiao YS, et al. Intratumoral neutrophils: a poor prognostic factor for hepatocellular carcinoma following resection. *J Hepatol* (2011) 54(3):497–505. doi: 10.1016/j.jhep.2010.07.044

128. Ilie M, Hofman V, Ortholan C, Bonnetaud C, Coelle C, Mouroux J, et al. Predictive clinical outcome of the intratumoral CD66b-positive neutrophil-to-CD8-positive T-cell ratio in patients with resectable nonsmall cell lung cancer. *Cancer* (2012) 118(6):1726–37. doi: 10.1002/cncr.26456

129. Jensen TO, Schmidt H, Moller HJ, Donskov F, Hoyer M, Sjoegren P, et al. Intratumoral neutrophils and plasmacytoid dendritic cells indicate poor prognosis and are associated with pSTAT3 expression in AJCC stage I/II melanoma. *Cancer* (2012) 118(9):2476–85. doi: 10.1002/cncr.26511

130. Trellakis S, Bruderek K, Dumitru CA, Gholaman H, Gu X, Bankfalvi A, et al. Polymorphonuclear granulocytes in human head and neck cancer: enhanced inflammatory activity, modulation by cancer cells and expansion in advanced disease. *Int J Cancer* (2011) 129(9):2183–93. doi: 10.1002/ijc.25892

131. Fossati G, Ricevuti G, Edwards SW, Walker C, Dalton A, Rossi ML. Neutrophil infiltration into human gliomas. *Acta Neuropathol* (1999) 98(4):349–54. doi: 10.1007/s004010051093

132. Rao HL, Chen JW, Li M, Xiao YB, Fu J, Zeng YX, et al. Increased intratumoral neutrophil in colorectal carcinomas correlates closely with Malignant phenotype and predicts patients' adverse prognosis. *PloS One* (2012) 7(1):e30806. doi: 10.1371/journal.pone.0030806

133. Li S, Cong X, Gao H, Lan X, Li Z, Wang W, et al. Tumor-associated neutrophils induce EMT by IL-17a to promote migration and invasion in gastric cancer cells. *J Exp Clin Cancer Res* (2019) 38(1):6. doi: 10.1186/s13046-018-1003-0

134. Hassan WA, ElBanna AK, Noufal N, El-Assmy M, Lotfy H, Ali RI. Significance of tumor-associated neutrophils, lymphocytes, and neutrophil-to-lymphocyte ratio in non-invasive and invasive bladder urothelial carcinoma. *J Pathol Transl Med* (2023) 57 (2):88–94. doi: 10.4132/jptm.2022.11.06

135. Yang M, Zhang G, Wang Y, He M, Xu Q, Lu J, et al. Tumour-associated neutrophils orchestrate intratumoural IL-8-driven immune evasion through Jagged2 activation in ovarian cancer. *Br J Cancer* (2020) 123(9):1404–16. doi: 10.1038/s41416-020-1026-0

136. Khalid F, Takagi K, Sato A, Yamaguchi M, Guestini F, Miki Y, et al. Interleukin (IL)-17A in triple-negative breast cancer: a potent prognostic factor associated with intratumoral neutrophil infiltration. *Breast Cancer* (2023) 30(5):748–57. doi: 10.1007/s12282-023-01467-0

137. Powell DR, Huttenlocher A. Neutrophils in the tumor microenvironment. *Trends Immunol* (2016) 37(1):41–52. doi: 10.1016/j.it.2015.11.008

138. Schmidt H, Bastholt L, Geertsen P, Christensen IJ, Larsen S, Gehl J, et al. Elevated neutrophil and monocyte counts in peripheral blood are associated with poor survival in patients with metastatic melanoma: a prognostic model. *Br J Cancer* (2005) 93(3):273–8. doi: 10.1038/sj.bjc.6602702

139. Governa V, Trella E, Mele V, Tornillo L, Amicarella F, Cremonesi E, et al. The interplay between neutrophils and CD8(+) T cells improves survival in human colorectal cancer. *Clin Cancer Res* (2017) 23(14):3847–58. doi: 10.1158/1078-0432.CCR-16-2047

140. Droeser RA, Hirt C, Eppenberger-Castori S, Zlobec I, Viehl CT, Frey DM, et al. High myeloperoxidase positive cell infiltration in colorectal cancer is an independent favorable prognostic factor. *PloS One* (2013) 8(5):e64814. doi: 10.1371/journal.pone.0064814

141. Zhou G, Peng K, Song Y, Yang W, Shu W, Yu T, et al. CD177+ neutrophils suppress epithelial cell tumourigenesis in colitis-associated cancer and predict good prognosis in colorectal cancer. *Carcinogenesis* (2018) 39(2):272–82. doi: 10.1093/carcin/bgx142

142. Galdiero MR, Bianchi P, Grizzi F, Di Caro G, Basso G, Ponzetta A, et al. Occurrence and significance of tumor-associated neutrophils in patients with colorectal cancer. *Int J Cancer* (2016) 139(2):446–56. doi: 10.1002/ijc.30076

143. Ponzetta A, Carriero R, Carnevale S, Barbagallo M, Molgora M, Perucchini C, et al. Neutrophils driving unconventional T cells mediate resistance against murine sarcomas and selected human tumors. *Cell* (2019) 178(2):346–60 e24. doi: 10.1016/j.cell.2019.05.047

144. Yvan-Charvet L, Ng LG. Granulopoiesis and neutrophil homeostasis: A metabolic, daily balancing act. *Trends Immunol* (2019) 40(7):598–612. doi: 10.1016/j.it.2019.05.004

145. Liu F, Wu HY, Wesselschmidt R, Kornaga T, Link DC. Impaired production and increased apoptosis of neutrophils in granulocyte colony-stimulating factor receptor-deficient mice. *Immunity* (1996) 5(5):491–501. doi: 10.1016/S1074-7613(00)80504-X

146. Walker F, Zhang HH, Matthews V, Weinstock J, Nice EC, Ernst M, et al. IL6/sIL6R complex contributes to emergency granulopoietic responses in G-CSF- and GM-CSF-deficient mice. *Blood* (2008) 111(8):3978–85. doi: 10.1182/blood-2007-10-119636

147. Zhu YP, Padgett L, Dinh HQ, Marcovecchio P, Blatchley A, Wu R, et al. Identification of an early unipotent neutrophil progenitor with pro-tumoral activity in mouse and human bone marrow. *Cell Rep* (2018) 24(9):2329–41 e8. doi: 10.1016/j.celrep.2018.07.097

148. Calzetti F, Finotti G, Tamassia N, Bianchetto-Aguilera F, Castellucci M, Cane S, et al. CD66b(-)CD64(dim)CD115(-) cells in the human bone marrow represent neutrophil-committed progenitors. *Nat Immunol* (2022) 23(5):679–91. doi: 10.1038/s41590-022-01189-z

149. Evrard M, Kwok IWH, Chong SZ, Teng KWW, Becht E, Chen J, et al. Developmental analysis of bone marrow neutrophils reveals populations specialized in expansion, trafficking, and effector functions. *Immunity* (2018) 48(2):364–79 e8. doi: 10.1016/j.immuni.2018.02.002

150. Eash KJ, Greenbaum AM, Gopalan PK, Link DC. CXCR2 and CXCR4 antagonistically regulate neutrophil trafficking from murine bone marrow. *J Clin Invest* (2010) 120(7):2423–31. doi: 10.1172/JCI41649

151. Adrover JM, Del Fresno C, Crainiciuc G, Cuartero MI, Casanova-Acebes M, Weiss LA, et al. A neutrophil timer coordinates immune defense and vascular protection. *Immunity* (2019) 50(2):390–402 e10. doi: 10.1016/j.immuni.2019.01.002

152. Marin-Esteban V, Youn J, Beaupain B, Jaracz-Ros A, Barlogis V, Fenneteau O, et al. Biallelic CXCR2 loss-of-function mutations define a distinct congenital neutropenia entity. *Haematologica* (2022) 107(3):765–9. doi: 10.3324/haematol.2021.279254

153. De Filippo K, Rankin SM. CXCR4, the master regulator of neutrophil trafficking in homeostasis and disease. *Eur J Clin Invest* (2018) 48 Suppl 2(Suppl 2): e12949. doi: 10.1111/eci.12949

154. Manz MG, Boettcher S. Emergency granulopoiesis. *Nat Rev Immunol* (2014) 14 (5):302–14. doi: 10.1038/nri3660

155. Capucetti A, Albano F, Bonecchi R. Multiple roles for chemokines in neutrophil biology. *Front Immunol* (2020) 11:1259. doi: 10.3389/fimmu.2020.01259

156. Mollica Poeta V, Massara M, Capucetti A, Bonecchi R. Chemokines and chemokine receptors: new targets for cancer immunotherapy. *Front Immunol* (2019) 10:379. doi: 10.3389/fimmu.2019.00379

157. Jamieson T, Clarke M, Steele CW, Samuel MS, Neumann J, Jung A, et al. Inhibition of CXCR2 profoundly suppresses inflammation-driven and spontaneous tumorigenesis. *J Clin Invest* (2012) 122(9):3127–44. doi: 10.1172/JCI61067

158. SenGupta S, Subramanian BC, Parent CA. Getting TANned: How the tumor microenvironment drives neutrophil recruitment. *J Leukoc Biol* (2019) 105(3):449–62. doi: 10.1002/JLB.3RI0718-282R

159. Yu PF, Huang Y, Han YY, Lin LY, Sun WH, Rabson AB, et al. TNFalpha-activated mesenchymal stromal cells promote breast cancer metastasis by recruiting CXCR2(+) neutrophils. *Oncogene* (2017) 36(4):482–90. doi: 10.1038/onc.2016.217

160. Gijsbers K, Gouwy M, Struyf S, Wuyts A, Proost P, Opdenakker G, et al. GCP-2/CXCL6 synergizes with other endothelial cell-derived chemokines in neutrophil mobilization and is associated with angiogenesis in gastrointestinal tumors. *Exp Cell Res* (2005) 303(2):331–42. doi: 10.1016/j.yexcr.2004.09.027

161. Zhou SL, Dai Z, Zhou ZJ, Chen Q, Wang Z, Xiao YS, et al. CXCL5 contributes to tumor metastasis and recurrence of intrahepatic cholangiocarcinoma by recruiting infiltrative intratumoral neutrophils. *Carcinogenesis* (2014) 35(3):597–605. doi: 10.1093/carcin/bgt397

162. Lee LF, Hellendall RP, Wang Y, Haskill JS, Mukaida N, Matsushima K, et al. IL-8 reduced tumorigenicity of human ovarian cancer in *vivo* due to neutrophil infiltration. *J Immunol* (2000) 164(5):2769–75. doi: 10.4049/jimmunol.164.5.2769

163. SenGupta S, Hein LE, Parent CA. The recruitment of neutrophils to the tumor microenvironment is regulated by multiple mediators. *Front Immunol* (2021) 12:734188. doi: 10.3389/fimmu.2021.734188

164. Charles KA, Kulbe H, Soper R, Escorcio-Correia M, Lawrence T, Schultheis A, et al. The tumor-promoting actions of TNF-alpha involve TNFR1 and IL-17 in ovarian cancer in mice and humans. *J Clin Invest* (2009) 119(10):3011–23. doi: 10.1172/JCI39065

165. Fridlender ZG, Sun J, Kim S, Kapoor V, Cheng G, Ling L, et al. Polarization of tumor-associated neutrophil phenotype by TGF-beta: "N1" versus "N2" TAN. *Cancer Cell* (2009) 16(3):183–94. doi: 10.1016/j.ccr.2009.06.017

166. Sionov RV, Fridlender ZG, Granot Z. The multifaceted roles neutrophils play in the tumor microenvironment. *Cancer Microenviron* (2015) 8(3):125–58. doi: 10.1007/s12307-014-0147-5

167. Montaldo E, Lusito E, Bianchessi V, Caronni N, Scala S, Basso-Ricci L, et al. Cellular and transcriptional dynamics of human neutrophils at steady state and upon stress. *Nat Immunol* (2022) 23(10):1470–83. doi: 10.1038/s41590-022-01311-1

168. Salcher S, Sturm G, Horvath L, Untergasser G, Kuempers C, Fotakis G, et al. High-resolution single-cell atlas reveals diversity and plasticity of tissue-resident neutrophils in non-small cell lung cancer. *Cancer Cell* (2022) 40(12):1503–20 e8. doi: 10.1016/j.ccell.2022.10.008

169. Peng H, Wu X, Liu S, He M, Tang C, Wen Y, et al. Cellular dynamics in tumour microenvironment along with lung cancer progression underscore spatial and evolutionary heterogeneity of neutrophil. *Clin Transl Med* (2023) 13(7):e1340. doi: 10.1002/ctm2.1340

170. Sorin M, Rezanejad M, Karimi E, Fiset B, Desharnais L, Perus LJM, et al. Single-cell spatial landscapes of the lung tumour immune microenvironment. *Nature* (2023) 614(7948):548–54. doi: 10.1038/s41586-022-05672-3

171. Ng MSF, Kwok I, Tan L, Shi C, Cerezo-Wallis D, Tan Y, et al. Deterministic reprogramming of neutrophils within tumors. *Science* (2024) 383(6679):eadf6493. doi: 10.1126/science.adf6493

172. Canli O, Nicolas AM, Gupta J, Finkelmeier F, Goncharova O, Pesic M, et al. Myeloid cell-derived reactive oxygen species induce epithelial mutagenesis. *Cancer Cell* (2017) 32(6):869–83 e5. doi: 10.1016/j.ccell.2017.11.004

173. Butin-Israeli V, Bui TM, Wiesolek HL, Mascarenhas L, Lee JJ, Mehl LC, et al. Neutrophil-induced genomic instability impedes resolution of inflammation and wound healing. *J Clin Invest* (2019) 129(2):712–26. doi: 10.1172/JCI122085

174. Wculek SK, Bridgeman VL, Peakman F, Malanchi I. Early neutrophil responses to chemical carcinogenesis shape long-term lung cancer susceptibility. *iScience* (2020) 23(7):101277. doi: 10.1016/j.isci.2020.101277

175. Houghton AM, Rzymkiewicz DM, Ji H, Gregory AD, Egea EE, Metz HE, et al. Neutrophil elastase-mediated degradation of IRS-1 accelerates lung tumor growth. *Nat Med* (2010) 16(2):219–23. doi: 10.1038/nm.2084

176. Lerman I, Garcia-Hernandez ML, Rangel-Moreno J, Chiriboga L, Pan C, Nastiuk KL, et al. Infiltrating myeloid cells exert protumorigenic actions via neutrophil elastase. *Mol Cancer Res* (2017) 15(9):1138–52. doi: 10.1158/1541-7786.MCR-17-0003

177. Wada Y, Yoshida K, Tsutani Y, Shigematsu H, Oeda M, Sanada Y, et al. Neutrophil elastase induces cell proliferation and migration by the release of TGF-alpha, PDGF and VEGF in esophageal cell lines. *Oncol Rep* (2007) 17(1):161–7. doi: 10.3892/or.17.1.161

178. El Rayes T, Catena R, Lee S, Stawowczyk M, Joshi N, Fischbach C, et al. Lung inflammation promotes metastasis through neutrophil protease-mediated degradation of Tsp-1. *Proc Natl Acad Sci U S A* (2015) 112(52):16000–5. doi: 10.1073/pnas.1507294112

179. Wculek SK, Malanchi I. Author Correction: Neutrophils support lung colonization of metastasis-initiating breast cancer cells. *Nature* (2019) 571(7763):E2. doi: 10.1038/s41586-019-1328-7

180. Ardi VC, Kupriyanova TA, Deryugina EI, Quigley JP. Human neutrophils uniquely release TIMP-free MMP-9 to provide a potent catalytic stimulator of angiogenesis. *Proc Natl Acad Sci U S A* (2007) 104(51):20262–7. doi: 10.1073/pnas.0706438104

181. Yang L, Liu Q, Zhang X, Liu X, Zhou B, Chen J, et al. DNA of neutrophil extracellular traps promotes cancer metastasis via CCDC25. *Nature* (2020) 583 (7814):133–8. doi: 10.1038/s41586-020-2394-6

182. Gershkovitz M, Caspi Y, Fainsod-Levi T, Katz B, Michaeli J, Khawaled S, et al. TRPM2 mediates neutrophil killing of disseminated tumor cells. *Cancer Res* (2018) 78 (10):2680–90. doi: 10.1158/0008-5472.CAN-17-3614

183. Matlung HL, Babes L, Zhao XW, van Houdt M, Treffers LW, van Rees DJ, et al. Neutrophils kill antibody-opsonized cancer cells by trogoptosis. *Cell Rep* (2018) 23 (13):3946–59 e6. doi: 10.1016/j.celrep.2018.05.082

184. Singhal S, Bhojnagarwala PS, O'Brien S, Moon EK, Garfall AL, Rao AS, et al. Origin and role of a subset of tumor-associated neutrophils with antigen-presenting cell features in early-stage human lung cancer. *Cancer Cell* (2016) 30(1):120–35. doi: 10.1016/j.ccell.2016.06.001

185. Pylaeva E, Korschunow G, Spyra I, Bordbari S, Siakaeva E, Ozel I, et al. During early stages of cancer, neutrophils initiate anti-tumor immune responses in tumor-draining lymph nodes. *Cell Rep* (2022) 40(7):111171. doi: 10.1016/j.celrep.2022.111171

186. Tosti N, Cremonesi E, Governa V, Basso C, Kancherla V, Coto-Llerena M, et al. Infiltration by IL22-producing T cells promotes neutrophil recruitment and predicts favorable clinical outcome in human colorectal cancer. *Cancer Immunol Res* (2020) 8 (11):1452–62. doi: 10.1158/2326-6066.CIR-19-0934

187. Rice CM, Davies LC, Subleski JJ, Maio N, Gonzalez-Cotto M, Andrews C, et al. Tumour-elicited neutrophils engage mitochondrial metabolism to circumvent nutrient limitations and maintain immune suppression. *Nat Commun* (2018) 9(1):5099. doi: 10.1038/s41467-018-07505-2

188. Veglia F, Tyurin VA, Blasi M, De Leo A, Kossenkov AV, Donthireddy L, et al. Fatty acid transport protein 2 reprograms neutrophils in cancer. *Nature* (2019) 569 (7754):73–8. doi: 10.1038/s41586-019-1118-2

189. Coffelt SB, Kersten K, Doornebal CW, Weiden J, Vrijland K, Hau CS, et al. IL-17-producing gammadelta T cells and neutrophils conspire to promote breast cancer metastasis. *Nature* (2015) 522(7556):345–8. doi: 10.1038/nature14282

190. Schmielau J, Finn OJ. Activated granulocytes and granulocyte-derived hydrogen peroxide are the underlying mechanism of suppression of t-cell function in advanced cancer patients. *Cancer Res* (2001) 61(12):4756–60.

191. Liu CY, Wang YM, Wang CL, Feng PH, Ko HW, Liu YH, et al. Population alterations of L-arginase- and inducible nitric oxide synthase-expressed CD11b+/CD14 (-)/CD15+/CD33+ myeloid-derived suppressor cells and CD8+ T lymphocytes in patients with advanced-stage non-small cell lung cancer. *J Cancer Res Clin Oncol* (2010) 136(1):35–45. doi: 10.1007/s00432-009-0634-0

192. Rodriguez PC, Ernstoff MS, Hernandez C, Atkins M, Zabaleta J, Sierra R, et al. Arginase I-producing myeloid-derived suppressor cells in renal cell carcinoma are a subpopulation of activated granulocytes. *Cancer Res* (2009) 69(4):1553–60. doi: 10.1158/0008-5472.CAN-08-1921

193. Li P, Lu M, Shi J, Hua L, Gong Z, Li Q, et al. Dual roles of neutrophils in metastatic colonization are governed by the host NK cell status. *Nat Commun* (2020) 11 (1):4387. doi: 10.1038/s41467-020-18125-0

194. Condamine T, Kumar V, Ramachandran IR, Youn JI, Celis E, Finnberg N, et al. ER stress regulates myeloid-derived suppressor cell fate through TRAIL-R-mediated apoptosis. *J Clin Invest* (2014) 124(6):2626–39. doi: 10.1172/JCI74056

195. Veglia F, Perego M, Gabrilovich D. Myeloid-derived suppressor cells coming of age. *Nat Immunol* (2018) 19(2):108–19. doi: 10.1038/s41590-017-0022-x

196. Lee BR, Chang SY, Hong EH, Kwon BE, Kim HM, Kim YJ, et al. Elevated endoplasmic reticulum stress reinforced immunosuppression in the tumor microenvironment via myeloid-derived suppressor cells. *Oncotarget* (2014) 5 (23):12331–45. doi: 10.18632/oncotarget.2589

197. Bonavita E, Bromley CP, Jonsson G, Pelly VS, Sahoo S, Walwyn-Brown K, et al. Antagonistic inflammatory phenotypes dictate tumor fate and response to immune checkpoint blockade. *Immunity* (2020) 53(6):1215–29 e8. doi: 10.1016/j.immuni.2020.10.020

198. Teijeira A, Garasa S, Gato M, Alfaro C, Migueliz I, Cirella A, et al. CXCR1 and CXCR2 chemokine receptor agonists produced by tumors induce neutrophil extracellular traps that interfere with immune cytotoxicity. *Immunity* (2020) 52 (5):856–71 e8. doi: 10.1016/j.immuni.2020.03.001

199. Cheng Y, Li H, Deng Y, Tai Y, Zeng K, Zhang Y, et al. Cancer-associated fibroblasts induce PDL1+ neutrophils through the IL6-STAT3 pathway that foster immune suppression in hepatocellular carcinoma. *Cell Death Dis* (2018) 9(4):422. doi: 10.1038/s41419-018-0458-4

200. He G, Zhang H, Zhou J, Wang B, Chen Y, Kong Y, et al. Peritumoural neutrophils negatively regulate adaptive immunity via the PD-L1/PD-1 signalling pathway in hepatocellular carcinoma. *J Exp Clin Cancer Res* (2015) 34:141. doi: 10.1186/s13046-015-0256-0

201. Noman MZ, Desantis G, Janji B, Hasmim M, Karray S, Dessen P, et al. PD-L1 is a novel direct target of HIF-1alpha, and its blockade under hypoxia enhanced MDSC-mediated T cell activation. *J Exp Med* (2014) 211(5):781–90. doi: 10.1084/jem.20131916

202. Xu W, Dong J, Zheng Y, Zhou J, Yuan Y, Ta HM, et al. Immune-checkpoint protein VISTA regulates antitumor immunity by controlling myeloid cell-mediated inflammation and immunosuppression. *Cancer Immunol Res* (2019) 7(9):1497–510. doi: 10.1158/2326-6066.CIR-18-0489

203. Wang TT, Zhao YL, Peng LS, Chen N, Chen W, Lv YP, et al. Tumour-activated neutrophils in gastric cancer foster immune suppression and disease progression through GM-CSF-PD-L1 pathway. *Gut* (2017) 66(11):1900–11. doi: 10.1136/gutjnl-2016-313075

204. Sun R, Xiong Y, Liu H, Gao C, Su L, Weng J, et al. Tumor-associated neutrophils suppress antitumor immunity of NK cells through the PD-L1/PD-1 axis. *Transl Oncol* (2020) 13(10):100825. doi: 10.1016/j.tranon.2020.100825

205. Eruslanov EB, Bhojnagarwala PS, Quatromoni JG, Stephen TL, Ranganathan A, Deshpande C, et al. Tumor-associated neutrophils stimulate T cell responses in early-stage human lung cancer. *J Clin Invest* (2014) 124(12):5466–80. doi: 10.1172/JCI77053

206. Mysore V, Cullere X, Mears J, Rosetti F, Okubo K, Liew PX, et al. FcgammaR engagement reprograms neutrophils into antigen cross-presenting cells that elicit acquired anti-tumor immunity. *Nat Commun* (2021) 12(1):4791. doi: 10.1038/s41467-021-24591-x

207. Costantini C, Calzetti F, Perbellini O, Micheletti A, Scarponi C, Lonardi S, et al. Human neutrophils interact with both 6-sulfo LacNAc+ DC and NK cells to amplify NK-derived IFNgamma: role of CD18, ICAM-1, and ICAM-3. *Blood* (2011) 117 (5):1677–86. doi: 10.1182/blood-2010-06-287243

208. Riise RE, Bernson E, Aurelius J, Martner A, Pesce S, Della Chiesa M, et al. TLR-stimulated neutrophils instruct NK cells to trigger dendritic cell maturation and promote adaptive T cell responses. *J Immunol* (2015) 195(3):1121–8. doi: 10.4049/jimmunol.1500709

209. Lattanzi G, Strati F, Diaz-Basabe A, Perillo F, Amoroso C, Protti G, et al. iNKT cell-neutrophil crosstalk promotes colorectal cancer pathogenesis. *Mucosal Immunol* (2023) 16(3):326–40. doi: 10.1016/j.mucimm.2023.03.006

210. Ogura K, Sato-Matsushita M, Yamamoto S, Hori T, Sasahara M, Iwakura Y, et al. NK cells control tumor-promoting function of neutrophils in mice. *Cancer Immunol Res* (2018) 6(3):348–57. doi: 10.1158/2326-6066.CIR-17-0204

211. Thoren FB, Riise RE, Ousback J, Della Chiesa M, Alsterholm M, Marcenaro E, et al. Human NK Cells induce neutrophil apoptosis via an NKp46- and Fas-dependent mechanism. *J Immunol* (2012) 188(4):1668–74. doi: 10.4049/jimmunol.1102002

212. Bernson E, Christenson K, Pesce S, Pasanen M, Marcenaro E, Sivori S, et al. Downregulation of HLA class I renders inflammatory neutrophils more susceptible to NK cell-induced apoptosis. *Front Immunol* (2019) 10:2444. doi: 10.3389/fimmu.2019.02444

213. Brostjan C, Oehler R. The role of neutrophil death in chronic inflammation and cancer. *Cell Death Discovery* (2020) 6:26. doi: 10.1038/s41420-020-0255-6

214. Puga I, Cols M, Barra CM, He B, Cassis L, Gentile M, et al. B cell-helper neutrophils stimulate the diversification and production of immunoglobulin in the marginal zone of the spleen. *Nat Immunol* (2011) 13(2):170–80. doi: 10.1038/ni.2194

215. Garner H, de Visser KE. Immune crosstalk in cancer progression and metastatic spread: a complex conversation. *Nat Rev Immunol* (2020) 20(8):483–97. doi: 10.1038/s41577-019-0271-z

216. Mantovani A, Cassatella MA, Costantini C, Jaillon S. Neutrophils in the activation and regulation of innate and adaptive immunity. *Nat Rev Immunol* (2011) 11(8):519–31. doi: 10.1038/nri3024

217. van Gisbergen KP, Sanchez-Hernandez M, Geijtenbeek TB, van Kooyk Y. Neutrophils mediate immune modulation of dendritic cells through glycosylation-

dependent interactions between Mac-1 and DC-SIGN. *J Exp Med* (2005) 201(8):1281–92. doi: 10.1084/jem.20041276

218. Gong T, Liu L, Jiang W, Zhou R. DAMP-sensing receptors in sterile inflammation and inflammatory diseases. *Nat Rev Immunol* (2020) 20(2):95–112. doi: 10.1038/s41577-019-0215-7

219. Chen GY, Nunez G. Sterile inflammation: sensing and reacting to damage. *Nat Rev Immunol* (2010) 10(12):826–37. doi: 10.1038/nri2873

220. Moynihan KD, Opel CF, Szeto GL, Tzeng A, Zhu EF, Engreitz JM, et al. Eradication of large established tumors in mice by combination immunotherapy that engages innate and adaptive immune responses. *Nat Med* (2016) 22(12):1402–10. doi: 10.1038/nm.4200

221. Carmi Y, Spitzer MH, Linde IL, Burt BM, Prestwood TR, Perlman N, et al. Allogeneic IgG combined with dendritic cell stimuli induce antitumour T-cell immunity. *Nature* (2015) 521(7550):99–104. doi: 10.1038/nature14424

222. Zhu EF, Gai SA, Opel CF, Kwan BH, Surana R, Mihm MC, et al. Synergistic innate and adaptive immune response to combination immunotherapy with anti-tumor antigen antibodies and extended serum half-life IL-2. *Cancer Cell* (2015) 27 (4):489–501. doi: 10.1016/j.ccell.2015.03.004

223. Hagerling C, Gonzalez H, Salari K, Wang CY, Lin C, Robles I, et al. Immune effector monocyte-neutrophil cooperation induced by the primary tumor prevents metastatic progression of breast cancer. *Proc Natl Acad Sci U S A* (2019) 116 (43):21704–14. doi: 10.1073/pnas.1907660116

224. Kumar V, Donthireddy L, Marvel D, Condamine T, Wang F, Lavilla-Alonso S, et al. Cancer-associated fibroblasts neutralize the anti-tumor effect of CSF1 receptor blockade by inducing PMN-MDSC infiltration of tumors. *Cancer Cell* (2017) 32 (5):654–68 e5. doi: 10.1016/j.ccell.2017.10.005

225. Salvagno C, Ciampricotti M, Tuit S, Hau CS, van Weverwijk A, Coffelt SB, et al. Therapeutic targeting of macrophages enhances chemotherapy efficacy by unleashing type I interferon response. *Nat Cell Biol* (2019) 21(4):511–21. doi: 10.1038/s41556-019-0298-1

frontiers | Frontiers in Immunology

TYPE Original Research
PUBLISHED 07 November 2024
DOI 10.3389/fimmu.2024.1472433

OPEN ACCESS

EDITED BY
Ombretta Melaiu,
University of Rome Tor Vergata, Italy

REVIEWED BY
Marina Macchini,
San Raffaele Hospital (IRCCS), Italy
Gabriella Pietra,
University of Genoa, Italy

*CORRESPONDENCE
Andrea Doni
andrea.doni@humanitasresearch.it

†These authors have contributed equally to this work

RECEIVED 29 July 2024
ACCEPTED 08 October 2024
PUBLISHED 07 November 2024

CITATION
Erreni M, Fumagalli MR, D'Anna R, Sollai M, Bozzarelli S, Nappo G, Zanini D, Parente R, Garlanda C, Rimassa L, Terracciano LM, Biswas SK, Zerbi A, Mantovani A and Doni A (2024) Depicting the cellular complexity of pancreatic adenocarcinoma by Imaging Mass Cytometry: focus on cancer-associated fibroblasts. *Front. Immunol.* 15:1472433. doi: 10.3389/fimmu.2024.1472433

Depicting the cellular complexity of pancreatic adenocarcinoma by Imaging Mass Cytometry: focus on cancer-associated fibroblasts

Marco Erreni[1,2†], Maria Rita Fumagalli[1†], Raffaella D'Anna[1], Mauro Sollai[3], Silvia Bozzarelli[4], Gennaro Nappo[2,5], Damiano Zanini[1], Raffaella Parente[1], Cecilia Garlanda[2,6], Lorenza Rimassa[2,4], Luigi Maria Terracciano[2,3], Subhra K. Biswas[7], Alessandro Zerbi[2,5], Alberto Mantovani[2,6,8] and Andrea Doni[1*]

[1]Unit of Multiscale and Nanostructural Imaging, IRCCS Humanitas Research Hospital, Milan, Italy, [2]Department of Biomedical Sciences, Humanitas University, Milan, Italy, [3]Pathology Unit, IRCCS Humanitas Research Hospital, Milan, Italy, [4]Medical Oncology and Hematology Unit, Humanitas Cancer Center, IRCCS Humanitas Research Hospital, Milan, Italy, [5]Pancreatic Surgery Unit, IRCCS Humanitas Research Hospital, Milan, Italy, [6]IRCCS Humanitas Research Hospital, Milan, Italy, [7]Singapore Immunology Network (SIgN), Agency for Science, Technology and Research (A*STAR), Singapore, Singapore, [8]William Harvey Research Institute, Queen Mary University of London, London, United Kingdom

Introduction: Pancreatic ductal adenocarcinoma (PDAC) represents the complexity of interaction between cancer and cells of the tumor microenvironment (TME). Immune cells affect tumor cell behavior, thus driving cancer progression. Cancer-associated fibroblasts (CAFs) are responsible of the desmoplastic and fibrotic reaction by regulating deposition and remodeling of extracellular matrix (ECM). As tumor-promoting cells abundant in PDAC ECM, CAFs represent promising targets for novel anticancer interventions. However, relevant clinical trials are hampered by the lack of specific markers and elusive differences among CAF subtypes. Indeed, while single-cell transcriptomic analyses have provided important information on the cellular constituents of PDACs and related molecular pathways, studies based on the identification of protein markers in tissues aimed at identifying CAF subtypes and new molecular targets result incomplete.

Methods: Herein, we applied multiplexed Imaging Mass Cytometry (IMC) at single-cell resolution on 8 human PDAC tissues to depict the PDAC composing cells, and profiling immune cells, endothelial cells (ECs), as well as endocrine cells and tumor cells.

Results: We focused on CAFs by characterizing up to 19 clusters distinguished by phenotype, spatiality, and interaction with immune and tumor cells. We report evidence that specific subtypes of CAFs (CAFs 10 and 11) predominantly are enriched at the tumor-stroma interface and closely associated with tumor cells.

CAFs expressing different combinations of FAP, podoplanin and cadherin-11, were associated with a higher level of CA19-9. Moreover, we identified specific subsets of FAP^+ and $podoplanin^+$/$cadherin\text{-}11^+$ CAFs enriched in patients with negative prognosis.

Discussion: The present study provides new general insights into the complexity of the PDAC microenvironment by defining phenotypic heterogeneities and spatial distributions of CAFs, thus suggesting different functions of their subtypes in the PDAC microenvironment.

KEYWORDS

multiplexed histopathology, Imaging Mass Cytometry, pancreatic cancer, tumor microenvironment, cancer-associated fibroblasts (CAFs)

1 Introduction

Pancreatic ductal adenocarcinoma (PDAC) is one of the most lethal types of cancer, with a 5-years survival rate of 11% only (1). This poor prognosis is mainly due to the inability to detect the disease until late, often metastatic, tumor stage (2). Further, diagnosis is complicated by the asymptomatic evolution of the disease, the lack of diagnostic biomarkers, the absence of attributable risk factors for the majority of patients and the difficult-to-access anatomical location of the pancreas, which limits the routine screening intervention (3, 4). Although 10-15% of cases can be ascribed to germline mutations or known risk factors, the majority of PDAC develops as a consequence of accumulating mutations in several genes, including *KRAS*, *p53*, *SMAD4* and *CDKN2A*, which results in the formation of pre-cancerous lesions, such as Pancreatic Intraepithelial Neoplasia (PanIN) and Intrapapillary Mucinous Neoplasia (IPMN), that possibly evolve to invasive cancer (5–8). Beside mutations that drive the neoplastic morphological alterations of pancreatic epithelial cells, PDAC is characterized by a massive infiltration of activated cancer-associated fibroblasts (CAFs), responsible for the deposition of extracellular matrix components and leading to a desmoplastic reaction, that shapes a tumor microenvironment (TME) composed by a dense stroma, a leaky vascular system and suppressive immune cell populations (9–11). The resulting TME, which can develop up to the 90% of the entire tumor mass, is indeed the main responsible of the heterogeneity, aggressive biology and resistance to therapy of the disease (9, 12). Although the limit in the 5-years survival rate, PDAC survival statistics have doubled over the past decades, due to the improved therapeutic approaches and clinical care (13).

Cell heterogeneity in PDAC has been widely investigated using single-cells transcriptomic approaches, but only few studies analyzed the protein expressed by the different cell subpopulations that compose the PDAC microenvironment (14–16). In the last decade, multiplexed Imaging Mass Cytometry (IMC) has emerged as a powerful technology to dissect the cell landscape of several TME (17–19). IMC combines conventional histology with mass cytometry to identify up to 35-40 metal-tagged antibodies, avoiding limitations related to fluorescence-based imaging technologies, including autofluorescence and spectral overlap (17, 20). Although several studies used conventional immunohistochemistry or fluorescence-based imaging to target markers of PDAC microenvironment (15, 16, 21, 22), fewer are the investigations conducted using the multiplexed IMC technology (23, 24). In addition, these studies mainly focused on the immune cell composition in the PDAC microenvironment, with a limited analysis of the CAF phenotype and localization.

In this manuscript, we applied a 31-antibody panel to define the organization and composition of the PDAC tumor microenvironment by IMC. We focused on the phenotype and the spatial localization of different CAF subpopulations, together with their relationship with immune, endothelial cells (ECs) and tumor cells. With this approach, we provide a comprehensive analysis of the PDAC microenvironment with the aim of better defining its cellular complexity, thereby identifying subtypes and cell signatures of relevance and useful in diagnosis and instrumental for new treatment strategies.

2 Materials and methods

2.1 Human samples and study design

The analyzed cohort includes 8 patients diagnosed with PDAC surgically resected at the Humanitas Research Hospital between 2022 and 2023. Patients' histopathological and clinical features are listed in Supplementary Table 1. Patients had not received any therapy before resection. Written informed consent was obtained for each patient included in the study. The study protocol was in accordance with ethical guidelines established in the 1975 Declaration of Helsinki and was approved by the local ethical committee (Authorization n° 3801).

2.2 Histopathological evaluation

5µm-thick formalin-fixed, paraffin-embedded (FFPE) sections from PDAC tissue blocks were deparaffinized in xylen and rehydrated through a graded alcohol series. Tissue sections were stained with Hematoxylin (Histo-Line Laboratories, Pantigliate (MI) - Italy) for 15 minutes, extensively washed in H_2O for 10 minutes, and then stained with Eosin (Histo-Line Laboratories, Pantigliate (MI) - Italy) for 7 minutes. After a rapid wash in H_2O, slides were dehydrated through a graded alcohol series, washed in xylene and then mounted with Eukitt (Sigma-Aldrich, St. Louis, Missouri, USA). Whole-slide scans were acquired by a ZEISS Axio Scan Z1 Slide Scanner and visualized with QuPath software (version 0.5.1).

2.3 Tissue staining

2µm-thick FFPE sections from PDAC tissue blocks were deparaffinized in xylen and rehydrated through a graded alcohol series. Slides were then incubated with EDTA, pH 9 antigen retrieval solution (Agilent Technologies, Santa Clara, CA 95051, USA) in a water bath at 98°C for 20 minutes, followed by a 10-minutes cooling down in antigen retrieval solution and by an additional 10-minutes cooling down in distilled water. To prevent non-specific antibody binding, slides were incubated in PBS supplemented with Ca^{2+} and Mg^{2+} (PBS^{2+}) (Lonza, Basel, Switzerland) supplemented with 0.1% Triton X-100, 3% BSA (Sigma-Aldrich, St. Louis, Missouri, USA), 5% Normal Mouse (Biosera, Cholet, France)/Rat(Sigma-Aldrich, St. Louis, Missouri, USA)/Rabbit(Dako, Agilent Technologies, Santa Clara, CA 95051, USA)/Goat(Sigma-Aldrich, St. Louis, Missouri, USA)/Sheep (Sigma-Aldrich, St. Louis, Missouri, USA) serum, for 45 minutes at room temperature in a humified chamber. Slides were then incubated with the metal-conjugated antibody mix, diluted in PBS^{2+} supplemented with 0.01% Triton X-100, 0.3% BSA (Sigma-Aldrich, St. Louis, Missouri, USA), 0.5% Normal Mouse (Biosera, Cholet, France)/Rat(Sigma-Aldrich, St. Louis, Missouri, USA)/Rabbit(Dako, Agilent Technologies, Santa Clara, CA 95051, USA)/Goat(Sigma-Aldrich, St. Louis, Missouri, USA), Sheep (Sigma-Aldrich, St. Louis, Missouri, USA) Serum, overnight at 4°C in a humified chamber. Slides were washed 4 times, 5 minutes each, in PBS^{2+} 0.05% Tween–20 (Merck, Darmstadt, Germany). For nuclear staining, tissues were then incubated with 0.3 µM Ir191/193 (Standard Biotools, South San Francisco, CA, USA) in PBS^{2+} for 30 minutes at room temperature. After incubation, tissue sections were washed 3 times, 3 minutes each, in PBS^{2+} 0.05% Tween-20. Finally, sections were washed for 30 seconds in ultrapure H_2O to remove salt leftovers and quickly airdried. The list of 31 metal-conjugated antibodies used in this study is reported in Supplementary Table 2. Metal-tagged antibodies recognizing alpha smooth muscle actin (αSMA), CD163, CD20, CD66b and collagen-I were purchased from Standard Biotools. The remaining antibodies were conjugated to lanthanide isotypes using the Maxpar® X8 Antibody Labelling Kit (Standard Biotools, South San Francisco, CA, USA) according to the manufacturer's instructions and resuspended in PBS^{2+} and 0.05% NaN_3. Titration tests were performed for each metal-conjugated antibody to optimize the staining protocol.

2.4 IMC data acquisition

Images were acquired with a Hyperion Imaging System (Standard Biotools, South San Francisco, CA, USA). To ensure system stability, the Hyperion Imaging System was routinely calibrated following the manufacturer's instructions. For each patient, 2 consecutive sections were cut and stained for H&E and IMC staining, respectively, as previously described. On the H&E-dedicated slides, 3 to 5 regions of interest (ROIs), corresponding to tumor regions, were selected by a specialized pathologist. The same regions were then identified on the IMC dedicated slides and 1 mm^2 ROIs were ablated with a UV laser, with a frequency of 200Hz, at a resolution of approximately 1$µm^2$. IMC acquired regions were then revised by a specialized pathologist to confirm the presence of the neoplastic tissue. Antibodies that showed high level of background signal in tumor tissue or did not exhibit a clear staining pattern were excluded from the analysis, resulting in a final panel of 31 metal-tagged antibodies.

2.5 Data analysis

IMC image analysis was performed using a custom pipeline as previously described (25). Briefly, hot pixel removal (radius=2, threshold=50) was performed on single–channel images extracted from mcd files. For each channel, low–intensity thresholds were manually settled based on visual inspection and a cutoff was set to at the top 99.99% percentile of expression (or at least at an intensity value of 10 dual counts) calculated over all the considered ROIs. Gaussian filter (r=2) was applied exclusively to estimate of pan-Cytokeratin+ (Pan-Ck^+), $CD45^+$, $CD31^+$ and fibroblast activation protein (FAP^+) positive area to avoid bias due to missing nuclear signal and small debrids.

Tiffs substacks containing the complete list of channels relevant for segmentation and cell classification were created. Ilastik (v1.3.3post3) (26) and CellProfiler (v4.2.1) (27) were used to perform single–pixel classification and cell segmentation. R EBImage package (v4.36) (28) was used to obtain channel intensity and shape parameters for each cell. Objects with area < 10$µm^2$, area larger than 1000$µm^2$, mean intensity higher than 2 in more than 15 markers, and lower than 0.01 in the markers used for Uniform Manifold Approximation and Projection (UMAP) analysis were discarded. No more than 2% of the cells were discarded based on these criteria.

Following inverse hyperbolic sine transformation and normalization of the data between 1% and 99% of the overall signal, UMAP (https://CRAN.R-project.org/package=umap, v0.2.8) and PhenoGraph (v 0.99) (k=60) algorithms were used for dimensional reduction and clustering analysis. Clusters were assigned to five different cellular populations (tumor, immune,

ECs, CAFs, pancreatic islets). PhenoGraph analysis (k=20) was then performed on the five subsets separately, in order to identify clusters of cells misannotated. After reassignment of all the cells to the correct populations, cells were re-clustered (k=20) and annotated into more specific subpopulations, as described in the Results section.

Neighboring cells were identified as those located within 30µm from cells borders using 3D interaction Fiji plugin (mcib3D v4.1.5). Interaction counts score were determined using patch method (p=1) from the imcRtools package (v1.9.0, permutation test n=5000). Patch method gives for a reference subpopulation, and each ROI, the fraction of its cells that have at least one neighbor in the target subpopulation. Cells subpopulations with less than 10 cells for ROI were not included in the statistics. For each pair of cell subtypes, permutation test over their positions allows to obtain an estimate of p-value associated to the observed number of interactions compared to those expected by chance. Interactions were tested separately for each ROI, and considered significant when p-value < 0.01. A score +1 or -1 was associated to each significantly positive or negative (more or less associated than expected by random model) interaction. Non-significant interactions were given score zero. The resulting scores, averaged over all the considered ROIs, were represented in heatmaps. For CAF subtypes, the minimum distance from each cell and tumor cells was evaluated with Cdist function (Rdist v0.05) using center of mass. For each cell we calculated the abundance of different neighboring cells (identified, as above, in a radius <30µm) subpopulation. We considered 29 classes, taking into account tumors and endothelial cells as aggregated macro populations, while subpopulations of CAFs and immune cells were considered in detail. The abundance normalized vectors were used as input for kmeans clustering (k=10, 1500 iterations, 10 initialization sets). The resulting clusters were manually annotated, based on center coordinates and cell subtype enrichment, to identify neighborhoods regions similar in composition (Supplementary Table 3).

Relative enrichment of CAFs subtypes in the groups identified by clinical parameters was defined ad –Log10 of the false discovery rate (fdr) from hypergeometric test for the good prognosis group and +Log10 of fdr for bad prognosis group. Thus, larger positive values indicate enrichment in the good prognosis group, while large negative values are indicative of enrichment in the bad prognosis group. Values of fdr were capped to 10^{-10}. Values fdr > 0.001 were set to 1, corresponding to enrichment score 0.

2.6 Image processing and statistics

Representative images were prepared using ImageJ (Fiji, version 1.54f) software. Gaussian filter was applied to representative images to increase their quality. GraphPad Prism software (version 9.0.2), dittoSeq (v1.6.0) and ggplot2 (v3.4) R packages were used to prepare graphs and to performed statistical analysis. Two-sample, two sided Kolmogorov-Smirnov (KS) test was used to compare distances distribution. Hypergeometric test was performed based on HypeR package (29). False discovery correction was applied to all p-values and reported as p-adjusted (padj).

3 Results

3.1 The cellular TME of PDAC

Multiple staining protocols combined with IMC technology at single-cell resolution (Figure 1A) were applied to human tissues of PDAC (n=8) (Supplementary Table 1). A total of 34 ROIs (1mm^2 range of n=3-5 per patient) were selected for acquisition, based on histopathological evaluation, including both neoplastic glands from PDAC (with various grades of differentiation) and stromal tissue, with the aim of acquiring regions similarly divided between PDAC and remaining TME (23±11% Pan-Ck$^+$ area, n=34 PDAC). As stated in Supplementary Table 2 and shown in Supplementary Figure 1A, tissue sections were stained with 31 metal-tagged antibodies detecting classical markers of tumor cells (Pan-Ck, Ck-7), pancreatic islets (peptide C); monocytic (CD45, CD68), polymorphonuclear (CD66b, MMP-9) and lymphoid (CD45, CD3, CD8, CD20) immune cells; cells composing the blood vessel wall, including vascular ECs (CD31, CD34), smooth muscle cells (CD146) and pericytes (CD146, αSMA); lymphatic ECs (CD31, podoplanin). Detection of differential markers subtyped the cells of mesenchymal origin (vimentin, desmin, cadherin-11, podoplanin, CD74, S100A4, CD44, FAP), which vary according to the functional differentiation and specialization in sites of cancer tissue (30–32). In addition, a definition of the diversity of ECM components (collagen-I, collagen-3A, collagen-IV, fibrinogen, pentraxin 3 (PTX3)) served to assess a functional association with different cell types in the proximity, such as functionality and stability of tumor blood vessels by measuring collagen IV-rich coverage (33). Additional markers included CD206, CD163 and HLA-DR, to reveal a functional state of tumor-associated macrophage (TAM) (M1 versus M2 polarization), whereas evaluation of carbonic anhydrase 9 (CA-IX) expression defined the cancer cell capable in sustaining local acidosis, and hence in favoring cancer progression (34) (Supplementary Figure 1A).

In all PDAC tissues analyzed, Pan-Ck$^+$ regions are randomly arranged and surrounded by a dense desmoplastic and collagenous stroma enriched of αSMA and vimentin. Dispersed blood vessels (2.1±1.5% CD31$^+$ area n=34 ROIs) and immune cells (15.7±8.2% CD45$^+$ area; n=34 ROIs) enclosed the tumor cells (Figures 1B, C). Isolated epithelial peptide C$^+$/FAP$^+$ pancreatic islets (35) (0.4±0.6% peptide C$^+$ area, range 0-2.3%, 0.8±1.9% FAP$^+$ range 0-9%; n=34 ROIs) were distinguished from Pan-Ck$^+$ cells (Figure 1D).

In a single-cell segmentation analysis, we generated a mask for each ROI of PDAC identifying a total number of 122827 cells (range 12080-18643 cells for n=8 PDAC) (a representative image of single-cell segmentation is shown in Supplementary Figure 1B). PhenoGraph analysis generated 32 different clusters, subdivided in tumor cells (Pan-Ck$^+$ and Ck-7$^+$), immune cells (CD45$^+$, CD3$^+$, CD68$^+$, CD66b$^+$, CD20$^+$), ECs (CD31$^+$, CD34$^+$, podoplanin$^+$), CAFs (CD45$^-$, Pan-Ck$^-$, Ck-7$^-$, CD31$^-$, αSMA$^+$, vimentin$^+$, CD74$^+$, CD44$^+$, S100A4$^+$, FAP$^+$, podoplanin$^+$, cadherin-11$^+$, desmin$^+$), pancreatic islets (peptide C$^+$) and stated as other cells for not expressing specific markers. UMAP representation of the annotated cluster is shown in in Figure 1E; Supplementary

10.3389/fimmu.2024.1472433

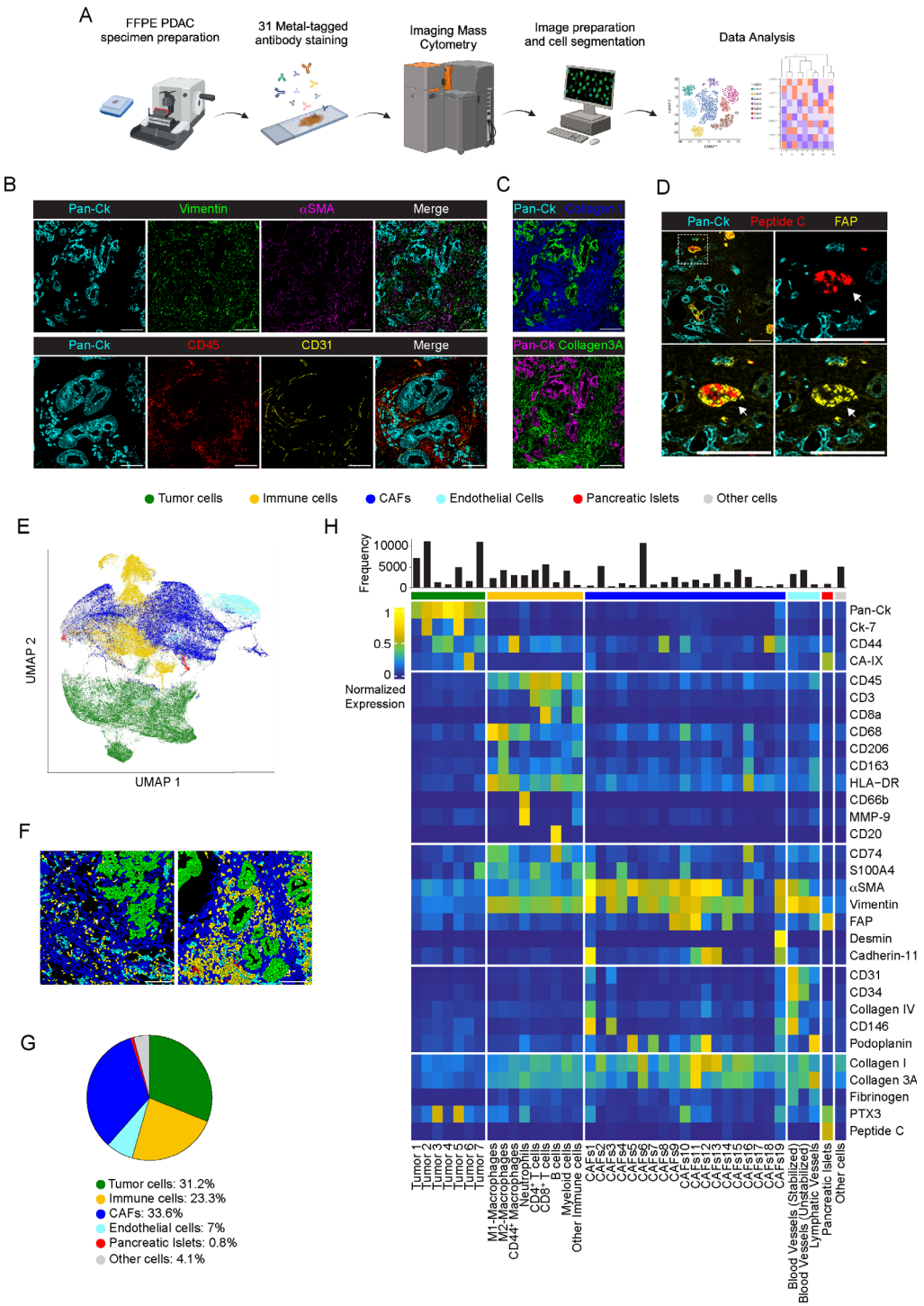

FIGURE 1
Cellular landscape in PDAC by IMC. **(A)** Schematic view of the IMC analysis workflow. **(B)** Representative images out of 34 acquired ROIs (n=8 PDAC) showing extracted signal contribution of Pan-Ck (cyan), vimentin (green), αSMA (magenta), CD45 (red), CD31 (yellow) and correspondent merged image. Bar: 200μm. **(C)** Upper panel, representative images out of 34 acquired ROIs (n=8 PDAC) showing signal contribution of Pan-Ck (green) and Collagen I (blue). Bar: 200μm. Lower panel, representative images out of 34 acquired ROIs (n=8 PDAC) showing Pan-Ck (magenta) and Collagen 3A (green). Bar: 200μm. **(D)** Representative images out of 34 acquired ROIs (n=8 PDAC) showing Pan-Ck (cyan), peptide C (red) and FAP (yellow). White arrow in the inset indicates the pancreatic islet expressing peptide C (red) and FAP (yellow). Bar: 200μm. **(E)** UMAP representation of PDAC cells annotated into tumor cells, immune cells, CAFs, ECs, pancreatic islet and other cells. **(F)** Representative reconstructed images showing the localization within the PDAC tissues of the segmented cells (black contours) corresponding to tumor cell (green), immune cells (yellow), CAF (blue), ECs (cyan), pancreatic islets (red) and other (gray) cell clusters. **(G)** Frequency of cells belonging to tumor cell (green), immune cell (yellow), CAF (blue), ECs (cyan), pancreatic islets (red) and other cell (gray) clusters, as in the legend. Bar: 200μm. **(H)** Heatmap referring to the normalized expression of each single markers of the acquired images (n=34 ROIs; n=8 PDAC) after PhenoGraph analysis, among the different clusters.

Figure 2A and, per single patient, in Supplementary Figure 2B. Representative images of the distribution of annotated cell subtypes in PDAC tissue are shown in Figure 1F.

CAFs represented the most abundant cell population identified (n=41339 cells, n=8 PDAC; range 21-43.6% per PDAC) and corresponded to 33.6% of the annotated cells, compared with tumor cells (n=38284; 31.2%, n=8; range 22.5-37.2% per PDAC), immune cells (n=28661 cells, 23.3%, n=8; range 12.7-45.5% per PDAC) and ECs (n=8596 cells, 7%, n=8; range 2.9-12.2% per PDAC) (Figure 1G). 4.1% of cells (n=5070; n=8; range 0.6-10.4% per PDAC) were not specifically annotated. The clusters identified were homogeneously represented among the different PDAC patients, with a diversity of relative abundance more associated with specific subtypes of CAFs and tumor cells (Supplementary Figure 2B).

As shown in the averaged intensity-based heatmap (Figure 1H) and in line with transcriptomic studies in PDAC (36), tumor cells were further reclassified into 7 different subtypes, based on the expression of Pan-Ck, Ck-7, CD44, S100A4 and CA-IX. Although PTX3 was recognized as a molecule predominantly associated with cells of mesenchymal origin in PDAC (37), two clusters of tumor cells (Tumor 3, Pan-Ck$^+$ PTX3$^+$; Tumor 5, Pan-Ck$^+$ Ck-7$^+$ PTX3$^+$) were identified based on its high expression. Immune cells were identified as myeloid cells (CD45$^+$, CD68$^-$, CD206$^+$) and as a whole subtyped in M1-like (CD45$^+$, CD68$^+$, HLA-DR$^+$, CD74$^+$), M2-like macrophages (CD45$^+$, CD68$^+$, CD206$^+$, CD163$^+$) or CD44-expressing macrophages (CD45$^+$, CD68$^+$, CD44$^+$); neutrophils (CD45$^+$, CD66b$^+$); CD4$^+$ T cells (CD45$^+$, CD3$^+$, CD8$^-$) and CD8$^+$ T cells (CD45$^+$, CD3$^+$, CD8$^+$); B cells (CD45$^+$, CD20$^+$) (Figure 1H). On the basis on the selective expression of markers of pericytes (αSMA, CD146) and coverage of a collagen-IV$^+$ basement (38), blood vessels were distinguished into functioning and stabilized (CD31$^+$, CD34$^+$, Collagen-IV$^+$, CD146$^+$, αSMA$^+$, cadherin-11$^+$) from non-stabilized (CD31$^+$, CD34$^+$, collagen-IV$^-$, CD146$^-$) tumor neo-angiogenesis, as well as in CD31$^+$ podoplanin$^+$ lymphatic vessels (Figure 1H). As reported, CAFs represent a multitude of potentially dynamic and plastic subgroups that change their gene expression profiles based on the stimuli from the environment (39), thereby influencing tumor progression through the tissue fibrotic reaction, the regulation of tissue biomechanical property and the modulation of the immune response to chemotherapy (11). Therefore, detection of multiple CAF markers, including αSMA, vimentin, S100A4, CD74, FAP, desmin, cadherin-11, CD34, CD146, CD44, CA-IX, podoplanin, collagen-I, collagen-3A and PTX3, served to discriminate the subpopulation of CAFs having a different functional impact in PDAC. As shown in Figure 1H, CAFs were classified into 19 different clusters.

3.2 Profiling of cancer cells

Tumor cells (n=38284; 31.2%, n=8; range 22.5-37.2% per PDAC) were annotated into 7 different subtypes, based on the expression of Pan-Ck, cytokeratin 7 (Ck-7), CD44, S100A4, PTX3, CA-IX, CD74 (Figures 2A, B). Although the expression levels changed among the subtypes, all tumor cells expressed Pan-Ck. A cluster with an exclusive expression of Pan-Ck alone corresponded to 18.8% (n=8; range 1.1-73.5% per PDAC) of tumor cells (Tumor 1), whereas majority of tumor cells expressed both Pan-Ck and Ck-7 (Tumor 2, n=8; range 1.1-74.0% per PDAC). Some clusters expressed a combination of markers associated with tumor proliferation and invasiveness (40), such as CD44, S100A4, CD74 and MMP-9 (Tumor 7, 29.1%, n=8; range 0.7-81.5% per PDAC) (Figure 2A–C). In particular, expression of CD44, a classical marker associated with epithelial-to-mesenchymal transition and poor prognosis of PDAC progression and metastasis (41, 42), was found associated with Tumor 3 (3.6%, range 0.2-9.0% per PDAC), Tumor 4 (2.2%, range 0-10.0% per PDAC) and Tumor 7 subtypes (Figures 2A–C). Few cells in the Tumor 6 subtype (4.1%, n=8; range 0.2-11.5% per PDAC) expressed the hypoxic marker CA-IX (Figures 2B, D). Therefore, as shown by IMC analysis, PDAC consists of a phenotypic diversity (n=7 identified clusters) of tumor cells potentially associated with different capacity for tumorigenesis and metastasis. As shown by UMAP in Supplementary Figure 3, for the same clusters, heterogeneity in the expression of the same markers was observed among the PDAC patients analyzed.

PTX3 is a humoral innate immune molecule produced by macrophages (43) and mesenchymal cells (37), which plays a role of extrinsic oncosuppressor of cancer by regulating complement-dependent tumor-promoting inflammation (43). On the other hand, PTX3 was found elevated in PDAC tissue and associated with an increased capacity of cancer cells to invade ECM (37). As observed in other tumors, PTX3 produced by cancer cells promote tumor progression by promoting invasiveness and migration (44, 45). Interestingly, we found that the Tumor 5 (12.9%, range 0-43.7% per PDAC, Figure 2D), expressing Pan-Ck, Ck-7 and PTX3 was almost exclusively found in PDAC #1 and #3 only, counting for the 90% of all identified Tumor 5 cells (Figure 2E), who were diagnosed with distant metastasis at the time of surgery (Supplementary Table 1). Co-expression of Pan-Ck, Ck-7 and PTX3 is restricted to a specific subset of cells (34.5% in PDAC#1; 43.7% in PDAC#3) (Figure 2F, white arrows and Figure 2G, red arrows), compared to the neighbor cells which lack the expression of Ck-7 (Figure 2F, white arrowheads and Figure 2G, red arrowheads), thus suggesting in an attempt to speculate the identification of subpopulation of PDAC cells associated with high tumor metastatic potential.

3.3 Profiling of immune cells in PDAC

In immune cell population (n=28661 cells), a functional specialization of macrophage was defined based on the expression of classical M1 (CD68$^+$, HLA-DR$^+$, CD74$^+$) or M2 (CD68$^+$, CD163$^+$, CD206$^+$) markers. The percentage of M2-like macrophages (14.7%, range 6.5-26.8% per PDAC) was higher compared to M1-like macrophages (8.2%, range 1.7-24.4% per PDAC), thus indicating a propensity for M2 deviation in the tumor microenvironment of PDAC, and hence sustained tumorigenesis, immune evasion, and metastasis formation (46, 47) (Figures 3A, B). A distinguished cluster of macrophages showed exclusive enrichment in CD44 (10.8%, range

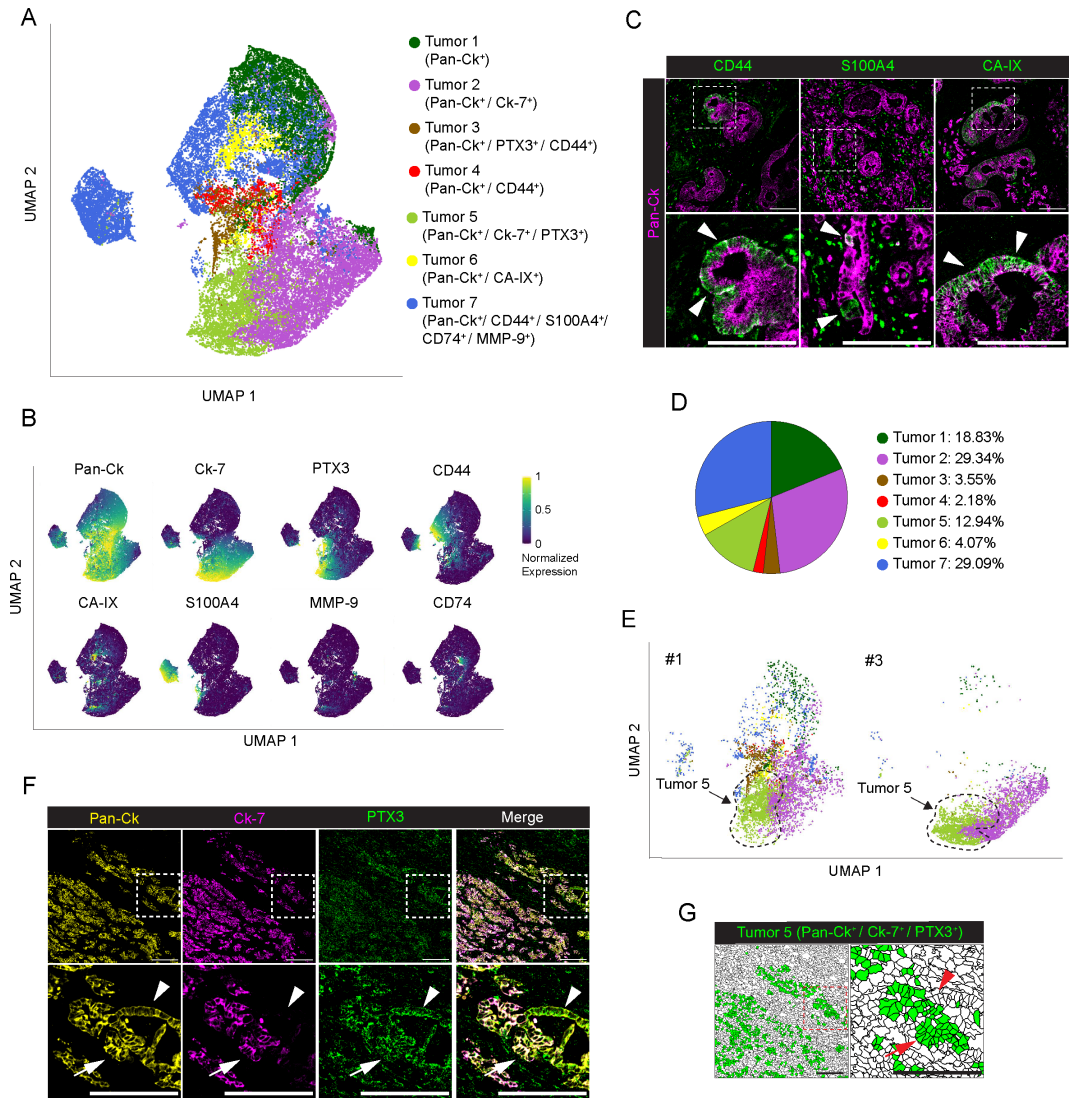

FIGURE 2
Profiling of tumor cells in PDAC. **(A)** UMAP representation of PDAC tumor cells annotated to 7 tumor cell subtypes, colors as in legend. **(B)** UMAP representation of the normalized expression of single markers in segmented cells annotated as tumor cells. **(C)** Representative images out of 34 acquired ROIs (n=8 PDAC) showing Pan-Ck (magenta) signal in combination with CD44 (green, left panel), S100A4 (green, middle panel) and CA-IX (green, right panel). White arrowheads on the onset (bottom) indicate tumor cells expressing CD44 (left panel), S100A4 (middle panel) and CA-IX (right panel). Bar: 200μm. **(D)** Frequency of cells belonging to the identified tumor subtypes, over the total number of tumor cells, as in legend. **(E)** UMAP representation of the subset of tumor cells in PDAC #1 and #3. Black-dotted line is a guide for the eye. Colors and UMAP coordinates as in **(A)**. **(F)** Representative images of Pan-Ck (yellow), Ck-7 (magenta) and PTX3 (green) signal in the PDAC #1. White arrows and white arrowheads in the inset show tumor cells co-expressing Pan-Ck/Ck-7/PTX3 (Tumor 5) or Pan-Ck/PTX3 alone, respectively. Bar: 200μm. **(G)** Representative images of the same region represented in **(F)**, showing the tissue localization of segmented cells (black contours) annotated as Tumor 5 (green) in PDAC #1. Red arrows and red arrowheads in the inset show tumor cells co-expressing Pan-Ck/Ck-7/PTX3 (Tumor 5) or Pan-Ck/PTX3 alone, respectively. Bar: 200μm.

1.5-35.9% per PDAC), and lower expression of HLA-DR and CD74, or of CD163 and CD206 (Figures 1H, 3E, F, yellow arrowheads). In PDAC, the same macrophage subtype was recently described to belong to the vascular niche and to be distinguished by a pro-angiogenic gene signature (24). Noteworthy, distribution of macrophages around Pan-Ck tumor cells is shown in Figure 3F, with M2-like macrophages expressing higher levels of CD163 and CD206 (Figure 3F, white arrows) and M1-like macrophages expressing higher levels of HLA-DR and CD74 (Figure 3F, white arrowheads). In addition, as previously shown in Figure 1H, S100A4 expression was higher in M2-like macrophages compared to M1-like macrophages, suggesting their pro-tumorigenic activity (48). The remaining subtypes of immune cells identified were found to be CD66b$^+$ neutrophils; CD3$^+$, CD4$^+$ (CD8$^-$) T cells; CD3$^+$, CD8$^+$ T cells; CD20$^+$ B cells; and eventually CD68$^-$, CD206$^+$ myeloid dendritic cells (Figure 3A; Supplementary Figures 4A, B). T cells represent the 34.8% of the tumor infiltrating cells (range 19.7-51.3%; n=8 PDAC), with CD8$^+$ and CD4$^+$ T cells counting for the 19.6% (range 8.4-32.2%; n=8) and 15.19% (range 5.1-26.2%; n=8) of T lymphocytes, respectively (Figures 3B, C: CD3$^+$, CD8$^-$, white arrowheads, CD3$^+$, CD8$^+$, white arrows). On the contrary, B cells poorly infiltrate tumor tissue (4.46%; range 0.1-13.3%; n=8)

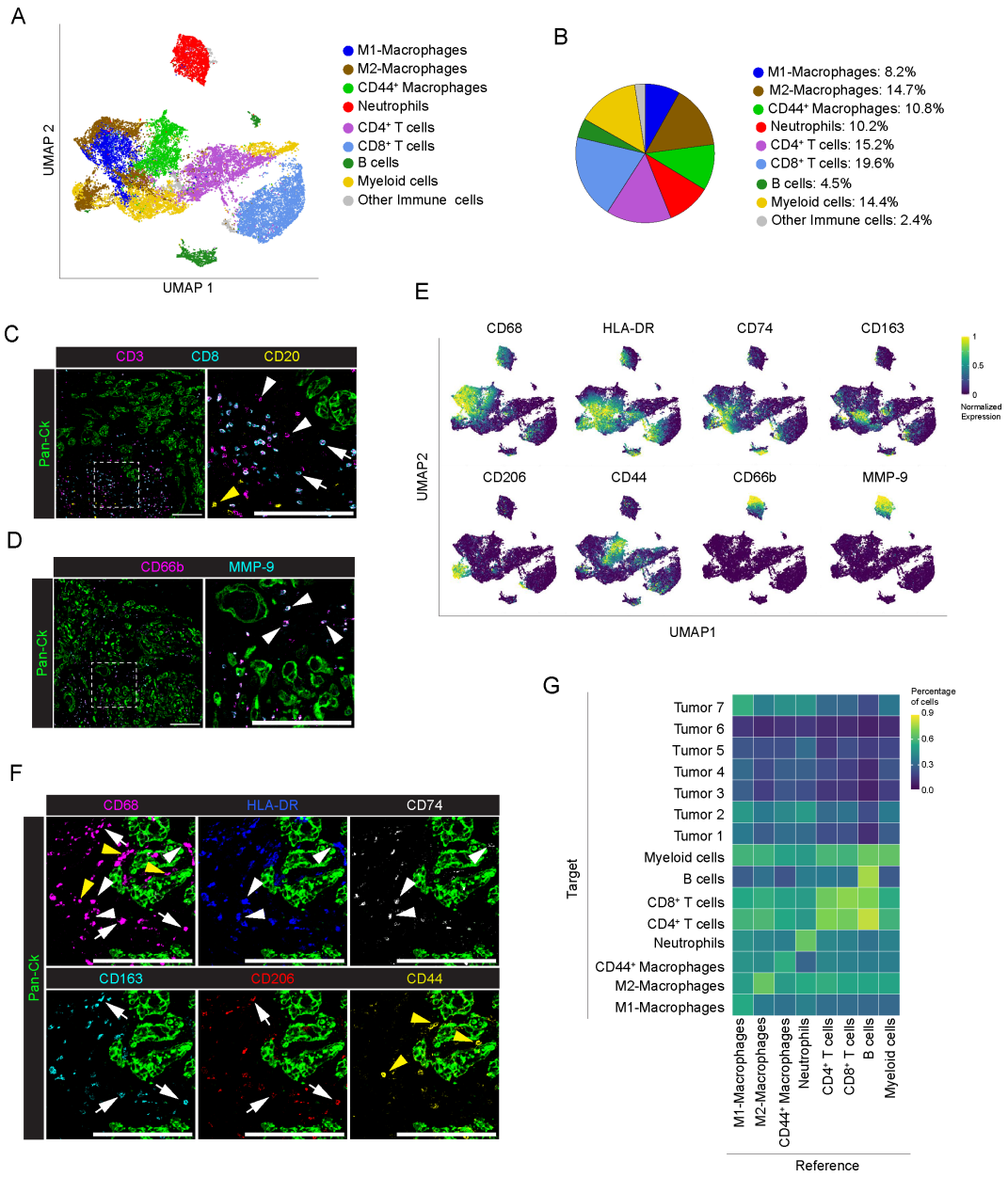

FIGURE 3
Profiling of immune cells in PDAC. **(A)** UMAP representation of immune cells in PDAC (n=8 PDAC), as in legend. **(B)** Frequency of cells belonging to the identified immune cell subpopulations, over the total number of immune cells, as in legend. **(C)** Representative images out of 34 acquired ROIs (n=8 PDAC) showing signal contribution of Pan-Ck (green) CD3 (magenta) CD8 (cyan) and CD20 (yellow). White arrowheads, white arrows and yellow arrows in the inset indicate CD4 T cells (identified as $CD3^+/CD8^-$ T cells), $CD8^+$ T cells and B cells respectively. Bar: 200µm. **(D)** Representative images out of 34 acquired ROIs (n=8 PDAC) showing Pan-Ck (green), $CD66b^+$ neutrophils (magenta) and $MMP\text{-}9^+$ (cyan). Arrowheads in the inset indicate $CD66b^+$ neutrophils expressing MMP-9. Bar: 200µm. **(E)** UMAP representation of the normalized expression of immune cell markers for the identification of macrophages subpopulation (M1 macrophages as $CD68^+/HLA\text{-}DR^{high}/CD74^{high}$, M2 macrophages as $CD68^+/CD163^{high}/CD206^{high}$ and $CD44^+$ macrophages as $CD68^+/CD44^+$) and neutrophils ($CD66b^+/MMP\text{-}9^+$). **(F)** Representative images out of 34 acquired ROIs (n=8 PDAC) showing the extracted signal contribution of Pan-Ck (green), CD68 (magenta), HLA-DR (blue) CD74 (gray), CD163 (cyan), CD206 (red) and CD44 (yellow). White arrowheads indicate M1 macrophages as $CD68^+/HLA\text{-}DR^{high}/CD74^{high}$, white arrows indicate M2 macrophages as $CD68^+/CD163^{high}/CD206^{high}$, yellow arrows indicate $CD44^+$ macrophages as $CD68^+/CD44^+$. Bar: 200µm. **(G)** Results of the neighboring cell analysis, as heatmap, showing the average percentage of each indicated cell subtype (Reference) that are in proximity (≤ 30µm distance) to each indicated cell subpopulations (Target).

(Figures 3B, C; yellow arrowheads). Neutrophil cluster (10.2%; range 0.2-29.3%; n=8) (Figure 3B) infiltrating tumor tissues were identified based on the expression of CD66b and high levels MMP-9 stored into their tertiary granules (Figures 3D, E). As observed in tumor cell profiling, immune cell composition of the TME is heterogeneous among the analyzed patients: neutrophil abundance was higher in PDAC #1, (29.4%) #2 (20.5%), #3 (9.8%) and #6 (15.9%); PDAC #2 showed a highest frequency of both M1-like (24.4%) and M2-like (26.8%) macrophages; $CD44^+$ were abundant in PDAC #4 (35.9%) and #8 (19.5%) (Supplementary Figure 4C).

Analysis of the frequency of cells (Reference) in close proximity (<30µm) with other cell types (Target) showed a preferential neighboring of B cells to both $CD4^+$ (72 ± 28% of B cells) and $CD8^+$ T cells (81 ± 21% of B cells) whereas no interaction was observed between immune cells and PDAC, with the exception of a weak association with $CD44^+$ macrophages (59 ± 24% of cells *vs* all the Tumor subtypes), M1-like macrophages (67 ± 20% of cells *vs* all the Tumor subtypes) and neutrophils (65 ± 25% of cells *vs* all tumor subtypes) (Figure 3G; Supplementary Figure 5).

3.4 Profiling of CAFs in PDAC

CAFs are tumor-promoting cells abundant in the ECM with a multifaceted phenotype (49, 50) and promising targets for new anticancer interventions (11, 51). In the present study, major efforts were therefore directed towards the identification of profiling markers of the different functional activities of CAFs in PDAC. Single-cell segmentation and PhenoGraph analysis identified n=41339 total CAFs (33.8% on total cells, n=8 PDAC; range 21-43.5% per PDAC tissue) annotated into 19 different subtypes, based on the differential expression of CD44, CA-IX, CD74, S100A4, αSMA, vimentin, FAP, desmin, cadherin-11, CD34, CD146, podoplanin, collagen I, collagen 3A and PTX3 (Figure 4A; Supplementary Figure 5A). As with immune cells, a phenotypic heterogeneity in the CAF population was found among the analyzed patients, although no specific CAF subtype was restricted to individual patients (Supplementary Figure 5B). According to the literature (49), most of the CAFs identified belonged to clusters 2 (12.7%, n=8; range 4.6-44.4%), 6 (26.4%, n=8; range 7-43.6%) and 15 (10.7%, n=8; range 2.4-30.6%) which express almost exclusively αSMA and vimentin (Figures 4A, B) and correspond to

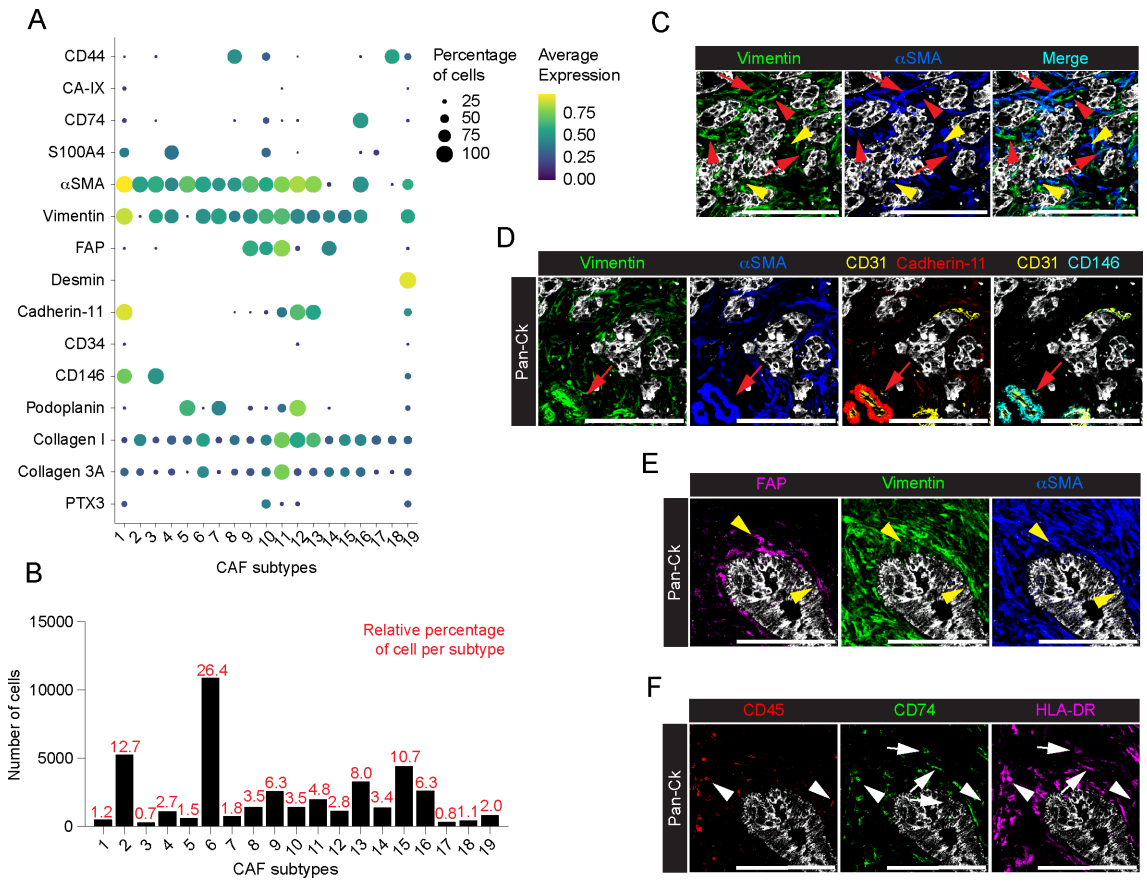

FIGURE 4
Profiling of CAFs in PDAC. **(A)** Dot plot showing each CAF marker average normalized expression and the relative percentage of positive cells, among the annotated CAF subtypes. **(B)** Barplot showing the relative percentage of cells among the identified subtypes on total CAFs. **(C)** Representative images out of 34 acquired ROIs (n=8 PDAC) of Pan-Ck (gray), vimentin (green) and αSMA (blue). Red arrows indicate cells co-expressing vimentin and αSMA. Red arrowheads and yellow arrowheads indicate cell expressing vimentin or αSMA only. Bar, 200µm. **(D)** Representative images out of 34 acquired ROIs (n=8 PDAC) showing the extracted signal contribution of Pan-Ck (gray), vimentin (green), αSMA (blue), CD31 (yellow), cadherin-11 (red) and CD146 (cyan). Red arrow indicates $CD31^+$ blood vessel (yellow) covered by $vimentin^+/αSMA^+/cadherin\text{-}11^+/CD146^+$ pericytes. Bar, 200µm. **(E)** Representative images out of 34 acquired ROIs (n=8 PDAC) showing the extracted signal contribution of Pan-Ck (gray), FAP (magenta), vimentin (green) and αSMA (blue). Yellow arrowheads indicate CAFs co-expressing FAP, vimentin and αSMA surrounding $Pan\text{-}Ck^+$ tumor cells. Bar, 200µm. **(F)** Representative images out of 34 acquired ROIs (n=8 PDAC) showing the extracted signal contribution of Pan-Ck (gray), CD45 (red), CD74 (green) and HLA-DR (magenta). White arrowheads indicate immune cells ($CD45^+$) expressing CD74 and HLA-DR, while white arrows indicate CAFs ($CD45^-$) expressing CD74 and HLA-DR. Bar: 200µm.

myofibroblast-like CAFs (myCAFs). In a further dissection of myCAFs, while CAFs 6 show a concomitant expression of αSMA and vimentin (Figures 4A, C, red arrows), CAFs 2 and CAFs 15 were expressing αSMA or vimentin alone, respectively (Figures 4A, C, red arrowhead: αSMA^+ CAFs 2; yellow arrowhead: $vimentin^+$ CAFs 15). Distinctly, the αSMA^+ $vimentin^+$ clusters CAFs 1 (1.2%, n=8; range 0.2-2.5%) and CAFs 3 (0.7%, n=8; range 0.2-2.9%) were patently identified as pericytes, exhibiting the expression of markers of mesenchymal origin, included cadherin-11 and CD146, and are associated $CD31^+$ ECs (Figure 4D). In addition to the expression of αSMA and vimentin, CAFs 9 (6.3%, n=8; range 0.04-20.4%), 10 (3.5%, n=8; range 0.4-9.2%), 11 (4.8%, n=8; range 0.2-18%) and 14 (3.4%, n=8; range 0.3-12.9%) showed higher expression of FAP, also in combination with S100A4 and PTX3 (CAFs 10) or cadherin-11 (CAFs 11), thus identifying phenotypically different subtypes and emphasizing their functional evolution and plasticity in PDAC (e.g. myCAF *vs.* inflammartory CAFs (iCAFs)) (52, 53) (Figure 4E). Interestingly, FAP^+ αSMA^+ subtypes were localized closer to tumor cells compared to the previously identified myCAFs (Figure 4E) (average minimal distance from the tumor cells: CAFs 9, 29.7 ± 25.5μm, n=2591 cells; CAFs 10, 36.6 ± 60.2μm, n=1437 cells; CAFs 11, 32.5 ± 36.9μm, n=1980 cells; *vs.* CAFs 2, 68.0 ± 63.3μm, n=5254 cells; CAFs 6, 95.7 ± 108.0μm, n=10905 cells; CAFs 15, 61.3 ± 79.7μm; n=4430 cells; p-value < 10^{-15} KS test for all conditions), as well as to the FAP^+ αSMA^- CAFs 14 subpopulation (56.4 ± 54.7μm, n= 1389; p-value < 10^{-15} KS test). Other subtypes identified included CAFs 19 distinguished by higher expression of desmin (2.0%, n=8; range 0.3-4.7%) (Figures 4A, B); CAFs 16 (6.3%, n=8; range 3.2-9.2%), the only cluster that showed a distinctive expression of CD74 and HLA-DR but lacking of CD45 expression (Figure 4F, white arrows), thus suggesting the overt identification of CAFs having immunological properties in PDAC, the so-called antigen-presenting CAFs (apCAFs) (54); the poorly represented CAFs 18 (1.1%, n=8; range 0.04-4.7%) and CAFs 8 (3.5%, n=8; range 0.3-6.7%) expressed high levels of CD44, alone (CAFs 18), or in combination with elevated αSMA and Vimentin (CAF 8) (Figures 4A, B); CAFs 5 (1.5%, n=8; range 0-7.7%), CAFs 7 (1.8%, n=8; range 0.2-7.2%) and CAFs 12 (2.8%, n=8; range 0-15.2%) showed expression of podoplanin, a well-defined CAF predictive marker of PDAC progression (55), in combination with αSMA (CAFs 5), αSMA and vimentin (CAFs 7), or with αSMA and vimentin and cadherin-11 (CAFs 12), (Figures 4A, B). In contrast to proteomic studies on CAFs in breast cancer (56), no consistent association between CD34 expression and CAFs was observed (Figure 4A). As expected, many of the clusters of CAFs that included CAFs 2, 6, 11, 12 and 13 (Figure 4A), were associated with collagen I and 3A, pointing to them as major players involved in a continuous interaction with the regions of the tumor tissue associated with deposition and remodeling of ECM (57).

A spatial association between cell subpopulations was evaluated by neighboring analysis, highlighting pairwise association between specific cell types, and neighborhood enrichment, aimed to identify larger regions homogeneous in cell composition (Figure 5). In association with a high phenotype diversity of CAFs, neighboring cell analysis revealed the presence of high heterogeneity in their spatial relationship with other cells in PDAC (Figure 5A). Except for CAFs 6, which showed an association with CAFs 2, 4, 8, 13 and 16 (fraction of CAFs 6 neighboring CAFs 2, 51 ± 27%; CAFs 4, 30 ± 19%; CAFs 8, 34 ± 18%; CAFs 13, 36 ± 23%; CAFs 16, 50 ± 20%; n= 10905 cells), no specific relationship was found between them. As expected, CAFs 1 and 3, identified as αSMA^+ $vimentin^+$ $CD146^+$ pericytes, (Figures 4A, D) were spatially associated with ECs (Figure 5A). In particular, CAFs 1 significantly associated with $CD146^+$ and collagen IV^+ $CD31^+$ ECs (Figure 1E; Supplementary Figure 5, score 0.57 ± 0.51), thus suggesting a role in controlling blood vessel functionality.

In addition, CAF FAP^+ subtypes (CAFs 9, 10 and 11) preferentially localized in proximity with Pan-CK+ cells (CAFs 9 86 ± 10%, n=2575 cells; CAFs 10 76 ± 19%, n=1405 cells; CAFs 11 80 ± 17%, n=1929 cells) (Figure 5A).

A consistent spatial association between CAFs and immune cells was observed (Figure 5A). Considering the subtypes of immune cells identified (Figures 5B, C), CAFs 1 and CAFs 3, identified as pericytes, showed an interaction, respectively, with $CD4^+$ T cells (Figure 5B, score 0.07 ± 0.47) and myeloid cells (Figure 5B, score 0.14 ± 0.38). Moreover, CAFs 3 were associated with $CD44^+$ macrophages (Figure 5C, score 0.29 ± 0.49) and M2-like macrophages (Figure 5C, score 0.43 ± 0.53). Of note, CAFs 1 and 3 mainly differ by the expression of cadherin-11 (Figure 1E), whose expression has been associated to anti-tumor immune response in a genetic mouse model of PDAC (58). Similarly, $podoplanin^+$ CAFs 7 were found in association with $CD4^+$ T cells (Figure 5B, score 0.06 ± 0.44) and $CD44^+$ macrophages (Figure 5B, 0.06 ± 0.25). FAP^+ CAFs 10 and 11 interacted preferentially with $CD44^+$ macrophages (Figure 5B, CAFs 10, score 0.04 ± 0.36; CAFs 11, score 0.1 ± 0.3) while FAP^+ CAFs 14 showed relationship with M1-like macrophages (Figure 5B, score 0.11 ± 0.47). These CAF subtypes were observed in the peritumoral niche around $Pan\text{-}Ck^+$ cells, in correspondence with an enrichment of macrophages (Figures 3H, 4G, E). As evidence for an identification of a CAF cluster with immunoregulatory properties (apCAFs) in PDAC, $CD4^+$ T cells were observed significantly close to CAFs 16 (Figure 5C, score 0.09 ± 0.445).

We then investigated the presence of patterns of localized enrichment resulting in the identification of 10 classes of regions similar in cellular composition (neighborhoods, Figures 5D, E). Thus, each ROI can be divided into sub-regions highlighting spatial adjacent cells belonging to different spatial context (59) (Figure 5D). The analysis shows that regions identified as tumor-stroma interface are particularly enriched of FAP^+ CAFs 10 and CAFs 11 (*padj<0.001*, Figure 5E; Supplementary Table 3), in agreement with the evidence resulting from the neighboring analysis (Figures 4E, 5A). In addition, CAFs 1, expressing pericyte markers, were enriched in perivascular region (*padj<0.001*). We also identified three neighborhoods of immune cells, enriched either in B cells and $CD8^+$ T cells (Lymphoid Cell Enriched Stroma), or neutrophils and $CD44^+$ and M1-like macrophages (Myeloid Enriched Stroma 1) or myeloid cells and $CD44^+$ macrophages (Myeloid Enriched Stroma 2), with distinct spatial distribution in the ROIs (Figures 5D, E). Several CAF subtypes were associated with the immune enriched neighborhoods. Among them, apCAFs (CAFs 16) were associated

with Lymphoid Cell Enriched Stroma and Myeloid Cell Enriched Stroma 2 (*padj<0.001*, Figure 5D; Supplementary Table 3).

To evaluate an association between CAF subtypes and PDAC progression, we evaluate their distribution in patients with circulating levels of carbohydrate antigen 19-9 (CA19-9) (60), disease-free survival (DFS) and survival status (Supplementary Table 1). We divided patients into high CA19-9 (n=5) and low CA19-9 (n=3), setting a threshold level of 100IU/L, as previously reported (61). We found that FAP$^+$ CAFs, namely CAFs 9, CAFs 10, CAFs 11 and CAFs 14, as well as podoplanin$^+$ cadherin-11$^+$ CAFs12 were enriched in patients with higher level of CA19-9 (*padj<0.001*) (Figures 6A, D–F; Supplementary Figure 6A). Interestingly, CAFs 12, as well as podoplanin$^+$ CAFs 5 are also associated with a worst DFS (n= 4 patients, DFS<13.5 months, *padj <0.001*) (Figures 6B, D; Supplementary Figure 6B). Similarly, CAFs 12 were associated to a shorter survival (n=3 patients, survival<18 months, *padj<0.001*)

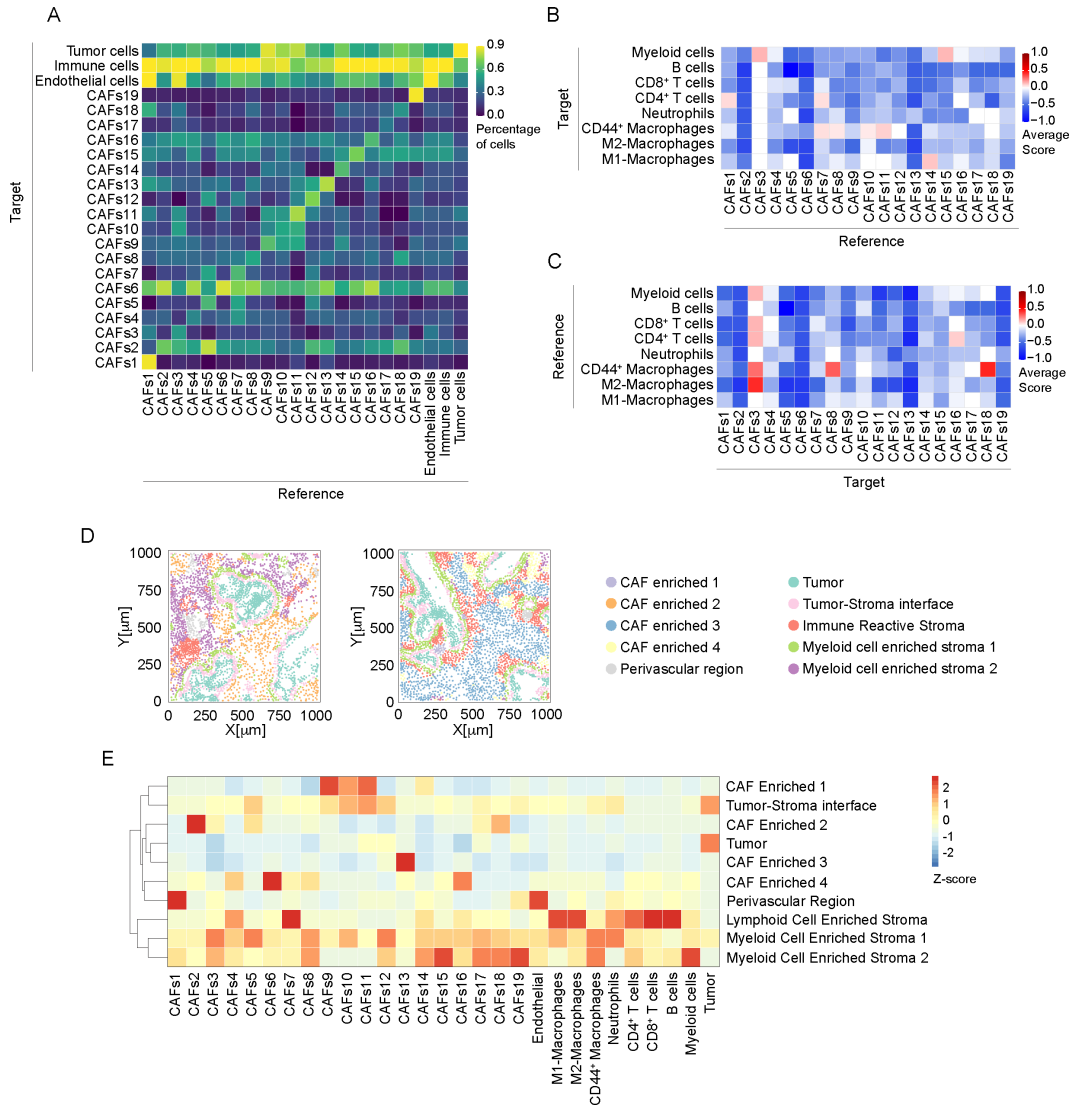

FIGURE 5
Neighborhood analysis of CAFs in PDAC. **(A)** Results of the single cell neighboring analysis, as heatmap, showing the average percentage of each indicated cell subtype (Reference) that are in proximity (≤ 30µm radius) to cells of each indicated subpopulation (Target). **(B)** Heatmap showing the average proximity score for each pair of cell phenotypic subpopulations of CAF (Reference) to immune cells (Target). Positive (red) or negative (blue) values indicate that a specific pair of phenotypes is neighboring significantly more often or significantly less often, respectively, than expected from a randomized placement, as described in Material and Methods. 30µm radius is considered for cell-to-cell proximity, as in **(A)**. **(C)** Heatmap, showing the average proximity score for each pair of cell phenotypic subpopulations, as in B, assuming immune cells as Reference populations and CAF subtypes as Target. **(D)** Representative spatial distribution of cellular neighborhoods, identified as regions with similar cellular composition, as described in Material and Methods, into two different ROIs (out of n=34). Each dot represents the center of mass of a single cell, dot color corresponds to annotated neighborhood, as in legend. Annotation was performed based on enrichment analysis reported in Supplementary Table 3. **(E)** Relative abundance of cellular populations across the annotated cellular neighborhoods as in **(D)** Values are normalized by column.

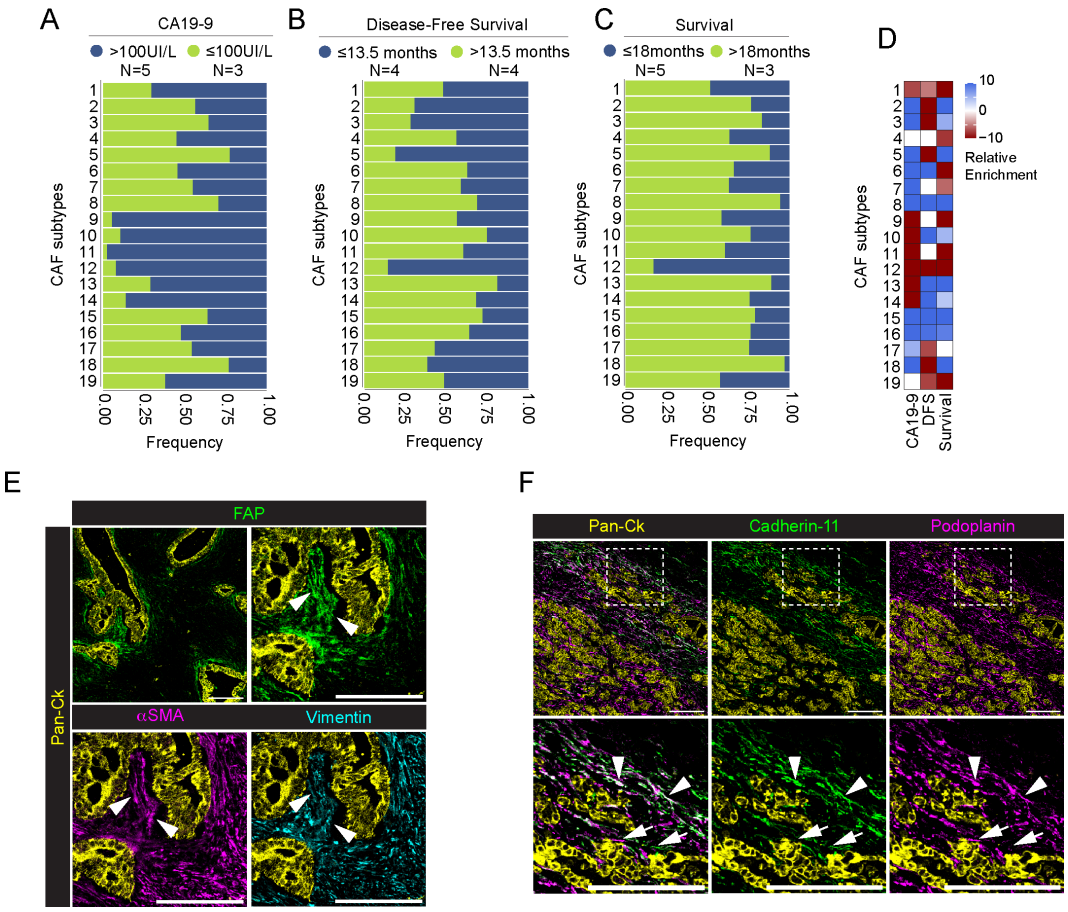

FIGURE 6
Association between CAFs and patients' levels of CA19-9, disease-free survival and survival status. **(A-C)** Barplot showing frequency of each CAF subpopulation in association with patients' pre-operative levels of CA19-9 [**(A)**, blue >100IU/l, green ≤100IU/l], disease-free survival [**(B)**, blue ≤13.5 months, green >13.5 months] and overall survival [**(C)**, blue ≤18 months, green >18 months) (PDAC n=8 total)]. Data are reported as frequency normalized over the total number of cells in each CAF group and annotated according to patient status. Number of patient in each group is reported in legend. **(D)** Relative enrichment score of each CAF subtype in the good (red) or bad (lightblue) prognosis group for three different clinical parameters as above. Higher absolute values correspond to more significant enrichment, values closer to zero are less significant. P-value adjusted > 0.001 are set to enrichment 0. **(E)** Representative images out of 34 acquired ROIs (n=8 PDAC) showing the extracted signal contribution of Pan-Ck (yellow), FAP (green), αSMA (magenta) and vimentin (cyan). White arrowheads indicate CAFs co-expressing FAP, vimentin and αSMA surrounding Pan-Ck$^+$ tumor cells. Bar, 200μm. **(F)** Representative images out of 34 acquired ROIs (n=8 PDAC) showing the extracted signal contribution of Pan-Ck (yellow), cadherin-11 (green) and podoplanin (magenta) (Upper panel). White arrows and arrowheads in close up images (lower panel) show podoplanin$^+$ CAFs and cadherin-11$^+$ podoplanin$^+$ CAFs, respectively. Bar, 200μm.

(Figures 6C, D; Supplementary Figure 6C). Higher frequency of CAFs 12 (81%) was found in the metastatic patient #1. Figure 6F show the concomitant infiltration of podoplanin$^+$ cadherin-11$^-$ CAFs 5 (white arrow) and podoplanin$^+$ cadherin-11$^+$ CAFs 12 (white arrowheads), close to tumor cells. Finally, CAFs 1, expressing the conventional pericyte markers, are associated with higher CA19-9 levels and worst patients prognosis (*padj<0.001*) (Figures 6A-D; Supplementary Figure 6). On the other hand, CD44$^+$ CAFs 8, vimentin$^+$ CAFs 15 and apCAFs (CAFs 16) are associated with lower CA19-9 levels, as well as longer DFS and survival (*padj<0.001*) (Figures 6A-D; Supplementary Figure 6).

Overall, single-cell resolution IMC analyses shed light on the phenotypic and spatial complexity of associated PDAC infiltrating CAFs, reflecting their possible functional differences that contribute to disease progression.

4 Discussion

Over the last years, several transcriptomic studies described the heterogeneity of CAFs in PDAC, underlying their pivotal role in disease progression and resistance to therapy. Analyses of gene expression profile and spatial location led to the identification of three main CAF subtypes, named myCAFs, iCAFs and apCAFs (52, 62, 63). Although transcriptomic approaches have the potential to identify thousands of genes and new signatures in tissues, a correlation between mRNA and protein can be limited by several factors, including post-transcriptional machinery (64). For this reason, several studies combined single-cell RNA analysis and multiplexed imaging to provide a comprehensive analysis of diseased tissue. Recent studies report the relevance of using IMC complementary to transcriptomics for the purpose of defining the

phenotype of cell subpopulations previously revealed by transcriptional approaches (54, 56, 65). On the other hand, while transcriptomic analysis has provided important information on the molecular pathways involved in the activation and differentiation of CAFs in PDAC, only a few studies have investigated their phenotype profiling by protein detection.

In the present work, we applied IMC to investigate cellular composition of 8 PDAC patients. By using a 31-antibody panel, IMC allowed us to describe the tissue architecture, identifying different subtypes of cancer cells, immune cells, ECs and CAFs. In addition, neighborhood analysis implemented the phenotypic data, providing information about the spatial localization of distinct cellular subtypes and their relationship within tumor tissue.

PDACs are characterized by a marked degree of both inter-tumor and intra-tumor heterogeneity in the histomorphology of tumor cells (66). These morphological differences coexist in the same tissues and are associated with distinct gene profiles and generally correlate with disease outcome (67, 68). In addition, morphological heterogeneity can be randomly observed even between immediately adjacent tumor cells, with a gradual transition from one morphological type to another (66). Recently, the concept of morpho-biotypes has been introduced to describe the diverse morphological and spatial organization of PDAC cells with different gene expression profiles, leading to the classification of PDAC into "glandular", "transitional" and "undifferentiated" (69). In our IMC analysis, we identified 7 different tumor cell subtypes. Beside the common expression of Pan-Ck, tumor cells were characterized by the expression of markers associated with tumor progression, epithelial-to-mesenchymal transition, and resistance to therapy, such as CD44, S100A4 and CA-IX (41, 70, 71). As reported (72) we also observed a marked degree of inter-tumor variability, with some subtypes of tumor cells whose expression was limited to specific patients in our cohort. We identified a subset of tumor cells expressing Pan-Ck, Ck-7 and PTX3, associated with the only two patients in our cohort having distant metastasis at the time of the diagnosis and surgery. Interestingly, a cancer-derived PTX3 production has been associated with tumor progression in several type of cancer, including melanoma, cervical cancer, hepatocellular carcinoma and glioma (44, 45, 73, 74), possible consequence of its role in remodeling ECM (75–77) that occurs in acidic microenvironments (76), an hallmark in cancer (78).

PDAC is generally considered an "immunologically cold" tumor, showing intrinsic properties that lead to the evasion of an effective immune response (79, 80). Almost 90% of PDACs show mutation in KRAS, which is associated to the secretion of granulocyte-macrophages colony-stimulating factor (GM-CSF) and the consequent recruitment of immunosuppressive myeloid cells, as well as the upregulation of programmed death ligand-1 (PD-L1) (81, 82). In addition, the recruitment of regulatory immune cells and the secretion of chemokine and cytokine, such as CXCL12, IL-10 and TGFβ, contribute to the generation of an immunosuppressive microenvironment (83). However, we identified that PDAC is predominantly accompanied by infiltration of M2-like macrophages, consistent with their association with tumor progression, recurrence and metastatic spread in PDAC patients (46). In addition, we identified a distinct population of $CD44^+$ macrophages. Recently, $CD44^+$ macrophages have been described in PDAC tissue as a subtype of HLA-DR^{Low} macrophages enriched in the vascular niche and possibly promoting neovascularization (24). Our analysis confirmed the presence of this phenotype, with lower HLA-DR expression compared to M1-like macrophages: differently, we found that, compared to the other immune cells, $CD44^+$ macrophages, together with M1-like macrophages and neutrophils, are the only immune cells showing a weak spatial interaction with tumor cells. Moreover, our neighborhood analysis (Figures 3G, 5D) showed that immune cells are generally excluded from tumor cell-enriched areas, confirming the immune suppressive microenvironment of PDAC tissue.

As widely described (12, 49, 84), CAFs play a pivotal role in the PDAC development and therapeutic response, by regulating the composition and the structure of the ECM, contributing to the generation of an immune-suppressive environment and influencing PDAC cell proliferation, invasion and drug resistance (11, 84). CAFs have been classified on the basis of their phenotype and function into myCAFs, having high expression of αSMA and located in proximity to tumor cells, iCAFs, showing IL-6^{high} inflammatory feature and located away from neoplastic cells, and apCAFs, expressing MHC-II and CD74, whose function is still matter of study (49, 54). Beside this classification, a variety of markers have been used to define CAFs, but most of them are shared among CAF and non-CAF cell type, thus requiring a further identification of subtype specific markers (85). In our study, we combined the expression of 11 established CAF markers (56, 65), resulting in the definition of 19 different CAF subtypes having distinct phenotype, tissue localization and relationship with other cells. We found that the vast majority of CAFs expressed αSMA and vimentin, thus suggesting the identification of the myCAF phenotype. αSMA^+ $Vimentin^+$ myCAFs can be further distinguished into distinct subtypes, based on the differential expression of other CAF markers, such as CD146, S100A4, podoplanin, FAP, CD44 and cadherin-11. αSMA and vimentin can be concomitantly (CAFs 6) or alternatively expressed (CAFs 2 and CAFs 15). Recently, it has been demonstrated that higher vimentin expression in CAFs is associated with a significantly shorter patient survival. In addition, CAFs expressing vimentin alone, without the expression of αSMA, represent an independent predictor of poor prognosis (86). In addition to myCAFs, we identified a subtype of CAF expressing CD74 and HLA-DR (CAFs 16), likely corresponding to apCAFs (54). Unlike professional antigen-presenting cells, apCAFs did not express costimulatory molecules, such as CD40, CD80 and CD86: it has been hypothesized that MHC-II expressed by apCAFs might act as a decoy receptor for $CD4^+$ T cells, inhibiting their clonal expansion, inducing anergy and promoting differentiation into T-regulatory cells, thus contributing to the generation of an immunosuppressive microenvironment (62, 87). In line with this observation, our neighborhood analysis revealed a spatial relationship between $CD4^+$ T cells and CAFs 16 (apCAFs), suggesting a possible immunomodulatory activity.

Generally, CAFs localized in proximity to different immune cell-enriched regions associated with M2-like macrophages, $CD44^+$ macrophages, T cells and myeloid cells. Recently, in mouse models

of PDAC, is has been demonstrated that *Cdh11* deficiency alters the molecular profile of fibroblasts, reduces the expression of immunosuppressive cytokines and increases the anti-tumor immunity (58, 88).

Podoplanin has emerged as a robust marker for CAFs in PDAC, showing a correlation with worst patients' prognosis (54, 89). More recently, it has been described a role of podoplanin-positive CAFs in the regulation of immune cell infiltration in PDAC and other tumors (90, 91). In our study, we identified 3 different CAF subtypes expressing podoplanin: among them, CAFs 7 also showed a significant spatial relationship with $CD4^+$ T cells and $CD44^+$ macrophages, suggesting a possible immune modulatory activity of this CAF population.

FAP is considered another well-defined CAF marker in PDAC. FAP^+ CAFs are the main repository for CXCL12 in PDAC tumor microenvironment: CXCL12 promotes T cell spatial exclusion, and pharmacological inhibition of CXCL12-CXCR4 interaction results in T cell accumulation in tumor tissue and fostering of immune checkpoint blockade (92). In addition, FAP^+ CAFs contribute to ECM desmoplasia, leading to the formation of a dense ECM which limit T cell proximity to PDAC tumor cells (93–96). In our analysis, we found 4 distinct CAF subtypes expressing FAP (CAFs 9, 10, 11 and 14): among this, CAFs 10 and 11 were the only CAF subtypes significantly enriched in tumor-stroma interface region and strictly associated to tumor cells. Moreover, we observed a significant spatial relationship between CAFs 10 and $CD44^+$ macrophages, possibly regulating their recruitment and activity. Given the described role of FAP^+ CAFs in regulating desmoplastic reaction and $CD44^+$ macrophages as highly phagocytic cells, in an attempt to speculate these cells can cooperate to a ECM remodeling niche that promotes tumor cell invasion and PDAC progression (42, 94, 97).

CA19-9 is a validated marker to establish PDAC progression, with a good sensitivity (61, 98). Even if the number of patients included in this study is not sufficient to provide reliable correlation between CAF subtypes and patients prognosis, we report that CAFs expressing different combination of FAP, podoplanin and cadherin-11, were associated with higher level of CA19-9.

Recently, expression of αSMA by pericytes, induced by cancer cell-derived exosomes, has been associated with an alteration to the morphology and bio-mechanical properties of pericytes, which significantly correlate with vascular leakiness and hypoxia in PDAC (99), thus compromising the stability of tumor vasculature and hence affecting therapy efficacy. Interestingly, CAFs 1, which expressed higher levels of αSMA compared to the other identified pericyte subtype (CAFs 3), were enriched in perivascular regions, and resulted associated with a worst patients conditions.

In addition to CAFs 1, CAFs 12 cells, expressing podoplanin and cadherin-11, are associated with higher levels of CA19-9 as well as shorter DFS and overall survival. This result is in accordance with the recently observed association between the expression of podoplanin and cadherin-11 and the expansion of mesothelial cells that contribute to stromal deposition and desmoplastic reaction in early neoplastic lesions in mouse (87). In our cohort, majority of CAFs 12 were expressed by the metastatic patient#1, suggesting a possible correlation with PDAC metastatic capability. In line with this observation, podoplanin expression by CAFs has been associated with PDAC progression and invasion (55). On the other side, CAFs 15 and CAFs 16 are associated with lower CA19-9 levels and better patient prognosis. As previously reported, we identified CAFs 16 as apCAFs, based on the concomitant expression of CD74 and HLA-DR (54). Although apCAFs have been generally linked to the generation of an immunomodulatory microenvironment (62, 87), they may exert more complicated immune-regulating functions. For example, in breast cancer, $MHC\text{-}II^+$ CAFs were associated with T regulatory cells and resistance to immunotherapy but also correlated with patient survival (100–102). In addition, in lung cancer, $MHC\text{-}II^+$ CAFs enhanced $CD4^+$ T cell cancer immunity (103).

In conclusion, our IMC analysis provided an overview of the complexity of the PDAC tumor microenvironments, showing how cancer and stromal cells with different phenotypic characteristics co-exist within the same tissue. In particular, the classification of 19 distinct CAF subtypes, characterized by different combination of fibroblast markers and by a peculiar spatial localization and relationship with surrounding cells, underlies the high plasticity of CAFs in PDAC and their complex role in PDAC progression, leading to the potential identification of new targets for the diagnosis and the treatment of PDAC patients.

Data availability statement

The raw data supporting the conclusions of this article will be made available by the authors, without undue reservation.

Ethics statement

The studies involving humans were approved by Comitato Etico Territoriale Lombardia 5, Via Alessandro Manzoni 56, 20089 Rozzano (Milano). The studies were conducted in accordance with the local legislation and institutional requirements. The participants provided their written informed consent to participate in this study.

Author contributions

ME: Conceptualization, Data curation, Formal analysis, Investigation, Methodology, Validation, Visualization, Writing – original draft. MF: Data curation, Formal analysis, Methodology, Software, Validation, Visualization, Writing – original draft. RD: Data curation, Formal analysis, Software, Writing – review & editing. MS: Resources, Writing – review & editing. SB: Resources, Writing – review & editing. GN: Resources, Writing – review & editing. DZ: Investigation, Writing – review & editing. RP: Investigation, Writing – review & editing. CG: Funding acquisition, Supervision, Writing – review & editing. LR: Writing – review & editing, Resources. LT: Resources, Supervision, Writing – review & editing. SB: Supervision, Writing – review & editing. AZ: Resources, Supervision, Writing – review & editing. AM: Supervision,

Writing – review & editing. AD: Conceptualization, Funding acquisition, Project administration, Supervision, Writing – original draft, Writing – review & editing.

Funding

The author(s) declare financial support was received for the research, authorship, and/or publication of this article. This study was funded by Ministero degli Affari Esteri e della Cooperazione Internazionale (MAECI; Project no. 2023-23683652-ITALIA-SINGAPORE 2023-2026), ITALY -SINGAPORE SCIENCE AND TECHNOLOGY COOPERATION, A*STAR (Grant No. R22I0IR118) and EU funding within the MUR PNRR Italian network of excellence for advanced diagnosis (Project no. PNC-E3-2022-23683266 PNC-HLS-DA). This work was partially supported by "Ricerca Corrente" funding from Italian Ministry of Health to IRCCS Humanitas Research Hospital.

Acknowledgments

IMC workflow in Figure 1A has been created with BioRender.com.

Conflict of interest

LR reports grant/research funding to institution from Agios, AstraZeneca, BeiGene, Eisai, Exelixis, Fibrogen, Incyte, IPSEN, Lilly, MSD, Nerviano Medical Sciences, Roche, Servier, Taiho Oncology, TransThera Sciences, and Zymeworks; consulting fees from AbbVie, AstraZeneca, Basilea, Bayer, Bristol Myers Squibb, Elevar Therapeutics, Exelixis, Genenta, Hengrui, Incyte, IPSEN, IQVIA, Jazz Pharmaceuticals, MSD, Nerviano Medical Sciences, Roche, Servier, Taiho Oncology, and Zymeworks; lecture fees from AstraZeneca, Bayer, Bristol Myers Squibb, Guerbet, Incyte, IPSEN, Roche, and Servier; and travel expenses from AstraZeneca.

The remaining authors declare that the research was conducted in the absence of any commercial or financial relationships that could be construed as a potential conflict of interest.

The author(s) declared that they were an editorial board member of Frontiers, at the time of submission. This had no impact on the peer review process and the final decision.

The reviewer MM declared a shared affiliation, with no collaboration, with the authors to the handling editor at the time of the review.

Publisher's note

Supplementary material

The Supplementary Material for this article can be found online at: https://www.frontiersin.org/articles/10.3389/fimmu.2024.1472433/full#supplementary-material

References

1. Siegel RL, Miller KD, Fuchs HE, Jemal A. Cancer statistics, 2022. *CA Cancer J Clin*. (2022) 72:7–33. doi: 10.3322/caac.21708

2. Halbrook CJ, Lyssiotis CA, Pasca di Magliano M, Maitra A. Pancreatic cancer: advances and challenges. *Cell*. (2023) 186:1729–54. doi: 10.1016/j.cell.2023.02.014

3. Petersen GM. Familial pancreatic cancer. *Semin Oncol*. (2016) 43:548–53. doi: 10.1053/j.seminoncol.2016.09.002

4. Cronin KA, Scott S, Firth AU, Sung H, Henley SJ, Sherman RL, et al. Annual report to the nation on the status of cancer, part 1: national cancer statistics. *Cancer*. (2022) 128:4251–84. doi: 10.1002/cncr.34479

5. Kanda M, Matthaei H, Wu J, Hong SM, Yu J, Borges M, et al. Presence of somatic mutations in most early-stage pancreatic intraepithelial neoplasia. *Gastroenterology*. (2012) 142:730–3.e9. doi: 10.1053/j.gastro.2011.12.042

6. Waddell N, Pajic M, Patch AM, Chang DK, Kassahn KS, Bailey P, et al. Whole genomes redefine the mutational landscape of pancreatic cancer. *Nature*. (2015) 518:495–501. doi: 10.1038/nature14169

7. Cancer Genome Atlas Research Network. Electronic address aadhe, Cancer Genome Atlas Research N. Integrated Genomic Characterization of Pancreatic Ductal Adenocarcinoma. *Cancer Cell*. (2017) 32:185–203 e13. doi: 10.1016/j.ccell.2017.07.007

8. Fujikura K, Hosoda W, Felsenstein M, Song Q, Reiter JG, Zheng L, et al. Multiregion whole-exome sequencing of intraductal papillary mucinous neoplasms reveals frequent somatic KLF4 mutations predominantly in low-grade regions. *Gut*. (2021) 70:928–39. doi: 10.1136/gutjnl-2020-321217

9. Ho WJ, Jaffee EM, Zheng L. The tumour microenvironment in pancreatic cancer - clinical challenges and opportunities. *Nat Rev Clin Oncol*. (2020) 17:527–40. doi: 10.1038/s41571-020-0363-5

10. Liot S, Balas J, Aubert A, Prigent L, Mercier-Gouy P, Verrier B, et al. Stroma involvement in pancreatic ductal adenocarcinoma: an overview focusing on extracellular matrix proteins. *Front Immunol*. (2021) 12:612271. doi: 10.3389/fimmu.2021.612271

11. Zhang T, Ren Y, Yang P, Wang J, Zhou H. Cancer-associated fibroblasts in pancreatic ductal adenocarcinoma. *Cell Death Dis*. (2022) 13:897. doi: 10.1038/s41419-022-05351-1

12. Pereira BA, Vennin C, Papanicolaou M, Chambers CR, Herrmann D, Morton JP, et al. Caf subpopulations: A new reservoir of stromal targets in pancreatic cancer. *Trends Cancer*. (2019) 5:724–41. doi: 10.1016/j.trecan.2019.09.010

13. Siegel RL, Miller KD, Wagle NS, Jemal A. Cancer statistics, 2023. *CA Cancer J Clin*. (2023) 73:17–48. doi: 10.3322/caac.21763

14. Tsujikawa T, Kumar S, Borkar RN, Azimi V, Thibault G, Chang YH, et al. Quantitative multiplex immunohistochemistry reveals myeloid-inflamed tumor-immune complexity associated with poor prognosis. *Cell Rep*. (2017) 19:203–17. doi: 10.1016/j.celrep.2017.03.037

15. Steele NG, Carpenter ES, Kemp SB, Sirihorachai VR, The S, Delrosario L, et al. Multimodal mapping of the tumor and peripheral blood immune landscape in human pancreatic cancer. *Nat Cancer*. (2020) 1:1097–112. doi: 10.1038/s43018-020-00121-4

16. Yousuf S, Qiu M, Voith von Voithenberg L, Hulkkonen J, Macinkovic I, Schulz AR, et al. Spatially resolved multi-omics single-cell analyses inform mechanisms of immune dysfunction in pancreatic cancer. *Gastroenterology*. (2023) 165:891–908.e14. doi: 10.1053/j.gastro.2023.05.036

17. Giesen C, Wang HA, Schapiro D, Zivanovic N, Jacobs A, Hattendorf B, et al. Highly multiplexed imaging of tumor tissues with subcellular resolution by mass cytometry. *Nat Methods*. (2014) 11:417–22. doi: 10.1038/nmeth.2869

18. Le Rochais M, Hemon P, Pers JO, Uguen A. Application of high-throughput imaging mass cytometry hyperion in cancer research. *Front Immunol*. (2022) 13:859414. doi: 10.3389/fimmu.2022.859414

19. Zhao C, Germain RN. Multiplex imaging in immuno-oncology. *J Immunother Cancer*. (2023) 11:e006923. doi: 10.1136/jitc-2023-006923

20. Chang Q, Ornatsky OI, Siddiqui I, Loboda A, Baranov VI, Hedley DW. Imaging mass cytometry. *Cytometry A*. (2017) 91:160–9. doi: 10.1002/cyto.a.23053

21. Byrne KT, Betts CB, Mick R, Sivagnanam S, Bajor DL, Laheru DA, et al. Neoadjuvant selicrelumab, an agonist Cd40 antibody, induces changes in the tumor microenvironment in patients with resectable pancreatic cancer. *Clin Cancer Res*. (2021) 27:4574–86. doi: 10.1158/1078-0432.CCR-21-1047

22. Wattenberg MM, Colby S, Garrido-Laguna I, Xue Y, Chang R, Delman D, et al. Intratumoral cell neighborhoods coordinate outcomes in pancreatic ductal adenocarcinoma. *Gastroenterology*. (2024) 166:1114–29. doi: 10.1053/j.gastro.2024.01.013

23. Yoon S, Li H, Quintanar L, Armstrong B, Rossi JJ. Uncovering differently expressed markers and heterogeneity on human pancreatic cancer. *Transl Oncol*. (2020) 13:100749. doi: 10.1016/j.tranon.2020.100749

24. Sussman J, Kim NY, Kemp SB, Traum D, Katsuda T, Kahn BM, et al. Multiplexed imaging mass cytometry analysis characterizes the vascular niche in pancreatic cancer. *Cancer Res*. (2024) 84(14):2364–76. doi: 10.1158/0008-5472.CAN-23-2352

25. Erreni M, Fumagalli MR, Zanini D, Candiello E, Tiberi G, Parente R, et al. Multiplexed imaging mass cytometry analysis in preclinical models of pancreatic cancer. *Int J Mol Sci*. (2024) 25:1389. doi: 10.3390/ijms25031389

26. Berg S, Kutra D, Kroeger T, Straehle CN, Kausler BX, Haubold C, et al. Ilastik: interactive machine learning for (Bio)Image analysis. *Nat Methods*. (2019) 16:1226–32. doi: 10.1038/s41592-019-0582-9

27. Stirling DR, Swain-Bowden MJ, Lucas AM, Carpenter AE, Cimini BA, Goodman A. Cellprofiler 4: improvements in speed, utility and usability. *BMC Bioinf*. (2021) 22:433. doi: 10.1186/s12859-021-04344-9

28. Pau G, Fuchs F, Sklyar O, Boutros M, Huber W. Ebimage–an R package for image processing with applications to cellular phenotypes. *Bioinformatics*. (2010) 26:979–81. doi: 10.1093/bioinformatics/btq046

29. Federico A, Monti S. Hyper: an R package for geneset enrichment workflows. *Bioinformatics*. (2020) 36:1307–8. doi: 10.1093/bioinformatics/btz700

30. Kalluri R, Zeisberg M. Fibroblasts in cancer. *Nat Rev Cancer*. (2006) 6:392–401. doi: 10.1038/nrc1877

31. Uccelli A, Moretta L, Pistoia V. Mesenchymal stem cells in health and disease. *Nat Rev Immunol*. (2008) 8:726–36. doi: 10.1038/nri2395

32. Kalluri R. The biology and function of fibroblasts in cancer. *Nat Rev Cancer*. (2016) 16:582–98. doi: 10.1038/nrc.2016.73

33. Carmeliet P, Jain RK. Molecular mechanisms and clinical applications of angiogenesis. *Nature*. (2011) 473:298–307. doi: 10.1038/nature10144

34. McDonald PC, Chafe SC, Dedhar S. Overcoming hypoxia-mediated tumor progression: combinatorial approaches targeting pH regulation, angiogenesis and immune dysfunction. *Front Cell Dev Biol*. (2016) 4:27. doi: 10.3389/fcell.2016.00027

35. Segerstolpe A, Palasantza A, Eliasson P, Andersson EM, Andreasson AC, Sun X, et al. Single-cell transcriptome profiling of human pancreatic islets in health and type 2 diabetes. *Cell Metab*. (2016) 24:593–607. doi: 10.1016/j.cmet.2016.08.020

36. Zhang S, Fang W, Zhou S, Zhu D, Chen R, Gao X, et al. Single cell transcriptomic analyses implicate an immunosuppressive tumor microenvironment in pancreatic cancer liver metastasis. *Nat Commun*. (2023) 14:5123. doi: 10.1038/s41467-023-40727-7

37. Goulart MR, Watt J, Siddiqui I, Lawlor RT, Imrali A, Hughes C, et al. Pentraxin 3 is a stromally-derived biomarker for detection of pancreatic ductal adenocarcinoma. *NPJ Precis Oncol*. (2021) 5:61. doi: 10.1038/s41698-021-00192-1

38. van Splunder H, Villacampa P, Martinez-Romero A, Graupera M. Pericytes in the disease spotlight. *Trends Cell Biol*. (2024) 34:58–71. doi: 10.1016/j.tcb.2023.06.001

39. Brichkina A, Polo P, Sharma SD, Visestamkul N, Lauth M. A quick guide to CAF subtypes in pancreatic cancer. *Cancers (Basel)*. (2023) 15:2614. doi: 10.3390/cancers15092614

40. Jordan AR, Racine RR, Hennig MJ, Lokeshwar VB. The role of CD44 in disease pathophysiology and targeted treatment. *Front Immunol*. (2015) 6:182. doi: 10.3389/fimmu.2015.00182

41. Zhao S, Chen C, Chang K, Karnad A, Jagirdar J, Kumar AP, et al. CD44 expression level and isoform contributes to pancreatic cancer cell plasticity, invasiveness, and response to therapy. *Clin Cancer Res*. (2016) 22:5592–604. doi: 10.1158/1078-0432.CCR-15-3115

42. Chen C, Zhao S, Zhao X, Cao L, Karnad A, Kumar AP, et al. Gemcitabine resistance of pancreatic cancer cells is mediated by igf1r dependent upregulation of CD44 expression and isoform switching. *Cell Death Dis*. (2022) 13:682. doi: 10.1038/s41419-022-05103-1

43. Bonavita E, Gentile S, Rubino M, Maina V, Papait R, Kunderfranco P, et al. PTX3 is an extrinsic oncosuppressor regulating complement-dependent inflammation in cancer. *Cell*. (2015) 160:700–14. doi: 10.1016/j.cell.2015.01.004

44. Ying TH, Lee CH, Chiou HL, Yang SF, Lin CL, Hung CH, et al. Knockdown of pentraxin 3 suppresses tumorigenicity and metastasis of human cervical cancer cells. *Sci Rep*. (2016) 6:29385. doi: 10.1038/srep29385

45. Rathore M, Girard C, Ohanna M, Tichet M, Ben Jouira R, Garcia E, et al. Cancer cell-derived long pentraxin 3 (PTX3) promotes melanoma migration through a toll-like receptor 4 (Tlr4)/Nf-Kappab signaling pathway. *Oncogene*. (2019) 38:5873–89. doi: 10.1038/s41388-019-0848-9

46. Yang S, Liu Q, Liao Q. Tumor-associated macrophages in pancreatic ductal adenocarcinoma: origin, polarization, function, and reprogramming. *Front Cell Dev Biol*. (2020) 8:607209. doi: 10.3389/fcell.2020.607209

47. Mantovani A, Allavena P, Marchesi F, Garlanda C. Macrophages as tools and targets in cancer therapy. *Nat Rev Drug Discovery*. (2022) 21:799–820. doi: 10.1038/s41573-022-00520-5

48. Liu S, Zhang H, Li Y, Zhang Y, Bian Y, Zeng Y, et al. S100a4 enhances protumor macrophage polarization by control of PPAR-gamma-dependent induction of fatty acid oxidation. *J Immunother Cancer*. (2021) 9:e002548. doi: 10.1136/jitc-2021-002548

49. Geng X, Chen H, Zhao L, Hu J, Yang W, Li G, et al. Cancer-associated fibroblast (CAF) heterogeneity and targeting therapy of CAFs in pancreatic cancer. *Front Cell Dev Biol*. (2021) 9:655152. doi: 10.3389/fcell.2021.655152

50. Stouten I, van Montfoort N, Hawinkels L. The tango between cancer-associated fibroblasts (CAFs) and immune cells in affecting immunotherapy efficacy in pancreatic cancer. *Int J Mol Sci*. (2023) 24:8707. doi: 10.3390/ijms24108707

51. Yamashita K, Kumamoto Y. CAFs-associated genes (Cafgs) in pancreatic ductal adenocarcinoma (PDAC) and novel therapeutic strategy. *Int J Mol Sci*. (2024) 25:6003. doi: 10.3390/ijms25116003

52. Ohlund D, Handly-Santana A, Biffi G, Elyada E, Almeida AS, Ponz-Sarvise M, et al. Distinct populations of inflammatory fibroblasts and myofibroblasts in pancreatic cancer. *J Exp Med*. (2017) 214:579–96. doi: 10.1084/jem.20162024

53. Xu Y, Li W, Lin S, Liu B, Wu P, Li L. Fibroblast diversity and plasticity in the tumor microenvironment: roles in immunity and relevant therapies. *Cell Commun Signal*. (2023) 21:234. doi: 10.1186/s12964-023-01204-2

54. Elyada E, Bolisetty M, Laise P, Flynn WF, Courtois ET, Burkhart RA, et al. Cross-species single-cell analysis of pancreatic ductal adenocarcinoma reveals antigen-presenting cancer-associated fibroblasts. *Cancer Discovery*. (2019) 9:1102–23. doi: 10.1158/2159-8290.CD-19-0094

55. Shindo K, Aishima S, Ohuchida K, Fujiwara K, Fujino M, Mizuuchi Y, et al. Podoplanin expression in cancer-associated fibroblasts enhances tumor progression of invasive ductal carcinoma of the pancreas. *Mol Cancer*. (2013) 12:168. doi: 10.1186/1476-4598-12-168

56. Cords L, Tietscher S, Anzeneder T, Langwieder C, Rees M, de Souza N, et al. Cancer-associated fibroblast classification in single-cell and spatial proteomics data. *Nat Commun*. (2023) 14:4294. doi: 10.1038/s41467-023-39762-1

57. Perez VM, Kearney JF, Yeh JJ. The PDAC extracellular matrix: A review of the ECM protein composition, tumor cell interaction, and therapeutic strategies. *Front Oncol*. (2021) 11:751311. doi: 10.3389/fonc.2021.751311

58. Peran I, Dakshanamurthy S, McCoy MD, Mavropoulos A, Allo B, Sebastian A, et al. Cadherin 11 promotes immunosuppression and extracellular matrix deposition to support growth of pancreatic tumors and resistance to gemcitabine in mice. *Gastroenterology*. (2021) 160:1359–72 e13. doi: 10.1053/j.gastro.2020.11.044

59. Schurch CM, Bhate SS, Barlow GL, Phillips DJ, Noti L, Zlobec I, et al. Coordinated cellular neighborhoods orchestrate antitumoral immunity at the colorectal cancer invasive front. *Cell*. (2020) 182:1341–59 e19. doi: 10.1016/j.cell.2020.07.005

60. van Oosten AF, Groot VP, Dorland G, Burkhart RA, Wolfgang CL, van Santvoort HC, et al. Dynamics of serum CA19-9 in patients undergoing pancreatic cancer resection. *Ann Surg*. (2024) 279:493–500. doi: 10.1097/SLA.0000000000005977

61. Ballehaninna UK, Chamberlain RS. The clinical utility of serum CA 19-9 in the diagnosis, prognosis and management of pancreatic adenocarcinoma: an evidence based appraisal. *J Gastrointest Oncol*. (2012) 3:105–19. doi: 10.3978/j.issn.2078-6891.2011.021

62. Hosein AN, Huang H, Wang Z, Parmar K, Du W, Huang J, et al. Cellular heterogeneity during mouse pancreatic ductal adenocarcinoma progression at single-cell resolution. *JCI Insight*. (2019) 5:e129212. doi: 10.1172/jci.insight.129212

63. Dominguez CX, Muller S, Keerthivasan S, Koeppen H, Hung J, Gierke S, et al. Single-cell RNA sequencing reveals stromal evolution into lrrc15(+) myofibroblasts as a determinant of patient response to cancer immunotherapy. *Cancer Discovery*. (2020) 10:232–53. doi: 10.1158/2159-8290.CD-19-0644

64. Haider S, Pal R. Integrated analysis of transcriptomic and proteomic data. *Curr Genomics*. (2013) 14:91–110. doi: 10.2174/1389202911314020003

65. Cords L, Engler S, Haberecker M, Ruschoff JH, Moch H, de Souza N, et al. Cancer-associated fibroblast phenotypes are associated with patient outcome in non-small cell lung cancer. *Cancer Cell*. (2024) 42:396–412 e5. doi: 10.1016/j.ccell.2023.12.021

66. Verbeke C. Morphological heterogeneity in ductal adenocarcinoma of the pancreas - does it matter? *Pancreatology*. (2016) 16:295–301. doi: 10.1016/j.pan.2016.02.004

67. NK S, Wilson GW, Grant RC, Seto M, O'Kane G, Vajpeyi R, et al. Morphological classification of pancreatic ductal adenocarcinoma that predicts molecular subtypes and correlates with clinical outcome. *Gut*. (2020) 69:317–28. doi: 10.1136/gutjnl-2019-318217

68. Juiz N, Elkaoutari A, Bigonnet M, Gayet O, Roques J, Nicolle R, et al. Basal-like and classical cells coexist in pancreatic cancer revealed by single-cell analysis on biopsy-derived pancreatic cancer organoids from the classical subtype. *FASEB J*. (2020) 34:12214–28. doi: 10.1096/fj.202000363RR

69. Di Chiaro P, Nacci L, Arco F, Brandini S, Polletti S, Palamidessi A, et al. Mapping functional to morphological variation reveals the basis of regional extracellular matrix subversion and nerve invasion in pancreatic cancer. *Cancer Cell*. (2024) 42:662–81.e10. doi: 10.1016/j.ccell.2024.02.017

70. Che P, Yang Y, Han X, Hu M, Sellers JC, Londono-Joshi AI, et al. S100a4 promotes pancreatic cancer progression through a dual signaling pathway mediated by Src and focal adhesion kinase. *Sci Rep*. (2015) 5:8453. doi: 10.1038/srep08453

71. McDonald PC, Chafe SC, Brown WS, Saberi S, Swayampakula M, Venkateswaran G, et al. Regulation of ph by carbonic anhydrase 9 mediates survival of pancreatic cancer cells with activated KRAS in response to hypoxia. *Gastroenterology*. (2019) 157:823–37. doi: 10.1053/j.gastro.2019.05.004

72. Milan M, Diaferia GR, Natoli G. Tumor cell heterogeneity and its transcriptional bases in pancreatic cancer: A tale of two cell types and their many variants. *EMBO J*. (2021) 40:e107206. doi: 10.15252/embj.2020107206

73. Tung JN, Ko CP, Yang SF, Cheng CW, Chen PN, Chang CY, et al. Inhibition of pentraxin 3 in glioma cells impairs proliferation and invasion in vitro and in vivo. *J Neurooncol*. (2016) 129:201–9. doi: 10.1007/s11060-016-2168-z

74. Song T, Wang C, Guo C, Liu Q, Zheng X. Pentraxin 3 overexpression accelerated tumor metastasis and indicated poor prognosis in hepatocellular carcinoma via driving epithelial-mesenchymal transition. *J Cancer*. (2018) 9:2650–8. doi: 10.7150/jca.25188

75. Erreni M, Manfredi A, Garlanda C, Mantovani A, Rovere-Querini P. The long pentraxin PTX3: A prototypical sensor of tissue injury and a regulator of homeostasis. *Immunol Rev*. (2017) 280:112–25. doi: 10.1111/imr.12570

76. Doni A, Musso T, Morone D, Bastone A, Zambelli V, Sironi M, et al. An acidic microenvironment sets the humoral pattern recognition molecule PTX3 in a tissue repair mode. *J Exp Med*. (2015) 212:905–25. doi: 10.1084/jem.20141268

77. Doni A, Stravalaci M, Inforzato A, Magrini E, Mantovani A, Garlanda C, et al. The long pentraxin PTX3 as a link between innate immunity, tissue remodeling, and cancer. *Front Immunol*. (2019) 10:712. doi: 10.3389/fimmu.2019.00712

78. Boedtkjer E, Pedersen SF. The acidic tumor microenvironment as a driver of cancer. *Annu Rev Physiol*. (2020) 82:103–26. doi: 10.1146/annurev-physiol-021119-034627

79. Ullman NA, Burchard PR, Dunne RF, Linehan DC. Immunologic strategies in pancreatic cancer: making cold tumors hot. *J Clin Oncol*. (2022) 40:2789–805. doi: 10.1200/JCO.21.02616

80. Hartupee C, Nagalo BM, Chabu CY, Tesfay MZ, Coleman-Barnett J, West JT, et al. Pancreatic cancer tumor microenvironment is a major therapeutic barrier and target. *Front Immunol*. (2024) 15:1287459. doi: 10.3389/fimmu.2024.1287459

81. Bayne LJ, Beatty GL, Jhala N, Clark CE, Rhim AD, Stanger BZ, et al. Tumor-derived granulocyte-macrophage colony-stimulating factor regulates myeloid inflammation and T cell immunity in pancreatic cancer. *Cancer Cell*. (2012) 21:822–35. doi: 10.1016/j.ccr.2012.04.025

82. Coelho MA, de Carne Trecesson S, Rana S, Zecchin D, Moore C, Molina-Arcas M, et al. Oncogenic ras signaling promotes tumor immunoresistance by stabilizing PD-L1 mRNA. *Immunity*. (2017) 47:1083–99.e6. doi: 10.1016/j.immuni.2017.11.016

83. Karamitopoulou E. Tumour microenvironment of pancreatic cancer: immune landscape is dictated by molecular and histopathological features. *Br J Cancer*. (2019) 121:5–14. doi: 10.1038/s41416-019-0479-5

84. Rebelo R, Xavier CPR, Giovannetti E, Vasconcelos MH. Fibroblasts in pancreatic cancer: molecular and clinical perspectives. *Trends Mol Med*. (2023) 29:439–53. doi: 10.1016/j.molmed.2023.03.002

85. Kobayashi H, Enomoto A, Woods SL, Burt AD, Takahashi M, Worthley DL. Cancer-associated fibroblasts in gastrointestinal cancer. *Nat Rev Gastroenterol Hepatol*. (2019) 16:282–95. doi: 10.1038/s41575-019-0115-0

86. Maehira H, Miyake T, Iida H, Tokuda A, Mori H, Yasukawa D, et al. Vimentin expression in tumor microenvironment predicts survival in pancreatic ductal adenocarcinoma: heterogeneity in fibroblast population. *Ann Surg Oncol*. (2019) 26:4791–804. doi: 10.1245/s10434-019-07891-x

87. Huang H, Wang Z, Zhang Y, Pradhan RN, Ganguly D, Chandra R, et al. Mesothelial cell-derived antigen-presenting cancer-associated fibroblasts induce expansion of regulatory T cells in pancreatic cancer. *Cancer Cell*. (2022) 40:656–73.e7. doi: 10.1016/j.ccell.2022.04.011

88. Sebastian A, Martin KA, Peran I, Hum NR, Leon NF, Amiri B, et al. Loss of cadherin-11 in pancreatic ductal adenocarcinoma alters tumor-immune microenvironment. *Front Oncol*. (2023) 13:1286861. doi: 10.3389/fonc.2023.1286861

89. Hirayama K, Kono H, Nakata Y, Akazawa Y, Wakana H, Fukushima H, et al. Expression of podoplanin in stromal fibroblasts plays a pivotal role in the prognosis of patients with pancreatic cancer. *Surg Today*. (2018) 48:110–8. doi: 10.1007/s00595-017-1559-x

90. Suzuki J, Aokage K, Neri S, Sakai T, Hashimoto H, Su Y, et al. Relationship between podoplanin-expressing cancer-associated fibroblasts and the immune microenvironment of early lung squamous cell carcinoma. *Lung Cancer*. (2021) 153:1–10. doi: 10.1016/j.lungcan.2020.12.020

91. Neuzillet C, Nicolle R, Raffenne J, Tijeras-Raballand A, Brunel A, Astorgues-Xerri L, et al. Periostin- and podoplanin-positive cancer-associated fibroblast subtypes cooperate to shape the inflamed tumor microenvironment in aggressive pancreatic adenocarcinoma. *J Pathol*. (2022) 258:408–25. doi: 10.1002/path.6011

92. Feig C, Jones JO, Kraman M, Wells RJ, Deonarine A, Chan DS, et al. Targeting cxcl12 from fap-expressing carcinoma-associated fibroblasts synergizes with anti-pd-L1 immunotherapy in pancreatic cancer. *Proc Natl Acad Sci U.S.A*. (2013) 110:20212–7. doi: 10.1073/pnas.1320318110

93. Hartmann N, Giese NA, Giese T, Poschke I, Offringa R, Werner J, et al. Prevailing role of contact guidance in intrastromal T-cell trapping in human pancreatic cancer. *Clin Cancer Res*. (2014) 20:3422–33. doi: 10.1158/1078-0432.CCR-13-2972

94. Lo A, Wang LS, Scholler J, Monslow J, Avery D, Newick K, et al. Tumor-promoting desmoplasia is disrupted by depleting fap-expressing stromal cells. *Cancer Res*. (2015) 75:2800–10. doi: 10.1158/0008-5472.CAN-14-3041

95. Jiang H, Hegde S, Knolhoff BL, Zhu Y, Herndon JM, Meyer MA, et al. Targeting focal adhesion kinase renders pancreatic cancers responsive to checkpoint immunotherapy. *Nat Med*. (2016) 22:851–60. doi: 10.1038/nm.4123

96. Cheng CS, Yang PW, Sun Y, Song SL, Chen Z. Fibroblast activation protein-based theranostics in pancreatic cancer. *Front Oncol*. (2022) 12:969731. doi: 10.3389/fonc.2022.969731

97. Chen C, Zhao S, Karnad A, Freeman JW. The biology and role of CD44 in cancer progression: therapeutic implications. *J Hematol Oncol*. (2018) 11:64. doi: 10.1186/s13045-018-0605-5

98. Luo G, Jin K, Deng S, Cheng H, Fan Z, Gong Y, et al. Roles of CA19-9 in pancreatic cancer: biomarker, predictor and promoter. *Biochim Biophys Acta Rev Cancer*. (2021) 1875:188409. doi: 10.1016/j.bbcan.2020.188409

99. Natarajan V, Ha S, Delgado A, Jacobson R, Alhalhooly L, Choi Y, et al. Acquired alphasma expression in pericytes coincides with aberrant vascular structure and function in pancreatic ductal adenocarcinoma. *Cancers (Basel)*. (2022) 14:2448. doi: 10.3390/cancers14102448

100. Costa A, Kieffer Y, Scholer-Dahirel A, Pelon F, Bourachot B, Cardon M, et al. Fibroblast heterogeneity and immunosuppressive environment in human breast cancer. *Cancer Cell*. (2018) 33:463–79.e10. doi: 10.1016/j.ccell.2018.01.011

101. Kieffer Y, Hocine HR, Gentric G, Pelon F, Bernard C, Bourachot B, et al. Single-cell analysis reveals fibroblast clusters linked to immunotherapy resistance in cancer. *Cancer Discovery*. (2020) 10:1330–51. doi: 10.1158/2159-8290.CD-19-1384

102. Friedman G, Levi-Galibov O, David E, Bornstein C, Giladi A, Dadiani M, et al. Cancer-associated fibroblast compositions change with breast cancer progression linking the ratio of S100a4(+) and Pdpn(+) CAFs to clinical outcome. *Nat Cancer*. (2020) 1:692–708. doi: 10.1038/s43018-020-0082-y

103. Kerdidani D, Aerakis E, Verrou KM, Angelidis I, Douka K, Maniou MA, et al. Lung tumor MHCII immunity depends on in situ antigen presentation by fibroblasts. *J Exp Med*. (2022) 219:e20210815. doi: 10.1084/jem.20210815

frontiers | Frontiers in Immunology

TYPE Case Report
PUBLISHED 29 November 2024
DOI 10.3389/fimmu.2024.1477477

OPEN ACCESS

EDITED BY
Noah Isakov,
Ben-Gurion University of the Negev, Israel

REVIEWED BY
Nicola Tumino,
Bambino Gesù Children's Hospital (IRCCS), Italy
Francesco Fazi,
Sapienza University of Rome, Italy
Rachael Sugars,
Karolinska Institutet (KI), Sweden

*CORRESPONDENCE
Emanuela Marcenaro
emanuela.marcenaro@unige.it

RECEIVED 07 August 2024
ACCEPTED 11 November 2024
PUBLISHED 29 November 2024

CITATION
Rebaudi F, Rebaudi A, De Rosa A, Rebaudi AL, Pesce S, Greppi M, Roghi M, Boggio M, Candiani S and Marcenaro E (2024) Case report: Non-invasive cyto-salivary sampling and biomarker detection via ELISA versus histopathology for diagnosing oral potentially malignant disorders - Insights from a case-control study.
Front. Immunol. 15:1477477.
doi: 10.3389/fimmu.2024.1477477

Case report: Non-invasive cyto-salivary sampling and biomarker detection via ELISA versus histopathology for diagnosing oral potentially malignant disorders - Insights from a case-control study

Federico Rebaudi[1], Alberto Rebaudi[2], Alfredo De Rosa[3], Alberto Luigi Rebaudi[2], Silvia Pesce[1,4], Marco Greppi[1], Marco Roghi[5], Maurizio Boggio[4], Simona Candiani[4,6] and Emanuela Marcenaro[1,4]*

[1]Department of Experimental Medicine (DIMES), University of Genoa, Genoa, Italy, [2]Private Practice, Genova, Italy, [3]Multidisciplinary Department of Medical-Surgical and Dental Specialties, University of Campania "Luigi Vanvitelli", Naples, Italy, [4]IRCCS Ospedale Policlinico San Martino, Genoa, Italy, [5]Department of Oral Pathology, Istituto Stomatologico Italiano, Milan, Italy, [6]Department of Earth, Environmental and Life Sciences (DISTAV), University of Genoa, Genoa, Italy

Oral leukoplakia is classified among oral potentially malignant disorders (OPMDs) by the World Health Organization (WHO). The visual oral examination (VOE) is the most used method for identifying lesions in their early stages. Given that the diagnosis of oral cancer is often late, there is an urgent need for early detection and examination of oral lesions. Surgical biopsy represents the gold standard as a diagnostic method, but because it is invasive, it cannot be repeated for periodic checks. We report the case of a lesion on the buccal mucosa of a 65-year-old male patient with a malignant appearance. The patient underwent a novel non-invasive cyto-salivary sampling and ELISA immunoassay for tumor biomarker detection and biopsy with histopathological analysis. The rapid ELISA test results excluded signs of malignancy, providing valuable insights into the lesion's immunophenotypic profile, which were consistent with the histopathological examination findings. This case report highlights the clinical and histopathological characteristics of a lesion with the aspect of Proliferative Verrucous Leukoplakia (PVL), emphasizing its challenging diagnosis and management. The integration of non-invasive cytobrush sampling with biomarker analysis proved valuable in detecting specific tumor biomarkers, potentially indicating ongoing tumor transformation. Monitoring these markers

over time could enhance early detection and management strategies, thereby improving patient outcomes. This approach underscores the utility of non-invasive techniques in phenotyping oral lesions and supporting clinical decision-making in oral medicine.

KEYWORDS

oral potentially malignant disorders, cytobrush sampling, biomarker analysis, histopathology, immune checkpoints

1 Introduction

Leukoplakia is the most common and studied white oral lesion, classified as an oral potentially malignant disorder (OPMD). The World Health Organization (WHO) defines leukoplakia as "a predominantly white plaque of questionable risk, having excluded other known diseases or disorders that carry no increased risk for cancer." The global prevalence of leukoplakia in the adult population is approximately 4.11% (1). Clinically, leukoplakia is diagnosed by excluding other white lesions with distinct clinicopathological characteristics. There are two main variants: homogeneous leukoplakia and non-homogeneous leukoplakia. The latter generally carries a higher risk of neoplastic transformation and exhibits varying features based on color and surface texture (2). To diagnose leukoplakia accurately, it is essential to exclude other well-defined pathologies associated with specific risk factors. These include frictional keratosis linked to persistent local trauma, tobacco pouch keratosis often found in smokers, and oral candidiasis. Experts emphasize that the initial diagnosis of leukoplakia is provisional and should be confirmed through histopathological analysis (3). A particularly aggressive form of leukoplakia is Proliferative Verrucous Leukoplakia (PVL), which is associated with a higher risk of neoplastic progression. PVL often begins as one or multiple leukoplakias that gradually enlarge, eventually merging into a single large lesion (4). Clinically, it is characterized by the gradual, continuous expansion of alterations on the oral mucosal surface, typically keratinized, which can develop varied textures and, in some cases, nodular formations that may harden over time. While there is no single histopathological definition for PVL, clinical and histological correlation is crucial for diagnosis. Accurate photographic documentation should be collected before performing a biopsy to assist the pathologist in correlating clinical and histopathological features. PVL predominantly affects females, particularly the elderly (5). It is important to note that these lesions have a tendency toward malignant progression in about 50% of cases, with carcinomas potentially developing in non-contiguous areas, particularly in the gingiva, alveolar mucosa, buccal mucosa, palate, and dorsal tongue (6). Patients with PVL should be monitored over time, and biopsies should be performed in areas that are more verrucous or nodular to exclude potential dysplasia or cancerization. Managing these rare leukoplakias is challenging, as they are often large and multifocal, complicating surgical eradication. Various treatment modalities have been described, including photodynamic therapy, laser ablation, and medical therapies, though with limited success (7, 8). Surgical removal is considered the treatment of choice, despite a recurrence rate of 71.2% (9). The purpose of this study is to correlate results obtained from a non-invasive cytobrush sampling, developed using a high-sensitivity ELISA technique for the detection of six tumor biomarkers, with findings from traditional histopathological analyses (10).

2 Case description

A 65-year-old male patient presented with a cauliflower-like growth on the buccal mucosa that had developed approximately two months before the visit. Initially, the patient underestimated the lesion's significance and delayed seeking medical attention. Concerned about the rapid growth of the lesion, he consulted his general practitioner, who ordered hematological tests and referred him for a dental examination. The patient was generally healthy, although he had a significant smoking history of 20 cigarettes per day for 30 years and was a moderate drinker, consuming about one glass of wine per meal. General clinical and hematological tests revealed no abnormalities. During the specialist examination, an extensive lesion in the fornix mucosa was noted in the upper right quadrant, corresponding to teeth positions 14, 15, 16, and 17. A removable partial resin prosthesis with metal retention clips was present in the lesion area. The patient was advised to remove the prosthesis to prevent further irritation of the lesion. Palpation of the perioral and neck glands was unremarkable, and the patient reported no additional local symptoms. Despite the presence of the partial removable prosthesis, he experienced minimal discomfort, only noting the growth of the mass. Clinical examination revealed a large lesion measuring approximately 1.5 x 1.3 cm, exhibiting a papillomatous, verruciform, and irregular appearance, as shown in Figure 1A. The lesion had well-defined borders, multiple new growths, and was predominantly white with some red areas. It was located on the buccal mucosa adjacent to the right maxillary premolar and first molar. The patient had no other oral or extraoral lesions. Two biopsies were performed: a non-invasive cytobrush sampling for biomarker analysis followed by an

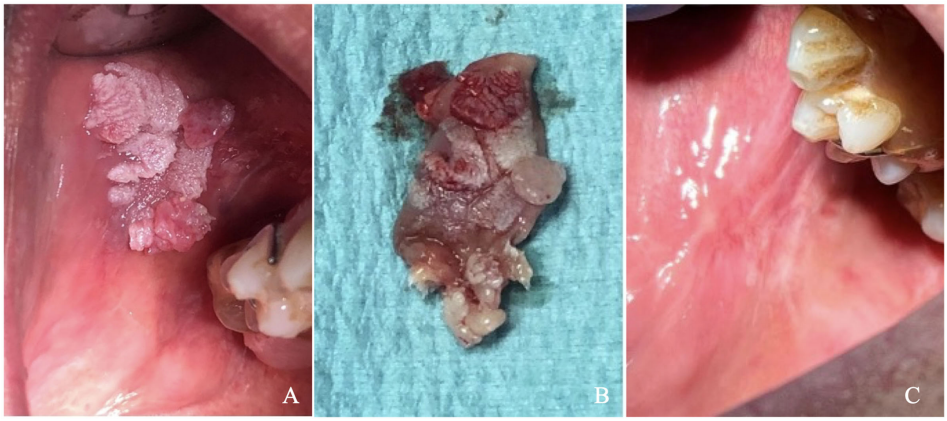

FIGURE 1
(A) Clinical picture showing the lesion **(B)** Excisional biopsy of the lesion immediately following surgery, **(C)** Healing of the biopsy site at 6-month follow-up.

excisional biopsy of the entire lesion. After rinsing the patient's mouth with saline, a cytosalivary sample was obtained using a cytobrush. Following the method described by Rebaudi et al., the cytobrush was gently rubbed with mild pressure and rotation over the lesion to collect cells and tissue fragments through exfoliation, taking care to avoid bleeding. The cytobrush tip was then placed into sealed Eppendorf vials, cataloged, and stored at 0-4°C before being sent to the laboratory in a refrigerated thermal box (10). Given that the lesion was less than 2 cm in size and lacked ulcerative necrotic features, it was decided to proceed with an excisional biopsy of the entire mass. After administering local anesthesia (Septodont, France), surgical excision was performed using a cold scalpel blade no. 15 (Hu Friedy, Chicago, USA). Silk sutures (Ethicon Inc., Somerville, New Jersey) were used for proper wound closure. The biopsy specimen, measuring 2 x 1.5 x 0.6 cm (Figure 1B), was placed in 10% formalin solution and sent to the pathologist for histopathological analysis.

2.1 Analysis

The analysis of biomarkers expressed by tissue fragments collected from an oral lesion through a cytobrush biopsy was conducted using two different disposable Stark Oral Screening® test kits (Stark S.a.r.l.):

- -Stark Oral Screening Quantitative Metabolic (REF: SOSFMTCKIT) for the detection of EGFR, p53, and Ki67.
- -Stark Oral Screening Quantitative NK Time (REF: SOSBHPDQNT) for the detection of B7-H6, PD-L1, and HLA-E.

After sampling the oral mucosa, the cytobrush is immersed in a lysis buffer, and the resulting protein suspension is analyzed. This test serves as a diagnostic aid and is processed automatically by a tabletop device (Femtohunter®) using the ELISA technique. The Stark Oral Screening® test is an *in vitro* diagnostic (IVD) tool that provides both qualitative and quantitative results based on a bioluminescent signal response, with a limit of detection (LOD) of 20 femtograms/microliter. Each chemiluminescent signal (S) detected by the Femtohunter® device is calibrated against the background noise (N), which is generated by non-specific luminescence on a control polyvinylidene difluoride (PVDF) membrane. The N value is subtracted from the S value detected on the PVDF membrane designated for the marker. A positive result (S - N > 0) indicates a specific signal for the target marker, confirming its presence in the sample. The positive value S is then divided by N to calculate a multiplication factor, allowing the operator to determine how many times the specific signal S is stronger than the background noise N (Signal-to-Noise ratio). The resulting S/N value is referred to as the FM (multiplication factor for the Femtohunter®) and is included in the Femtohunter® FM patient report. We observed the reproducibility of the results in previous applications of this test. This was done on a large cohort of patients with samples recovered at different time points (10).

The cytobrush analysis revealed the presence of 4 out of 6 biomarkers, with Femtohunter® FM values greater than or equal to the cutoff of 1.2. Specifically, two biomarkers, p53 and B7-H6, were negative, showing FM values below 1.2. Among the positive biomarkers, EGFR and HLA-E demonstrated clear positivity, with FM values of 1.6. Ki67 and PD-L1 were weakly positive, with values of 1.2 and 1.3, respectively. Therefore, the test is considered negative for malignant tumors, as the FM values for some biomarkers were below 1.2 (Figure 2).

Histopathological analysis of the mucosectomy specimen revealed submucosal tissue containing adipose and stretched muscular components. The surface exhibited a keratotic exophytic lesion composed of papillomatous epithelial projections, some of which were blunt and featured keratin-rich invaginations ("tapping"), without evident fibrovascular papillae. The squamous epithelium appeared thickened, intermittently para-keratotic, and acanthotic. Epithelial ridges displayed mild atypia and rare mitotic

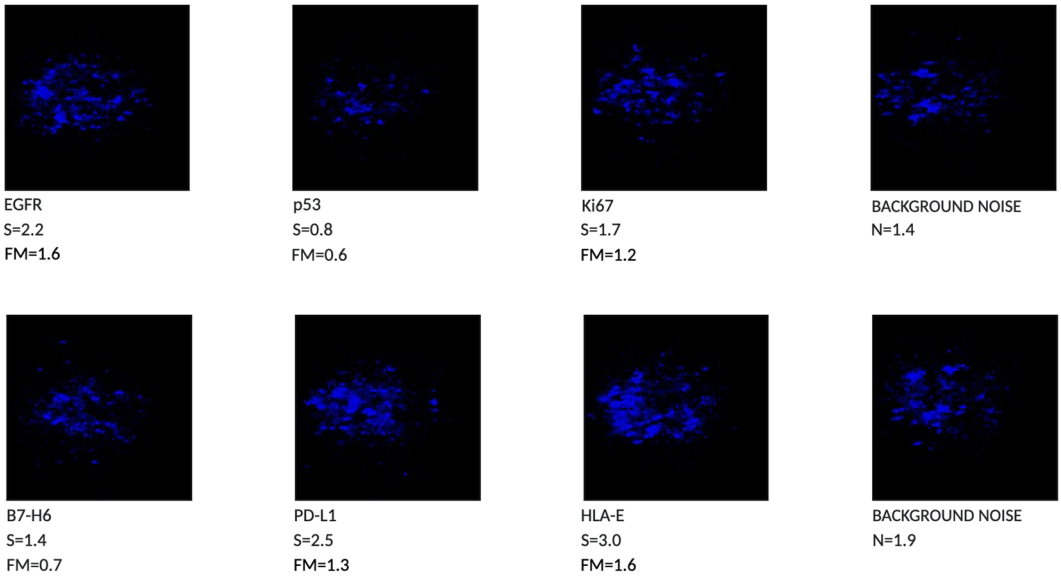

FIGURE 2
Chemiluminescent Phenotype of a lesion with aspect of Proliferative Verrucous Leukoplakia, 4 out of 6 biomarkers are positive (FM > than 1.2).

figures, with a tendency toward convergence and fusion. Although basal hyperplasia was not observed, focal cytopathic changes suggestive of viral infection ("koilocytosis") were present.

Based on the clinical and histological findings, a diagnosis of lesion with the aspect of Proliferative Verrucous Leukoplakia (PVL) was established (Figure 3). A clinical follow-up at six months showed complete healing of the sampling site with no signs of local recurrence (Figure 1C). Despite the absence of clinical indications of recurrence, ongoing monitoring of the patient is essential to ensure that future recurrences do not occur.

3 Discussion

Currently, there are no scientifically endorsed systems capable of identifying lesions in their early stages of tumor development (11) other than the traditional clinical Visual Oral Examination (VOE). Surgical biopsy remains the most effective method for collecting tissue for diagnosis (12) and is considered the gold standard. However, this method is invasive and cannot be performed repeatedly for follow-up checks, particularly in cases of large lesions that cannot be completely excised. Additionally, a biopsy

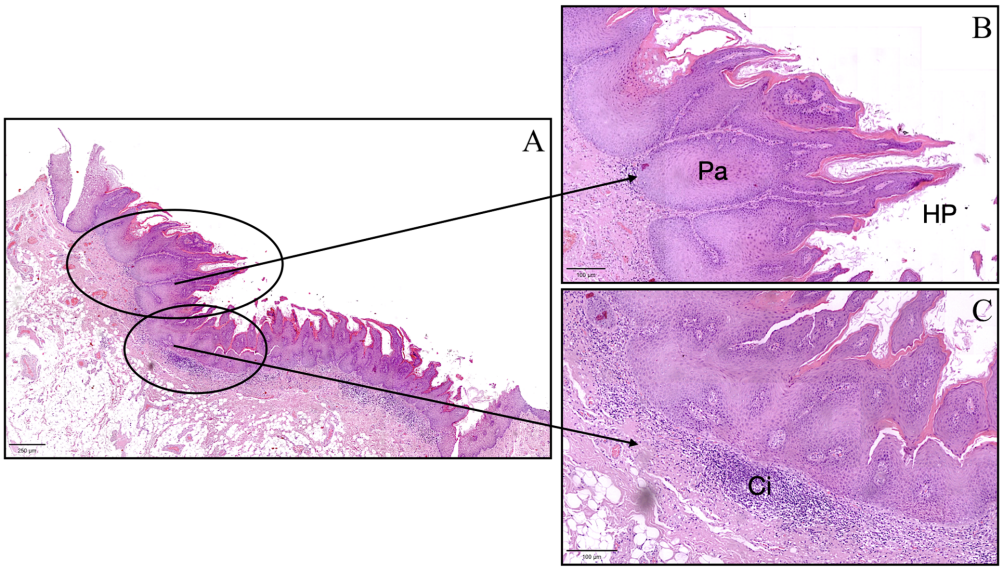

FIGURE 3
Histopathological image of the lesion with aspect of Proliferative Verrucous Leukoplakia showing pseudoinvasive aspects (Pa), hyperkeratosis and papillomatosis (HP), and chronic inflammatory infiltrate (Ci). **(A)** scale bar in **(A)** = 250 µm, scale bar in **(B, C)** = 100 µm.

only reflects a portion of the lesion, depending on the surgeon's discretion. The advantage of cytobrush sampling is its ability to detect tumor markers throughout the lesion, as sampling can encompass the entire lesion and its margins. Furthermore, since the cytobrush is a non-invasive method, it can be repeated periodically for monitoring. The case presented in this article examines the clinical and histopathological aspects of an irregular, cauliflower-like lesion with a papillomatous verruciform appearance. Proliferative Verrucous Leukoplakia (PVL) is a relatively uncommon condition with a higher prevalence in elderly women. A hallmark of this condition is its constant growth, which can occur even in non-contiguous areas, with a high estimated risk of cancerization at 50% (13). The histopathological diagnosis is challenging because there is no unique definition for this form of leukoplakia; clinical and histological correlation is essential for an accurate diagnosis (5, 6). The role of human papillomavirus (HPV) in this type of lesion is controversial. Some studies, such as those by Palefsky et al. (1995) (14), have detected HPV in many PVL cases, while others have found no evidence of HPV in PVL (15, 16). In the case described, histopathological analysis revealed the presence of HPV, characterized by focal, attenuated cytopathic features suggestive of viral infection, known as "koilocytosis." Since this lesion could not be classified as PVL due to incomplete clinical and histopathological correspondence, it was categorized as a lesion with aspects of PVL. The Femtohunter® is an automatic ELISA developer device that performs chemiluminescence analysis on samples taken by cytobrush and submitted to the Stark Oral Screening® IVD test. Results are provided as a graphical image (Figure 2), along with analytical data of the markers, and a patient report is printed. The Stark Oral Screening® test is a patient-side *in vitro* diagnostic (IVD) and quantitative test based on bioluminescent signal response (10). The biomarker analysis of the cytobrush revealed the presence of 4 out of 6 positive biomarkers. These biomarkers were considered positive because their FM values were greater than or equal to the cutoff of 1.2. Two biomarkers, p53 (FM 0.6) and B7-H6 (FM 0.7), were negative. Among the positive biomarkers, EGFR and HLA-E showed clear positivity, with FM values of 1.6. Ki67 and PD-L1 exhibited weak positivity, with values of 1.2 and 1.3, respectively. The test results indicate a negative outcome for a malignant tumor, as a positive diagnosis requires all six biomarkers to have FM values greater than 1.2 (10). Analyzing the Individual Markers in Detail:

-PD-L1 is a transmembrane protein expressed in various types of tumors, including Oral Squamous Cell Carcinoma (OSCC) (17, 18). When bound to the inhibitory checkpoint PD-1 (originally identified on T cells and more recently on NK cells), PD-L1 compromises the ability of cytotoxic immune cells to eliminate the tumor (19–21). Pharmacological treatments exist that inhibit the PD-1/PD-L1 axis, leading to improved survival in OSCC patients (22). The presence of PD-L1 in OPMDs has been documented in several studies (23, 24). Notably, a study by Dave et al. (25) demonstrated that PD-L1 could be present in a precancerous lesion even years before potential malignant transformation, aligning with our findings of weak but detectable expression of this marker (FM 1.3).

-Moderately elevated expression of Ki67 has been reported by Fettig et al. (2000) (26) in a study analyzing 10 cases of PVL. In this study, Ki67 expression was not correlated with the level of epithelial alterations. In another study involving 12 patients, Gouvea et al. (2010) (27) found Ki67 expression in PVL lesions. Our case also exhibited low positivity for this marker, consistent with the aforementioned studies (FM 1.2).

-EGFR is a transmembrane receptor that regulates signaling involved in cell proliferation and differentiation. Numerous studies have shown that leukoplakia often exhibits overexpression of EGFR, which correlates with a higher risk of malignant transformation (28). This suggests that EGFR could serve as a biological marker for identifying high-risk subgroups of OPMDs (29). In our case, we observed high levels of EGFR expression (FM 1.6).

-Altered expression of HLA-E, the ligand for the inhibitory checkpoint NKG2A (found on NK cells), has been noted in oral inflammatory/pre-tumoral conditions (17, 24, 30). The expression of molecules such as HLA-E and PD-L1 is independent of the oral lesion's histopathological grade; levels of these molecules are comparable in OPMDs and oral squamous cell carcinomas (24), with FM 1.6 in our case.

-B7-H6 (31), a member of the B7 family of immune modulators, was originally identified as a ligand for NKp30 (32), a receptor on NK cells. Expression of B7-H6 on tumor cell surfaces can enhance susceptibility to NK cell-mediated attacks. Several studies suggest that a soluble form of B7-H6 could be released by tumor cells, affecting NKp30 surface expression and preventing effective anti-tumor activity (33, 34). B7-H6 is expressed in various tumor types but absent in normal tissues, aligning with its sub-threshold expression in this lesion with precancerous characteristics (FM 0.7).

-Alteration or mutation of the p53 gene is among the most common events in human carcinogenesis (35). The mutated protein is not easily degradable, accumulating in cancer cells and leading to immunohistochemical overexpression, which is a marker of poor prognosis. Overexpression of p53 may decrease the sensitivity of tumor cells to chemotherapy, indicating an increased risk of progression to oral cancer among OPMDs (34, 36). In our case, both B7-H6 and p53 levels were low, with p53 at FM 0.6, below the cutoff value of 1.2.

In conclusion, our findings indicate that 4 out of 6 markers are positive, suggesting that OPMDs may already express tumor markers, in contrast to healthy mucosal tissue where these markers are generally absent (10). Our approach utilizes fresh tissue fragments through exfoliation and a highly sensitive ELISA, allowing us to identify biomarkers that might otherwise remain undetected. While immunohistochemistry can provide valuable information, it typically struggles to visualize biomarkers at such low expression levels. This underscores the potential of our

approach for early identification of at-risk patients, allowing for proactive management strategies.

Furthermore, we noted that in inflamed tissues, initial marker expression was typically elevated but decreased as inflammation resolved. This variability highlights the necessity of considering the dynamic nature of inflammation when interpreting biomarker results across different contexts. By recognizing these patterns, we can better differentiate between precancerous states and normal tissue, enhancing our understanding of oral pathologies. By utilizing this innovative screening method, we can enhance our ability to monitor patients over time, allowing for the timely detection of changes that may signify malignant transformation.

Monitoring the expression of these biomarkers over time could provide valuable insights into ongoing tumor transformation, facilitating timely intervention. Vigilant monitoring is essential for ensuring early diagnosis, which significantly improves patient prognosis.

Regular assessment using this non-invasive technique can empower clinicians to make informed decisions regarding patient care, ultimately leading to better treatment outcomes.

Furthermore, the use of a rapid, non-invasive system that is well-tolerated by patients for detecting tumor biomarkers could serve as an effective screening tool. This approach would aid in the phenotyping of oral lesions and provide critical information for improved management and treatment outcomes. Incorporating such screening methods into routine clinical practice could revolutionize our approach to managing OPMDs, fostering a proactive rather than reactive strategy in oral cancer prevention.

Data availability statement

The raw data supporting the conclusions of this article will be made available by the authors, without undue reservation.

Ethics statement

This study was carried out in accordance with the recommendations of the ethical standards of the institutional and/or national research committee. The protocol was approved by the ethics committee of the Liguria Region, Genova, Italy (n.127/2022-DB id12223). The subject gave written informed consent in accordance with the Declaration of Helsinki. Written informed consent for publication of their clinical details and/or clinical images was obtained from the patient/parent/guardian/relative of the patient. The studies were conducted in accordance with the local legislation and institutional requirements. The participants provided their written informed consent to participate in this study. Ethical approval was not required for the study involving animals in accordance with the local legislation and institutional requirements because We did not use animal samples or other animal material. Written informed consent was obtained from the individual(s) for the publication of any potentially identifiable images or data included in this article.

Author contributions

FR: Conceptualization, Data curation, Formal analysis, Investigation, Methodology, Validation, Writing – original draft. AR: Conceptualization, Data curation, Formal analysis, Investigation, Methodology, Writing – review & editing. ALR: Conceptualization, Data curation, Investigation, Methodology, Writing – review & editing. ADR: Writing – review & editing, Validation, Visualization. SP: Data curation, Supervision, Writing – review & editing, Visualization. MG: Data curation, Formal analysis, Writing – review & editing. MR: Methodology, Validation, Visualization, Writing – review & editing. MB: Data curation, Formal analysis, Methodology, Writing – review & editing. SC: Data curation, Supervision, Writing – review & editing, Validation. EM: Conceptualization, Data curation, Formal analysis, Funding acquisition, Investigation, Methodology, Project administration, Resources, Software, Supervision, Validation, Visualization, Writing – original draft, Writing – review & editing.

Funding

The author(s) declare that financial support was received for the research, authorship, and/or publication of this article. The research leading to these results has received funding from Fondazione AIRC under IG 2021 – ID. 26037 project – P.I. EM. Additional grants from University of Genova: PRIN-MIUR 2022, grant n. 2022YCKH7K-P.I. EM; PRIN-MIUR PNRR 2022, grant n. P2022PKFNB P.I. SP.

Acknowledgments

The authors want to thank: Riccardo Moffa, Angelo Simone Parodi, Dr. Giuseppe Di Meo, Dr. Francesca Carrano (Stark Sarl Monaco) and Dr. Marta Giacobbe.

Conflict of interest

The authors declare that the research was conducted in the absence of any commercial or financial relationships that could be construed as a potential conflict of interest.

The author(s) declared that they were an editorial board member of Frontiers, at the time of submission. This had no impact on the peer review process and the final decision.

Publisher's note

References

1. Mello FW, Miguel AFP, Dutra KL, Porporatti AL, Warnakulasuriya S, Guerra ENS, et al. Prevalence of oral potentially Malignant disorders: A systematic review and meta-analysis. *J Oral Pathol Med*. (2018) 47:633–40. doi: 10.1111/jop.2018.47.issue-7

2. Bin WS. Oral epithelial dysplasia and premalignancy. *Head Neck Pathol*. (2019) 13:423–39. doi: 10.1007/s12105-019-01020-6

3. Warnakulasuriya S, Kujan O, Aguirre-Urizar JM, Bagan JV, González-Moles MÁ, Kerr AR, et al. Oral potentially Malignant disorders: A consensus report from an international seminar on nomenclature and classification, convened by the WHO Collaborating Centre for Oral Cancer. *Oral Dis*. (2021) 27:1862–80. doi: 10.1111/odi.13704

4. Campisi G, Giovannelli L, Ammatuna P, Capra G, Colella G, Di Liberto C, et al. Proliferative verrucous vs conventional leukoplakia: no significantly increased risk of HPV infection. *Oral Oncol*. (2004) 40:835–40. https://linkinghub.elsevier.com/retrieve/pii/S1368837504000673.

5. Upadhyaya JD, Fitzpatrick SG, Cohen DM, Bilodeau EA, Bhattacharyya I, Lewis JS, et al. Inter-observer variability in the diagnosis of proliferative Verrucous leukoplakia: clinical implications for oral and maxillofacial surgeon understanding: A collaborative pilot study. *Head Neck Pathol*. (2019) 14:156–65. https://europepmc.org/articles/PMC7021885.

6. Cabay RJ, Morton TH, Epstein JB. Proliferative verrucous leukoplakia and its progression to oral carcinoma: a review of the literature. *J Oral Pathol Med*. (2007) 36:255–61. doi: 10.1111/j.1600-0714.2007.00506.x

7. Lodi G, Franchini R, Warnakulasuriya S, Varoni EM, Sardella A, Kerr AR, et al. Interventions for treating oral leukoplakia to prevent oral cancer. *Cochrane Database Syst Rev*. (2016) 7:92–3. doi: 10.1002/14651858.CD001829.pub4

8. Gondivkar SM, Gadbail AR, Choudhary MG, Vedpathak PR, Likhitkar MS. Photodynamic treatment outcomes of potentially-malignant lesions and Malignancies of the head and neck region: A systematic review. *J Investig Clin Dent*. (2018) 9(1). doi: 10.1111/jicd.2018.9.issue-1

9. Abadie WM, Partington EJ, Fowler CB, Schmalbach CE. Optimal management of proliferative verrucous leukoplakia: A systematic review of the literature. *Otolaryngol Head Neck Surg*. (2015) 153:504–11. doi: 10.1177/0194599815586779

10. Rebaudi F, De Rosa A, Greppi M, Pistilli R, Pucci R, Govoni FA, et al. A new method for oral cancer biomarkers detection with a non-invasive cyto-salivary sampling and rapid-highly sensitive ELISA immunoassay: a pilot study in humans. *Front Immunol*. (2023) 14:1216107. doi: 10.3389/fimmu.2023.1216107

11. Cicciù M, Cervino G, Fiorillo L, D'Amico C, Oteri G, Troiano G, et al. Early diagnosis on oral and potentially oral Malignant lesions: A systematic review on the VELscope® Fluorescence method. *Dent J (Basel)*. (2019) 7(3):93. doi: 10.3390/dj7030093

12. Shanti RM, Tanaka T, Stanton DC. Oral biopsy techniques. *Dermatol Clin*. (2020) 38:421–7. doi: 10.1016/j.det.2020.05.003

13. Villa A, Menon RS, Kerr AR, De Abreu Alves F, Guollo A, Ojeda D, et al. Proliferative leukoplakia: Proposed new clinical diagnostic criteria. *Oral Dis*. (2018) 24:749–60. doi: 10.1111/odi.12830

14. Palefsky JM, Silverman S, Abdel-Salaam M, Daniels TE, Greenspan JS. Association between proliferative verrucous leukoplakia and infection with human papillomavirus type 16. *J Oral Pathol Med*. (1995) 24:193–7. doi: 10.1111/j.1600-0714.1995.tb01165.x

15. García-López R, Moya A, Bagan JV, Pérez-Brocal V. Retrospective case-control study of viral pathogen screening in proliferative verrucous leukoplakia lesions. *Clin Otolaryngol*. (2014) 39:272–80. doi: 10.1111/coa.12291

16. Bagan JV, Jimenez Y, Murillo J, Gavaldá C, Poveda R, Scully C, et al. Lack of association between proliferative verrucous leukoplakia and human papillomavirus infection. *J Oral Maxillofac Surg*. (2007) 65:46–9. doi: 10.1016/j.joms.2005.12.066

17. André P, Denis C, Soulas C, Bourbon-Caillet C, Lopez J, Arnoux T, et al. Anti-NKG2A mAb is a checkpoint inhibitor that promotes anti-tumor immunity by unleashing both T and NK cells. *Cell*. (2018) 175:1731. doi: 10.1016/j.cell.2018.10.014

18. Pesce S, Greppi M, Tabellini G, Rampinelli F, Parolini S, Olive D, et al. Identification of a subset of human natural killer cells expressing high levels of programmed death 1: A phenotypic and functional characterization. *J Allergy Clin Immunol*. (2017) 139:335–346.e3. doi: 10.1016/j.jaci.2016.04.025

19. Lenouvel D, González-Moles MÁ, Talbaoui A, Ramos-García P, González-Ruiz L, Ruiz-Ávila I, et al. An update of knowledge on PD-L1 in head and neck cancers: Physiologic, prognostic and therapeutic perspectives. *Oral Dis*. (2020) 26:511–26. doi: 10.1111/odi.13088

20. Topalian SL, Taube JM, Anders RA, Pardoll DM. Mechanism-driven biomarkers to guide immune checkpoint blockade in cancer therapy. *Nat Rev Cancer*. (2016) 16:275–87. doi: 10.1038/nrc.2016.36

21. Chamoto K, Yaguchi T, Tajima M, Honjo T. Insights from a 30-year journey: function, regulation and therapeutic modulation of PD1. *Nat Rev Immunol*. (2023) 23:682–95. doi: 10.1038/s41577-023-00867-9

22. Ferris RL, Blumenschein G, Fayette J, Guigay J, Colevas AD, Licitra L, et al. Nivolumab vs investigator's choice in recurrent or metastatic squamous cell carcinoma of the head and neck: 2-year long-term survival update of CheckMate 141 with analyses by tumor PD-L1 expression. *Oral Oncol*. (2018) 81:45. doi: 10.1016/j.oraloncology.2018.04.008

23. De Souza Malaspina TS, Gasparoto TH, Costa MRSN, De Melo EF, Ikoma MRV, Damante JH, et al. Enhanced programmed death 1 (PD-1) and PD-1 ligand (PD-L1) expression in patients with actinic cheilitis and oral squamous cell carcinoma. *Cancer Immunol Immunother*. (2011) 60:965–74. doi: 10.1007/s00262-011-1007-5

24. Gonçalves AS, Mosconi C, Jaeger F, Wastowski IJ, Aguiar MCF, Silva TA, et al. Overexpression of immunomodulatory mediators in oral precancerous lesions. *Hum Immunol*. (2017) 78:752–7. doi: 10.1016/j.humimm.2017.09.003

25. Dave K, Ali A, Magalhaes M. Increased expression of PD-1 and PD-L1 in oral lesions progressing to oral squamous cell carcinoma: a pilot study. *Sci Rep*. (2020) 10 (1):9705. doi: 10.1038/s41598-020-66257-6

26. Fettig A, Anthony Pogrel M, Silverman S, Bramanti TE, DaCosta M, Regezi JA, et al. Proliferative verrucous leukoplakia of the gingiva. *Oral Surg Oral Med Oral Pathol Oral Radiol Endod*. (2000) 90(6):723–30. doi: 10.1067/moe.2000.108950

27. Gouvêa AF, Vargas PA, Coletta RD, Jorge J, Lopes MA. Clinicopathological features and immunohistochemical expression of p53, Ki-67, Mcm-2 and Mcm-5 in proliferative verrucous leukoplakia. *J Oral Pathol Med*. (2010) 39:447–52. doi: 10.1111/j.1600-0714.2010.00889.x

28. Ries J, Vairaktaris E, Agaimy A, Bechtold M, Gorecki P, Neukam FW, et al. The relevance of EGFR overexpression for the prediction of the Malignant transformation of oral leukoplakia. *Oncol Rep*. (2013) 30:1149–56. doi: 10.3892/or.2013.2545

29. Meka NJ, Ugrappa S, Velpula N, Kumar S, Maloth KN, Kodangal S, et al. Quantitative immunoexpression of EGFR in oral potentially Malignant disorders: oral leukoplakia and oral submucous fibrosis. *J Dent Res Dent Clin Dent Prospects*. (2015) 9:166. doi: 10.15171/joddd.2015.031

30. Salomé B, Sfakianos JP, Ranti D, Daza J, Bieber C, Charap A, et al. NKG2A and HLA-E define an alternative immune checkpoint axis in bladder cancer. *Cancer Cell*. (2022) 40:1027–43.e9. https://europepmc.org/article/med/36099881.

31. Brandt CS, Baratin M, Yi EC, Kennedy J, Gao Z, Fox B, et al. The B7 family member B7-H6 is a tumor cell ligand for the activating natural killer cell receptor NKp30 in humans. *J Exp Med*. (2009) 206:1495–503. http://intl.jem.org/cgi/content/full/206/7/1495.

32. Pende D, Parolini S, Pessino A, Sivori S, Augugliaro R, Morelli L, et al. Identification and molecular characterization of NKp30, a novel triggering receptor involved in natural cytotoxicity mediated by human natural killer cells. *J Exp Med*. (1999) 190:1505–16. doi: 10.1084/jem.190.10.1505

33. Pesce S, Tabellini G, Cantoni C, Patrizi O, Coltrini D, Rampinelli F, et al. B7-H6-mediated downregulation of NKp30 in NK cells contributes to ovarian carcinoma immune escape. *Oncoimmunology*. (2015) 4(4):e1001224. doi: 10.1080/2162402X.2014.1001224

34. Wang J, Jin X, Liu J, Zhao K, Xu H, Wen J, et al. The prognostic value of B7-H6 protein expression in human oral squamous cell carcinoma. *J Oral Pathol Med*. (2017) 46:766–72. doi: 10.1111/jop.2017.46.issue-9

35. Carson DA, Lois A. Cancer progression and p53. *Lancet*. (1995) 346:1009–11. doi: 10.1016/S0140-6736(95)91693-8

36. Khan H, Gupta S, Husain N, Misra S, MPS N, Jamal N, et al. Correlation between expressions of Cyclin-D1, EGFR and p53 with chemoradiation response in patients of locally advanced oral squamous cell carcinoma. *BBA Clin*. (2014) 3:11–7. doi: 10.1016/j.bbacli.2014.11.004

frontiers | Frontiers in Immunology

TYPE Original Research
PUBLISHED 20 December 2024
DOI 10.3389/fimmu.2024.1506236

OPEN ACCESS

EDITED BY
Lorenzo Mortara,
University of Insubria, Italy

REVIEWED BY
Valeria Lucarini,
Sapienza University of Rome, Italy
Pengfei Xu,
University of California, Davis, United States

*CORRESPONDENCE
Elin Bernson
elin.bernson@gu.se

RECEIVED 04 October 2024
ACCEPTED 09 December 2024
PUBLISHED 20 December 2024

CITATION
Karlsson V, Stål E, Stoopendahl E, Ivarsson A, Leffler H, Lycke M, Sundqvist M, Sundfeldt K, Christenson K and Bernson E (2024) Elevated Galectin-3 levels in the tumor microenvironment of ovarian cancer – implication of ROS mediated suppression of NK cell antitumor response via tumor-associated neutrophils.
Front. Immunol. 15:1506236.
doi: 10.3389/fimmu.2024.1506236

Elevated Galectin-3 levels in the tumor microenvironment of ovarian cancer – implication of ROS mediated suppression of NK cell antitumor response via tumor-associated neutrophils

Veronika Karlsson[1,2], Ebba Stål[1], Emma Stoopendahl[1], Anton Ivarsson[1], Hakon Leffler[3], Maria Lycke[4], Martina Sundqvist[5], Karin Sundfeldt[1,4], Karin Christenson[2] and Elin Bernson[1,4]*

[1]Sahlgrenska Center for Cancer Research, University of Gothenburg, Gothenburg, Sweden, [2]Department of Oral Microbiology and Immunology, Institute of Odontology, Sahlgrenska Academy, University of Gothenburg, Gothenburg, Sweden, [3]Department of Laboratory Medicine, Lund University, Lund, Sweden, [4]Department of Obstetrics and Gynecology, Institute of Clinical Sciences, Sahlgrenska Academy, University of Gothenburg, Gothenburg, Sweden, [5]Department of Rheumatology and Inflammation Research, Institute of Medicine, Sahlgrenska Academy, University of Gothenburg, Gothenburg, Sweden

Introduction: Ovarian cancer is a lethal disease with low survival rates for women diagnosed in advanced stages. Current cancer immunotherapies are not efficient in ovarian cancer, and there is therefore a significant need for novel treatment options. The β-galactoside-binding lectin, Galectin-3, is involved in different immune processes and has been associated with poor outcome in various cancer diagnoses. Here, we investigated how Galectin-3 affects the interaction between natural killer (NK) cells and neutrophils in the tumor microenvironment of ovarian cancer.

Method: Ascites from the metastatic tumor microenvironment and cyst fluid from the primary tumor site were collected from patients with high-grade serous carcinoma (HGSC) together with peripheral blood samples. Galectin-3 concentration was measured in ascites, cyst fluid and serum or plasma. Neutrophils isolated from HGSC ascites and autologous blood were analyzed to evaluate priming status and production of reactive oxygen species. *In vitro* co-culture assays with NK cells, neutrophils and K562 target cells (cancer cell line) were conducted to evaluate NK cell viability, degranulation and cytotoxicity.

Results: High levels of Galectin-3 were observed in cyst fluid and ascites from patients with HGSC. Neutrophils present in HGSC ascites showed signs of priming; however, the priming status varied greatly among the patient samples. Galectin-3 induced production of reactive oxygen species in ascites neutrophils, but only from a fraction of the patient samples, which is in line with the heterogenous priming status of the ascites neutrophils. In co-cultures with NK cells and K562 target cells, we observed that Galectin-3-induced production of

reactive oxygen species in neutrophils resulted in decreased NK cell viability and lowered anti-tumor responses.

Conclusion: Taken together, our results demonstrate high levels of Galectin-3 in the tumormicroenvironment of HGSC. High levels of Galectin-3 may induce production of reactiveoxygen species in ascites neutrophils in some patients. In turn, reactive oxygen species produced by neutrophils may modulate the NK cell anti-tumor immunity. Together, this study suggests further investigation to evaluate if a Galectin-3-targeting therapy may be used in ovarian cancer.

KEYWORDS

galectin-3, ovarian cancer, NK cells, neutrophils, tumor immunology, ROS release, tumor microenvironment

1 Introduction

Ovarian carcinoma (OC) is the most lethal gynecologic malignancy among women, which can be attributed to late diagnosis of these patients and high recurrence frequency (1). The most common occurring epithelial ovarian carcinoma is high-grade serous carcinoma (HGSC), where many women are diagnosed at an advanced stage (Federation of Gynecology and Obstetrics [FIGO] stage III or IV) (2, 3). Current treatment strategy includes debulking surgery followed by platinum-based chemotherapy. However, as recurrence occurs in 70% of the patients, novel treatment options are of significant clinical need. Immunotherapy has emerged as a successful treatment option in several cancers but has not yet been proven as an efficient treatment for OC (4, 5). To improve or develop novel treatment options for OC patients, a better understanding of the immune microenvironment in OC is urgently needed. OC metastasis is commonly followed by the accumulation of fluid, or ascites, in the peritoneal cavity. The ascites contains both malignant cells, lymphocytes and granulocytes, and acellular components such as interleukin (IL)-6, IL-8, IL-10, transforming growth factor beta (TGF-ß) and vascular endothelial growth factor (VEGF) (6–8). The correlation between T cell infiltration to the OC tumor microenvironment and improved survival suggests that immunotherapy is a conceivable treatment option in the disease (9). However, despite a correlation between mutational burden and immune cell tumor infiltration, many OC tumors remain immunologically "cold" and do not evoke a specific T cell response (10). Thus, OC immunotherapy directed towards targets beyond cytotoxic T cells may present as a promising alternative.

Natural killer (NK) cells are innate lymphocytes that, in contrast to cytotoxic T cells, have the ability to detect and kill malignant cells without prior sensitization. Upon activation, NK cells exert their cytotoxic function through degranulation of lytic granules containing pore-forming proteins and proteases (11–13). We have recently demonstrated that a subset of tissue-resident NK cells in OC ascites display anti-tumor properties, suggesting that NK cells are a feasible immunotherapeutic target (7). However, the NK cell function in OC is impaired due to the immunosuppressive tumor microenvironment (4, 8, 14–17).

An immune-suppressor that has gained interest in cancer research is Galectin-3, a mammalian lectin with affinity for β-galactoside-containing glycoconjugates. Galectin-3 is involved in a number of different biological processes including inflammation, apoptosis, cell growth and angiogenesis (18–24). Blood levels of Galectin-3 are often increased during inflammatory conditions (18), however, high Galectin-3 blood levels have also been detected in several cancers including colon, head and neck, liver, gastric, endometrial, thyroid, skin, bladder and breast carcinomas (25, 26). Galectin-3 may promote tumorigenesis and metastasis through several mechanisms including induction of T cell apoptosis, inhibition of tumor cell apoptosis, promotion of angiogenesis, adhesion between tumor and endothelial cells, and promotion of tumor spread (25–27). Indeed, increased Galectin-3 blood levels have been associated with bad prognosis and/or relapse in breast, lung, and oral cancer (28–31). In OC, Galectin-3 can be detected on the cell surface of primary tumor cells and OC cell lines. Moreover, Mirandola et al. have demonstrated that inhibition of Galectin-3 reduces growth, invasion, migration, and drug resistance of OC cells *in vitro*, and interferes with the angiogenic potential of OC cells (27). Currently, Galectin-3 inhibition is being evaluated as potential treatment in both malignant and non-malignant conditions (25, 26).

Neutrophils are one type of immune cell present in OC ascites (32). Neutrophils are important effector cells in the first line of defense and eliminate pathogens through phagocytosis, degranulation of vesicles containing toxic and proteolytic factors, release of reactive oxygen species (ROS) and formation of neutrophil extracellular traps (NETs) (20, 33). While neutrophils circulating in peripheral blood are in a resting state, extravasation to

tissue usually results in a switch to a pre-activated, primed, state. Priming of neutrophils commonly includes degranulation of intracellular granules and secretory vesicles, which can be characterized as cleavage of surface-bound L-selectin (CD62L) and upregulation of granule localized receptors on the cell surface, including CD11b and CD66 (34–36). Secretory vesicles are most easily mobilized to the plasma membrane followed by gelatinase and specific granules; the granules requiring the most stimuli for mobilization are the azurophilic granules. Depending on the extent of stimuli, granule membrane-localized receptors are thus exposed on the neutrophil cell surface and matrix localized soluble factors are released to the extracellular environment (37, 38). Interestingly, degranulation of the gelatinase and specific granules exposes Galectin-3 binding sites on the surface of neutrophils that allow stimulation of the NADPH oxidase, as Galectin-3 stimulates ROS release in neutrophils extravasated into tissue or *in vitro* treated with TNF-α, but not in resting neutrophils from the blood circulation (39, 40).

ROS released by myeloid cells has been correlated to decreased NK cell cytotoxicity against myeloid leukemia cells (41). We hypothesized that Galectin-3 mediated ROS released from extravasated neutrophils in the metastatic environment of OC ascites would affect NK cell anti-tumor responses. Thus, in this study, we investigated the impact of Galectin-3 on the interaction between neutrophils, NK cells and tumor cells. Our data demonstrated the presence of soluble Galectin-3 in the primary and ascitic HGSC tumor microenvironment, together with the presence of degranulated neutrophils. We observed that the extent of degranulation varied among patient samples, and Galectin-3-induced ROS production by ascites neutrophils was apparent in a fraction of patients with HGSC. Using functional NK cell anti-tumor assays, we investigated how Galectin-3-induced ROS release from neutrophils impacted on NK cell functionality. Our results demonstrated a Galectin-3 mediated decrease of NK cell viability *via* neutrophil ROS release, with anti-tumor responses impeded by ROS.

2 Materials and methods

2.1 Patients and sample collection

This study includes biosamples from two cohorts of patients with confirmed or suspected HGSC. Ascites, cyst fluid and blood samples were collected from Cohort 1 (sampled during 2016), and ascites and blood samples were collected from Cohort 2 (sampled during 2020-2024). Sampling was carried out during de-bulking surgery or paracentesis prior to surgery at Sahlgrenska University Hospital, Gothenburg, Sweden, after informed written consent from patients. Only chemo naïve patients were included in the study. All histopathology evaluation was performed by a board-certified pathologist specializing in gynecological malignancies. Patient and tumor data were recorded regarding age, body mass index (BMI), smoking and FIGO stage (summarized in Tables 1, 2). Ten patients with HGSC were enrolled in Cohort 1 and 18 patients with HGSC were enrolled in Cohort 2. The studies were approved by the regional ethics board in Gothenburg (Dnr. 201-15) and the Swedish Ethical Review Authority (Dnr. 510-13) and performed according to the Helsinki declaration. Buffy coats and blood from healthy donors were obtained from the blood bank at the Sahlgrenska University Hospital, Gothenburg, Sweden. As the buffy coats and blood were provided anonymously and thereby could not be traced back to a specific donor, no ethical approval was needed in accordance with the Swedish legislation section code 4§ 3p SFS 2003:460 (Law on Ethical Testing of Research Relating to People).

2.2 Biosample preparation

Cohort 1: Cyst fluid, taken from surgically excised ovarian cysts, and ascites, aspirated at the time of midline incision, were collected in silicon dioxide tubes and frozen at -80°C within 4 hours after collection. Venous blood was collected in silicon dioxide tubes and

TABLE 1 Patient characteristics in Cohort 1.

Patient ID	Stage[a]	Age[b]	BMI[c]	Smoking[d]	Ascites Galectin-3 conc. (ng/mL)	Cyst fluid Galectin-3 conc. (ng/mL)	Serum Galectin-3 conc. (ng/mL)
1	IIIC	52	23	No	31.9	112.3	6.2
2	IIIC	40	21	No	110.4	111.9	7.2
6	IIIC	57	19.5	No	15.5	–	10.9
7	IIIC	64	20.6	No	15.8	115.3	9.8
10	IIIC	69	26.5	No	35.4	92.1	28.0
13	IVB	68	22.1	No	19.8	60.0	4.9
14	IVB	58	25	No	70.4	–	7.4
15	IIIC	48	23.9	No	26.4	82.6	8.4
18	IIIC	71	22.1	No	12.3	–	10.7
20	IIB	60	18.5	No	87.4	20.4	27.4

[a]FIGO stage [b]Age in years [c]Body mass index [d]Yes or no.

10.3389/fimmu.2024.1506236

TABLE 2 Patient characteristics in Cohort 2.

Patient ID[a]	Stage[b]	Age[c]	BMI[d]	Smoking[e]	Ascites volume (L)	Ascites Galectin-3 conc. (ng/mL)	Plasma Galectin-3 conc. (ng/mL)
4	IIIC	41	25.8	No	1.3	10.2	14.2
10	IIIC	73	27.1	No	1.3	32.9	10.7
12	IV	66	31.1	No	≥ 2	35.8	16.5
13	IIIA1	64	19.8	No	≥ 2	14.9	13.6
16	IIB	51	28.9	No	≥ 2	64.7	18.3
24	IVB	58	32.3	No	≥ 2	20.5	38.5
26	IIIC	46	33.9	No	≥ 2	16.8	12.4
28	IIIC	77	31.2	No	≥ 2	25.5	24.4
29	IIIC	65	20.4	No	0.2	64.2	17.7
30	IIIC	70	28.5	No	0.65	24.8	9.3
33	IIIC	55	39.4	Yes	≥ 2	55.1	18.8
35	IVB	60	41.3	No	0.57	44.2	28.6
36	IIIC	58	32.3	No	0.85	32.2	9.1
40	IIIC	60	18.8	No	1.5	8.3	16.4
45	IVB	50	23.4	No	0.4	145.8	14.4
48	IVB	52	19.9	No	1.9	34.5	20.5
49	IVA	65	24.7	No	≥ 2	40.6	19.4
54	IIIC	61	20.5	No	≥ 2	15.9	17.4

[a]Patients within this cohort were included in one earlier publication (7). [b]FIGO stage. [c]Age in years. [d]Body mass index. [e]Yes or no.

centrifuged, after which serum was transferred to new tubes and stored at -80°C.

Cohort 2: Venous blood was collected in EDTA tubes. For plasma collection, blood was centrifuged at 1000 x *g* (10 min, 4°C), after which plasma was transferred to new tubes and frozen at -80°C. Ascites was aspirated either at the time of midline incision, or through paracentesis, and collected in plastic collection bags. Cell-free ascites was obtained by centrifugation at 1000 x *g* (10 min, 4°C). Ascites was filtrated using 180 and 40 µm nylon net filters (Merck Millipore) to achieve a single cell suspension.

Erythrocytes were removed from ascites, venous blood and buffy coats with dextran sedimentation. This was followed by density gradient centrifugation with lymphoprep (STEMCELL Technologies) to obtain mononuclear cells and neutrophils. NK cells were isolated from the mononuclear cells using a negative NK isolation kit (Miltenyi Biotec) according to manufacturer's protocol. The neutrophils, obtained in the lymphoprep pellet, were treated with distilled H_2O to remove remaining erythrocytes by hypotonic lysis and then stored in Krebs-Ringer Glucose phosphate buffer (KRG; pH 7.3, supplemented with Ca^{2+} [1 mM]) on ice prior to subsequent analysis on the same day as isolated. For cell morphology and phenotype after isolation, see Supplementary Figures S1A, C. For some experiments the neutrophils were pre-treated with recombinant human TNF-α (10 ng/ml; Sigma-Aldrich) for 20 min at 37°C; neutrophils used as controls to these cells were kept on ice. When specified, blood neutrophils were incubated in cell-free cyst fluid (Cohort 1) or autologous cell-free ascites (Cohort 2) for 20 min at 37°C; neutrophils used as controls were incubated in KRG for 20 min at 37°C. Serum from healthy donors was obtained from venous blood by centrifugation and stored at -80°C.

2.3 Measurement of soluble Galectin-3

Paired biosamples of ascites, cyst fluid and serum (Cohort 1), or ascites and plasma (Cohort 2), from patients with confirmed HGSC and serum from age-matched healthy donors were analyzed for content of Galectin-3 using an enzyme-linked immunosorbent assay (ELISA) from BG Medicine according to the protocol provided by the manufacturer. The total protein concentration in the biosamples was determined by Pierce BCA Protein Assay (Thermo Scientific) according to manufacturer's instructions. Absorbance for Galectin-3 concentration was measured at 450 nm in a CLARIOstar plate reader (BMG Labtech), while absorbance for total protein concentration was measured at 562 nm in a FLUOstar Omega plate reader (BMG Labtech). Results were calculated in Microsoft Excel version 16.57 or later.

2.4 Detection of cell-bound Galectin-3

Cell-bound galectin-3 was analyzed on non-isolated leukocytes. Filtrated single cell ascites and blood from cohort 2 were treated with FACS lysing solution (BD FACS) according to manufacturer's instructions on the day of biosample collection. Thereafter, the fixated leukocytes were washed with PBS and immunostained for one hour at 4°C in darkness. Antibodies were diluted in PBS supplemented with 10% human serum. Neutrophils were distinguished from other leukocytes with BV786 anti-CD45 monoclonal antibody (clone HI30; BD Horizon) and light scattering, see Supplementary Figure S1B for gating. Galectin-3 binding was detected using PE anti-Galectin-3 monoclonal antibody (clone M3/38) with a matching isotype control (PE rat IgG2A, κ antibody), both purchased from BioLegend. All flow cytometry analysis in this study was performed using LSRFortessa (BD) and data were analyzed using FlowJo version 10.8.2 or later (BD Biosciences). Results are shown as median fluorescence intensity (MFI) if not stated otherwise.

2.5 Phenotypic analysis of neutrophil priming status

The priming status of neutrophils were phenotypically examined by analyzing the expression of CD11b, CD66, CD66b and CD62L on the cell surface by flow cytometry. Neutrophils were either kept on ice or pre-treated with TNF-α or incubated with cell-free ascites/cyst fluid (as described above), and thereafter washed in KRG and immunostained for 30 min at 4°C in darkness. The following fluorochrome-conjugated monoclonal antibodies were used for detection of surface markers: APC anti-CD11b (clone ICRF44), PE anti-CD66a,c,d,e (clone B1.1/CD66), FITC anti-CD66b (clone G10F5) and APC anti-CD62L (clone DREG-56), all antibodies were purchased from BD Pharmingen.

2.6 Production of recombinant Galectin-3

Recombinant human Galectin-3 was produced in *E. coli* and purified as previously described (39, 42). For some experiments Detoxi-Gel Endotoxin Removing Columns (Thermo Scientific) were used for endotoxin removal of Galectin-3 according to protocol provided by the manufacturer.

2.7 Measurement of neutrophil ROS production

Production of ROS by the neutrophil NADPH oxidase was measured with an isoluminol-amplified chemiluminescence system in the presence of horse radish peroxidase as described by Dahlgren et al. (43). Resting and TNF-α treated neutrophils were diluted in KRG and equilibrated in polypropylene tubes (1 ml system with 1 x 10^5 cells) in a six-channel Biolumat LB 9505 (Berthold Technologies) or in white 96-well plates (0.2 ml system with 5 x 10^5 cells) CLARIOstar plate reader (BMG Labtech) for 5 min at 37°C, with or without lactose (10 mM, Sigma Aldrich). After equilibration, cells were stimulated with recombinant human Galectin-3 (20 μg/ml), formyl-methionyl-leucyl-phenylalanine (fMLF; 100 nM, Sigma Aldrich) or phorbol 12-myristate 13-acetate (PMA; 50 nM, Sigma Aldrich) and the light emission, which reflect the superoxide anion production (the pre-cursor of all ROS), was recorded over time. The ROS levels measured using the Biolumat LB 9505 are expressed as mega counts per minute (Mcpm) and the ROS levels measured using the CLARIOstar plate reader are expressed as relative light units (RLU). For analysis of peak ROS values, the background level, i.e., the value recorded prior to stimulation was subtracted from the observed peak value. The results were analyzed using GraphPad Prism software version 10.2.0 or later (GraphPad Software).

2.8 NK cell viability, degranulation and cytotoxicity

NK cells and neutrophils were isolated from buffy coats from healthy donors using negative beads as described above. The human myelogenous leukemia cell line, K562, was provided by the Department of Infectious Diseases at the University of Gothenburg, Sweden. Complete medium used in assays contained RPMI 1640 (Gibco) and 10% heat-inactivated fetal calf serum. Neutrophils were pre-treated with TNF-α as described above. NK cells and neutrophils were co-incubated in a low attachment 96 well plate (Corning) at 1:1 or 2:1 ratio (NK:neutrophils) in medium only or with endotoxin free Galectin-3 (5 or 25 μg/ml), with or without the addition of SOD (50 U/ml, Worthington Biochemical) and endotoxin free catalase (200 U/ml, Worthington Biochemical), or diphenyleneiodonium (DPI; 3 μM, Sigma Aldrich), for 4 hours at 37°C with 5% CO_2. After 4 hours K562 cells, pre-labeled with CellTrace Violet (Invitrogen) according to manufacturer's protocol, were added at a 5:1 ratio (NK:K562) followed by BUV395 anti-CD107a monoclonal antibody (clone H4A3, BD Horizon) to measure NK cell degranulation, and then incubated for 20 hours at 37°C with 5% CO_2. Cells were labeled with BV711 anti-CD56 monoclonal antibody (clone NCAM 16.2, BD Horizon), for NK cell identification, and LIVE/DEAD Fixable Near-IR (1:1000, Invitrogen) to measure cell viability. Gating strategies are provided in Supplementary Figure S1D. The data was analyzed using flow cytometry as described above.

2.9 Statistical analysis

Statistical analysis was performed in GraphPad Prism version 10.2.0 or later. For comparison of two groups a Student's t-test was used. For multiple group comparisons with paired data, repeated measures one-way ANOVA or mixed-effects model using restricted maximum likelihood (REML) estimation was used. The mixed-effects model using REML estimation was used instead of one-way ANOVA when there were missing values in the data sets. For multiple group comparisons with no pairing, ordinary one-way ANOVA was used. More detailed information about the statistical

tests used in each experiment is stated in figure legends. Statistically significant differences were regarded as p-values < 0.05.

3 Results

3.1 Galectin-3 is present in the HGSC tumor microenvironment

Galectin-3 levels in ascites from 10 patients diagnosed with HGSC (Cohort 1, Table 1) were investigated using ELISA. The mean Galectin-3 concentration was significantly higher in ascites compared to paired serum samples from HGSC patients (Figure 1A; median 9.1 and 29.1 ng/ml in serum and ascites, respectively). Also, ovarian cyst fluid collected from the primary tumor site contained increased levels of Galectin-3 as compared to paired serum (median 92.1 ng/ml in cyst fluid). To verify that the higher level of Galectin-3 measured in ascites was not due to an increase in total protein concentration, the Galectin-3 level was normalized to total protein concentration. The relative Galectin-3 concentration (fraction of total protein concentration) was significantly higher in ascites compared to serum (Figure 1B; total protein concentration in ascites, serum and cyst fluid are displayed in Figure 1C). We repeated the analysis with samples from 18 patients with HGSC (Cohort 2, Table 2) and the results verified that the level of Galectin-3 was increased in HGSC ascites as compared to paired plasma (Figures 1D–F; median 16.9 and 32.6 ng/ml in plasma and ascites, respectively). To investigate if the increased levels of Galectin-3 were local or systemic, we measured the concentration of Galectin-3 and total protein concentration in serum from age-matched healthy donors (Supplementary Table S1, Figures 1G–I; median 9.1 ng/ml). Serum and plasma levels of Galectin-3 were similar between the two HGSC cohorts and healthy donors, suggesting that the increased levels of Galectin-3 are not systemic but localized to the tumor microenvironment.

3.2 Neutrophils in ascites from HGSC patients show signs of priming

Neutrophil response to stimuli is dependent on their priming status; resting peripheral blood neutrophils will respond differently to activating agonists as compared to extravasated (primed) neutrophils at the site of inflammation (44). As previously shown by others, Galectin-3 stimulates ROS production in primed, but not resting, neutrophils (39). Priming is most often associated with degranulation and subsequent alterations of receptors on the neutrophil cell surface. Similarly, *in vitro* treatment with TNF-α results in primed neutrophils, with altered surface expression (increased CD11b and CD66 and decreased CD62L), as well as a responsiveness to Galectin-3-induced ROS-release (33, 40). Therefore we used flow cytometry to investigate the cell surface expression of CD62L (L-selectin), CD11b (integrin alpha M), CD66a,c,d,e (hereafter referred to as CD66) and CD66b, surface markers characteristic for primed neutrophils, on HGSC ascites neutrophils as compared to autologous peripheral blood neutrophils. As shown in Figures 2A, B, surface expression of CD11b, CD66 and CD66b was upregulated on HGSC ascites neutrophils, while CD62L was shed, in comparison to blood neutrophils, indicating that neutrophils present in HGSC ascites display a primed phenotype. However, treatment with TNF-α *in vitro* led to additionally increased expression of CD11b, CD66 and CD66b, as well as lower expression of CD62L, which suggests that HGSC ascites neutrophils can be further primed (Figure 2B). The surface expression of CD11b, CD66 and CD66b, and percentage of $CD62L^+$ neutrophils, observed in blood neutrophils isolated from healthy donor buffy coats (Supplementary Figures S2A–D) was similar to blood neutrophils from OC patients, indicating priming of neutrophils in the tumor environment specifically.

We hypothesized that in addition to transmigration to the peritoneum, neutrophil priming may be induced by the tumor microenvironment in HGSC. Thus, we next tested whether cell-free ascites or cyst fluid from patients with HGSC could prime resting blood neutrophils. Peripheral blood neutrophils were incubated in autologous cell-free ascites or cyst fluid followed by measurement of cell surface expression of CD62L, CD11b, CD66 and CD66b. As shown in Figures 2C, D, peripheral blood neutrophils have higher expression of CD11b, CD66 and CD66b, and less expression of CD62L, on the cell surface after incubation in autologous HGSC cell-free ascites or cyst fluid. In relation to the priming induced by TNF-α treatment, neutrophils incubated in cell-free cyst fluid displayed a higher extent of priming compared to neutrophils incubated in cell-free ascites. Together, the results indicate that acellular components in the HGSC tumor microenvironment induces priming in neutrophils.

Upon priming, during the degranulation process, neutrophils expose additional Galectin-3-binding sites (39, 40). We thus investigated the level of Galectin-3 on the cell surface on HGSC ascites neutrophils. The amount of surface-bound Galectin-3 varied between samples, and we observed a trend of increased Galectin-3 bound to ascites neutrophils when compared to autologous peripheral blood neutrophils in two out of four patient samples, however the increase was not significant (Supplementary Figure S2E).

3.3 Galectin-3-induced ROS release in HGSC ascites neutrophils differ among patients

Earlier studies have shown that Galectin-3 induces ROS release in *in vivo* extravasated neutrophils and in neutrophils treated *in vitro* with ionomycin, fMLF, TNF-α or lipopolysaccharide (LPS) (39, 40, 45–47), while resting neutrophils, or neutrophils modestly stimulated in 22°C, did not respond to Galectin-3 with ROS release (39). The results from the study by Karlsson et al. imply that a certain amount of intracellular granules needs to be mobilized to the surface in order for a neutrophil to be able to respond with ROS release upon Galectin-3 stimulation. As OC ascites neutrophils displayed a primed phenotype, we next investigated whether Galectin-3 induces ROS release in these cells without prior TNF-α treatment *in vitro*. Figures 3A, B shows ROS release in ascites and peripheral blood neutrophils from three HGSC patients. While *in vitro* TNF-α

10.3389/fimmu.2024.1506236

treated neutrophils, from both HGSC ascites and peripheral blood, released ROS upon Galectin-3 stimulation (Figures 3C, D), only one patient sample of ascites neutrophils that were not pre-exposed to TNF-α *in vitro* responded to Galectin-3 with release of ROS with similar kinetics to Galectin-3-induced ROS release in TNF-α treated neutrophils (patient 30; Figures 3A–D). The ROS release curves from HGSC ascites neutrophils from the two other samples (patients 49 and 54) were similar to unstimulated peripheral blood neutrophils after Galectin-3 stimulation, with no or neglectable ROS release detected. When the Galectin-3 inhibitor lactose was added to the neutrophils, no Galectin-3 induced ROS was detected in any of the patient samples (Figures 3A–D). Both ascites and blood neutrophils

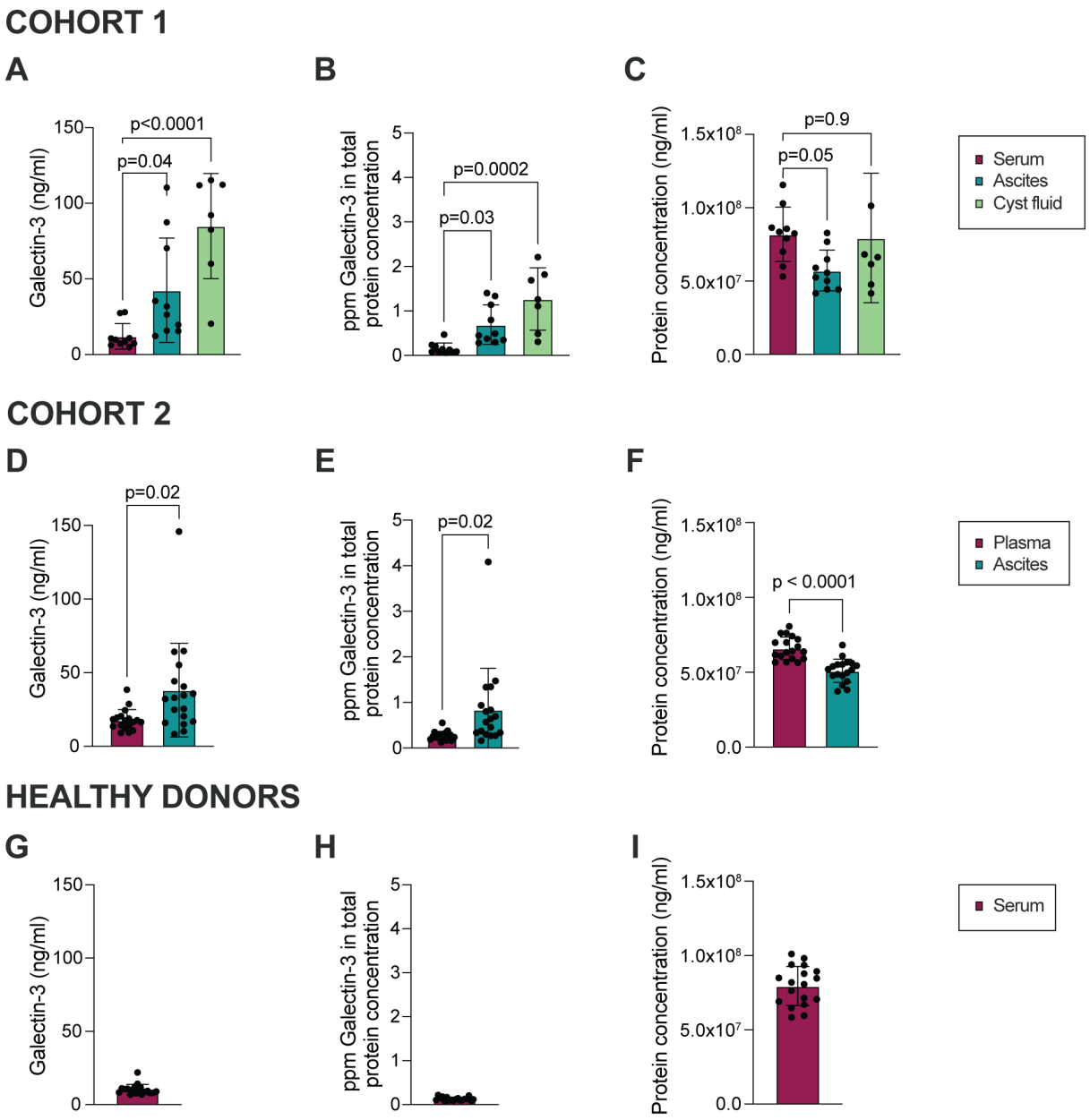

FIGURE 1
Galectin-3 is significantly higher in HGSC ascites and cyst fluid as compared to serum. **(A)** Galectin-3 concentration in ascites, cyst fluid and serum collected from patients with HGSC within Cohort 1. **(B)** Concentration of Galectin-3 in serum, ascites and cyst fluid normalized to total protein concentration, shown as parts per million (ppm; Cohort 1). **(C)** Total protein concentration in matched ascites, serum and cyst fluid (Cohort 1). **(D)** Galectin-3 concentration in ascites and plasma collected from patients with HGSC within Cohort 2. **(E)** Concentration of Galectin-3 in plasma and ascites when normalized to total protein concentration (ppm; Cohort 2). **(F)** Total protein concentration in matched ascites and plasma (Cohort 2). **(G)** Galectin-3 concentration in serum collected from healthy donors. **(H)** Concentration of Galectin-3 in serum when normalized to total protein concentration (ppm; healthy donors). **(I)** Total protein concentration in serum (healthy donors). Data is presented as mean ± SD, and statistically significant differences were evaluated by REML mixed-effects model followed by Šídák's multiple comparisons test **(A-C)** or paired Student's t-test **(D-F)**, n=7-10 in Cohort 1, n=18 in Cohort 2, n=18 in healthy donor cohort.

produced ROS after stimulation with PMA, and neutrophils from patients 49 and 54 also produced ROS after stimulation with fMLF (Supplementary Figure S3; neutrophils from patient 30 were not stimulated with fMLF). To understand why the ascites neutrophils responded differently across the patient samples, we plotted the ROS response to Galectin-3 against the priming status of the ascites neutrophils. As demonstrated in Figure 3E, the HGSC ascites neutrophils that released the highest amount of Galectin-3-induced ROS were also the most primed neutrophils (as measured by surface expression of CD66 and percentage of $CD62L^+$ neutrophils), however we had too few samples to statistically correlate the parameters to each other.

3.4 Galectin-3-induced ROS production decreases NK cell viability *in vitro* and impairs NK cell function against tumor cells

Exposure to ROS decreases the NK cell viability (41). We thus hypothesized that Galectin-3-induced ROS release in neutrophils may impact NK cell viability and hence their anti-tumor function. As shown in Figures 4A, B, co-incubation with NK cells and neutrophils resulted in decreased NK cell viability, which was further decreased when Galectin-3 was added to the setup. The addition of DPI, a known NADPH oxidase inhibitor, or SOD and

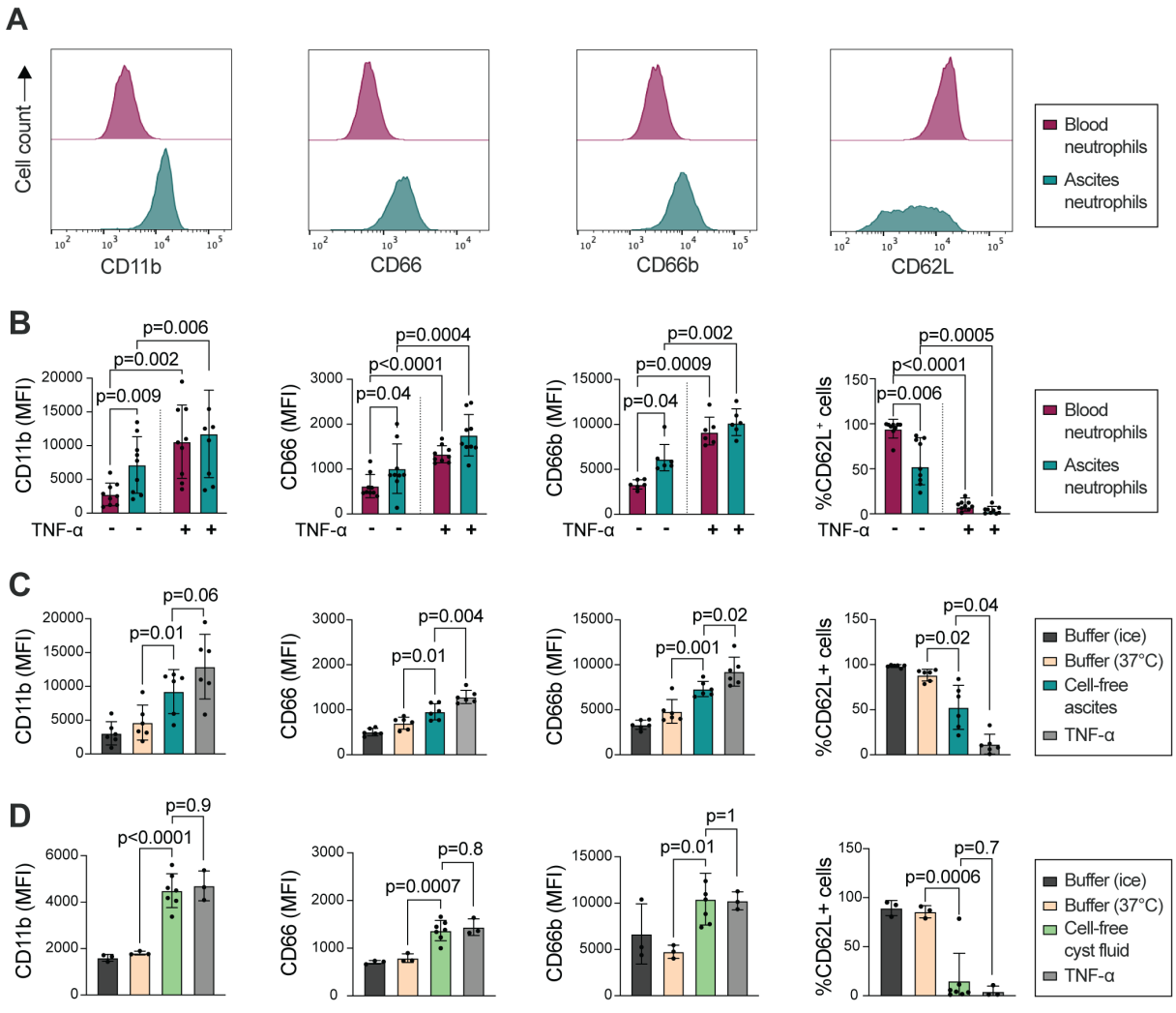

FIGURE 2
HGSC ascites neutrophils show signs of priming compared to autologous peripheral blood neutrophils. **(A)** Representative histograms of surface expression of CD11b, CD66, CD66b and CD62L. **(B)** Surface expression of CD11b, CD66, CD66b (MFI), and percentage of $CD62L^+$ neutrophils, on HGSC peripheral blood neutrophils (red) and HGSC ascites neutrophils (green) on unstimulated and TNF-α treated cells. **(C)** Surface expression of CD11b, CD66, CD66b (MFI), and percentage of $CD62L^+$ neutrophils, on HGSC peripheral blood neutrophils, after incubation in autologous cell-free HGSC ascites, buffer (KRG) or TNF-α at 37°C for 20 min, or kept in KRG on ice. **(D)** Surface expression of CD11b, CD66, CD66b (MFI), and percentage of $CD62L^+$ neutrophils, on healthy donor peripheral blood neutrophils that were incubated in cell-free HGSC cyst fluid, buffer (KRG) or TNF-α at 37°C for 20 min, or kept in KRG on ice. Blood neutrophils from 3 healthy donors were incubated in cell-free cyst fluid from 7 patients with HGSC. Data is presented as mean ± SD, and statistically significant differences were evaluated with repeated measures one-way ANOVA followed by Šídák's multiple comparisons test **(B-C)** and ordinary one-way ANOVA followed by Šídák's multiple comparisons test **(D)**, n=6-9 in **(B)**, n=6 in **(C)**, n=3/7 in **(D)**.

catalase that acts as ROS scavengers, restored the NK cell viability, indicating that the observed NK cell death is mediated *via* a ROS-mediated mechanism.

We next evaluated the NK cell anti-tumor effect in a co-culture assay with NK cells and target cells from the leukemic tumor cell line K562, an established model to measure NK cell reactivity towards tumor cells (48). Upon NK cell activation after interaction with ligands on target cells, NK cells release lytic granules containing Granzyme B and perforin that kill the target cell (49). In the presence, but not absence, of Galectin-3, addition of neutrophils to the co-culture decreased the NK cell degranulation significantly, as measured by percentage of NK cells expressing CD107a (Figure 4C). This was paralleled with a trend of increased viability of K562 cells, however the difference was not significant (Figure 4D; gating strategy in Supplementary Figure S1D). The addition of SOD and catalase to the assay restored NK cell degranulation, indicating that ROS-mediated NK cell death was responsible for their decreased anti-tumor activity (Figure 4C).

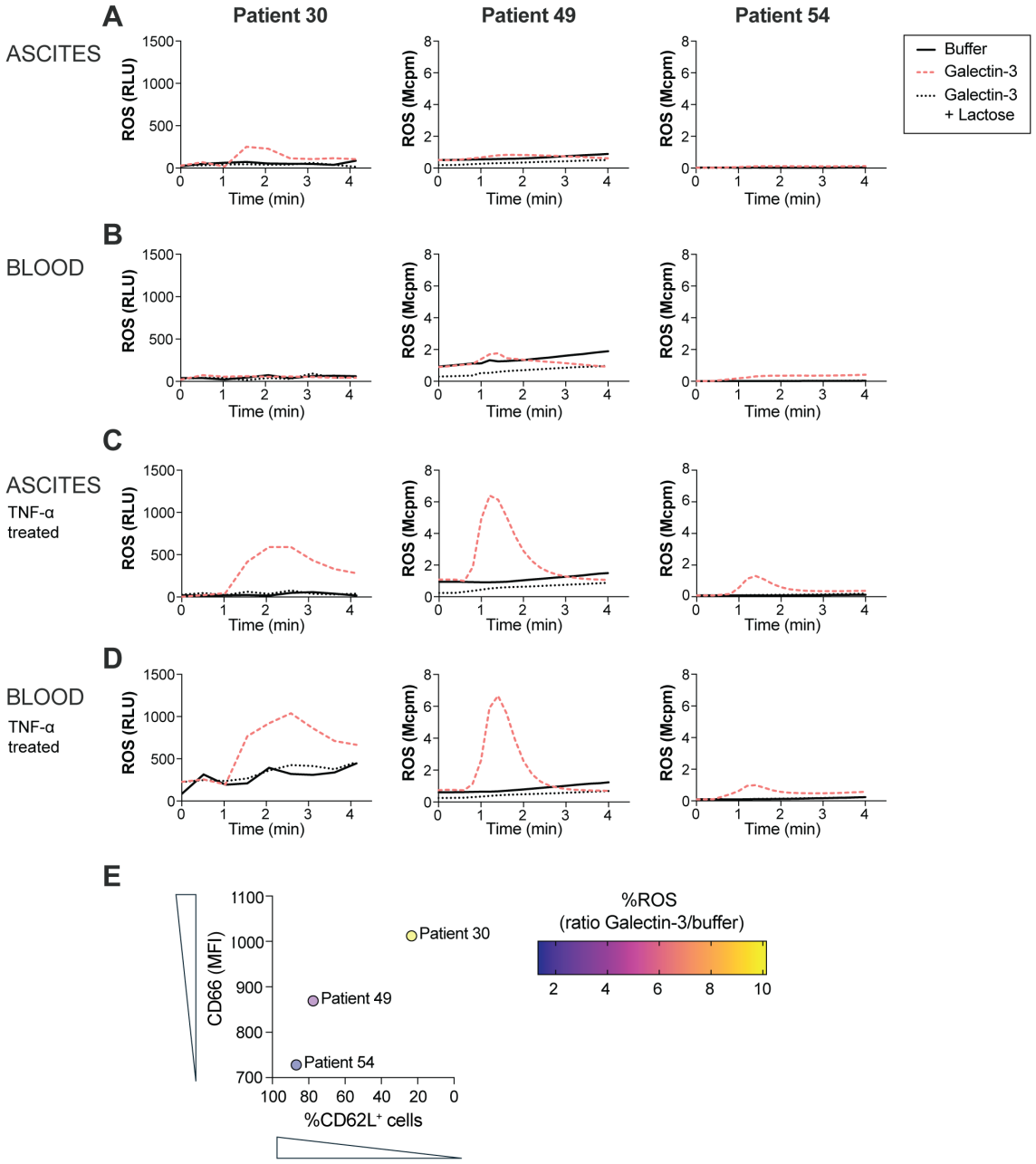

FIGURE 3
ROS release in ascites and peripheral blood neutrophils from three HGSC patients. **(A-D)** ROS release upon exposure to Galectin-3 (20 µg/ml) in untreated ascites **(A)** and blood **(B)** neutrophils, and TNF-α treated ascites **(C)** and blood **(D)** neutrophils in the presence or absence of lactose (10 mM). **(E)** Correlation between ROS release as measured by ratio of ROS peak value between ascites neutrophils stimulated with Galectin-3 and unstimulated (buffer) ascites neutrophils, and priming status as measured by surface expression of CD66 and percentage of $CD62L^+$ neutrophils, in HGSC ascites neutrophils from 3 patients with HGSC. ROS release in neutrophils from patient 30 was measured using CLARIOstar plate reader, while ROS release in neutrophils from patient 49 and 54 was measured using Biolumat LB 9505.

4 Discussion

In this study, we have investigated how the presence of Galectin-3 in high-grade serous carcinoma (HGSC) affects the immune-mediated anti-tumor response. Using samples from patients with HGSC we detected high levels of Galectin-3 in the ascites together with degranulated neutrophils. Furthermore, our *in vitro* functional assays with NK cells, neutrophils and tumor cells demonstrated a decreased NK cell response in the presence of Galectin-3. Taken together, the results from this study imply that Galectin-3 may decrease NK cell mediated tumor-killing *via* neutrophil ROS release.

Using patient samples from two cohorts of chemo naïve patients diagnosed with HGSC, we detected high levels of Galectin-3 in the tumor metastatic environment of ascites. We also detected high levels of Galectin-3 in HGSC cyst fluid, which is the fluid found surrounding the primary tumor in the ovary. These findings go in line with elevated levels of Galectin-3 reported in many other cancers including colon, head and neck, liver, gastric, endometrial, thyroid, skin and breast carcinomas (25). The Galectin-3 levels in serum or plasma measured in our cohorts were comparable to Galectin-3 serum and plasma levels in healthy subjects measured by us and others (46, 50, 51), indicating that Galectin-3 levels are specifically increased at the primary and metastatic tumor sites. In healthy conditions, Galectin-3 is found in most tissues, including the ovaries, but the expression is low compared to other tissues. Interestingly, Galectin-3 is not found in lymphoid tissues (52). The cellular source of Galectin-3 includes macrophages, neutrophils and epithelial cells (53). In malignant conditions, Galectin-3 can be produced by tumor cells, but also by stimulated lymphocytes. Thus, the increased Galectin-3 levels detected in OC ascites may be a result of increased production in tumor cells as well as increased inflammation in the peritoneum.

In addition to their essential role in host defense against pathogens, neutrophils regulate inflammation and activity of other leukocytes (54–56). In the malignant setting, the role of tumor-associated neutrophils is debated, where neutrophils may both inhibit and promote tumor growth and metastasis (57). High levels of neutrophils have been associated with worse outcome in several cancers including melanoma, renal and lung cancer (58–60), but the knowledge on neutrophils in OC is limited. A recent study suggested that neutrophils might promote OC metastasis, as ovarian tumor cells stimulate the release of NETs, and NETs bound to the tumor cells facilitate metastasis to the omentum (61). Activation of the NADPH oxidase, leading to production of ROS, is an important mechanism for neutrophil elimination of diverse microorganisms and regulation of inflammation (62–64). In addition, because ROS is toxic to tumor cells, the ROS-release by tumor-associated neutrophils may have an anti-tumor effect. However, also NK cells are sensitive to ROS, and addition of histamine dihydrochloride, which inhibits the formation of ROS, spares NK cells from undergoing ROS-induced apoptosis (41, 65).

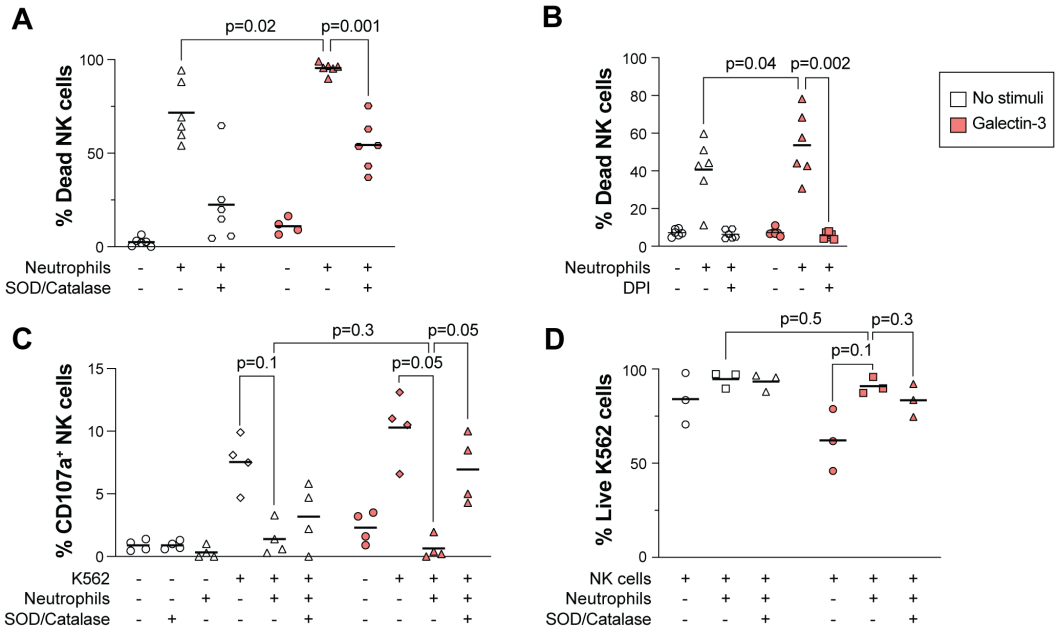

FIGURE 4
Galectin-3-induced ROS production in neutrophils decreases NK cell viability. **(A, B)** Impact of Galectin-3 on NK cell viability in presence or absence of neutrophils, measured as percentage of dead NK cells. NK cells and TNF-α treated neutrophils were co-incubated at a 2:1 **(A)** or 1:1 **(B)** ratio in medium only (no stimuli) or with Galectin-3 (25 or 5 µg/ml in A and B, respectively) overnight, with or without the addition of SOD and catalase **(A)** or DPI **(B)**. **(C, D)** NK cell degranulation as measured by CD107a expression **(C)** and viability of K562 cells **(D)** after overnight co-culture with NK cells, K562 cells and TNF-α treated neutrophils. Galectin-3 (25 µg/ml) and SOD/catalase were added as indicated. Horizontal lines represent mean. Statistically significant differences were evaluated by repeated measures one-way ANOVA followed by Šídák's multiple comparison test **(A-D)**, n=6 in **(A, B)**, n=4 in **(C)**, n=3 in **(D)**.

Indeed, immunotherapy with histamine dihydrochloride and low-dose IL-2 leads to improved clinical outcome in acute myeloid leukemia (66, 67).

Our data suggests that a fraction of HGSC patients harbor ascites neutrophils that respond to Galectin-3 with ROS release. It is well established that extracellular Galectin-3 mediates intracellular signaling, which impacts on cell function (24). Depending on the priming status of the neutrophil, different receptors may be ligated by Galectin-3, resulting in various intracellular signaling cascades. *In vitro* stimulation of neutrophils increases Galectin-3 binding proteins on the neutrophil surface, and only extravasated or *in vitro* stimulated neutrophils respond with ROS release upon Galectin-3 exposure (39). Earlier studies have suggested that Galectin-3 binding to CD66a and CD66b on *in vitro* stimulated neutrophils leads to activation of the NADPH oxidase complex (68). However, Galectin-3 binds to β-galactosides present at many different surface receptors, and induces respiratory burst in neutrophils in a carbohydrate- and dose-dependent manner, suggesting that several receptors may be involved in Galectin-3-induced ROS release (69). Generation of extracellular ROS is mediated by the assembly and activation of the NADPH oxidase, which *via* electron transport reduces O_2 to O_2^-. As O_2^- is very unstable, it quickly reacts with protons to form ROS such as H_2O_2 and HOCl, by the help of enzymatic reactivity. The signaling cascades that lead to activation of the NADPH oxidase depends on the stimuli; while fMLF induces NADPH oxidase activation via G-protein coupled receptors on the cell surface, PMA stimulates the intracellular protein kinase C (PKC) (70). Both signaling pathways eventually leads to phosphorylation of the NADPH oxidase components, resulting in ROS release. Despite many attempts to understand these complex signaling cascades, not all signaling pathways leading to NADPH oxidase activation are completely identified, including Galectin-3-induced NADPH oxidase activation and ROS release (71).

The fact that only one out of three patients' neutrophils responded with a low but clear ROS release upon Galectin-3 stimulation suggests that HGSC ascites neutrophils are primed to various extent. Analysis of surface markers demonstrated heterogeneity in degranulation between patients, and all ascites neutrophils could be further degranulated *in vitro*. Thus, the ascites neutrophil priming status varies between different donors as also observed for transmigrated neutrophils in inflamed joints of patients with inflammatory arthritis (72). As neutrophils from different patients varied in degree of degranulation, this may mean that also the level of Galectin-3 binding proteins varied on the neutrophil surface, resulting in differential Galectin-3-induced ROS-responses. The fact that the non-TNF-α treated ascites neutrophils that produced ROS upon Galectin-3 stimulation (patient 30) also were the most degranulated suggests that the extent of degranulation can be of importance for Galectin-3 responsiveness. On the other hand, degranulation is not always equivalent to priming status. In certain circumstances, neutrophils may respond with increased ROS production while they show no or little sign of degranulation (73, 74). For example, treatment with a G protein-coupled receptor (GPCR) internalization inhibitor (Barbadin) and endogenous hyaluronan acid increases GPCR-mediated ROS release without an increase of CD11b or cleavage of CD62L (73, 74). In the OC setting, it is plausible that the transmigration to the peritoneum leads to neutrophil activation. Moreover, ascites contains inflammatory reagents including TNF-α that can activate neutrophils (75). Indeed, we could demonstrate that resting neutrophils from autologous peripheral blood degranulate when exposed to cell-free ascites. In addition, neutrophil incubation in cyst fluid collected at the site of the primary tumor increased surface expression of granule markers and decreased the expression of CD62L. Thus, neutrophils present at the primary tumor site are likely also degranulated and primed.

Another possible explanation for the absence of ROS response to Galectin-3 in some HGSC ascites neutrophils is that they might express surface proteins that affect their response to Galectin-3. For example, Galectin-3C, a truncated version of Galectin-3 that lacks the N-domain but contains the carbohydrate recognition domain (CRD), inhibits Galectin-3-induced ROS release in neutrophils. The levels of Galectin-3C can be increased in situations where high amounts of primed neutrophils are present. Thus, even though additional binding of Galectin-3 to the cell surface of neutrophils is possible (neutrophils reach saturation at around 8 μM, as compared to a maximum of 4.4 nM measured in HGSC ascites in this study and 0.5 nM in healthy donor plasma), it will not induce more ROS production when high amounts of Galectin-3C is bound to the cell surface (40). Additionally, the binding of Galectin-3 in itself may affect the accessibility of surface proteins on the neutrophil as Galectins form lattices by crosslinking glycoproteins on the cell surface of neutrophils. The formation of lattices organizes cell surface-receptors, either by clustering certain receptors, or excluding receptors, thus regulating receptor signaling (76). Nevertheless, we did observe a Galectin-3-induced ROS release in ascites neutrophils from one out of three patients, and all ascites neutrophils responded to Galectin-3 when pre-treated with TNF-α. It is worth noting that the degree of ROS production observed in those experiments is lower when compared to the Galectin-3 response in blood neutrophils observed by others previously (39, 40). Though only observed in two patient samples, we noted a trend that ascites neutrophils responded with higher ROS production upon fMLF stimulation when compared to blood neutrophils. This may imply that ascites neutrophils have higher surface expression of formyl-peptide receptor 1 (FPR1), a receptor for fMLF. FPR1 is exposed on the neutrophil surface when neutrophils extravasate from the blood circulation, or after *in vitro* treatment with agents such as LPS or TNF-α (77–79). Again, these results indicate that ascites neutrophils from some HGSC patients may be in a primed state.

Using a co-culture setup with NK cells and primed neutrophils, we demonstrated that Galectin-3 induces NK cell death in a ROS-dependent manner. Addition of K562 tumor cells to the co-culture evoked NK cell degranulation; however, this was diminished in the presence of ROS produced by neutrophils. These findings suggest that Galectin-3 can contribute to a tumor-promoting environment in which NK cell-mediated tumor eradication is dampened in a neutrophil – Galectin-3-dependent pathway. Due to highly impeded NK cell degranulation when neutrophils were added to the co-culture, we could not detect a further decrease in NK cell

degranulation in the presence of Galectin-3. NK cells may also be suppressed by other factors in the complex tumor microenvironment of HGSC; OC ascites contains anti-inflammatory cytokines as well as myeloid-derived suppressor cells (MDSCs) and tumor-associated macrophages (TAMs) (80). A number of studies have shown that MDSCs decrease immune responses leading to increased tumor growth, and using a xenograft tumor model with primary human OC cells, MDSCs were shown to decrease T cell proliferation and anti-tumorigenic properties (81). The presence of cytokines such as IL-10 and TGF-ß, secreted by MDSCs, TAMs and other immune cells, as well as tumor cells, further suppress NK cells (80, 82, 83). For example, TGF-β downregulates the activating receptors NKp30 and NKG2D on NK cells resulting in decreased cytotoxicity (84). Moreover, the presence of soluble B7-H6, a ligand to NKp30, in OC ascites induced downregulation of NKp30, which correlated with impaired anti-tumor function of NK cells (15). Thus, combinatory treatments targeting several immune-evasion pathways in OC should be further investigated.

Galectin-3 may affect NK cell function by causing reduced activation *via* inhibition of activating NK cell receptors. One study reported that Galectin-3 can bind to MICA, which is a ligand to the activating NK cell receptor NKG2D, and that this Galectin-3-MICA complex caused disturbed interaction with NKG2D and thereby reduced NK cell killing of bladder cancer cells (85). It has also been proposed that Galectin-3, by acting as a soluble inhibitory ligand to the activating NK cell receptor NKp30, results in reduced NK cell cytotoxicity towards cervical cancer cells (86). Moreover, Galectin-3 binding to Integrin beta-1 (IGB1; CD29) on NK cells may induce secretion of the anti-inflammatory cytokine IL-10 (87), and Galectin-3 localized intracellularly in NK cells can affect NK cell degranulation, as inhibition of Galectin-3 increased the release of cytotoxic granules (88). Altogether, these studies suggest that Galectin-3 inhibits NK cell mediated tumor killing. However, contrarily to what others have reported, we did not observe decreased NK cell mediated cytotoxicity or decreased degranulation towards K562 target cells in the presence of Galectin-3.

Galectin-3 may be targeted by small molecule inhibitors such as GB0139 or monoclonal antibodies (18). Thus far, targeting Galectin-3 has shown promise for antiviral therapy (18), and Galectin-3-targeting drugs are now being evaluated in both malignant (bladder and colorectal cancer, multiple myeloma, B cell lymphoma, melanoma, chronic lymphocytic leukemia, non-small cell lung cancer) and non-malignant (fibrosis, non-alcoholic steatohepatitis, psoriasis) conditions (25). We have recently reported that NK cells present at the ascitic metastatic site in HGSC demonstrate anti-tumor capacity (7); however, further interventions may be required to overcome the immunosuppressive environment in ascites. Indeed, Galectin-3 is suggested as an immunotherapeutic target improving the outcome of inhibitory checkpoint inhibition in cancer immunotherapy, were Galectin-3 inhibition for example was demonstrated to augment the PD-L1 response in a mouse model of lung adenocarcinoma (89, 90). The results from this study demonstrate a ROS mediated decrease of the NK cell anti-tumor response. Thus, another therapeutic approach may be to inhibit ROS formation through treatment with histamine dihydrochloride as proven efficient in acute myeloid leukemia (66). Even though our studies have focused on the metastatic site of HGSC ascites, we also show that Galectin-3 levels are high in HGSC cyst fluid at the primary tumor site, and that neutrophils are degranulated when incubated in HGSC cyst fluid. Ultimately, these results suggest that Galectin-3 may affect NK cell mediated anti-tumor response also at the primary tumor site.

Murine models that mimic human conditions, such as xenograft mouse models, can generate valuable information about human biology that is challenging to obtain otherwise. Using a murine model to study if Galectin-3 induces neutrophil-dependent ROS mediated NK cell death and reduced cytotoxicity towards OC tumor cells *in vivo* could therefore be of interest for future perspectives. However, there are substantial differences between human and murine neutrophils, including receptor signaling pathways, granule proteins and regulation of NADPH oxidase activity (91), which have to be taken into consideration.

A limitation with this study is the low number of samples in certain experiments, including measurement of ROS activity. Nevertheless, despite a low number of samples we believe that this study provides new insights into the interplay between NK cells, neutrophils and Galectin-3.

In conclusion, we report that the high levels of Galectin-3 detected in the tumor microenvironment of HGSC may decrease NK cell eradication of tumor cells in a ROS-dependent manner. This study sheds light on the intricate immune cell interactions within the tumor microenvironment in OC and suggests further investigation to evaluate Galectin-3 as a potential immunotherapeutic target in OC.

Data availability statement

The original contributions presented in the study are included in the article/Supplementary Material. Further inquiries can be directed to the corresponding author.

Ethics statement

The studies involving humans were approved by the regional ethics board in Gothenburg (Dnr. 201-15) and the Swedish Ethical Review Authority (Dnr. 510-13). The studies were conducted in accordance with the local legislation and institutional requirements. The participants provided their written informed consent to participate in this study.

Author contributions

VK: Data curation, Formal analysis, Investigation, Methodology, Project administration, Validation, Visualization, Writing – original

draft, Writing – review & editing. EbS: Data curation, Formal analysis, Investigation, Visualization, Writing – review & editing. EmS: Data curation, Formal analysis, Investigation, Writing – review & editing. AI: Data curation, Formal analysis, Investigation, Writing – review & editing. HL: Supervision, Writing – review & editing. ML: Investigation, Supervision, Writing – review & editing. MS: Funding acquisition, Methodology, Supervision, Writing – review & editing. KS: Funding acquisition, Supervision, Writing – review & editing. KC: Conceptualization, Funding acquisition, Supervision, Writing – review & editing. EB: Conceptualization, Data curation, Formal Analysis, Funding acquisition, Investigation, Methodology, Project administration, Resources, Supervision, Validation, Visualization, Writing – original draft, Writing – review & editing.

Funding

The author(s) declare that financial support was received for the research, authorship, and/or publication of this article. This project was supported by the Swedish cancer foundation (20 0226 P 01 H; EB and CAN 2018/384; KS), the Swedish research council (2019-06328; EB), the Swedish Society for Medical Research (EB), the Swedish Society for Medicine (SLS-881711; EB), the Assar Gabrielsson foundation (BRG20-06, FB23-112; EB), Swedish state under the agreement between the Swedish government and the county councils, the ALF-agreement (965552; KS), Cancera and the Swedish Cancer Society (21-1848; KS), the Swedish state under the TUA-agreement (TUAGBG-916951 & TUAGBG-978190; KC), the Åke Wiberg Foundation (M21-0025 and M23-0193; MS), the Sahlgrenska International Starting Grant (GU2021/1070; MS), the King Gustaf the V 80-year foundation (FAI-2021-0804 and FAI-2022-0873; MS), the Rune and Ulla Almlövs Foundation (2023-418; MS), the Mary von Sydow foundation (4723; MS), the Magnus Bergwall foundation (2023-875; MS), the Swedish Rheumatism Association (R-995669; MS), the Wilhelm and Martina Lundgren Science Fund (2024-SA-4605; MS and 2022-4083; EB).

Acknowledgments

We acknowledge Birgitta Weijdegård for her assistance in measuring Galectin-3 in patient samples. We thank all patients who participated by donating biosamples to this study.

Conflict of interest

The authors declare that the research was conducted in the absence of any commercial or financial relationships that could be construed as a potential conflict of interest.

Generative AI statement

The author(s) declare that no Generative AI was used in the creation of this manuscript.

Publisher's note

Supplementary material

The Supplementary Material for this article can be found online at: https://www.frontiersin.org/articles/10.3389/fimmu.2024.1506236/full#supplementary-material

References

1. Siegel RL, Miller KD, Fuchs HE, Jemal A. Cancer statistic. *CA Cancer J Clin.* (2022) 72:7–33. doi: 10.3322/caac.21708

2. De Leo A, Santini D, Ceccarelli C, Santandrea G, Palicelli A, Acquaviva G, et al. What is new on ovarian carcinoma: integrated morphologic and molecular analysis following the new 2020 world health organization classification of female genital tumors. *Diagnostics (Basel).* (2021) 11:697. doi: 10.3390/diagnosQcs11040697

3. Prat J. Ovarian, fallopian tube and peritoneal cancer staging: rationale and explanation of new figo staging 2013. *Best Pract Res Clin Obstet Gynaecol.* (2015) 29:858–69. doi: 10.1016/j.bpobgyn.2015.03.006

4. Baci D, Bosi A, Gallazzi M, Rizzi M, Noonan DM, Poggi A, et al. The ovarian cancer tumor immune microenvironment (Time) as target for therapy: A focus on innate immunity cells as therapeutic effectors. *Int J Mol Sci.* (2020) 21:3125. doi: 10.3390/ijms21093125

5. Chardin L, Leary A. Immunotherapy in ovarian cancer: thinking beyond pd-1/pd-L1. *Front Oncol.* (2021) 11:795547. doi: 10.3389/fonc.2021.795547

6. Lai P, Rabinowich H, Crowley-Nowick PA, Bell MC, Mantovani G, Whiteside TL. Alterations in expression and function of signal-transducing proteins in tumor-associated T and natural killer cells in patients with ovarian carcinoma. *Clin Cancer Res.* (1996) 2:161–73.

7. Bernson E, Huhn O, Karlsson V, Hawkes D, Lycke M, Cazzetta V, et al. Identification of tissue-resident natural killer and T lymphocytes with anti-tumor properties in ascites of ovarian cancer patients. *Cancers (Basel).* (2023) 15:3363. doi: 10.3390/cancers15133362

8. Kim S, Kim B, Song YS. Ascites modulates cancer cell behavior, contributing to tumor heterogeneity in ovarian cancer. *Cancer Sci.* (2016) 107:1173–8. doi: 10.1111/cas.2016.107.issue-9

9. Wefers C, Lambert LJ, Torensma R, Hato SV. Cellular immunotherapy in ovarian cancer: targeting the stem of recurrence. *Gynecol Oncol.* (2015) 137:335–42. doi: 10.1016/j.ygyno.2015.02.019

10. Fan S, Gao X, Qin Q, Li H, Yuan Z, Zhao S. Association between tumor mutation burden and immune infiltration in ovarian cancer. *Int Immunopharmacol.* (2020) 89:107126. doi: 10.1016/j.intimp.2020.107126

11. Prager I, Watzl C. Mechanisms of natural killer cell-mediated cellular cytotoxicity. *J Leukoc Biol.* (2019) 105:1319–29. doi: 10.1002/JLB.MR0718-269R

12. Trinchieri G. Biology of natural killer cells. *Adv Immunol.* (1989) 47:187–376. doi: 10.1016/S0065-2776(08)60664-1

13. Wolf NK, Kissiov DU, Raulet DH. Roles of natural killer cells in immunity to cancer, and applications to immunotherapy. *Nat Rev Immunol.* (2023) 23:90–105. doi: 10.1038/s41577-022-00732-1

14. Gubbels JA, Claussen N, Kapur AK, Connor JP, Patankar MS. The detection, treatment, and biology of epithelial ovarian cancer. *J Ovarian Res.* (2010) 3:8. doi: 10.1186/1757-2215-3-8

15. Pesce S, Tabellini G, Cantoni C, Patrizi O, Coltrini D, Rampinelli F, et al. B7-H6-mediated downregulation of nkp30 in nk cells contributes to ovarian carcinoma immune escape. *Oncoimmunology*. (2015) 4:E1001224. doi: 10.1080/2162402X.2014.1001224

16. Nersesian S, Glazebrook H, Toulany J, Grantham SR, Boudreau JE. Naturally killing the silent killer: nk cell-based immunotherapy for ovarian cancer. *Front Immunol*. (2019) 10:1782. doi: 10.3389/fimmu.2019.01782

17. Carlsten M, Bjorkstrom NK, Norell H, Bryceson Y, Van Hall T, Baumann BC, et al. Dnax accessory molecule-1 mediated recognition of freshly isolated ovarian carcinoma by resting natural killer cells. *Cancer Res*. (2007) 67:1317–25. doi: 10.1158/0008-5472.CAN-06-2264

18. Stojanovic BS, Stojanovic B, Milovanovic J, Arsenijevic A, Dimitrijevic Stojanovic M, Arsenijevic N, et al. The pivotal role of galectin-3 in viral infection: A multifaceted player in host-pathogen interactions. *Int J Mol Sci*. (2023) 24:9617. doi: 10.3390/ijms24119617

19. Almkvist J, Karlsson A. Galectins as inflammatory mediators. *Glycoconj J*. (2002) 19:575–81. doi: 10.1023/B:GLYC.0000014088.21242.e0

20. Kolaczkowska E, Kubes P. Neutrophil recruitment and function in health and inflammation. *Nat Rev Immunol*. (2013) 13:159–75. doi: 10.1038/nri3399

21. Karlsson A, Christenson K, Matlak M, Bjorstad A, Brown KL, Telemo E, et al. Galectin-3 functions as an opsonin and enhances the macrophage clearance of apoptotic neutrophils. *Glycobiology*. (2009) 19:16–20. doi: 10.1093/glycob/cwn104

22. Linden JR, Kunkel D, Laforce-Nesbitt SS, Bliss JM. The role of galectin-3 in phagocytosis of candida albicans and candida parapsilosis by human neutrophils. *Cell Microbiol*. (2013) 15:1127–42. doi: 10.1111/cmi.2013.15.issue-7

23. Cockram TOJ, Puigdellivol M, Brown GC. Calreticulin and galectin-3 opsonise bacteria for phagocytosis by microglia. *Front Immunol*. (2019) 10:2647. doi: 10.3389/fimmu.2019.02647

24. Johannes L, Jacob R, Leffler H. Galectins at A glance. *J Cell Sci*. (2018) 131. doi: 10.1242/jcs.208884

25. Ahmed R, Anam K, Ahmed H. Development of galectin-3 targeting drugs for therapeutic applications in various diseases. *Int J Mol Sci*. (2023) 24:8116. doi: 10.3390/ijms24098116

26. Patwekar M, Sehar N, Patwekar F, Medikeri A, Ali S, Aldossri RM, et al. Novel immune checkpoint targets: A promising therapy for cancer treatments. *Int Immunopharmacol*. (2024) 126:111186. doi: 10.1016/j.intimp.2023.111186

27. Mirandola L, Nguyen DD, Rahman RL, Grizzi F, Yuefei Y, Figueroa JA, et al. Anti-galectin-3 therapy: A new chance for multiple myeloma and ovarian cancer? *Int Rev Immunol*. (2014) 33:417–27. doi: 10.3109/08830185.2014.911855

28. Weber M, Buttner-Herold M, Distel L, Ries J, Moebius P, Preidl R, et al. Galectin 3 expression in primary oral squamous cell carcinomas. *BMC Cancer*. (2017) 17:906. doi: 10.1186/s12885-017-3920-2

29. Capalbo C, Scafetta G, Filetti M, Marchetti P, Bartolazzi A. Predictive biomarkers for checkpoint inhibitor-based immunotherapy: the galectin-3 signature in nsclcs. *Int J Mol Sci*. (2019) 20:1607. doi: 10.3390/ijms20071607

30. Liu XH, Deng CX, Hu PC, Wang Y, Dong YH. Functional impact of galectin-3 and trail expression in breast cancer cells. *Eur Rev Med Pharmacol Sci*. (2017) 21:3626–33.

31. Wang LP, Chen SW, Zhuang SM, Li H, Song M. Galectin-3 accelerates the progression of oral tongue squamous cell carcinoma via A wnt/beta-catenin-dependent pathway. *Pathol Oncol Res*. (2013) 19:461–74. doi: 10.1007/s12253-013-9603-7

32. Sheid B. Angiogenic effects of macrophages isolated from ascitic fluid aspirated from women with advanced ovarian cancer. *Cancer Lett*. (1992) 62:153–8. doi: 10.1016/0304-3835(92)90186-Y

33. Nauseef WM, Borregaard N. Neutrophils at work. *Nat Immunol*. (2014) 15:602–11. doi: 10.1038/ni.2921

34. Kishimoto TK, Jutila MA, Berg EL, Butcher EC. Neutrophil mac-1 and mel-14 adhesion proteins inversely regulated by chemotactic factors. *Science*. (1989) 245:1238–41. doi: 10.1126/science.2551036

35. Kuhns DB, Long Priel DA, Gallin JI. Loss of L-selectin (Cd62l) on human neutrophils following exudation *in vivo*. *Cell Immunol*. (1995) 164:306–10. doi: 10.1006/cimm.1995.1174

36. Cowland JB, Borregaard N. Granulopoiesis and granules of human neutrophils. *Immunol Rev*. (2016) 273:11–28. doi: 10.1111/imr.2016.273.issue-1

37. Sengelov H, Follin P, Kjeldsen L, Lollike K, Dahlgren C, Borregaard N. Mobilization of granules and secretory vesicles during *in vivo* exudation of human neutrophils. *J Immunol*. (1995) 154:4157–65. doi: 10.4049/jimmunol.154.8.4157

38. Follin P, Briheim G, Dahlgren C. Mechanisms in neutrophil priming: characterization of the oxidative response induced by formylmethionyl-leucyl-phenylalanine in human exudated cells. *Scand J Immunol*. (1991) 34:317–22. doi: 10.1111/j.1365-3083.1991.tb01552.x

39. Karlsson A, Follin P, Leffler H, Dahlgren C. Galectin-3 activates the nadph-oxidase in exudated but not peripheral blood neutrophils. *Blood*. (1998) 91:3430–8. doi: 10.1182/blood.V91.9.3430

40. Sundqvist M, Welin A, Elmwall J, Osla V, Nilsson UJ, Leffler H, et al. Galectin-3 type-C self-association on neutrophil surfaces; the carbohydrate recognition domain regulates cell function. *J Leukoc Biol*. (2018) 103:341–53. doi: 10.1002/JLB.3A0317-110R

41. Mellqvist UH, Hansson M, Brune M, Dahlgren C, Hermodsson S, Hellstrand K. Natural killer cell dysfunction and apoptosis induced by chronic myelogenous leukemia cells: role of reactive oxygen species and regulation by histamine. *Blood*. (2000) 96:1961–8. doi: 10.1182/blood.V96.5.1961

42. Massa SM, Cooper DN, Leffler H, Barondes SH. L-29, an endogenous lectin, binds to glycoconjugate ligands with positive cooperativity. *Biochemistry*. (1993) 32:260–7. doi: 10.1021/bi00052a033

43. Dahlgren C, Bjornsdottir H, Sundqvist M, Christenson K, Bylund J. Measurement of respiratory burst products, released or retained, during activation of professional phagocytes. *Methods Mol Biol*. (2020) 2087:301–24. doi: 10.1007/978-1-62703-845-4_21

44. Miralda I, Uriarte SM, Mcleish KR. Multiple phenotypic changes define neutrophil priming. *Front Cell Infect Microbiol*. (2017) 7:217. doi: 10.3389/fcimb.2017.00217

45. Sundqvist M, Wekell P, Osla V, Bylund J, Christenson K, Savman K, et al. Increased intracellular oxygen radical production in neutrophils during febrile episodes of periodic fever, aphthous stomatitis, pharyngitis, and cervical adenitis syndrome. *Arthritis Rheum*. (2013) 65:2971–83. doi: 10.1002/art.v65.11

46. Sundqvist M, Osla V, Jacobsson B, Rudin A, Savman K, Karlsson A. Cord blood neutrophils display A galectin-3 responsive phenotype accentuated by vaginal delivery. *BMC Pediatr*. (2013) 13:128. doi: 10.1186/1471-2431-13-128

47. Almkvist J, Faldt J, Dahlgren C, Leffler H, Karlsson A. Lipopolysaccharide-induced gelatinase granule mobilization primes neutrophils for activation by galectin-3 and formylmethionyl-leu-phe. *Infect Immun*. (2001) 69:832–7. doi: 10.1128/IAI.69.2.832-837.2001

48. Wong WY, Wong H, Cheung SP, Chan E. Measuring natural killer cell cytotoxicity by flow cytometry. *Pathology*. (2019) 51:286–91. doi: 10.1016/j.pathol.2018.12.417

49. Long EO, Kim HS, Liu D, Peterson ME, Rajagopalan S. Controlling natural killer cell responses: integration of signals for activation and inhibition. *Annu Rev Immunol*. (2013) 31:227–58. doi: 10.1146/annurev-immunol-020711-075005

50. De Boer RA, Van Veldhuisen DJ, Gansevoort RT, Muller Kobold AC, Van Gilst WH, Hillege HL, et al. The fibrosis marker galectin-3 and outcome in the general population. *J Intern Med*. (2012) 272:55–64. doi: 10.1111/j.1365-2796.2011.02476.x

51. Sundqvist M, Andelid K, Ekberg-Jansson A, Bylund J, Karlsson-Bengtsson A, Linden A. Systemic galectin-3 in smokers with chronic obstructive pulmonary disease and chronic bronchitis: the impact of exacerbations. *Int J Chron Obstruct Pulmon Dis*. (2021) 16:367–77. doi: 10.2147/COPD.S283372

52. Farhad M, Rolig AS, Redmond WL. The role of galectin-3 in modulating tumor growth and immunosuppression within the tumor microenvironment. *Oncoimmunology*. (2018) 7:E1434467. doi: 10.1080/2162402X.2018.1434467

53. Diaz-Alvarez L, Ortega E. The many roles of galectin-3, A multifaceted molecule, in innate immune responses against pathogens. *Mediators Inflammation*. (2017) 2017:9247574. doi: 10.1155/2017/9247574

54. Rosales C. Neutrophil: A cell with many roles in inflammation or several cell types? *Front Physiol*. (2018) 9:113. doi: 10.3389/fphys.2018.00113

55. Mantovani A, Cassatella MA, Costantini C, Jaillon S. Neutrophils in the activation and regulation of innate and adaptive immunity. *Nat Rev Immunol*. (2011) 11:519–31. doi: 10.1038/nri3024

56. Riise RE, Bernson E, Aurelius J, Martner A, Pesce S, Della Chiesa M, et al. Tlr-stimulated neutrophils instruct nk cells to trigger dendritic cell maturation and promote adaptive T cell responses. *J Immunol*. (2015) 195:1121–8. doi: 10.4049/jimmunol.1500709

57. Masucci MT, Minopoli M, Carriero MV. Tumor associated neutrophils. Their role in tumorigenesis, metastasis, prognosis and therapy. *Front Oncol*. (2019) 9:1146. doi: 10.3389/fonc.2019.01146

58. Schmidt H, Bastholt L, Geertsen P, Christensen IJ, Larsen S, Gehl J, et al. Elevated neutrophil and monocyte counts in peripheral blood are associated with poor survival in patients with metastatic melanoma: A prognostic model. *Br J Cancer*. (2005) 93:273–8. doi: 10.1038/sj.bjc.6602702

59. Tessier-Cloutier B, Twa DD, Marzban M, Kalina J, Chun HE, Pavey N, et al. The presence of tumour-infiltrating neutrophils is an independent adverse prognostic feature in clear cell renal cell carcinoma. *J Pathol Clin Res*. (2021) 7:385–96. doi: 10.1002/cjp2.204

60. Bellocq A, Antoine M, Flahault A, Philippe C, Crestani B, Bernaudin JF, et al. Neutrophil alveolitis in bronchioloalveolar carcinoma: induction by tumor-derived interleukin-8 and relation to clinical outcome. *Am J Pathol*. (1998) 152:83–92.

61. Lee W, Ko SY, Mohamed MS, Kenny HA, Lengyel E, Naora H. Neutrophils facilitate ovarian cancer premetastatic niche formation in the omentum. *J Exp Med*. (2019) 216:176–94. doi: 10.1084/jem.20181170

62. Forsman H, Dahlgren C, Martensson J, Bjorkman L, Sundqvist M. Function and regulation of gpr84 in human neutrophils. *Br J Pharmacol*. (2024) 181:1536–49. doi: 10.1111/bph.v181.10

63. Nguyen GT, Green ER, Mecsas J. Neutrophils to the roscue: mechanisms of nadph oxidase activation and bacterial resistance. *Front Cell Infect Microbiol*. (2017) 7:373. doi: 10.3389/fcimb.2017.00373

64. Dahlgren C, Forsman H, Sundqvist M, Bjorkman L, Martensson J. Signaling by neutrophil G protein-coupled receptors that regulate the release of superoxide anions. *J Leukoc Biol*. (2024) 116:1334-51. doi: 10.1093/jleuko/qiae165

65. Brune M, Hansson M, Mellqvist UH, Hermodsson S, Hellstrand K. Nk cell-mediated killing of aml blasts: role of histamine, monocytes and reactive oxygen metabolites. *Eur J Haematol*. (1996) 57:312–9. doi: 10.1111/j.1600-0609.1996.tb01383.x

66. Brune M, Castaigne S, Catalano J, Gehlsen K, Ho AD, Hofmann WK, et al. Improved leukemia-free survival after postconsolidation immunotherapy with histamine dihydrochloride and interleukin-2 in acute myeloid leukemia: results of A randomized phase 3 trial. *Blood*. (2006) 108:88–96. doi: 10.1182/blood-2005-10-4073

67. Martner A, Thoren FB, Aurelius J, Hellstrand K. Immunotherapeutic strategies for relapse control in acute myeloid leukemia. *Blood Rev*. (2013) 27:209–16. doi: 10.1016/j.blre.2013.06.006

68. Feuk-Lagerstedt E, Jordan ET, Leffler H, Dahlgren C, Karlsson A. Identification of cd66a and cd66b as the major galectin-3 receptor candidates in human neutrophils. *J Immunol*. (1999) 163:5592–8. doi: 10.4049/jimmunol.163.10.5592

69. Robinson BS, Arthur CM, Evavold B, Roback E, Kamili NA, Stowell CS, et al. The sweet-side of leukocytes: galectins as master regulators of neutrophil function. *Front Immunol*. (2019) 10:1762. doi: 10.3389/fimmu.2019.01762

70. Karlsson A, Nixon JB, Mcphail LC. Phorbol myristate acetate induces neutrophil nadph-oxidase activity by two separate signal transduction pathways: dependent or independent of phosphatidylinositol 3-kinase. *J Leukoc Biol*. (2000) 67:396–404. doi: 10.1002/jlb.67.3.396

71. Dahlgren C, Lind S, Martensson J, Bjorkman L, Wu Y, Sundqvist M, et al. G protein coupled pattern recognition receptors expressed in neutrophils: recognition, activation/modulation, signaling and receptor regulated functions. *Immunol Rev*. (2023) 314:69–92. doi: 10.1111/imr.v314.1

72. Bjorkman L, Christenson K, Davidsson L, Martensson J, Amirbeagi F, Welin A, et al. Neutrophil recruitment to inflamed joints can occur without cellular priming. *J Leukoc Biol*. (2019) 105:1123–30. doi: 10.1002/JLB.3AB0918-369R

73. Niemietz I, Moraes AT, Sundqvist M, Brown KL. Hyaluronan primes the oxidative burst in human neutrophils. *J Leukoc Biol*. (2020) 108:705–13. doi: 10.1002/JLB.3MA0220-216RR

74. Sundqvist M, Holdfeldt A, Wright SC, Moller TC, Siaw E, Jennbacken K, et al. Barbadin selectively modulates fpr2-mediated neutrophil functions independent of receptor endocytosis. *Biochim Biophys Acta Mol Cell Res*. (2020) 1867:118849. doi: 10.1016/j.bbamcr.2020.118849

75. Browning L, Patel MR, Horvath EB, Tawara K, Jorcyk CL. Il-6 and ovarian cancer: inflammatory cytokines in promotion of metastasis. *Cancer Manag Res*. (2018) 10:6685–93. doi: 10.2147/CMAR.S179189

76. Brewer CF, Miceli MC, Baum LG. Clusters, bundles, arrays and lattices: novel mechanisms for lectin-saccharide-mediated cellular interactions. *Curr Opin Struct Biol*. (2002) 12:616–23. doi: 10.1016/S0959-440X(02)00364-0

77. Dahlgren C, Christophe T, Boulay F, Madianos PN, Rabiet MJ, Karlsson A. The synthetic chemoattractant trp-lys-tyr-met-val-dmet activates neutrophils preferentially through the lipoxin A(4) receptor. *Blood*. (2000) 95:1810–8. doi: 10.1182/blood.V95.5.1810.005k06_1810_1818

78. Sengelov H, Kjeldsen L, Borregaard N. Control of exocytosis in early neutrophil activation. *J Immunol*. (1993) 150:1535–43. doi: 10.4049/jimmunol.150.4.1535

79. Bylund J, Karlsson A, Boulay F, Dahlgren C. Lipopolysaccharide-induced granule mobilization and priming of the neutrophil response to helicobacter pylori peptide hp(2-20), which activates formyl peptide receptor-like 1. *Infect Immun*. (2002) 70:2908–14. doi: 10.1128/IAI.70.6.2908-2914.2002

80. Almeida-Nunes DL, Mendes-Frias A, Silvestre R, Dinis-Oliveira RJ, Ricardo S. Immune tumor microenvironment in ovarian cancer ascites. *Int J Mol Sci*. (2022) 23:10692. doi: 10.3390/ijms231810692

81. Cui TX, Kryczek I, Zhao L, Zhao E, Kuick R, Roh MH, et al. Myeloid-derived suppressor cells enhance stemness of cancer cells by inducing microrna101 and suppressing the corepressor ctbp2. *Immunity*. (2013) 39:611–21. doi: 10.1016/j.immuni.2013.08.025

82. Sinha P, Clements VK, Bunt SK, Albelda SM, Ostrand-Rosenberg S. Cross-talk between myeloid-derived suppressor cells and macrophages subverts tumor immunity toward A type 2 response. *J Immunol*. (2007) 179:977–83. doi: 10.4049/jimmunol.179.2.977

83. Trinchieri G. Interleukin-12 and the regulation of innate resistance and adaptive immunity. *Nat Rev Immunol*. (2003) 3:133–46. doi: 10.1038/nri1001

84. Castriconi R, Cantoni C, Della Chiesa M, Vitale M, Marcenaro E, Conte R, et al. Transforming growth factor beta 1 inhibits expression of nkp30 and nkg2d receptors: consequences for the nk-mediated killing of dendritic cells. *Proc Natl Acad Sci U.S.A*. (2003) 100:4120–5. doi: 10.1073/pnas.0730640100

85. Tsuboi S, Sutoh M, Hatakeyama S, Hiraoka N, Habuchi T, Horikawa Y, et al. A novel strategy for evasion of nk cell immunity by tumours expressing core2 O-glycans. *EMBO J*. (2011) 30:3173–85. doi: 10.1038/emboj.2011.215

86. Wang W, Guo H, Geng J, Zheng X, Wei H, Sun R, et al. Tumor-released galectin-3, A soluble inhibitory ligand of human nkp30, plays an important role in tumor escape from nk cell attack. *J Biol Chem*. (2014) 289:33311–9. doi: 10.1074/jbc.M114.603464

87. Chen Y, Zhang W, Cheng M, Hao X, Wei H, Sun R, et al. Galectin-3-itgb1 signaling mediates interleukin 10 production of hepatic conventional natural killer cells in hepatitis B virus transgenic mice and correlates with hepatocellular carcinoma progression in patients. *Viruses*. (2024) 16:737. doi: 10.3390/v16050737

88. Brittoli A, Fallarini S, Zhang H, Pieters RJ, Lombardi G. *In vitro*" Studies on galectin-3 in human natural killer cells. *Immunol Lett*. (2018) 194:4–12. doi: 10.1016/j.imlet.2017.12.004

89. Scafetta G, D'alessandria C, Bartolazzi A. Galectin-3 and cancer immunotherapy: A glycobiological rationale to overcome tumor immune escape. *J Exp Clin Cancer Res*. (2024) 43:41. doi: 10.1186/s13046-024-02968-2

90. Vuong L, Kouverianou E, Rooney CM, Mchugh BJ, Howie SEM, Gregory CD, et al. An orally active galectin-3 antagonist inhibits lung adenocarcinoma growth and augments response to pd-L1 blockade. *Cancer Res*. (2019) 79:1480–92. doi: 10.1158/0008-5472.CAN-18-2244

91. Nauseef WM. Human neutrophils not equal murine neutrophils: does it matter? *Immunol Rev*. (2023) 314:442–56. doi: 10.1111/imr.13154

frontiers | Frontiers in Immunology

TYPE Original Research
PUBLISHED 18 June 2025
DOI 10.3389/fimmu.2025.1537876

OPEN ACCESS

EDITED BY
Rosa Molfetta,
Sapienza University of Rome, Italy

REVIEWED BY
Daniel Olive,
Aix Marseille Université, France
Pierpaolo Correale,
Azienda Ospedaliera "Bianchi-Melacrino-Morelli", Italy

*CORRESPONDENCE
Doriana Fruci
doriana.fruci@opbg.net

†These authors have contributed equally to this work and share first authorship

RECEIVED 01 December 2024
ACCEPTED 22 May 2025
PUBLISHED 18 June 2025

CITATION
Romania P, Cifaldi L, Gragera P, D'Alicandro V, Caforio M, Folgiero V, Lucarini V, Melaiu O, Bei R, Locatelli F and Fruci D (2025) A genome-wide shRNA screen uncovers a novel potential ligand for NK cell activating receptors. *Front. Immunol.* 16:1537876. doi: 10.3389/fimmu.2025.1537876

A genome-wide shRNA screen uncovers a novel potential ligand for NK cell activating receptors

Paolo Romania[1†], Loredana Cifaldi[1,2†], Paula Gragera[1†], Valerio D'Alicandro[1], Matteo Caforio[1], Valentina Folgiero[1], Valeria Lucarini[1], Ombretta Melaiu[1,2], Roberto Bei[2], Franco Locatelli[1,3] and Doriana Fruci[1*]

[1]Bambino Gesù Children's Hospital, Istituto di Ricovero e Cura a Carattere Scientifico (IRCCS), Rome, Italy, [2]Department of Clinical Sciences and Translational Medicine, University of Rome "Tor Vergata", Rome, Italy, [3]Department of Life Sciences, Catholic University of the Sacred Heart, Rome, Italy

Introduction: Natural Killer (NK) cells play a key role in both innate and adaptive immune responses against viruses and tumor cells. Their function relies on the dynamic balance between activating and inhibitory signals, which are mediated by receptors that bind ligands expressed on target cells. While much is known about the function and expression patterns of NK cell activating receptors (NKARs), many of their ligands remain unidentified.

Methods: K562 cells were transduced with a shRNA library targeting 15,000 genes and co-cultured with NK cells from healthy donors. Surviving clones were tested in cytotoxicity and degranulation assays. PLAC1 was cloned from JEG3 cells in a lentiviral vector and transfected in K562 cells. PLAC1-related gene expression and survival data were obtained from the TCGA database and analyzed using R. PLAC1 and DSG2 expression in healthy tissues and NK cells was obtained from the HPA database and a GEO dataset.

Results: We identified ten candidate genes whose downregulation in K562 cells decreased NK cell-mediated cytotoxicity to levels comparable to silencing the MICA gene. The most promising candidates were functionally validated through single-target gene silencing and overexpression. Among them, the placenta-specific 1 (*PLAC1*) gene stood out, as its inhibition conferred the greatest protection to target cells from NK cell lysis, while overexpression of PLAC1 significantly increased NK cell degranulation. Importantly, PLAC1 was found to interact with NKAR fusion proteins, including NKG2D, DNAM1 NKp44 and NKp30, suggesting its potential involvement in NK cell function. PLAC1 is typically silent in normal tissues, with the exception of placental trophoblasts and testicular germ cells, but is markedly overexpressed in a wide range of tumors. Notably, its prognostic significance appears to be tumor-type specific, associating with either favorable or poor outcomes depending on the cancer context.

10.3389/fimmu.2025.1537876

Discussion: Our study identifies PLAC1 as a novel potential ligand for NKARs, suggesting it could be a valuable target for pharmacological strategies aimed at enhancing NK cell recognition. This finding holds promise for improving the efficacy of NK cell-based immunotherapies and advancing their clinical application.

KEYWORDS

NK cell, activating receptors, ligands, genome-wide screening, cancer immunotherapy, PLAC1, prognostic value

Introduction

Natural killer (NK) are cytolytic and cytokine-producing lymphocytes of the innate immune system, essential for immune regulation and antitumor and antiviral immunity (1). Their activity is tightly controlled by a balance between activating and inhibiting receptors that recognize ligands on the surface of target cells (2).

NK cell activation occurs when inhibitory receptors fail to engage their ligands, while activating receptors bind to their targets, shifting the signaling balance toward activation (3). This interplay determines whether NK cells are triggered to kill target cells (3). NK cell activating receptors (NKARs), such as NK group 2, member D (NKG2D), DNAX accessory molecule 1 (DNAM1) as well as natural cytotoxicity receptors (NCRs) NKp30, NKp44, and NKp46, recognize stress-induced ligands expressed during cellular transformation or viral infection (4). For instance, the homodimer NKG2D detects MICA, MICB, and ULBP family ligands in humans (5), and H60 and Rae1 in mice (6). DNAM-1 recognizes PVR and Nectin-2 (3, 7). Despite initial challenges, several NCR ligands have been identified. NKp30 binds BAT3, HCMV pp65, β-1,3-glucan, and the tumor-associated ligand B7-H6, promoting IFN-γ production and cytotoxicity (8–14). NKp44 and NKp46 bind viral hemagglutinins via sialylated glycans (15–17). NKp44 also recognizes NID1 and tumor-specific MLL5 (18, 19). NKp46 interacts with complement factor P and externalized calreticulin (20, 21).

Although much is known about the expression and function of NKARs, many ligands have not yet been unidentified. To uncover novel ligands for NKARs, we performed a genome-wide loss-of-function screening using stable gene knockdown in the human chronic myeloid leukemia cell line K562 (22, 23). This approach led to the identification of PLAC1 (24) as a potential ligand for NKARs.

Our findings demonstrate that modulating PLAC1 expression, through either inhibition or overexpression, significantly influences NK cell function and their interaction with NKARs such as NKG2D, DNAM-1, NKp44 and NKp30. Notably, PLAC1 is absent in normal tissues under steady-state conditions but is expressed across a wide range of hematopoietic and non-hematopoietic tumors, as well as in transformed cells. In these contexts, PLAC1 can activate allogenic NK cells. Furthermore, its expression has been linked to either favorable or poor prognosis, depending on the tumor type. Altogether, these findings suggest PLAC1 as a promising novel ligand for NKARs.

Results

Genome-wide screening identifies PLAC1 as a novel potential ligand for NK cell activating receptors

To uncover novel ligands for NKARs, we performed a genome-wide loss-of-function genetic screening using a pooled shRNA library targeting 15,000 human genes with multiple sequence-verified constructs (Figure 1A). On average, five shRNA designs were used per gene. We selected the K562 cell line as a target due to its expression of numerous ligands for NKARs, making it an ideal model for identifying genes involved in NK cell activation. K562 cells were transduced with the human lentiplex shRNA library (TRC 1.5) at a multiplicity of infection (MOI) ≤1 and selected with puromycin for 4 days. As a control, K562 cells were transduced with a non-targeting shRNA (shCTRL). The transduced cells were then cocultured with freshly isolated NK cells from five healthy donors (HD) at an effector-to-target (E:T) ratio of 15:1, with each donor added separately over three consecutive days. Surviving K562 cells, presumed to have silenced genes essential for NK cell-mediated activation, were selected based on viability and morphology via flow cytometry, and maintained as bulk populations or individual clones (Figure 1A).

Functional validation using NK cells from additional HDs and a standard ^{51}Cr release assay confirmed that K562 cells transduced with the shRNA library were more resistant to NK cell-mediated killing, compared to shCTRL cells (Figures 1B, C). The average lytic units (L.U.) at 30% lysis across three replicates (shLib 1-3) were significantly lower for K562-shLib cells (12.6) than for K562-shCTRL cells (17.5) (Figure 1B, right panel). Similarly, individual clones showed variable levels of resistance, with library-derived clones displaying an average L.U. at 20% of 18, compared to 31 for shCTRL cells (Figure 1C, right panel). Notably, the 10 clones with L.U. values below the average (<18) were also more resistant to killing by the NKL cell line (25) than the other clones (Figure 1D).

10.3389/fimmu.2025.1537876

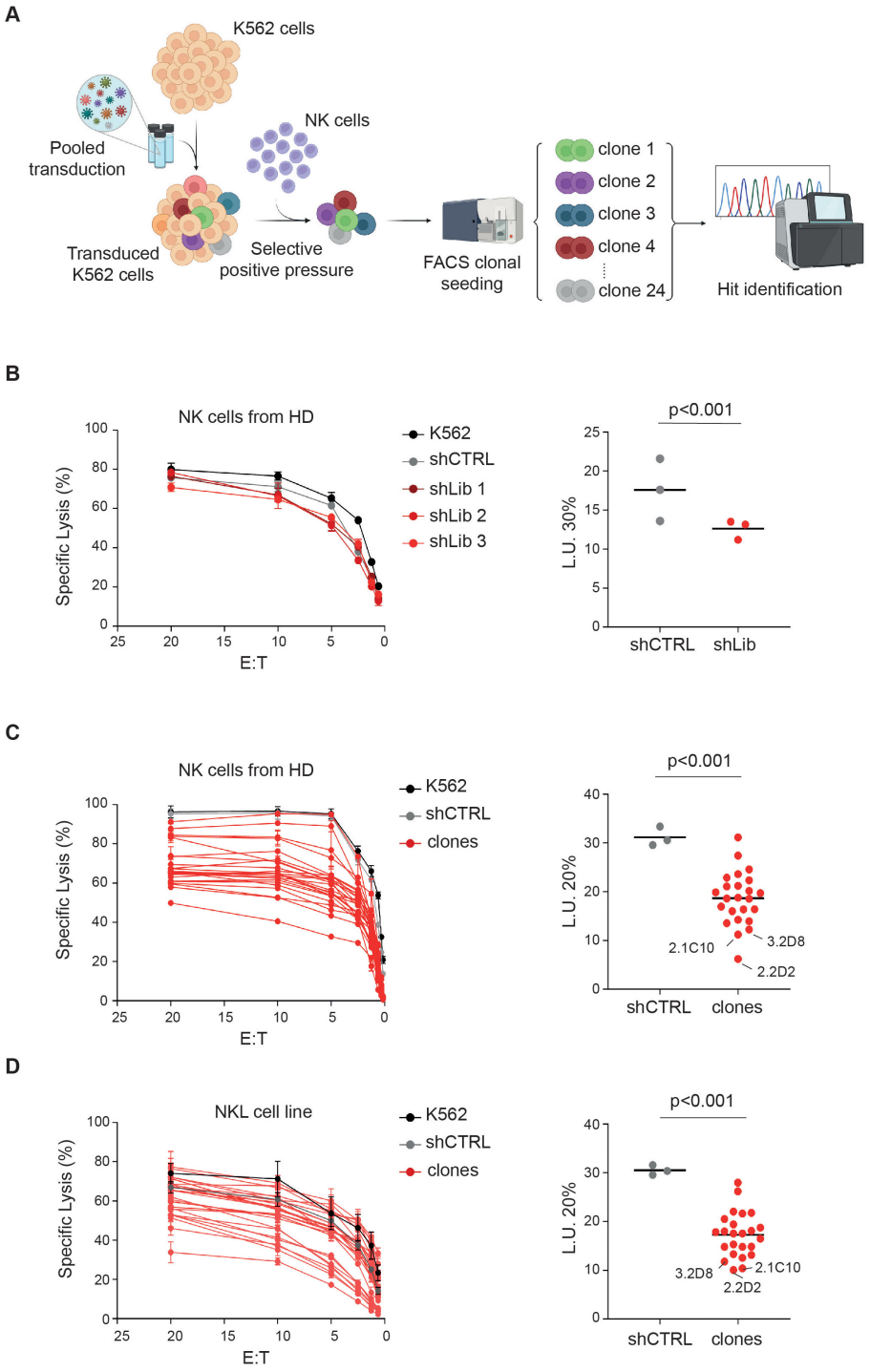

FIGURE 1
Genome-wide screening identifies new potential ligands for activating NK cell receptors. **(A)** Experimental scheme as detailed in the text. **(B-D)** NK cells derived from HD **(B, C)** and NKL cell line **(D)** were tested as effectors at the indicated E:T ratios in a standard ^{51}Cr-release assay using K562 cells infected with the lentiplex shRNA library that survived positive selection with NK cells, either as a polyclonal cell population **(B)** or as single clones **(C, D)**. Data from a representative of three independent experiments are shown. Specific lysis was converted to L.U. 30% **(B)** or 20% **(C, D)**. Dots, represent L.U. 30% or 20% of the effector/target pairs tested; horizontal bars indicate average values. *P* values were calculated by comparing with shCTRL and sh-bulk **(B)** or clones **(C, D)** (two-tailed paired Student *t* test). The scheme in A was created by BioRender.

To evaluate whether silencing a specific ligand could impair NK cell function, we tested NKL cell recognition of K562 cells with MICA knockdown, a known ligand for NKG2D. K562-shMICA cells exhibited protection levels comparable to the top 10 resistant clones, with a L.U. of 40 versus 20 for K562-shCTRL (Supplementary Figure S1).

DNA sequencing identified the silenced target genes in 15 out of 24 clones (Supplementary Table S1). The remaining 9 clones likely contained multiple shRNA inserts, preventing target identification. Among the identified genes, placenta-specific protein 1 (*PLAC1*, clone 2.2D2) (24), transcription factor 7 (*TCF7*, clone 2.1C10) (26), and Pleckstrin Homology Domain-Containing A5 (*PLEKHA5*, clone 3.2D8) (27) conferred strong resistance to NK cell-mediated lysis by both HD-derived NK cells and the NKL cell line (Figures 1C, D). *PLAC1* is associated with placental development (24), *TCF7* is involved in T cell differentiation (28), and *PLEKHA5* has been linked to the suppression of tumor metastasis (29).

Functional validation revealed that silencing PLAC1 significantly impaired NK cell degranulation, as indicated by reduced CD107a expression (Figure 2A; Supplementary Figure S2A). Both K562-shPLAC1 cells and the corresponding library clone (K562-2.2D2) decreased the frequency of $CD107a^+$ NK cells by nearly 50% compared to K562-shCTRL cells (0.60 and 0.48, respectively) (Figure 2A). In contrast, silencing TCF7 or PLEKHA5 had no significant effect on NK cell degranulation (Figure 2A). Based on these results and given its predicted membrane localization (30), we focused on PLAC1 as the most promising target. To further validate its role, PLAC1 was cloned from JEG3 cells and stably expressed in K562 cells (Figure 2B; Supplementary Figures S2B, C).

Overexpression of PLAC1 in K562 cells increased NK cell degranulation by 23%, with the frequency of $CD107a^+$ NK cells rising from 45.5% in K562-CTRL cultures to 59% in K562-PLAC1 cultures (Figure 2C). Since the overexpression of PLAC1 did not impact the expression of NKAR ligands MICA/B, ULBPs, Nectin-2, PVR, B7-H6, FAS and TRAIL-R2 (Figure 2D), the increased degranulation was attributed to a direct effect mediated by PLAC1.

These results highlight PLAC1's critical role in modulating NK cell function and suggest its potential as a novel ligand for NKARs.

PLAC1 modulates the binding of NK cell activating receptors to K562 cells

PLAC1 may influence NK cell function by serving as a ligand for NKARs. To test this hypothesis, we examined whether PLAC1 expression affects the binding of NKARs fusion proteins NKG2D, DNAM1, NKp30 and NKp44 to K562 cells overexpressing PLAC1. In this assay, K562 cells were stained with NKARs-Fc fusion proteins, NKG2D-Fc, DNAM1-Fc, NKp30-Fc and NKp44-Fc. Compared with control cells, overexpression of PLAC1 led to significantly increased binding of all fusion proteins tested in K562 cells (Figure 2E).

These results suggest that overexpression of PLAC1 results in increased interaction of these cells with the activating receptors NKG2D, DNAM1, NKp30, and NKp44, potentially amplifying the recognition and lysis of tumor cells by NK cells.

PLAC1 expression in tumors based on cancer genomic datasets

PLAC1 is highly expressed during development, particularly in placental tissues, including trophoblast giant cells and the labyrinthine layer derived from the trophoblast lineage (31). According to data from The Cancer Genome Atlas (TCGA), PLAC1 is virtually undetectable in most normal somatic tissues, with the exception of testicular germ cells, skeletal muscle, peritubular cells, and the placenta during gestation (Figure 3A; Supplementary Figure S3A). In contrast, PLAC1 is significantly upregulated in a wide range of tumor types compared to their normal tissue counterparts (Figure 3B). Elevated expression was observed in 15 distinct cancers, including bladder urothelial carcinoma (BLCA), breast invasive carcinoma (BRCA), cervical squamous cell carcinoma and endocervical adenocarcinoma (CESC), cholangiocarcinoma (CHOL), colon adenocarcinoma (COAD), esophageal carcinoma (ESCA), glioblastoma multiforme (GBM), head and neck squamous cell carcinoma (HNSC), kidney renal clear cell carcinoma (KIRC), lung adenocarcinoma (LUAD), lung squamous cell carcinoma (LUSC), prostate adenocarcinoma (PRAD), rectum adenocarcinoma (READ), stomach adenocarcinoma (STAD) and thyroid carcinoma (THCA) (Figure 3B; Supplementary Table S2). Interestingly, the prognostic relevance of PLAC1 expression appears to be highly tumor-specific. Elevated PLAC1 levels were associated with improved overall survival in ESCA, GBM and LUSC, and poorer prognosis in BLCA, CESC, CHOL, COAD, HNSC, KIRC and PRAD (Figure 3C; Supplementary Figures S3B, C). To assess the impact of threshold selection on survival outcomes, we conducted sensitivity analyses using multiple clinically and statistically relevant cut-offs—including the mean, median, and quartiles of PLAC1 expression (Supplementary Figures S3B). Although the strength and significance of the associations varied depending on the chosen threshold, consistent trends were observed, particularly in ESCA and LUSC, where the mean expression level reliably stratified survival outcomes (Supplementary Figures S3B, C).

These findings underscore the importance of careful threshold selection when utilizing PLAC1 as a prognostic biomarker and suggest that PLAC1 may serve as a context-dependent indicator of clinical outcome, with its prognostic value varying substantially across different tumor types.

To further explore the role of PLAC1 in NK cell activation, we analyzed its correlation with a NK cell gene signature (32) in tumor types where PLAC1 expression affects overall survival of patients. Notably, in tumors where high PLAC1 expression is associated with a favorable prognosis (ESCA, GBM, LUSC), we observed a positive

10.3389/fimmu.2025.1537876

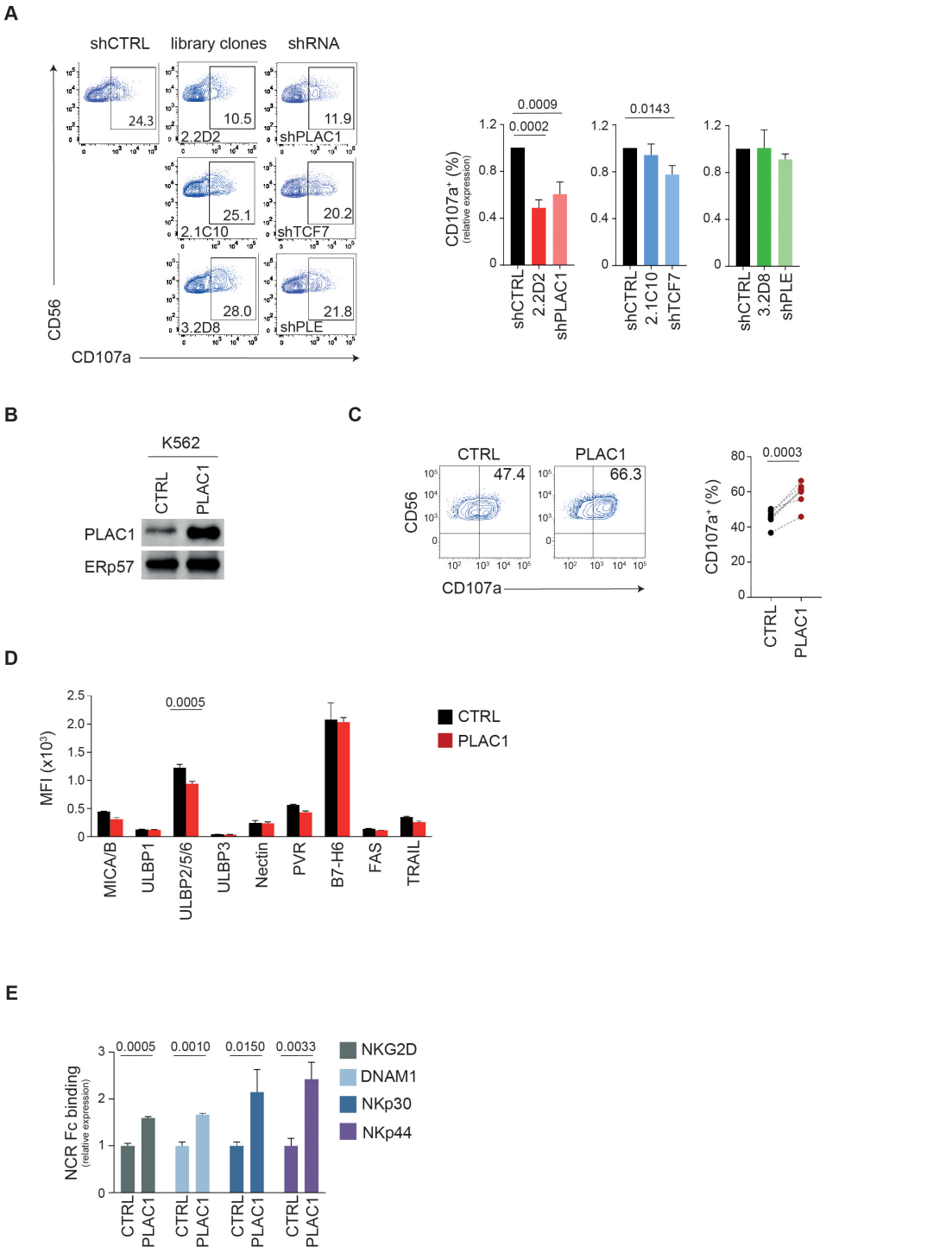

FIGURE 2
PLAC1 regulates the activity of NK cells. **(A)** Representative example of degranulation by human CD3$^-$CD56$^+$ NK cells from a HD, measured as CD107a cell-surface expression following stimulation with K562 cells transduced with the indicated library clones or specific shRNAs. The percentage of CD107a$^+$ NK cells is indicated. A representative of three independent experiments is reported. Summary of NK cell degranulation after stimulation with the indicated target cells with 5 HDs is reported on the right (Dunett's multiple comparisons test). **(B)** Immunoblotting of PLAC1 expression in K562 cells overexpressing PLAC1. **(C)** Representative example of degranulation by human CD3$^-$CD56$^+$ NK cells from a HD, measured as CD107a cell-surface expression following stimulation with K562 cells overexpressing PLAC1. Summary of NK cell degranulation of 7 donors after stimulation with the indicated cells is reported on the right (two-tailed paired Student *t* test). **(D)** Expression of the indicated ligands for NKARs in control and PLAC1-overexpressing K562 cells (Šídák's multiple comparisons test). **(E)** Relative intensity in NKAR-Fc protein binding on K562 overexpressing PLAC1 compared with K562-CTRL cells measured by flow cytometric analysis. Means ± SD of three independent experiments are shown (two-tailed unpaired Student *t* test).

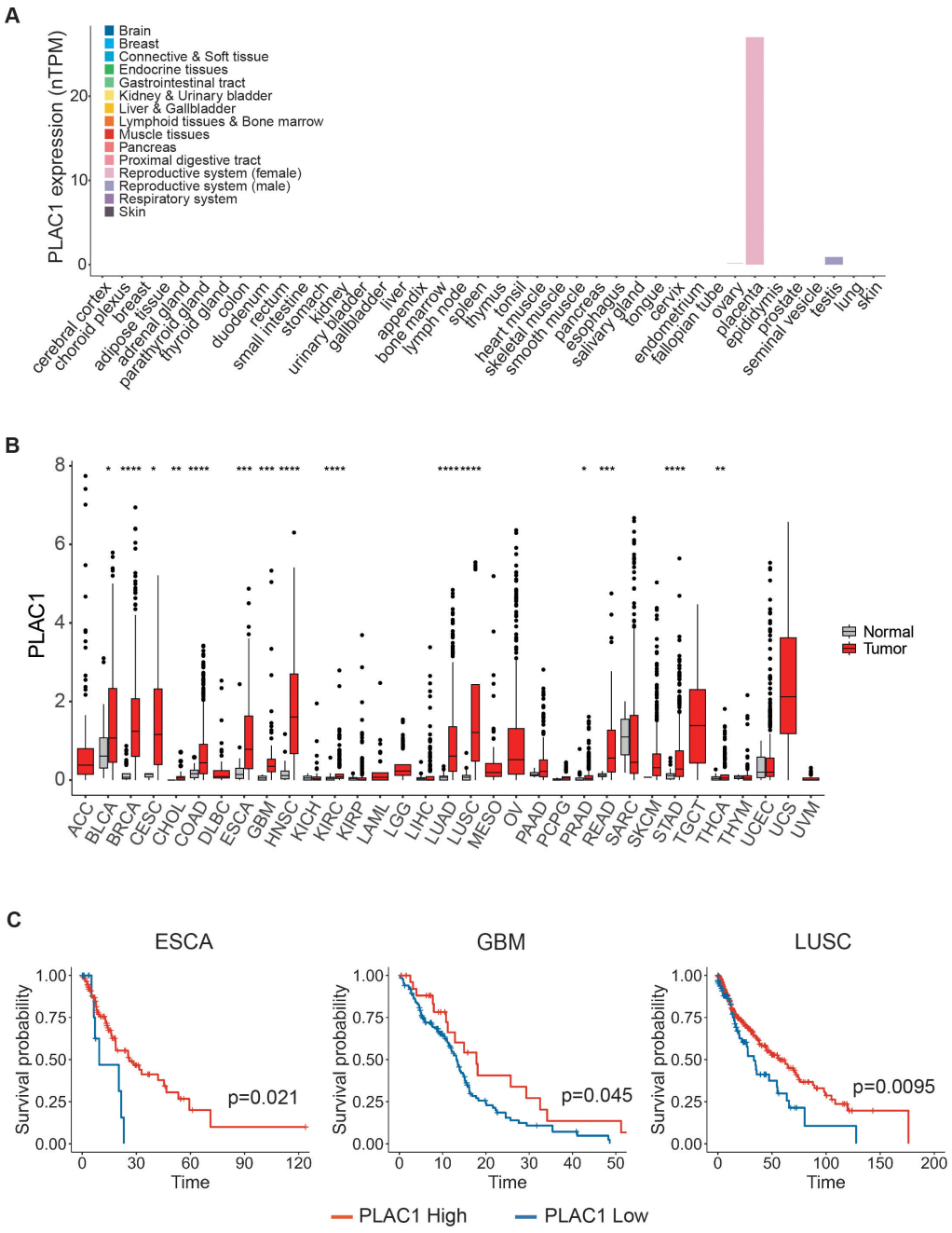

FIGURE 3
PLAC1 expression has prognostic value in tumors. **(A)** PLAC1 gene expression in the indicated normal human tissues. **(B)** The expression status of PLAC1 in 33 cancer types compared to the normal counterpart. **(C)** Kaplan-Meier curves show the duration of overall survival of the indicated tumor patients according to the PLAC1 gene expression. Statistically significant P values are indicated. * p<0.05, ** p<0.01, *** p<0.001, **** p<0.0001.

correlation between PLAC1 and the genes *XCL1*, *KLRC1* (NKG2A), *KLRC2* (NKG2C) and *TKTL1*, and a negative correlation with the *MLC1* gene (Figure 4). In contrast, these correlations were absent in tumor types where high PLAC1 expression was associated with poorer survival outcomes (BLCA, CESC, CHOL, COAD, HNSC, KIRC and PRAD). These findings further strengthen the association between PLAC1 and NK cell function in specific cancer contexts.

Desmoglein 2 is not expressed on NK cells

Recent studies have identified Desmoglein 2 (DSG2), a critical component of desmosomes, as a direct interaction partner of PLAC1 (30). Desmosomes are specialized adhesive protein complexes located at intercellular junctions, essential for maintaining tissue mechanical integrity (33). Given PLAC1's potential role as a ligand for NKARs,

we investigated whether DSG2 is expressed on NK cells. According to data from the Human Protein Atlas (HPA), DSG2 is primarily expressed in epithelial cells and trophoblasts (34). Among immune cells, DSG2 is predominantly found on dendritic cells (DC), with no significant expression detected on NK cells (11) (Supplementary Figure S4A). To further explore DSG2 expression in NK cells within an oncological context, we analyzed single-cell RNA sequencing (scRNA-seq) data from NK cells isolated from the bone marrow of HD and patients with acute myeloid leukemia (AML) (35). DSG2 was detected in fewer than 1% of total NK cells (approximately 0.3%), with no significant differences between healthy and AML conditions (Supplementary Figure S4B). In contrast, well-characterized NK cell receptors, such as NKp46 (*NCR1*), NKG2D (*KLRK1*), NKG2A (*KLRC1*), and DNAM1 (*CD226*) were expressed in a substantially higher proportion of NK cells, approximately 30%, 10%, 7%, and 1%, respectively (Supplementary Figure S4B). Finally, we evaluated the expression of DSG2 on the surface of NK cells purified from HDs. Unlike HeLa cells, which are known to express DSG2, NK cells from all donors analyzed did not express DSG2 (Supplementary Figure S4C).

Altogether, these finding indicate that DSG2 is not expressed on the surface of NK cells, neither in healthy conditions nor in cancerous states. Therefore, the interaction between PLAC1 and NK cells likely involves a receptor other than DSG2.

Discussion

This study identifies a novel role of PLAC1 as a potential ligand for NKARs, contributing to the recognition of tumor cells by NK cells. NKARs, such as NKG2D, DNAM-1 and NCRs NKp30, NKp44 and NKp46, interact with ligands frequently upregulated on tumor cells, thereby promoting NK cell activation, cytokine production and the elimination of tumor cells (1). PLAC1 appears to function similarly, although the precise mechanisms and receptor interactions have yet to be fully elucidated.

The *PLAC1* gene is primarily expressed in the placenta, where it plays a crucial role in fetal development (24). Its protein product is mainly localized on the surface of trophoblastic cells, where it contributes to cell adhesion processes and helps to maintain the maternal-fetal interface (31). Notably, PLAC1 is not expressed in other normal tissues but is detectable in a variety of cancers, making it an attractive target for cancer research due to its restricted expression pattern and immunogenic potential (36–38).

PLAC1 is classified as a cancer/testis antigen (CTA) (39), with elevated expression reported in several tumor types, including stomach (40), colon (41), liver (42), pancreas (43), prostate (44), ovary (45, 46), uterus (47), cervix (48), breast (49), lung (37), HNSC (38, 50) and nasopharynx carcinoma (51). Beyond its expression profile, PLAC1 has been implicated in promoting cancer cell proliferation, invasion, and migration (52). Several factors may explain PLAC1's role in cancer. For example, it might be ectopically expressed in tumors due to widespread epigenetic deregulation, without directly contributing to oncogenic processes. Its role could be context-dependent, becoming functionally relevant only in certain tumor types, disease stages, or microenvironmental conditions. Alternatively, PLAC1 may participate in broader molecular networks, where its effects are compensated by other mechanisms, making its individual contribution difficult to detect experimentally. Finally, PLAC1 might play a primarily immunological role, contributing to tumor immunogenicity rather than directly driving oncogenic transformation.

In this study, we employed a genome-wide loss-of-function screening approach to demonstrate that PLAC1 can act as a ligand for NKARs. This interaction enhances NK cell-mediated cytotoxicity against PLAC1-expressing tumor cells. Notably, overexpression of PLAC1 in K562 cells increased binding to NKAR-Fc fusion proteins, including NKG2D-Fc, DNAM1-Fc, NKp30-Fc and NKp44-Fc. These findings suggest that PLAC1 may function as a novel ligand for these receptors. Beyond its potential role as a direct ligand for NKARs, PLAC1 could also act as a cofactor for known ligands, modulating their interaction with NKARs through a mechanism distinct from merely inducing ligand expression. While the direct role of PLAC1 as an NKAR ligand remains to be fully validated, our findings underscore its impact on NK cell activation and tumor cell recognition. Further studies are required to determine whether PLAC1 interacts with an as-yet-unidentified NK cell receptor. The potential importance of PLAC1, compared to other tumor-mediated NK cell regulation mechanisms, lies in its role as a direct ligand for NKARs. Unlike stress-induced activation mechanisms such as MICA/B or ULBPs, PLAC1 offers an additional interaction with NK cells, potentially enhancing tumor recognition and killing. This makes PLAC1 a promising target for therapeutic strategies, particularly in tumors that express this antigen.

PLAC1 has been shown to interact with DSG2 in a choriocarcinoma model (30). DSG2 is a key component of desmosomes, structures essential for cell adhesion in epithelial and cardiac tissues (33). As a member of the cadherin superfamily, DSG2 plays diverse roles in cell adhesion and is implicated in both normal development and cancer progression (34, 53). Interestingly, DSG2 is highly expressed in epithelial and cardiac tissues but less so in immune cells, including NK cells, where its expression decreases during lymphocyte differentiation (11). While the role of DSG2 in NK cell function and its potential affinity for PLAC1 warrant further investigation, our data suggests that the interaction between PLAC1 and NK cells likely involves a receptor other than DSG2. Exploring the targeting of PLAC1 to enhance NK cell-mediated anti-tumor responses could lead to the development of new immunotherapies that increase NK cell cytotoxicity or harness PLAC1's immunogenic potential to improve cancer treatment outcomes. Further studies are needed to assess how PLAC1 influences tumor progression and whether targeting it can effectively modulate the tumor microenvironment.

In summary, the interaction between PLAC1 and NK cells represents a promising mechanism by which the immune system can recognize and eliminate PLAC1-expressing tumors. These findings provide new insights into tumor immunity and suggest potential strategies for cancer immunotherapy involving the modulation of PLAC1. Further studies are needed to unravel the

precise molecular pathways and to assess the therapeutic potential of PLAC1 in clinical settings.

Methods

Cell lines, patients, NK cells and reagents

All cell lines were obtained by ATCC and characterized every 6 months by HLA class I typing. Mycoplasma contamination was routinely detected by Mycoplasma Detection kit (Venor-GeM Advance). Cells were maintained in RPMI 1640 medium supplemented with 10% FBS (Gibco), 2 mM glutamine, 100 mg/ml penicillin and 50 mg/ml streptomycin (Euroclone).

Human NK cells were isolated from peripheral blood mononuclear cells (PBMC) of HDs by the RosetteSep NK-cell enrichment mixture method (StemCell Technologies) and Ficoll-Paque Plus (Lympholyte Cedarlane) centrifugation. NK cells with purity greater than 90% were suspended in NK MACS medium (Miltenyi Biotec) supplemented with NK MACS Supplement, AB serum and 500 IU/mL of recombinant human IL-2 (PeproTech) for 18 hours at 37°C.

Lentiviral infections and transfections

K562 cells were stable infected with a pooled shRNA human library from the RNAi consortium (TRC 1.5) consisting of over 150000 plasmid-based shRNA constructs targeting 15000 human genes (Sigma). On average, there were five shRNA designs for each gene target. K562 were stably transduced with a multiplicity of infection (MOI) ≤ 1 such that the majority of cells will be transduced with a single shRNA. Transduced cells were selected using 3 μg/ml puromycin for 4 days. As control K562 cell were infected with an shRNA (sgCTR). Transduced cells were cocultured with NK cells isolated from HD at an E:T ratio of 15:1 for 3 days. The surviving cells were FACS sorted for cell viability and morphology and seeded clonally in 96 well plates. The clones obtained were expanded and genomic DNA extracted by standard procedures. Lentiviral particles were generated in HEK293T cells by combining a pLKO.1 plasmid containing shRNA sequences, packaging plasmid pCMV-dR8.74, and envelope plasmid VSV-G/pMD2.G using TransIT-293 transfection reagent (MIRUS Bio LLC, Madison, WI, USA). K562 cells were infected by the spin inoculation method with lentivirus containing a nontarget shRNA control vector (SHC002) or either of MICA, PLAC1, TCF7 and PLEK shRNAs (clone ID: TRCN0000061288, TRCN0000061031, TRCN0000061677, and TRCN0000060846) targeting the indicated genes (Sigma-Aldrich).

PLAC1 cloning

Full-length cDNAs encoding human PLAC1 (accession number AF234654.1) was cloned from JEG3 cells in the lentiviral vector pRRL-CMV-PGK-GFP-WPRE (TWEEN) under the control of the CMV promoter. K562 cells were transfected with PLAC1 vector or empty vector using LipofectAMINE 2000 according to the manufacturer's instructions (Invitrogen Life Technologies). Stably transfected cells were sorted by FACS as GFP expressing cells.

DNA sequencing

Genomic DNA was isolated with standard procedures and primers designed to flank the shRNA hairpins were used to amplify the shRNA sequences. Hits identified by sequencing the PCR amplicon were matched to database.

Quantitative mRNA expression

Total RNA was extracted using TRIzol Reagent (Invitrogen). First-strand cDNA was synthesized using the SuperScript II First Strand cDNA synthesis kit (Invitrogen). Quantitative real-time PCR (qPCR) reactions were performed using pre-validated TaqMan gene expression assays from Applied Biosystems (Hs06598311_m1 for PLAC1, Hs01556515_m1 for TCF7, Hs01043767_m1 for PLEKHA5, Hs02786624_g1 for GAPDH). Relative gene expression was determined using the 2-ΔΔCt method with ß-actin as endogenous control.

Cytotoxicity and degranulation assay

NK cell cytotoxic activity and degranulation assay were performed by a standard 4-hour ^{51}Cr-release assay and flow cytometric analysis of cell-surface CD107a expression, respectively. In cytotoxicity assay K562 cells were labelled with ^{51}Cr [Amersham International; 100μCi (3.7 MBq)/1 x 10^6 cells] and co-cultured (5 x 10^3) with NK cells or NKL cell line at different E:T cell ratios, in 96-well plates round bottom in triplicates, and incubated at 37°C. At 4 hours of incubation, 25μL supernatant were removed, and the ^{51}Cr release was measured with TopCount NXT beta detector (PerkinElmer Life Sciences). The percentage of specific lysis by counts per minute (cpm) was determined as follows: 100 x (mean cpm experimental release – mean cpm spontaneous release)/(mean cpm total release - mean cpm spontaneous release). Specific lysis was converted to lytic units (L.U.) calculated from the curve of the percentage lysis (54) and defined as the number of NK cells required to produce 20% lysis of 10^6 target cells during the 4 hours of incubation. In degranulation assays, NK cells were co-cultured with K562 target cells at 1:1 ratio for 3 hours, in complete medium in the presence of anti-CD107a (diluted 1:100). During the last 2 hours, GolgiStop (BD Bioscences) was added at 1:500 dilution. Cells were firstly pre-stained with Live/Dead Kit (L/D), stained with anti-CD56, anti-CD3 and then, the expression of CD107a was evaluated in the $CD3^-CD56^+$ subset by flow cytometry.

10.3389/fimmu.2025.1537876

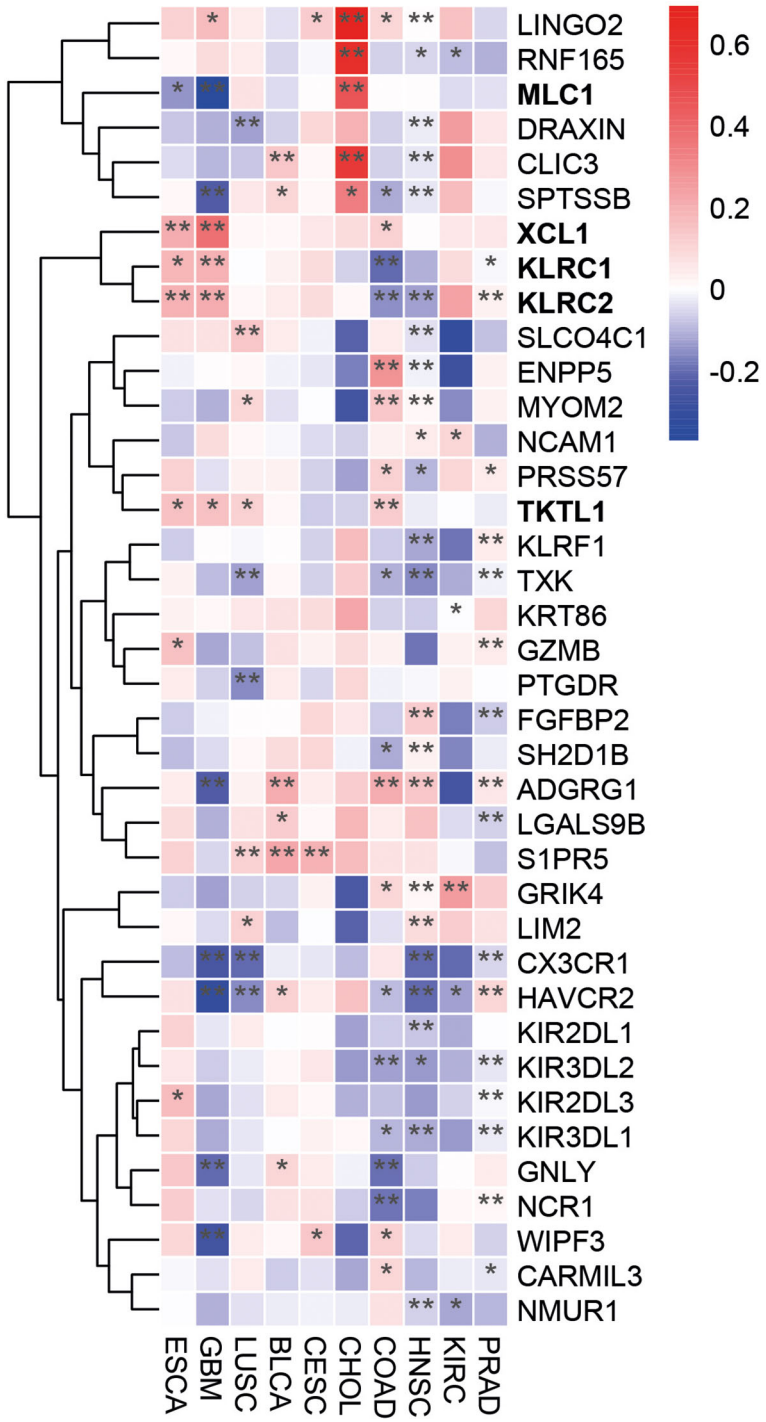

FIGURE 4
PLAC1 correlates with the expression of NK-cell signature genes in cancer. Heatmap showing the differential expression of NK cell marker genes in the indicated tumor types. The color scale is based on *z*-score-scaled gene expression. The z-score distribution ranges from −2 (blue) to 2 (red). Statistically significant P values are indicated; * p<0.05, ** p<0.01.

Antibodies for flow cytometry

The following antibodies were used: anti-CD3-Alexa-700 (UCHT1), anti-CD56-PE-Cy7 (B159), anti-CD107a-FITC (H4A3), anti-IgG1-FITC (A85-1), anti-IgM-PE (R6-60.2), anti-MICA/B-BV650 (6D4), anti-ULBP2/5/6-BV510 (165903), anti-CD155/PVR-BV605 (SKII.4), anti-CD112/Nectin-2-PE (R2.525), anti-CD95/FAS-BV421 (DX2), anti-CD262/TRAIL/R2-PE

(YM366), anti-ULBP1-PE (170818), anti-ULBP3-PE (166510), anti-FAS-BV421 (DX2), anti-B7-H6-BV421 (1A5), anti-DSG2-PE (6D8), purchased from BD Biosciences. For indirect staining, goat F (ab')2 Fragment anti-mouse IgG FITC (IM1619) was used. All these antibodies were used according to the manufacturers' protocol. Prior to surface staining, NK cells were pre-stained with Live/Dead™ Fixable Near-IR Dead Cell Stain Kit (Invitrogen). Flow cytometry was performed by using FACSCalibur, FACSCantoII or FACSFortessa X-20 (BD Biosciences) and analyzed by FlowJo Software. Recombinant human NKG2D-Fc, DNAM1-Fc, NKp30-Fc and NKp44-Fc chimera proteins were purchased from R&D. Cells were incubated with fusion proteins for 30 min in ice, washed twice and then incubated with PE-conjugated goat anti-human Fc antibody (Jackson ImmunoResearch Laboratories) for 30 min on ice, and propidium iodide was added to cells before flow analysis.

Western blotting

Equal amounts of protein extracts were resolved on 15% or 10% polyacrylamide gel for the detection of PLAC1 and MICA, respectively, and transferred on nitrocellulose membranes (Amersham Systems, Ge Healthcare Sciences). Filters were blocked with 5% (v/v) non-fat dry milk for 1 hour at room temperature, and then blotted with rabbit anti-human PLAC1 polyclonal antibody (kindly provided by Prof. Zarnani, Sina Biotech Co) or mouse anti-human PLAC1 (G1, Santa Cruz Biotechnology, Cat No 365919), and mouse anti-human MICA monoclonal antibody (Proteintech, Cat No. 66384-1-Ig) to recognize PLAC1 and MICA, respectively. Anti-ERp57, anti-β–actin or anti-GAPDH antibodies were used as loading control. After extensive washing with TBST, filters were incubated with peroxidase-coupled secondary antibody for 1 hour at room temperature. Reactivity was detected with the ECL Western Blotting Detection Kit (Amersham Systems, Ge Healthcare Life Sciences) and the protein bands were quantified using Image J.

Databases and data analysis

Pan-cancer gene expression data and clinical data from 33 tumor types were downloaded from The Cancer Genome Atlas (TCGA, https://portal.gdc.cancer.gov/, accessed April 5th, 2024) database. The survival curves using log-rank test of Kaplan-Meier overall survival (OS) and the forest-plots indicating hazard-ratio and 95% confidence intervals for different cut-off values for PLAC1 expression were conducted using the *survival* R package (version 3.4.0) under R version 4.4.1 (https://www.R-project.org/). P values<0.05 were considered significant. The expression of PLAC1 and DSG2 in healthy tissues and cell types was obtained from the Human Protein Atlas (HPA, http://www.proteinatlas.org/, accessed July 2nd, 2024) database. The Gene Expression Omnibus (GEO, https://www.ncbi.nlm.nih.gov/geo/, accessed September 6th, 2024) database was used to obtain normalized scRNA-seq data from NK cells (GSE159624).

Statistical analysis

For all data, statistical significance was evaluated using GraphPad software. Statistical tests performed are indicated in the figure legends. P values not exceeding 0.05 were considered to be statistically significant.

Data availability statement

The original contributions presented in the study are included in the article/Supplementary Material. Further inquiries can be directed to the corresponding author.

Ethics statement

The studies involving humans were approved by Ospedale Pediatrico Bambino Gesù. The studies were conducted in accordance with the local legislation and institutional requirements. The participants provided their written informed consent to participate in this study.

Author contributions

PR: Conceptualization, Data curation, Formal Analysis, Funding acquisition, Investigation, Methodology, Project administration, Resources, Software, Supervision, Validation, Visualization, Writing – original draft, Writing – review & editing. LC: Conceptualization, Data curation, Formal Analysis, Funding acquisition, Investigation, Methodology, Project administration, Resources, Software, Supervision, Validation, Visualization, Writing – original draft, Writing – review & editing. PG: Conceptualization, Data curation, Formal Analysis, Funding acquisition, Investigation, Methodology, Project administration, Resources, Software, Supervision, Validation, Visualization, Writing – original draft, Writing – review & editing. VD: Conceptualization, Data curation, Formal Analysis, Funding acquisition, Investigation, Methodology, Project administration, Resources, Software, Supervision, Validation, Visualization, Writing – original draft, Writing – review & editing. MC: Conceptualization, Data curation, Formal Analysis, Funding acquisition, Investigation, Methodology, Project administration, Resources, Software, Supervision, Validation, Visualization, Writing – original draft, Writing – review & editing. VF: Resources, Conceptualization, Data curation, Formal Analysis, Funding acquisition, Investigation, Methodology, Project administration, Software, Supervision, Validation, Visualization, Writing – original draft, Writing – review & editing. VL: Conceptualization, Data curation, Formal Analysis, Funding acquisition, Investigation, Methodology, Project administration, Resources, Software, Supervision, Validation, Visualization, Writing – original draft, Writing – review & editing. OM: Conceptualization, Data curation, Formal Analysis, Funding

acquisition, Investigation, Methodology, Project administration, Resources, Software, Supervision, Validation, Visualization, Writing – original draft, Writing – review & editing. RB: Conceptualization, Data curation, Formal Analysis, Funding acquisition, Investigation, Methodology, Project administration, Resources, Software, Supervision, Validation, Visualization, Writing – original draft, Writing – review & editing. FL: Conceptualization, Data curation, Formal Analysis, Funding acquisition, Investigation, Methodology, Project administration, Resources, Software, Supervision, Validation, Visualization, Writing – original draft, Writing – review & editing. DF: Conceptualization, Data curation, Formal Analysis, Funding acquisition, Investigation, Methodology, Project administration, Resources, Software, Supervision, Validation, Visualization, Writing – original draft, Writing – review & editing.

Funding

The author(s) declare that financial support was received for the research and/or publication of this article. This work was supported by grants awarded by the European Union's Horizon 2020 research and Innovation program under the Marie Skłodowska-Curie Actions grant agreement No 954992 (CAPSTONE-ETN) (D. Fruci), the Associazione Italiana Ricerca sul Cancro (AIRC) IG18495 (D. Fruci) and IG24345 (D. Fruci), the Italian Ministry of Health with Ricerca Finalizzata No. PE-2011-02351866 (D. Fruci) and Current Research funds (D. Fruci), PRIN2022/ 20223RRASS/CUP: E53D23001190006 (L. Cifaldi) and PRIN PNRR2022/ P2022XZKBM/CUP: E53D23015290001 (L. Cifaldi). This research was also supported by fellowships from the Fondazione Umberto Veronesi (FUV) (V. Lucarini and O. Melaiu) and a CAPSTONE-ETN H2020 Early-Stage Researchers (P. Gragera).

Conflict of interest

The authors declare that the research was conducted in the absence of any commercial or financial relationships that could be construed as a potential conflict of interest.

Generative AI statement

The author(s) declare that no Generative AI was used in the creation of this manuscript.

Publisher's note

Supplementary material

The Supplementary Material for this article can be found online at: https://www.frontiersin.org/articles/10.3389/fimmu.2025.1537876/full#supplementary-material

SUPPLEMENTARY FIGURE 1
Related to Figure 1. MICA inhibition confers protection of K562 cells from NK cell-mediated lysis. **(A)** Representative immunoblotting analysis of MICA expression on K562 cells infected with lentiviruses carrying control shRNA (shMICA-) or shRNA targeting the *MICA* gene (shMICA+). Densitometric analysis of GAPDH-normalized MICA expression from three independent experiments is shown below. **(B)** Flow-cytometry analysis of MICA expression in the indicated cell lines. The percentage of MICA-positive K562 cells is shown. **(C)** K562-shMICA and K562-shCTRL cells were assayed as targets of NK cells at the indicated E:T ratios in a standard ^{51}Cr-release assay. A representative of five independent experiments is reported. **(D)** Specific lysis of C was converted to L.U. 20%. Dots, L.U. 20% of the effector/target pairs tested; horizontal bars, average values. *P* values, compared with K562-shMICA and K562-shCTRL cells (two-tailed paired Student *t* test).

SUPPLEMENTARY FIGURE 2
Related to Figure 2. PLAC1 regulates the activity of NK cells. **(A)** qPCR of PLAC1, TCF7 and PLEKHA5 expression in K562 cells transduced with lentiviral vectors encoding either control shRNA (shCTRL) or shRNA targeting PLAC1, TCF7 or PLEKHA5 genes (two-tailed unpaired Student *t* test). **(B)** qPCR of PLAC1 expression in K562 cells overexpressing PLAC1 (two-tailed unpaired Student *t* test).

SUPPLEMENTARY FIGURE 3
Related to Figure 3 PLAC1 expression has prognostic value in tumors. **(A)** PLAC1 gene expression in the indicated human cell types. **(B)** Kaplan-Meier curves show the duration of overall survival of the indicated tumor patients according to the PLAC1 gene expression. **(C)** Forest plots showing hazard ratio and 95% confident intervals of the full range of cutoff values of the indicated tumor patients according to the PLAC1 gene expression. Log-rank test with Miller and Siegmund P-value correction was used. Statistically significant P values are indicated.

SUPPLEMENTARY FIGURE 4
Desmoglein 2 expression in tumor cells and NK cells. **(A)** DSG2 expression in the indicated human cells. **(B)** Density plots of DSG2 expression of NK cells from scRNA-seq of HD and AML patients (GSE159624). **(C)** Representative flow-cytometry analyses of DSG2 expression in HeLa cells and NK cells from a HD. Summary of DSG2 expression in NK cells from 3 HDs is reported on the right.

References

1. Quatrini L, Della Chiesa M, Sivori S, Mingari MC, Pende D, Moretta L. Human NK cells, their receptors and function. *Eur J Immunol.* (2021) 51:1566–79. doi: 10.1002/eji.202049028

2. Lanier LL. Up on the tightrope: natural killer cell activation and inhibition. *Nat Immunol.* (2008) 9:495–502. doi: 10.1038/ni1581

3. Biassoni R, Cantoni C, Pende D, Sivori S, Parolini S, Vitale M, et al. Human natural killer cell receptors and co-receptors. *Immunol Rev.* (2001) 181:203–14. doi: 10.1034/j.1600-065X.2001.1810117.x

4. Lanier LL. NK cell receptors. *Annu Rev Immunol.* (1998) 16:359–93. doi: 10.1146/annurev.immunol.16.1.359

5. Zingoni A, Molfetta R, Fionda C, Soriani A, Paolini R, Cippitelli M, et al. NKG2D and its ligands: "One for all, all for one. *Front Immunol*. (2018) 9:476. doi: 10.3389/fimmu.2018.00476

6. Gonzalez S, Lopez-Soto A, Suarez-Alvarez B, Lopez-Vazquez A, Lopez-Larrea C. NKG2D ligands: key targets of the immune response. *Trends Immunol*. (2008) 29:397–403. doi: 10.1016/j.it.2008.04.007

7. Cifaldi L, Doria M, Cotugno N, Zicari S, Cancrini C, Palma P, et al. DNAM-1 activating receptor and its ligands: how do viruses affect the NK cell-mediated immune surveillance during the various phases of infection? *Int J Mol Sci*. (2019) 20. doi: 10.3390/ijms20153715

8. Pogge von Strandmann E, Simhadri VR, von Tresckow B, Sasse S, Reiners KS, Hansen HP, et al. Human leukocyte antigen-B-associated transcript 3 is released from tumor cells and engages the NKp30 receptor on natural killer cells. *Immunity*. (2007) 27:965–74. doi: 10.1016/j.immuni.2007.10.010

9. Arnon TI, Achdout H, Levi O, Markel G, Saleh N, Katz G, et al. Inhibition of the NKp30 activating receptor by pp65 of human cytomegalovirus. *Nat Immunol*. (2005) 6:515–23. doi: 10.1038/ni1190

10. Li SS, Ogbomo H, Mansour MK, Xiang RF, Szabo L, Munro F, et al. Identification of the fungal ligand triggering cytotoxic PRR-mediated NK cell killing of Cryptococcus and Candida. *Nat Commun*. (2018) 9:751. doi: 10.1038/s41467-018-03014-4

11. Bagger FO, Kinalis S, Rapin N. BloodSpot: a database of healthy and Malignant haematopoiesis updated with purified and single cell mRNA sequencing profiles. *Nucleic Acids Res*. (2019) 47:D881–5. doi: 10.1093/nar/gky1076

12. Brandt CS, Baratin M, Yi EC, Kennedy J, Gao Z, Fox B, et al. The B7 family member B7-H6 is a tumor cell ligand for the activating natural killer cell receptor NKp30 in humans. *J Exp Med*. (2009) 206:1495–503. doi: 10.1084/jem.20090681

13. Cao G, Wang J, Zheng X, Wei H, Tian Z, Sun R. Tumor therapeutics work as stress inducers to enhance tumor sensitivity to natural killer (NK) cell cytolysis by up-regulating NKp30 ligand B7-H6. *J Biol Chem*. (2015) 290:29964–73. doi: 10.1074/jbc.M115.674010

14. Semeraro M, Rusakiewicz S, Minard-Colin V, Delahaye NF, Enot D, Vely F, et al. Clinical impact of the NKp30/B7-H6 axis in high-risk neuroblastoma patients. *Sci Transl Med*. (2015) 7:283ra255. doi: 10.1126/scitranslmed.aaa2327

15. Mandelboim O, Lieberman N, Lev M, Paul L, Arnon TI, Bushkin Y, et al. Recognition of haemagglutinins on virus-infected cells by NKp46 activates lysis by human NK cells. *Nature*. (2001) 409:1055–60. doi: 10.1038/35059110

16. Ho JW, Hershkovitz O, Peiris M, Zilka A, Bar-Ilan A, Nal B, et al. H5-type influenza virus hemagglutinin is functionally recognized by the natural killer-activating receptor NKp44. *J Virol*. (2008) 82:2028–32. doi: 10.1128/JVI.02065-07

17. Dong XY, Peng JR, Ye YJ, Chen HS, Zhang LJ, Pang XW, et al. Plac1 is a tumor-specific antigen capable of eliciting spontaneous antibody responses in human cancer patients. *Int J Cancer*. (2008) 122:2038–43. doi: 10.1002/ijc.v122:9

18. Gaggero S, Bruschi M, Petretto A, Parodi M, Del Zotto G, Lavarello C, et al. Nidogen-1 is a novel extracellular ligand for the NKp44 activating receptor. *Oncoimmunology*. (2018) 7:e1470730. doi: 10.1080/2162402X.2018.1470730

19. Baychelier F, Sennepin A, Ermonval M, Dorgham K, Debre P, Vieillard V. Identification of a cellular ligand for the natural cytotoxicity receptor NKp44. *Blood*. (2013) 122:2935–42. doi: 10.1182/blood-2013-03-489054

20. Narni-Mancinelli E, Gauthier L, Baratin M, Guia S, Fenis A, Deghmane AE, et al. Complement factor P is a ligand for the natural killer cell-activating receptor NKp46. *Sci Immunol*. (2017) 2. doi: 10.1126/sciimmunol.aam9628

21. Sen Santara S, Lee DJ, Crespo A, Hu JJ, Walker C, Ma X, et al. The NK cell receptor NKp46 recognizes ecto-calreticulin on ER-stressed cells. *Nature*. (2023) 616:348–56. doi: 10.1038/s41586-023-05912-0

22. Zamai L, Mariani AR, Zauli G, Rodella L, Rezzani R, Manzoli FA, et al. Kinetics of *in vitro* natural killer activity against K562 cells as detected by flow cytometry. *Cytometry*. (1998) 32:280–5. doi: 10.1002/(SICI)1097-0320(19980801)32:4<280::AID-CYTO4>3.0.CO;2-M

23. Diehl P, Tedesco D, Chenchik A. Use of RNAi screens to uncover resistance mechanisms in cancer cells and identify synthetic lethal interactions. *Drug Discov Today Technol*. (2014) 11:11–8. doi: 10.1016/j.ddtec.2013.12.002

24. Cocchia M, Huber R, Pantano S, Chen EY, Ma P, Forabosco A, et al. PLAC1, an Xq26 gene with placenta-specific expression. *Genomics*. (2000) 68:305–12. doi: 10.1006/geno.2000.6302

25. Robertson MJ, Cochran KJ, Cameron C, Le JM, Tantravahi R, Ritz J. Characterization of a cell line, NKL, derived from an aggressive human natural killer cell leukemia. *Exp Hematol*. (1996) 24:406–15.

26. Zhu Y, Wang W, Wang X. Roles of transcriptional factor 7 in production of inflammatory factors for lung diseases. *J Transl Med*. (2015) 13:273. doi: 10.1186/s12967-015-0617-7

27. Tran TT, Rane CK, Zito CR, Weiss SA, Jessel S, Lucca L, et al. Clinical significance of PDCD4 in melanoma by subcellular expression and in tumor-associated immune cells. *Cancers (Basel)*. (2021) 13. doi: 10.3390/cancers13051049

28. Zhang J, Lyu T, Cao Y, Feng H. Role of TCF-1 in differentiation, exhaustion, and memory of CD8(+) T cells: A review. *FASEB J*. (2021) 35:e21549. doi: 10.1096/fj.202002566R

29. Liu J, Adhav R, Miao K, Su SM, Mo L, Chan UI, et al. Characterization of BRCA1-deficient premalignant tissues and cancers identifies Plekha5 as a tumor metastasis suppressor. *Nat Commun*. (2020) 11:4875. doi: 10.1038/s41467-020-18637-9

30. Chen Y, Stagg C, Schlessinger D, Nagaraja R. PLAC1 affects cell to cell communication by interacting with the desmosome complex. *Placenta*. (2021) 110:39–45. doi: 10.1016/j.placenta.2021.06.001

31. Jackman SM, Kong X, Fant ME. Plac1 (placenta-specific 1) is essential for normal placental and embryonic development. *Mol Reprod Dev*. (2012) 79:564–72. doi: 10.1002/mrd.22062

32. Shembrey C, Foroutan M, Hollande F. A new natural killer cell-specific gene signature predicting recurrence in colorectal cancer patients. *Front Immunol*. (2022) 13:1011247. doi: 10.3389/fimmu.2022.1011247

33. Brooke MA, Nitoiu D, Kelsell DP. Cell-cell connectivity: desmosomes and disease. *J Pathol*. (2012) 226:158–71. doi: 10.1002/path.v226.2

34. Awad MM, Dalal D, Cho E, Amat-Alarcon N, James C, Tichnell C, et al. DSG2 mutations contribute to arrhythmogenic right ventricular dysplasia/cardiomyopathy. *Am J Hum Genet*. (2006) 79:136–42. doi: 10.1086/504393

35. Crinier A, Dumas PY, Escaliere B, Piperoglou C, Gil L, Villacreces A, et al. Single-cell profiling reveals the trajectories of natural killer cell differentiation in bone marrow and a stress signature induced by acute myeloid leukemia. *Cell Mol Immunol*. (2021) 18:1290–304. doi: 10.1038/s41423-020-00574-8

36. Koslowski M, Sahin U, Mitnacht-Kraus R, Seitz G, Huber C, Tureci O. A placenta-specific gene ectopically activated in many human cancers is essentially involved in Malignant cell processes. *Cancer Res*. (2007) 67:9528–34. doi: 10.1158/0008-5472.CAN-07-1350

37. Yang L, Zha TQ, He X, Chen L, Zhu Q, Wu WB, et al. Placenta-specific protein 1 promotes cell proliferation and invasion in non-small cell lung cancer. *Oncol Rep*. (2018) 39:53–60.

38. Meng X, Liu Z, Zhang L, He Y. Plac1 remodels the tumor immune evasion microenvironment and predicts therapeutic response in head and neck squamous cell carcinoma. *Front Oncol*. (2022) 12:919436. doi: 10.3389/fonc.2022.919436

39. Li Y, Chu J, Li J, Feng W, Yang F, Wang Y, et al. Cancer/testis antigen-Plac1 promotes invasion and metastasis of breast cancer through Furin/NICD/PTEN signaling pathway. *Mol Oncol*. (2018) 12:1233–48. doi: 10.1002/mol2.2018.12.issue-8

40. Liu F, Shen D, Kang X, Zhang C, Song Q. New tumour antigen PLAC1/CP1, a potentially useful prognostic marker and immunotherapy target for gastric adenocarcinoma. *J Clin Pathol*. (2015) 68:913–6. doi: 10.1136/jclinpath-2015-202978

41. Ren Y, Lv Y, Li T, Jiang Q. High expression of PLAC1 in colon cancer as a predictor of poor prognosis: A study based on TCGA data. *Gene*. (2020) 763:145072. doi: 10.1016/j.gene.2020.145072

42. Wu Y, Lin X, Di X, Chen Y, Zhao H, Wang X. Oncogenic function of Plac1 on the proliferation and metastasis in hepatocellular carcinoma cells. *Oncol Rep*. (2017) 37:465–73. doi: 10.3892/or.2016.5272

43. Yin Y, Zhu X, Huang S, Zheng J, Zhang M, Kong W, et al. Expression and clinical significance of placenta-specific 1 in pancreatic ductal adenocarcinoma. *Tumour Biol*. (2017) 39:1010428317699131. doi: 10.1177/1010428317699131

44. Ghods R, Ghahremani MH, Madjd Z, Asgari M, Abolhasani M, Tavasoli S, et al. High placenta-specific 1/low prostate-specific antigen expression pattern in high-grade prostate adenocarcinoma. *Cancer Immunol Immunother*. (2014) 63:1319–27. doi: 10.1007/s00262-014-1594-z

45. Tchabo NE, Mhawech-Fauceglia P, Caballero OL, Villella J, Beck AF, Miliotto AJ, et al. Expression and serum immunoreactivity of developmentally restricted differentiation antigens in epithelial ovarian cancer. *Cancer Immun*. (2009) 9:6.

46. Devor EJ, Gonzalez-Bosquet J, Warrier A, Reyes HD, Ibik NV, Schickling BM, et al. p53 mutation status is a primary determinant of placenta-specific protein 1 expression in serous ovarian cancers. *Int J Oncol*. (2017) 50:1721–8. doi: 10.3892/ijo.2017.3931

47. Devor EJ, Leslie KK. The oncoplacental gene placenta-specific protein 1 is highly expressed in endometrial tumors and cell lines. *Obstet Gynecol Int*. (2013) 2013:807849. doi: 10.1155/2013/807849

48. Devor EJ, Reyes HD, Gonzalez-Bosquet J, Warrier A, Kenzie SA, Ibik NV, et al. Placenta-specific protein 1 expression in human papillomavirus 16/18-positive cervical cancers is associated with tumor histology. *Int J Gynecol Cancer*. (2017) 27:784–90. doi: 10.1097/IGC.0000000000000957

49. Yuan H, Wang X, Shi C, Jin L, Hu J, Zhang A, et al. Plac1 is a key regulator of the inflammatory response and immune tolerance in mammary tumorigenesis. *Sci Rep*. (2018) 8:5717. doi: 10.1038/s41598-018-24022-w

50. Hayashi R, Nagato T, Kumai T, Ohara K, Ohara M, Ohkuri T, et al. Expression of placenta-specific 1 and its potential for eliciting anti-tumor helper T-cell responses in head and neck squamous cell carcinoma. *Oncoimmunology*. (2020) 10:1856545. doi: 10.1080/2162402X.2020.1856545

51. Lin C, Qian P, Zhang Y, Liu Z, Dai K, Sun D. Plac1 promotes nasopharyngeal carcinoma cells proliferation, migration and invasion via Furin/NICD/PTEN pathway. *Tissue Cell*. (2021) 69:101480. doi: 10.1016/j.tice.2020.101480

52. Mahmoudian J, Ghods R, Nazari M, Jeddi-Tehrani M, Ghahremani MH, Ghaffari-Tabrizi-Wizsy N, et al. PLAC1: biology and potential application in cancer immunotherapy. *Cancer Immunol Immunother*. (2019) 68:1039–58. doi: 10.1007/s00262-019-02350-8

53. Myo Min KK, Ffrench CB, McClure BJ, Ortiz M, Dorward EL, Samuel MS, et al. Desmoglein-2 as a cancer modulator: friend or foe? *Front Oncol*. (2023) 13:1327478.

54. Villanueva J, Lee S, Giannini EH, Graham TB, Passo MH, Filipovich A, et al. Natural killer cell dysfunction is a distinguishing feature of systemic onset juvenile rheumatoid arthritis and macrophage activation syndrome. *Arthritis Res Ther*. (2005) 7:R30–37.

Frontiers in Immunology

Explores novel approaches and diagnoses to treat immune disorders.

The official journal of the International Union of Immunological Societies (IUIS) and the most cited in its field, leading the way for research across basic, translational and clinical immunology.

Discover the latest Research Topics

See more →

Frontiers

Avenue du Tribunal-Fédéral 34
1005 Lausanne, Switzerland
frontiersin.org

Contact us

+41 (0)21 510 17 00
frontiersin.org/about/contact